INTERNATIONAL DOCTORATE SCHOOL IN
CLINICAL AND EXPERIMENTAL MEDICINE

XXXIV CYCLE

Curriculum: Nanomedicine, medicinal and pharmaceutical sciences

University of Modena and Reggio Emilia

Doctoral Thesis

Design and Synthesis of Boron Containing Compounds and Their Use as Antibacterial Agents

PhD Candidate:

Dr. Maria Luisa Introvigne

Supervisor:

Prof. Fabio Prati

Co-supervisor:

Prof. Emilia Caselli

PhD Coordinator:

Giuseppe Biagini

Index

Abbreviations

ADC - *Acinetobacter* Derived Cephalosporinases

AIDS – Acquired Immunodeficiency Disease Syndrome

AML – Acute Myeloid Leukemia

ATX LPA – Autotaxin – Lysophosphatidic Acid

BATSI – Boronic Acid Transition State Inhibitors

BNCT – Boron Neutron Capture Therapy

Ca – Carbonic anhydrase

CAZ – Ceftazidime

DCM – dichloromethane

DPP – Dipeptidyl Peptidase

ER – Estrogen Receptor

ESBL – Extended Spectrum β-lactamases

FAP – Fibroblast Activating Protein

FDA – Food and Drug Administration

FEP – Cefepime

G-CSF – Granulocyte Colony Stimulating Factor

GLP-1 – Glucagon Like Peptide

HDAC – Histone deacetylase I

HIV – Human immunodeficiency virus

HNE – Human neutrophile elastase

IAV – Influenza A Virus

IC_{50} – Inhibitory concentration 50%

K_i – Inhibition constant

KPC – *K. pneumoniae* carbapenemases

LD_{50} – letal dose 50%

MAPK - mitogen-activated protein kinase

MBL – Metallo β-lactamases

MDM2 – Mouse Double Minute 2

MDR – Multi-drug Resistant

MIC – Minimum inhibitory concentration

Mp – Melting point

MRSA – Meticillin Resistant *S. aureus*

MS – Mass spectroscopy

NA – Neuraminidase

NFk-B – nuclear factor-kappa-light-chain-enhancer of activated B cells

NMR – Nuclear Magnetic Resonance

PBP – Penicillin Binding Proteins

PDE – Phosphodiesterase

ROS – Reactive oxygen species

SBL – Serine β-lactamases

SERD – Estrogen Receptor Down Regulator

THF – tetrahydrofuran

TLC – Thin Layer Chromatography

WHO – World Health Organization

English Abstract

There are only five boron-containing compounds on the pharmaceutical market, but several boronates are in clinical or preclinical phases. The most important therapeutic fields of application are the anti-cancer and the anti-bacterial ones. As anti-bacterials, boronic compounds are adjuvants of commonly used β-lactam antibiotics to avoid bacterial resistance, impairing the main mechanism that is the production of β-lactamases (BL). Boronic Acids are often called Transition State Inhibitors (BATSIs), because they inhibit BL by reversibly forming a tetrahedral adduct that resembles the high-energy intermediate of acylation-deacylation step.

My doctoral project was focused on the design and synthesis of inhibitors active against all classes of BL: class A and class C BL (Serine BL), class B (Metallo BL) and/or class D enzymes (Serine BL). Starting from the structure of an in house lead BATSI, **S02030**, bioisosteric replacements of the amide chain with either a triazole or a sulphonamide allowed the identification of promising scaffolds.

I obtained a library of 26 1,2,3-triazoles BATSIs displaying a good inhibitory activity against two of the most clinically relevant SBL: the *Acinetobacter* Derived Cephalosporinases ADC-7 (K_is from 0.090 μM to 33 μM) and the *Klebsiella pneumoniae* carbapenemase, KPC-2 (K_is from 1 nM to 1 μM). These compounds proved able to restore cephalosporin susceptibility at a fixed concentration of 4 μg/mL. X-Ray crystal structures and docking studies showed that α-triazolylboronic acids display some important interactions with conserved residues in the active site of ADC-7 and KPC-2 enzymes.

To extend the activity of such α-triazolylboronic acids against class B, Metallo BL (MBLs), I decorated these molecules with several zinc binding groups. Indeed, MBLs possess one or two zinc ions in their catalytic pocket. Seven compounds were synthesized and preliminary *in vitro* tests highlighted a promising activity on VIM-2 (IC_{50}= 7.7 μM).

Moving from these inhibitors, the X-Ray structure of OXA-24/40, a class D β-lactamases, allowed the rational design of β-triazolylboronic acids, possessing an extra methylene group between the triazole and the boronic moiety. A series of 10 molecules were synthesized and they are ready to be tested on OXA enzymes.

The bioisosteric replacement of the amide with sulphonamide led to the synthesis of a series of sulphonamide BATSIs, where compound ***12f*** proved to be a good inhibitor of class D β-lactamases in the nanomolar range (OXA 24/40, K_i = 0.300 μM), thus representing the first example of class D β-lactamase inhibitor in our laboratory.

Moreover, I faced the optimization of the lead BATSI **S02030** by the insertion of different substituents on the R_1 acylamido chain. The result was the discovery of ***19e*** (***MB076)***, a good inhibitor of both class A (KPC-2, IC_{50} = 0.132 μM) and class C β- lactamases (ADC-7, K_i = 0.020 μM). It was tested *in*

vitro (in combination with Cefepime, MIC decreased from 16 μg/mL to 0.5 μg/mL in KPC-2 expressing strains) and, given its ability of restoring antibiotic activity, I set up a large-scale synthesis for *in vivo* tests on animal models. Moreover, analogues of this compound were synthesized aiming to obtain orally bioavailable derivatives.

The aims we achieved suggest that BATSIs are an effective solution in the fight against antimicrobial resistance and some preliminary studies highlighted the possible applications of these compounds in different therapeutic areas.

Italian Abstract

Ci sono solo cinque composti boronici sul mercato farmaceutico, ma diversi boronati sono in fase clinica o preclinica. I più importanti campi di applicazione terapeutici sono l'antitumorale e l'antibatterico. Come antibatterici, i composti boronici sono adiuvanti degli antibiotici β-lattamici per evitare la resistenza batterica, compromettendo il meccanismo principale di quest'ultima che è la produzione di β-lattamasi (BL). Gli acidi boronici sono spesso chiamati inibitori dello stato di transizione (BATSI), perché inibiscono BL formando in modo reversibile un addotto tetraedrico che assomiglia all'intermedio ad alta energia della fase di acilazione-deacilazione.

Il mio progetto di dottorato si è concentrato sulla progettazione e sintesi di inibitori attivi contro tutte le classi di BL: classe A e classe C BL (Serina BL), classe B (Metallo BL) e/o classe D (Serina BL). Partendo dalla struttura del BATSI **S02030,** precedentemente sintetizzato nel nostro laboratorio, sostituzioni bioisosteriche della catena ammidica con un triazolo o una sulfonammide hanno permesso di identificare scaffold promettenti.

Ho ottenuto una libreria di 26 1,2,3-triazoli che mostrano una buona attività inibitoria contro due delle SBL clinicamente più rilevanti: *Acinetobacter* Derived Cephalosporinase, ADC-7 (K_is da 0,090 μM a 33 μM) e *Klebsiella pneumoniae* carbapenemasi, KPC-2 (K_is da 1 nM a 1 μM). Questi composti sono in grado di ripristinare la suscettibilità alle cefalosporine a una concentrazione fissa di 4 μg/mL. Strutture cristalline a raggi X e studi di docking hanno mostrato che gli acidi α-triazolilboronici interagiscono con i residui conservati nel sito attivo degli enzimi ADC-7 e KPC-2.

Per estendere l'attività di tali acidi α-triazolilboronici contro la classe B, Metallo BL (MBLs), ho decorato queste molecole con diversi gruppi leganti lo zinco. Infatti, le MBLs possiedono uno o due ioni zinco nella tasca catalitica. Sono stati sintetizzati sette composti e test preliminari *in vitro* hanno evidenziato un'attività promettente su VIM-2 (IC_{50}= 7,7 μM).

A partire da questi inibitori, la struttura a raggi X di OXA-24/40, una β-lattamasi di classe D, ha permesso la progettazione di acidi β-triazolilboronici, che possiedono un gruppo metilenico extra tra il triazolo e l'acido boronico. Dieci molecole sono state sintetizzate e sono pronte per essere testate su OXA 24/40.

La sostituzione bioisosterica dell'ammide con una sulfonammide ha portato alla sintesi di una serie di sulphonamide- BATSI, tra i quali il composto ***12f*** si è dimostrato un buon inibitore degli enzimi di classe D nell'intervallo nanomolare (OXA 24/40, K_i = 0,300 μM), rappresentando così il primo esempio di inibitore di classe D nel nostro laboratorio.

Inoltre, ho affrontato l'ottimizzazione del BATSI **S02030** mediante l'inserimento di diversi sostituenti sulla catena acilammidica R_1. Il risultato è stata la scoperta di ***19e*** (***MB076***), buon inibitore sia di β-lattamasi di classe A (KPC-2, IC_{50} = 0,132 μM) che di classe C (ADC-7, K_i = 0,020 μM). È stato testato *in vitro* (in combinazione con Cefepime, la MIC diminuisce da 16 μg/mL a 0,5 μg/mL in ceppi che esprimono KPC-2) e, data la sua capacità di ripristinare l'attività antibiotica, ho messo a punto una sintesi su larga scala per test *in vivo* su modelli animali. Inoltre, sono stati sintetizzati analoghi di questo composto allo scopo di ottenere derivati biodisponibili per via orale.

Gli obiettivi raggiunti dimostrano che i BATSI sono una soluzione efficace nella lotta alla resistenza antimicrobica e alcuni studi preliminari hanno evidenziato possibili applicazioni di questi composti in aree terapeutiche diverse.

1 Introduction

1.1 Boron

Boronic chemistry is an exciting area of science and it is gaining more and more importance. Scientific articles concerning boron can be found from the beginning of '900 and demonstrate the presence of this element in almost every field of life. Boron is present in the environment, found in the form of borates in the oceans, sedimentary rocks, coal, shale and in some soils. Boron is extracted from surface deposits located in few desert regions of the world (in particular, California and Turkey) and is used for glass and ceramic industry, detergent industry, fertilizer industry and in fire retardants.[1] Boron is an essential micronutrient for plants, involved in their structural integrity and in their metabolism. In animals it is a regulator of calcium and bone metabolism and it may be involved in cerebral function too, thanks to its effects on the transport across membranes.[2] Boron derivatives as boronic acids and esters, benzoxaboroles, benzoxaborines, diazaborines and amine cyanoboranes have been studied for synthetic, biological, pharmaceutical and medical aims since the late 1990's and their potential in medicinal chemistry has rapidly increased and has been globally recognized.

1.1.1 The element Boron

Boron is the fifth atom of the periodic table, in the period 2 and group 13 and it exists in nature as two stable isotopes (^{10}B and ^{11}B). Boron lacks two valence electrons and has an empty *p*-orbital: it is trivalent and can bind with other elements to form either trigonal planar sp^2 structures, such as boronic acids in their neutral form (pKa of boronic acids is between 4 and 10), or tetrahedral structures, such as anionic boronates where the boron atom convert to a sp^3-hybridized form by coordination of a hydroxyl group (Figure 1).[2,3] The affinity of boron, and boronic acids in particular, for oxygen makes it able to form complexes with compounds bearing two hydroxyl groups in adjacent position, like sugars and their derivatives. These complexes are formed also in living organisms where they can bind calcium ions. Moreover, thanks to its empty orbital, boron acts as Lewis acid, it can easily react with nucleophiles and it can be involved in proton transfer in cells.[2]

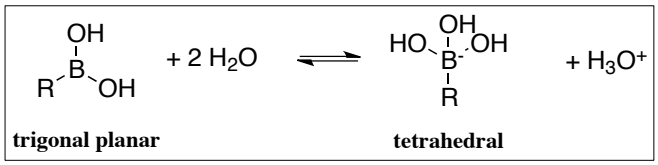

Figure 1. Sp^2 and sp^3 hybridization of boron in boronic acids.

1.1.2 Boron in bacteria

The first natural product where trace amounts of boron were found is Boromycin (Figure 2), isolated at the beginning of 20th century from *Streptomyces antibioticus*. In this compound the boron is present as tetrahedral borate due to coordination by two distal 1,2-diols and this arrangement is fundamental for inducing the folding of polyols into compact structures.[4] The complex structure of Boromycin was elucidated through chemical degradation studies and by X-ray crystal structure analysis. This

compound demonstrated antibiotic activity against Gram-positive bacteria, some fungi and protozoa, but not against Gram-negative bacteria. It interacts with the cytoplasmic membrane of these organisms and damages the permeability barrier for potassium ions.[5] About ten years later Aplasmomycin was isolated from *Streptomyces griseus*: this macrolide has a structure similar to that of Boromycin and demonstrated an anti-plasmodium activity.

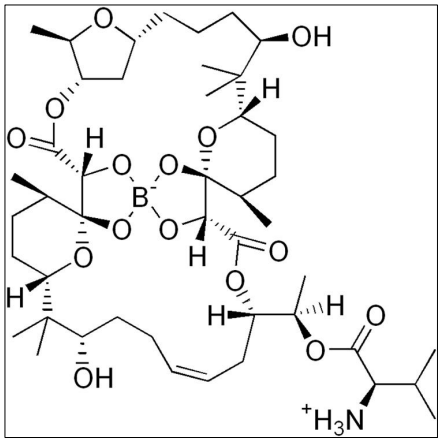

Figure 2. Structure of Boromycin.

1.1.3 Boron in plants

Boron is an essential micronutrient in plants. Studies on the importance of boron in this field were conducted starting from the 19th century. For example, Winifred et al. in 1924 reported the effects of boronic acid supplementation in broad bean plants (*Vicia faba*): in the absence of boron the plant dies after a short time in a characteristic manner correlated with disorganization of the vascular tissues, breaking down and discoloration of cells.[6] Boron is present in the plant cell wall membrane where it forms complexes with polysaccharide moieties with structural functions.[4] Boric acid is important also for protein synthesis, germination, pollination, nitrogen fixation and metabolism. In membranes boron is involved in transport systems. Boron deficiency causes a reduction in the calcium and phosphate uptake from cells and is also correlated to an increase of reactive oxygen species.[2,4] There are important differences among different species in the levels of boron required for optimum growth and at high doses boron is also toxic for plants and used as herbicidal.[7]

1.1.4 Boron in animals

In 1967 the World Health Organization (WHO) declared the boron as a "probably essential element" for humans[8] even if its role in mammalian biological systems is not fully understood. The main sources of dietary boron are fruits, vegetables, tubers, nuts and legumes for a consumption of 1-2 mg *per day* in adults. Complexes formed by boron with polyhydroxyl ligands (like sugars) are broken easily in the body and boron is absorbed in the form of $B(OH)_3$ in which it is found in biological fluids. It interacts with other nutrients and plays a regulatory role in the metabolism of minerals and lipids. It was demonstrated that lack of boron in the diet reduces growth in developing rats, while boron supplementation is effective in different fields of animal and human physiology. In particular,

boron seems to interact with bone metabolism: it enhances the synthesis of steroid hormones, such as testosterone and β-estradiol and this is directly related to an increase in absorption of calcium and phosphorus. The effect of boron supplementation is very similar to those of vitamin D supplementation and it is an important strategy in the treatment of bone loss in elderly people and post-menopausal women.[2,4] Boron is also implicated in maintaining the integrity of membranes in the brain and it seems to influence electrical activity. Experiments in elderly humans demonstrated an effect of boron intake in improving performance of various cognitive and psychomotor tasks.[2]

1.2 Boron and synthetic chemistry

Boron containing agents have been firstly recognized and developed as a very versatile reagent in the field of synthetic chemistry. Thanks to its vacant *p*-orbital, boron can easily interact with nucleophiles undergoing useful transformations from boron-containing building blocks to valuable products. Natural products don't possess C-B bonds in their structures, but the biological activity of numerous synthetic molecules containing C-B bonds, boronic acids and esters in particular, was demonstrated.[9] Therefore, it was important to develop synthetic methods to create C-B bonds and introduce a boronic acid or ester into molecules. Several techniques have been studied and different functional groups are now recognized as useful to reach this aim.

1.2.1 Synthesis of boronic acids and esters

Although boronic acids are not found in nature, they can be derived synthetically from primary sources of boron such as boric acid, which is made by the acidification of borax with carbon dioxide. Borate esters (Figure 3), the main precursors for boronic acid derivatives, are made by simple dehydration of boric acid with alcohols.

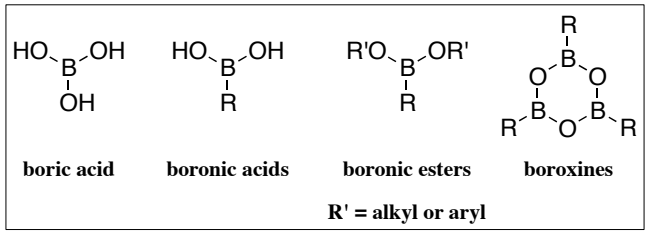

Figure 3. Oxygenated organoboron compounds.

Boronic acids possess unique properties as mild organic Lewis acids, they have a mitigated reactivity profile, high stability and they are relatively easy to handle. Moreover, because of their low toxicity and their ultimate degradation into the environmentally friendly boric acid, boronic acids can be considered "green" compounds. They are solids that tend to exist as mixtures of oligomeric anhydrides, in particular the cyclic six-membered boroxines (Figure 3). This is one of the reasons because the corresponding boronic esters are often preferred as synthetic intermediates.

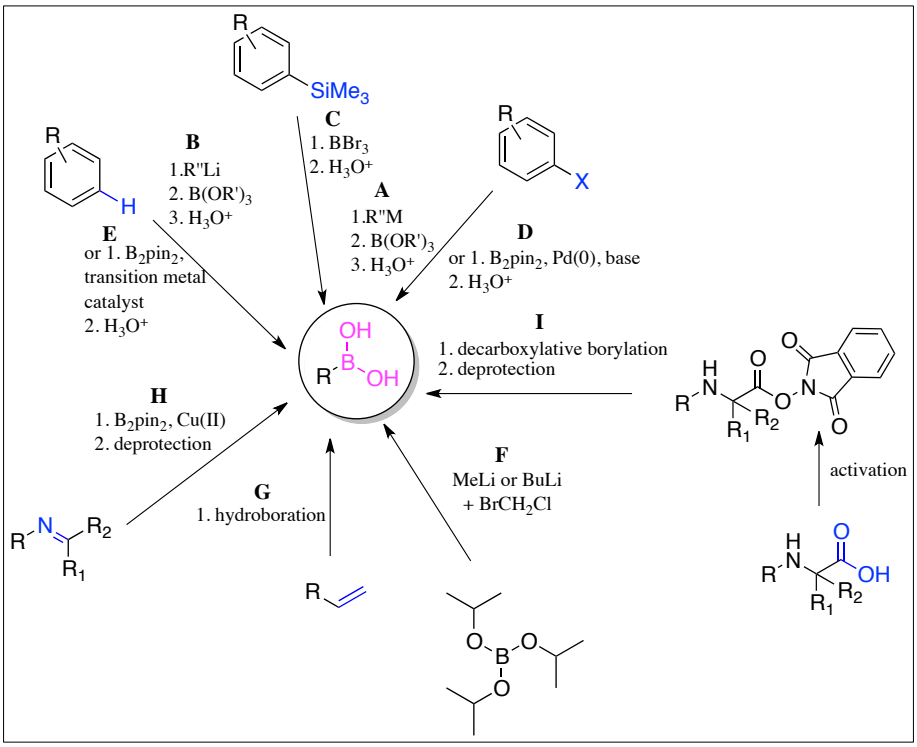

Figure 4. Synthetic methods to obtain boronic acids.

Arylboronic acids

Arylboronic acids are very popular in medicinal chemistry because of their role as cross-coupling partners for the synthesis of biaryl units. Several methods are now available for their synthesis[10]:

- Reaction of hard organometallic intermediated (i.e. lithium or magnesium) with a borate ester at low temperature. The organometallic intermediated can be obtained as Grignard reagent from an aryl halide (**A**, Figure 4)) or through ortho-lithiation of arenes containing ortho-directing groups (such as amines, ethers etc, **B**).
- Trialkylaryl silanes or stannanes can undergo direct transmetallation with boron halides such as boron tribromide. The arylboron dibromide product is then hydrolysed using an aqueous acidic workup (**C**).
- Cross-coupling reaction of diboronyl esters, such as boron bispinacolate (B_2pin_2), with aryl bromides, iodides, and triflates under palladium catalysis (**D**). Standard conditions for the coupling reaction involve $PdCl_2$ as catalyst, with potassium acetate as the base in a polar aprotic solvent.
- Direct boronylation of arenes through a transition metal promoted C-H functionalization (**E**). The reaction requires an iridium or rhodium catalyst and a diboronyl ester or a dialkoxyborane as boron donor.

Alkylboronic acids

Compared to arylboronic acids, alkylboronic acids and esters are less stable and for a long time they have found limited use as synthetic intermediates aside for their oxidation into alcohols. Indeed, also in the synthesis of boronic acids in medicinal chemistry, usually boronic esters are deprotected only in the final steps of the process. Among the reactions to obtain these compounds there are[10]:

- Trapping of organomagnesium and organolithium intermediates with borates (**F**, Figure 4). Methylboronic esters, for example, are made using the condensation of MeLi and triisopropylborate. The useful α-chloromethylboronate reagents can be made with the *in situ* trapping variant whereby BuLi is added to a mixture of $BrCH_2Cl$ and triisopropylborate.
- Catalyzed and un-catalyzed hydroboration of alkenes (**G**). In this way enantiopure alkylboronic esters can be obtained.
- Borylation of imines using B_2pin_2 as boron donor (**H**). Ellman at al. performed a substrate-controlled asymmetric borylation of imines[11,12]: they use a Cu(II) catalyst for the borilation of *N-tert*-butanesulfinyl imines in the presence of B_2pin_2. From the protected pinacolate derivative, the trifluoroborate compound and/or the free boronic acid can be easily obtained.
- Decarboxylative borylation of carboxylic acids (**I**).[13] The redox-active ester of a carboxylic acid is converted to the corresponding boronate in three steps: (i) preparation of the catalytic $NiCl_2$•6 H_2O/ ligand solution or suspension, (ii) preparation of the $[B_2pin_2Me]Li$ complex and (iii) decarboxylative borylation Ni-catalyzed. More recently an easier method was reported where $Cu(acac)_2$ is used and the reaction works in less then half an hour.[14]

Boronic esters

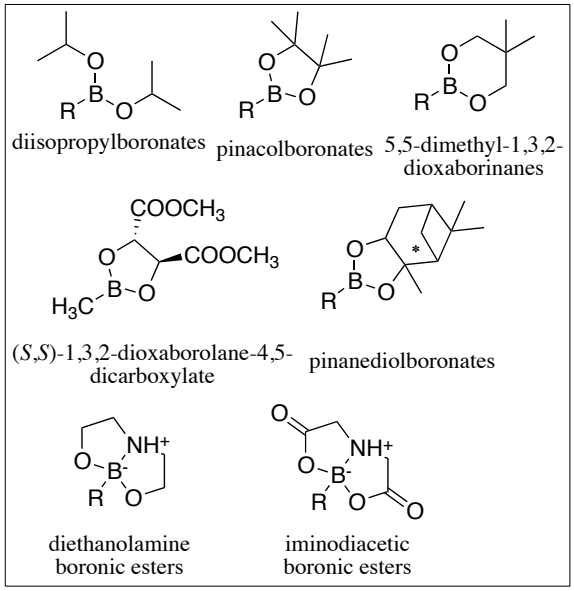

Figure 5. Examples of common boronic esters.

Replacement of the hydroxyl groups of boronic acids by alkoxy or aryloxy groups provides esters (Figure 5), which are less polar and easier to handle than corresponding acids. Indeed, many of them

serve as protecting groups to reduce the reactivity of C-B bonds and some of them are also chiral and can be use as inducers in stereoselective reactions.

Boronic esters can be synthesised from corresponding boronic acids and alcohols or diols. The reaction is an equilibrium, where the forward reaction is favoured when the boronate product is insoluble in the reaction solvent. Otherwise, it can be driven by azeotropic distillation of the water produced with the use of dehydrating agents, such as $MgSO_4$. Another method to obtain boronic esters is by transesterification of smaller dialkyl boronates (i.e. diisopropyl boronate) with distillation of the volatile alcohol by-product.

Stereoselective modifications of boronic acids and esters

Starting from the alkyl boronates or bromo-methaneboronates, Matteson asymmetric homologation[15,16] is the most commonly used method for the synthesis of α-amido and β-amidoboronic[17] acids in a highly stereocontrolled manner (Scheme 1), allowing the isolation of the chloroalkylboronate in nearly enantiomerically pure form (e.e. > 97%). Since pinanediol is commercially available in both enantiomeric forms, alpha-chloroboronates can be obtained in both configurations. Moreover, β-substituted and α-β-disubstituted β-aminoboronic acids can be obtained using this synthetic method.[18]

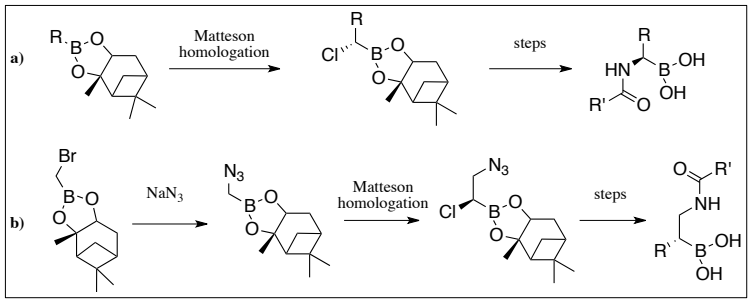

Scheme 1. a) Synthesis of α-amidoboronic acids. b) Synthesis of β-amidoboronic acids.

1.2.2 Benzoxaboroles and benzoxaborines

Benzoxaboroles are five-membered cyclic half esters of boronic acids and they were first synthesized in 1957.[19] They are implicated in organic synthesis, supramolecular chemistry, glycopeptide recognition and medicinal chemistry where they demonstrated antifungal, antiparasitic, antibacterial and anticancer activities. In general their synthesis involves the nucleophilic addition to *o*-formylphenylboronic acids where the carbonyl group of the aldehyde is hydrogen bonded to the boronic acid and thus activated for the nucleophilic attack and cyclization to form the oxaborole ring (Scheme 2).[20]

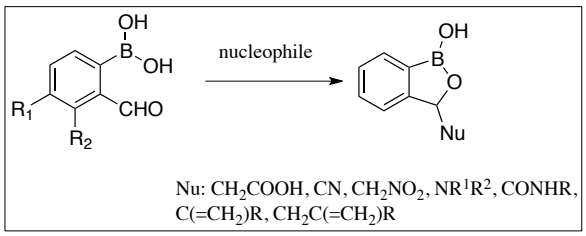

Scheme 2. General synthesis of benzoxaboroles.

The synthesis of benzoxaboroles was optimized by several research groups to insert different kind of nucleophiles in position 3 on the oxaborole ring, such as secondary amines[21], indoles, α-bromomethylacrylates, phosphate groups, benzylisonitrile (to

insert an amide group), enolate (aldol reaction) and olefins (Wittig reaction). Moreover, benzoxaboroles can be obtained through other methods, starting from *o*-benzylalcohols[22], *o*-bromobenzaldehyde[23], *o*-bromophenylboronate[24], haloarenes (Miyaura borylation)[25], Ru-catalyzed cyclotrimerization of alkynes (schemes not reported).[26]

Benzoxaborines are very similar to benzoxaboroles with one more carbon atom in the oxaborine ring. They showed antiprotozoal and antibacterial activities as β-lactamase inhibitors. Benzoxaborines are obtained in a way similar to benzoxaboroles, starting from protected *o*-bromophenethyl alcohols (Scheme 3).

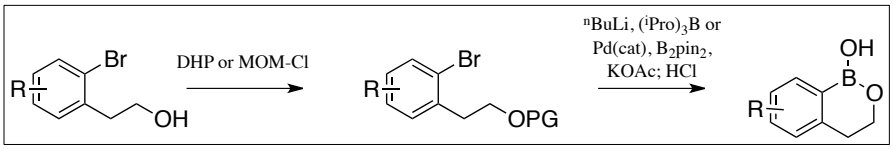

Scheme 3. General synthesis of benzoxaborines

Boron-containing compounds are gaining more and more interest in the field of medicinal chemistry because of their electronic and physicochemical properties which make them really promising in the development of new therapeutic agents. Therefore, there is a proportionally growing interest for the discovery and optimization of synthetic procedures to obtain these compounds.

1.3 *Therapeutic potential of boron-containing compounds*

Boron was commonly considered toxic for a long time and this is the reason for its only recent appearance in medicinal chemistry. This belief came from the presence of boric acid as an ingredient in ant poisons, and from Velcade® (**bortezomib**, Figure 6), the first boron-containing drug on the market used for the treatment of multiple myeloma.

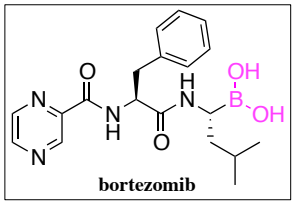

Figure 6. Structure of bortezomib, proteasome inhibitor for the treatment of multiple myeloma.

The toxicity of **bortezomib** is due to its mechanism of action and is not caused by the presence of boron in the molecule. Moreover, boric acid has a LD_{50} of 2660 mg/kg which is very close to that of table salt (NaCl – LD_{50} 3000 mg/kg).[27] As described before, boron is present in nature, in different kind of fruit and vegetables; boric acid is also a component of eye wash and vaginal creams and is used as a buffer for biological assays. Therefore, boron is to be considered not intrinsically toxic and, in fact, it is now present in five approved drugs on the market and in a lot of molecules under investigation in clinical and preclinical trials.

Organoboron compounds can exploit the ability of boron to interact with nucleophiles, forming covalent bonds and to switch between its trigonal – planar structure to the tetrahedral anionic structure. This represents a great potential when boron interacts with active site nucleophiles into biological targets and makes it unique among electrophiles commonly present in drugs. For example, Plescia et al.[28] compared the electrophilicity of the boronic acid with that of an aldehyde group in the reaction with the hydroxyl group of a serine protease. The reactions of both groups result in a stable

tetrahedral intermediate and are effective in inhibiting the enzyme. However, aldehydes are highly reactive and, therefore, they can cause oxidative stress in humans, cytotoxicity and carcinogenic consequences.

Boron is also able to bind diols with high affinity and reversibility: in this way boron can interact with hydroxyl groups of carbohydrates. Carbohydrates are often present on cellular surfaces and are part of signal pathways involved in the development and progression of different diseases.

Another important characteristic is the capacity of ^{10}B to absorb neutrons, delivering lithium nuclei and high-energy α-particles. This ability has been exploited to develop Boron Neutron Capture Therapies (BNCTs) for cancer.[29]

The aim of this chapter is to highlight the most important boron-containing compounds on the market and under investigation for the treatment of different diseases.

1.3.1 Anti-cancer agents

Boronic compounds have been studied for the treatment of cancer addressing numerous targets.

Proteasome inhibitors

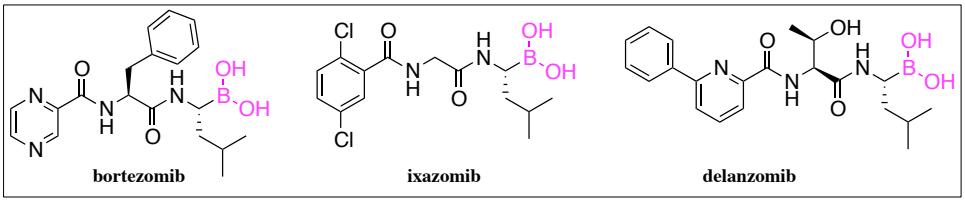

Figure 7. Boronic acid based proteasome inhibitors.

First of all, starting from the discovery of **bortezomib** (Figure 7), research continues for compounds active as proteasome inhibitors. The proteasome is the enzymatic complex present in mammalian cells that recognises ubiquitinated proteins and degrades them to small peptides and amino acids. If this system is inhibited, proteins accumulate in the cell and cause its apoptosis (Figure 8).

Bortezomib was the first boron-containing drug approved by the Food and Drug Administration (FDA) in 2003 for the treatment of multiple myeloma. It was designed starting from the structure of the first synthetic peptide proteasome inhibitor, the aldehyde proteasome inhibitors. Peptidyl aldehydes were not selective inhibitors of proteasome, they were not stable against oxidation and they had poor bioavailability. Therefore, the aldehyde moiety was replaced with a boronic acid, known to be more selective and stable.[30] Indeed, the boronic acid interacts covalently with the hydroxyl group of threonine-1 present at the *N*-terminal of the β-5 subunit of the proteasome.[29]

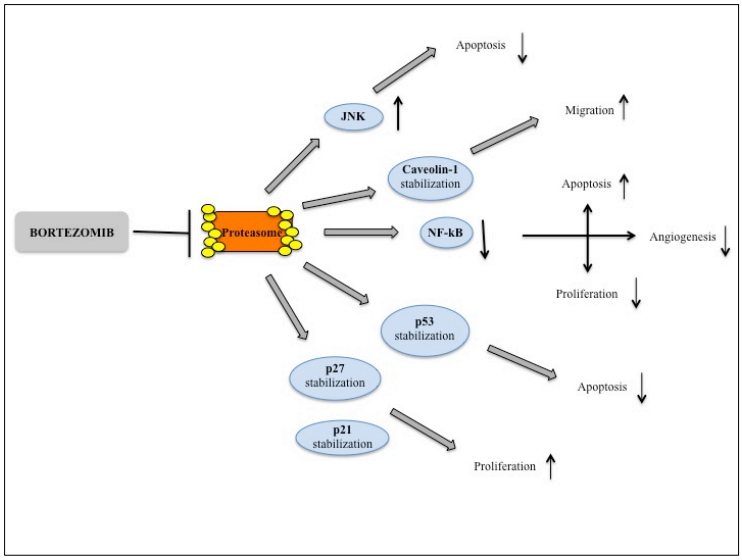

Figure 8. Effects of proteasome inhibition by **bortezomib** (modified from *Expert Opinion on Therapeutic Targets* **2007**, *11:12*, 1571-1586).[31]

Velcade® now is also on phase III clinical trial for the treatment of diffuse large cell B lymphoma and on phase II for the treatment of glioma, graft-versus-host disease, myelodysplastic syndrome, non-small cell lung cancer, Acute Myeloid Leukaemia (AML) and different kinds of lymphoma (https://adis.springer.com/share-url/20211019T165157915). However, **bortezomib** demonstrated also several side effects, such as cardiovascular disorders, nausea and neurologic disorders, not associated with boron itself, but due to the drug's mechanism of action.[27,32] The use of **bortezomib** is also limited by its requirement for parenteral administration (intravenous or subcutaneous).

In 2015, FDA approved **ixazomib** (Ninlaro®, Figure 7) for use in the treatment of multiple myeloma. This orally-bioavailable proteasome inhibitor is a **bortezomib** analogue, but it has physicochemical properties distinct from its lead compound.[33] **Delanzomib** (Figure 7) is another **bortezomib** analogue, proteasome inhibitor, studied for the treatment of multiple myeloma and other cancer diseases. It overcame phase I clinical trials, but it was discontinued after phase II trials due to limited efficacy (https://adis.springer.com/share-url/20211019T165242723).[34]

The problem of peptide boronic acids is their pharmacokinetic profile and the rapid inactivation *in vivo*. Different strategies were tried to overcome these concerns: proline-like boronic acids[35], curcumin analogues[36] and urea-containing peptide boronic acids[37] were synthesized and proved to be good proteasome inhibitors even if none of them is in clinical trials yet.

Dipeptidyl peptidase 8 and 9 (DPP 8/9) inhibitors

Although proteasome inhibition is the most promising target for boron-compounds in the anti-cancer field, more recently, they were described for their activity against different targets. Dipeptidyl peptidase 8 and 9 (DPP8/9) are serine proteases involved in the development of different tumours and deregulated immune responses.

Talabostat or Val-Boro-Pro (Figure 9) is a dipeptidic boronic acid that was firstly discovered as inhibitor of DPP4, a dipeptdyl peptidase, which specifically cleaves two N-terminal amino acids of a peptidic chain, when they are followed by a proline or alanine residue. This enzyme is involved in the deactivation of the glucagon-like peptide 1 (GLP-1), a hormone responsible for the increase of insulin release from the pancreas when blood levels of glucose are enhanced. Therefore, the first target treatment for **talabostat** was diabetes. Then, it was discovered to be not selective and to inhibit also DPP8/9 and fibroblast activating protein (FAP), a protein involved in the structural formation and stabilization of cancer cells, and it was studied as promising anti-cancer agent.[38] This compound reached phase III clinical trials, but it was discontinued because of its limited efficacy and lack of selectivity, which causes low patient tolerance at doses high enough for anti-cancer activity.[39] However, **talabostat** continues to be studied and it is in preclinical phase for AML, and in phase I/II for pancreatic cancer, prostate cancer and solid tumours (https://adis.springer.com/share-url/20211019T165419525).

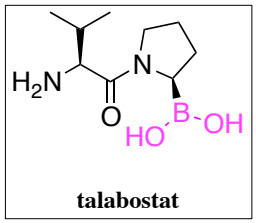

Figure 9. Structure of **talabostat**, inhibitor of DPP4, DPP 8/9 and FAP.

Histone deacetylase I (HDAC I) inhibitors

Histone deacetylase I (HDAC I) is overexpressed in different cancer cell lines and in particular in multiple myeloma cells where its enhanced presence causes resistance to **bortezomib**.[40] Inhibition of HDAC causes histone over-acetylation and consequently inhibition of cell growth and apoptosis. The mechanism of deacetylation is mediated by a zinc ion that coordinates a carbonyl group of the substrate: a tetrahedral transition state is formed and stabilized by the interaction between zinc and oxygen. The tetrahedral anionic form of a boronic acid can play the same role, being stabilized in the active pocket of the enzyme. Some boronic acids with α-amino acidic moieties were tested as HDAC inhibitors and demonstrated to be active in the nanomolar range. In particular Zhou et al. synthesized a series of dual inhibitors of HDAC and proteasome based on the structures of **bortezomib**. Among these, the best inhibitor was compound **1** (Figure 10) with an IC_{50} of 8.98 nM against a **bortezomib** resistant multiple myeloma cell line.[41] However, there are no boronic compounds as HDAC inhibitors in preclinical or clinical phases of development yet.

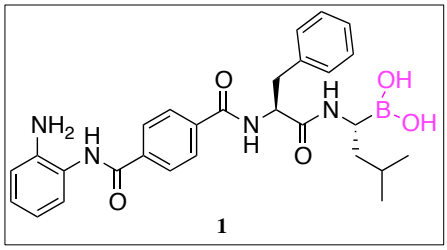

Figure 10. HDAC inhibitor with activity in the nanomolar range (IC_{50} = 8.98 nM).

Boronic acid moiety can improve PK-PD profiles of anti-cancer drugs

Fulvestrant acts as an estrogen-receptor down regulator (SERD) by a competitive bond to the estrogen receptor α (ERα). The problem of fulvestrant for the therapy of breast cancer is the first pass metabolism, which causes its glucuronidation and reduces its bioavailability. The boronic acid

analogue of fulvestrant (**2**, Figure 11) proved to improve the pharmacokinetic profile of this drug, without modifying its pharmacological profile.[42]

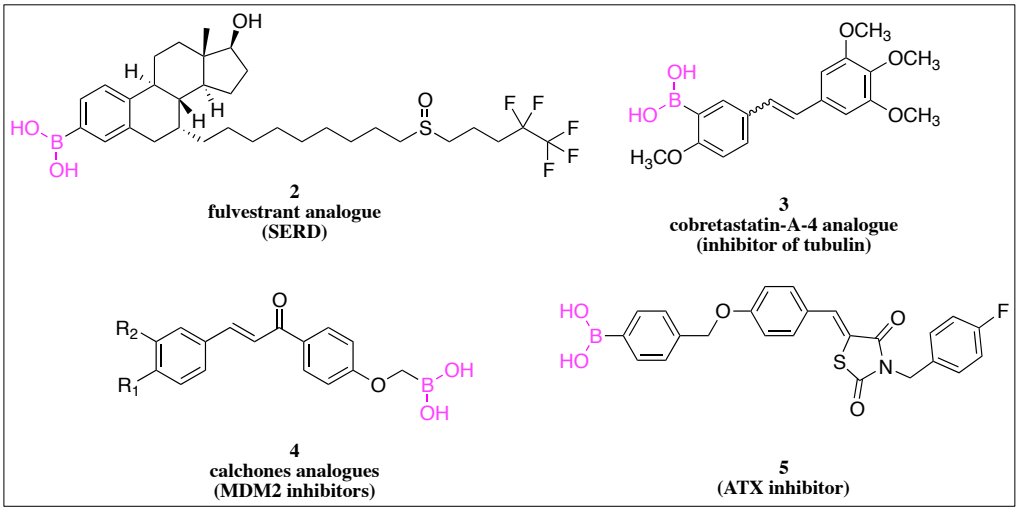

Figure 11. Boronic groups introduced to improve pharmacological skills.

Based on the fact that boronic acids could act as bioisoster for aromatic phenol groups, boron-containing analogues of cobrestatin A-4 where synthesised, improving the solubility of the parental compound. Cobrestatin A-4 binds the colchicine's binding site of tubulin which is involved in cellular division: the boronic acid analogue **3** (Figure 11) enhanced the bioavailability and also the anti-proliferative activity of this anti-cancer drug.[43]

Another case in which the bioisosteric properties of boronic compounds were exploited was the synthesis of analogues of chalcones, a class of anti-cancer agents suffering a lack in selectivity against cancer cells. The boronic analogues of calchones (general structure **4**, Figure 11) were designed to be more selective, targeting the mouse double minute 2 (MDM2) oncoprotein, a negative regulator of p53. The "genome guardian", p53, is a tumour suppressor protein that promotes apoptosis, autophagy, senescence and growth arrest in cancer cells. MDM2 inactivates p53 and, thus, promotes cell proliferation. Boronic-containing calchones demonstrated improved selectivity and activity in breast cancer cells, and also in human colon carcinoma cells with values of inhibition in the low micromolar range.[44]

The autotaxin-lysophosphatidic acid (ATX-LPA) signalling pathway is involved in chronic inflammation, fibrosis and tumour progression. LPA binds different receptors on mammalian cells, thus it is not a good target for anti-cancer therapies, while the inhibition of ATX can be a good strategy. Different boronates has been synthesized to improve the activity of existing compounds, compound **5** (Figure 11) was the best one, demonstrating a 400-fold enhanced inhibition.[45]

Boronic acids as anti-cancer prodrugs

Boronic acids and their esters are oxidized by H_2O_2 and other reactive oxygen species (ROS) that are usually present in cancer cells in higher amounts than healthy cells. This oxidation produces the corresponding alcohol and boric acid, not toxic for human cells.[46] Therefore, in different studies, the hydroxyl group of active compounds has been replaced with a boronic group to achieve the selective release of the drug in cancer cells. Examples of this strategy are new aromatic nitrogen mustards with boronic esters or boronic acids as ROS-based activators[47]; the 10-boronic acid substituted camptothecin prodrug (Figure 12) for targeting release of camptothecin, which inhibits the enzyme topoisomerase I, involved in DNA replication[48] and the boronic acid prodrugs of crizotinib (Figure 12) designed to enhance the cancer cells specificity of this tyrosine kinase inhibitor.[49]

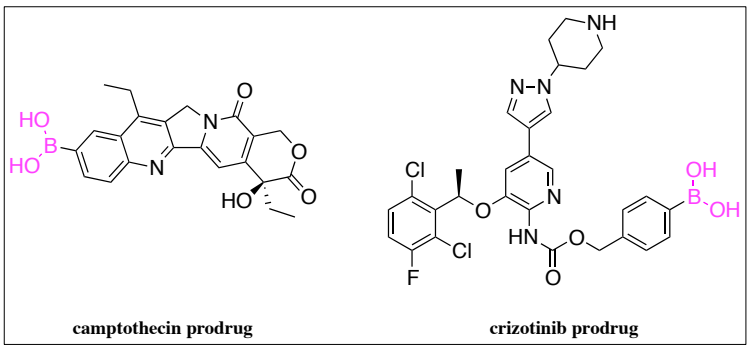

Figure 12. Anti-cancer prodrugs activated by oxidation of the boronic acid to the corresponding hydroxyl group.

1.3.2 Anti-viral agents

Since 1990's the ability of boron compounds to form multiple hydrogen bonds or covalent adducts made them interesting in the treatment of several viral infections.

Hepatitis C Virus (HCV)

Hepatitis C virus (HCV) is responsible for liver infections, leading to liver cirrhosis and hepatocellular carcinomas. The two main targets of HCV are NS3 protease and the non-nucleoside RNA-dependent RNA polymerase, NS5B.

NS3 protease is important for the transcriptional process and the development of a mature HCV: peptide boronates bind covalently the catalytic serine in the active site, forming an anionic tetrahedral intermediate and inhibiting the enzyme. Several peptide boronates were synthesised to target NS3 protease and, in particular, macrocyclic analogues of known protease inhibitors (not shown), such as danoprevir and vaniprevir, were obtained and demonstrated activity in the low to sub-nanomolar range.[50,51]

Other molecules, which demonstrated good activity against HCV are **GSK5852** and **GSK8175** (Figure 13). They are both inhibitors of NS5B polymerase. **GSK5852** showed nanomolar inhibition of NS5B (IC_{50} = 50 nM) and it was able to start clinical trials where it demonstrated a statistically significant

reduction in serum HCV ribonucleic acid (RNA) following a single dose of 420 mg (−1.33 $\log_{10}$ copies/mL) compared with placebo (−0.09 $\log_{10}$ copies/mL) at 24 h postdose in subjects infected with hepatitis C virus. However, it was discontinued because of its short plasma half-life (5h) *in vivo*, probably due to benzylic oxidation.[52]

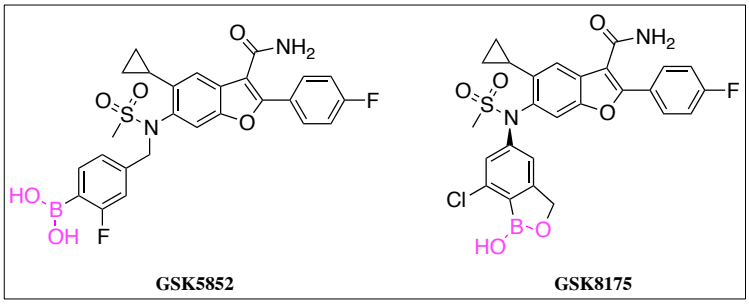

Figure 13. Compounds for the treatment of HCV: they both reached clinical trials, but they were discontinued.

A backup program was initiated to remove metabolic liabilities associated with **GSK5852** and a second-generation of NS5B inhibitors, including **GSK8175** was obtained. **GSK8175** is the *N*-phenylbenzoxaborole analogue of **GSK5852** that showed low *in vivo* clearance across preclinical species and broad-spectrum activity against HCV replicons. In clinical studies, **GSK8175** displayed a 60–63h half-life and a robust decrease in viral RNA levels in HCV-infected patients, thereby validating the hypothesis that reducing benzylic oxidation would improve human pharmacokinetics and lower efficacious doses.[53] As at September 2021, also **GSK8175** was discontinued after it entered phase III clinical trials because it was not so active as expected in human volunteers (https://adis.springer.com/share-url/20211019T165513294). Although no compounds have been able to reach the market yet, mostly because of pharmacokinetic issues, the high level of development reached by GSK compounds demonstrated that boronic acids are potent inhibitors of this class of viruses.

Other viruses

Other viruses targeted by boronic compounds are human immunodeficiency virus type 1 (HIV), Influenza A virus (IAV) and the family of flaviviruses.

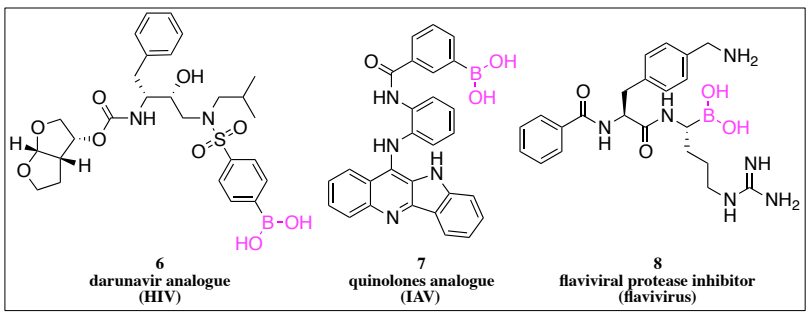

Figure 14. Anti-viral boron-containing compounds active against HIV (**6**), IAV (**7**) or flaviviruses (**8**).

Acquired Immune Deficiency Syndrome (AIDS) appears after the infection by human immunodeficiency virus type 1 (HIV). Boronic compounds have been developed against two targets:

the HIV-1 aspartic acid protease and the Rev Response Element (RRE), an RNA sequence important for virus proliferation. In particular, against HIV-1 aspartic acid protease a boronic acid analogue of darunavir, compound **6** (Figure 14), showed a low-nanomolar inhibition and good cellular activity[54].

Influenza A virus (IAV) is able to enter into the host cell thanks to the interaction between its glycoprotein, neuraminidase (NA), and the glycan receptor on the host cell. The capacity of boron compounds to interact with glycans was exploited to design boronic acid derivatives of quinolones as inhibitors of IA virus (an example is compound **7**, Figure 14). Quinolones have been used as substrates because they are known DNA-binding agents with anti-viral activities: the boronic derivatives demonstrated to prevent the access of viral ribonucleoprotein (RNP) into the nucleus of the host cell, thus, interfering with DNA replication of the virus. Moreover, these compounds are able to inhibit mitogen-activated protein kinase (MAPK) and nuclear factor-kappa B (NF-kB) signalling cascades, which are involved in viral replication too.[55]

A number of infections, like *Zika*, *West Nile* and *Dengue virus infections* are caused by flaviviruses and the inhibition of flaviviral proteases is an important target to treat diseases associated with these infections. Dipeptide boronic acids, such as compound **8** (Figure 14), demonstrated to bind flaviviral proteases 1000 fold better than their amide or carboxylic acid analogues. Besides its high affinity for the target, compound **8** is relatively ineffective in cellular assays, probably because of the high polarity, which makes the passage through cell membranes difficult.[56]

Although several boron-containing compounds have been studied in the field of anti-viral agents, no molecules reached the market and there is a lack of compounds also in clinical phases of development. Therefore, it is important to notice that there are plenty of possibilities for boronic compounds in this field.

1.3.3 Boronic compounds as anti-infective agents with different targets

Targeting leucyl-tRNA synthetases

Among the five boron containing compounds already on the market, one is **tavaborole** (Kerydin®, Figure 15), an anti-fungal agent, approved in 2014 by FDA for the treatment of onychomycosis.[57] It is a 5-fluorobenzoxaborole and acts as fungal leucyl-tRNA synthetase inhibitor.

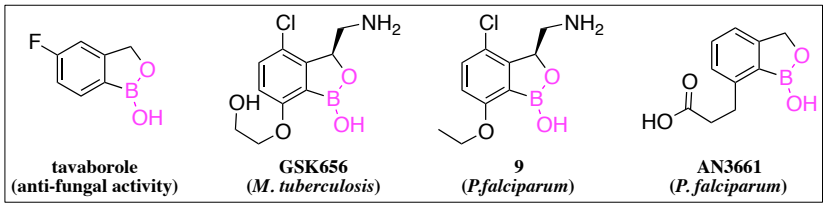

Figure 15. Boronic compounds inhibitors of leucyl-tRNA synthetase.

The amminoacyl- tRNA synthetase family of enzymes is responsible for the attachment of specific amino acids to their corresponding tRNA, an essential passage for protein synthesis. Starting from **tavaborole**, several benzoxaboroles have been reported to be inhibitors of leucyl- tRNA synthetase in a variety of microorganisms: for example, 3-aminomethyl-benzoxaboranes were synthesised to target the leucyl- tRNA synthetase of *Mycobatcterium tuberculosis* and **GSK656** (Figure 15) was identified as clinical candidate, it has completed phase I clinical trials and is now in phase II for the treatment of pulmonary tuberculosis.[58] Compound **9** (Figure 15) was not admitted to clinical trial for the treatment of tuberculosis for its lack of selectivity. This concern was avoided with the introduction of a hydroxyl group on the alkyl chain in **GSK656**. However, **9** showed inhibitory activity against other microorganism and, in particular, it demonstrated nanomolar antimalarial activity against four strains of *P. falciparum*.[59] Starting from compound **9**, Sonoiki et al. synthesised compound **AN3661** (Figure 15) that demonstrated an even greater activity against different strains of *P. falciparum* and it showed orally bioavailability in mice models too.[60]

Targets for the treatment of fungal, mycobacterial and parasitic infections

More targets were addressed, such as BlaC, the single chromosomally encoded β-lactamases in *M. tuberculosis*[61] or the proteasome of *P. falciparum*[62,63] as targets for antimalarial compounds. Several studies concerning boronic compounds for the treatment of fungal, mycobacterial and parasitic infections are ongoing and it is important to notice the involvement of two companies in this field: GlaxoSmithKline and Anacor Pharmaceuticals (acquired by Pfizer in 2016). AN5568 or **acoziborole** (Figure 16) is a benzoxaborole from Anacor Pharmaceuticals in clinical phase II/III for the treatment of African trypanosomiasis[64], which is one field of interest for this company, together with malaria (**AN3661**, Figure 15), cryptosporidiosis (**AN7973**, Figure 16) and infections caused by animal ectoparasites, such as *D.variabilis* (American dog ticks), *C.felis* (cat fleas), *Leishmania* and *Wolbachia*.[65]

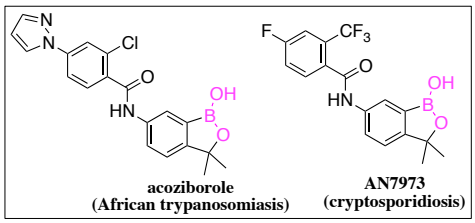

Figure 16. Boronic compounds for the treatment of parasitic infections developed by Anacor Pharmaceuticals.

1.3.4 Boron-containing compounds in the treatment of other important diseases

Crisaborole (Eucrisa®, Figure 17) was approved by the FDA in 2016. It is an inhibitor of phosphodiesterase 4 (PDE4) and cytokine release factor, both involved in inflammatory response. **Crisaborole** is on the market for the treatment of eczema and atopic dermatitis.[66] Phosphodiesterases

(PDEs) are the enzymes responsible for the hydrolysis of cAMP and cGMP in different signalling cascades. Similar to **crisaborole** are compounds **AN2898** and compound **20** (Figure 17). If compared to **crisaborole**, **AN2898** possesses only one extra nitrile on the benzyl ring. Its activity was promising and it completed phase II clinical trials, but Anacor Pharmaceuticals did not list the product on its latest pipeline, so its development appears to be discontinued (https://adis.springer.com/share-url/20211019T165624463). Compound **20** is an analogue of **crisaborole** that demonstrated nanomolar activity against several PDE4 isoforms and showed also to suppress the production of cytokines implicated in atopic dermatitis.[67] This molecule is not in clinical trials yet, but its activity is encouraging.

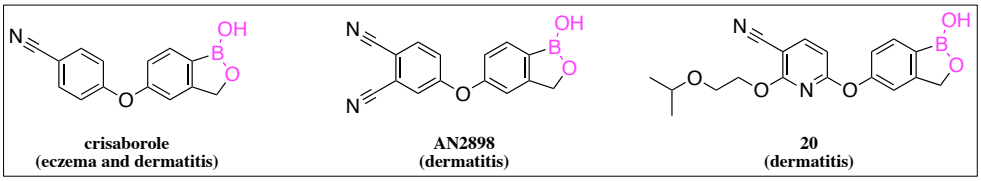

Figure 17. Boronic compounds active as PDE4 inhibitors.

Targets for the anti-inflammatory activity of boronic compounds are also the human neutrophil elastase (HNE)[68], autotaxin (ATX)[69], NLRP3 inflammasome[70], chemokine receptors[71] and carbonic anhydrase (CA).

Some boronic compounds have been developed for the treatment of Alzheimer's disease (cyclic boronic acid derivatives and curcumin analogues)[72], as anticoagulants (boronic acid thrombin inhibitors and inhibitors of factor Xia)[73,74] and for the treatment of diabetes (dipeptide boronic acids as DPP4 inhibitors).[75] Among the DPP4 inhibitors, compound **PHX1149** (dutogliptin, Figure 18) is of particular concern because, although it is no longer under investigation for the treatment of diabetes, it is now in phase II clinical trial for the treatment of myocardial infarction in a combination therapy together with granulocyte-colony stimulating factor (G-CSF).[76]

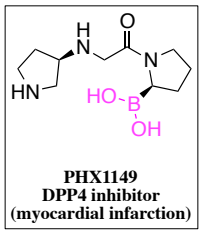

Figure 18. Dutogliptin, boronic compound in phase II clinical trial.

1.3.5 *Anti-bacterial agents*

One of the major challenges for medicinal chemistry nowadays is the development of new anti-bacterial agents, able to overcome the increasing emergence of resistance against existing drugs. Antibiotics are becoming less effective, their ability to treat common infectious diseases is decreasing and this leads to higher medical costs, prolonged hospital stays and increased mortality (Figure 19). Resistance is growing among Gram-positive and Gram-negative bacteria. The WHO priority list[77] assigned as critical *Acinetobacter baumannii*, *Pseudomonas aeruginsa* and *Enterobacteriaceae*, which are part of the big family of "ESKAPE" pathogens (*Enterococcus faecium*, *Staphylococcus aureus*,

Klebsiella pneumonia, *Acinetobacter baumannii*, *Pseudomonas aeruginosa* and *Enterobacter* species). These bacteria currently cause the majority of world-wide hospital infections and "escape" the effects of antibacterial drugs due to high prevalence of cephalosporin and carbapenem resistance and to their ability to survive in adverse environmental conditions.[78]

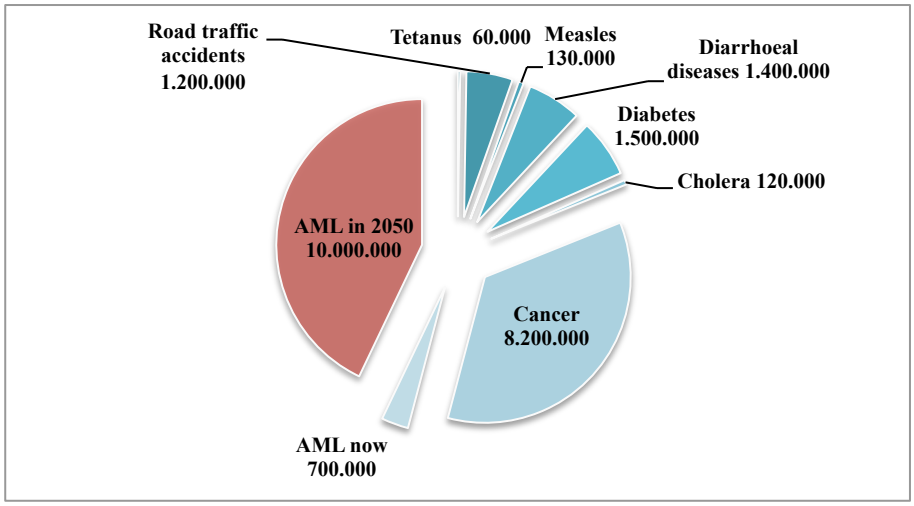

Figure 19. Deaths attributable to anti-microbial resistance (AMR) every year compared to other major causes of death. The estimated number of AMR will increase to 10 million by 2050 (modified from *Advanced Science*, **2020**, *7*, 1901872).[79]

Antibiotics are classified on the basis of their mechanism of action: interference with bacterial cell wall, DNA or RNA synthesis, lysis of bacterial membrane, inhibition of protein synthesis and inhibition of metabolic pathways. Among different classes of antibiotics there are:

(i) *Glycopeptides*, which inhibit peptidoglycan synthesis: vancomycin and second-generation glycopeptides, such as dalbavancin, oritavancin and telavancin.

(ii) *Oxazolidinones*, which inhibit protein synthesis via binding the 50S ribosome: linezolid and tedizolid.

(iii) *Fluoroquinolones*, that directly target DNA gyrase and/or topoisomerase IV, essential in DNA replication: ciprofloxacin, delafloxacin (approved in 2017), finafloxacin and the *new non-fluorinated quinolones* with simultaneous activity on DNA gyrase and topoisomerase IV, ozenoxacin and nemonoxacin.

(iv) *Aminoglycosides*, that inhibits bacterial protein synthesis: the newest is plazomicin (approved in 2018).

(v) *Tetracyclines*, which inhibit protein synthesis: levofloxacin, the last generation eravacycline (approved in 2018) and the aminomethylcycline, omedacycline (approved in 2018).

(vi) β-Lactams, that target Penicillin Binding Proteins (PBPs), responsible of transpeptidase and carboxypeptidase reactions during the building of bacterial cell wall: different classes, such as penicillins, cephalosporins, carbapenem, monobactams.[79]

Boronic acids have been studied since the 19th century for their potential activity in the field of anti-microbials: the electrophilicity of the boron is comparable to that of the carbonyl in the β-lactam ring of β-lactam antibiotics. Therefore, from the beginning, boronic acids were synthesised to either imitate or potentiate the activity of this class of antimicrobials. In fact, it is possible to differentiate two categories of molecules: boronates investigated for their intrinsic antibiotic activity and boronic acids as adjuvant of β-lactam antibiotics to overcome resistance.

1.3.5.1 Intrinsic antibiotic activity

Although the properties of boric acid as anti-bacterial agents have been known since the 19th century[80], recently it was itself newly investigated in clinical trials as a component of creams for the treatment of bacterial vaginosis.[81]

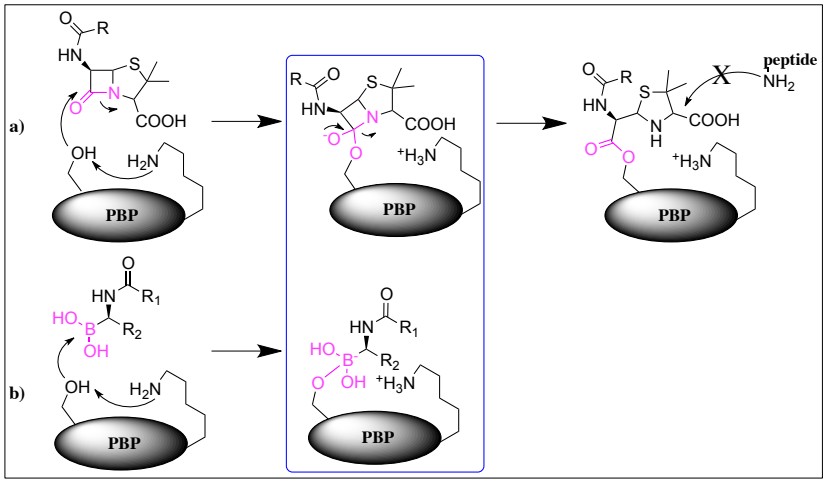

Scheme 4. a) Mechanism of action of β-lactam antibiotics. **b)** Boronic acids as inhibitors of PBPs. The blue square highlights the mimesis between β-lactam and boronic acid in the formation of the acylation transition state.

Different studies have been performed to prove the ability of boronic acids as PBPs inhibitors, even if no compounds reached clinical trials. Peptidyl boronic acid compounds were obtained to provide insights into the mechanism of action of PBPs through crystal structures, but they also demonstrated inhibitory activity in the micromolar range.[82,83]

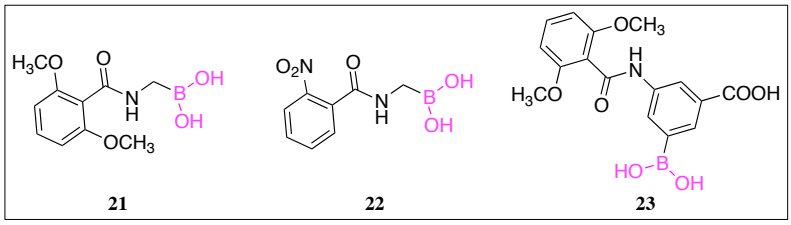

Figure 20. PBPs inhibitors.

Acyclic boronic acids have been synthesised as inhibitors of PBPs for their ability to be attacked by serine residues and, thus, to mimic the transition state of acylation of PBPs (Scheme 4): compounds

21[84] (IC_{50} = 1.3 μM, Figure 20) and **23**[85] (IC_{50} = 20 μM, Figure 20) were identified as promising inhibitors in two different studies. Among analogues of **21**, **22** (Figure 20) was the best one, with improved inhibitory activity (IC_{50} = 0.6 μM).[86] Moreover, a recent crystallographic study reported that different boronic compounds are able to react with PBPs: in particular, boronic acids form a tricovalent complex, while benzoxaboroles form dicovalent complexes as shown in Figure 21.[87]

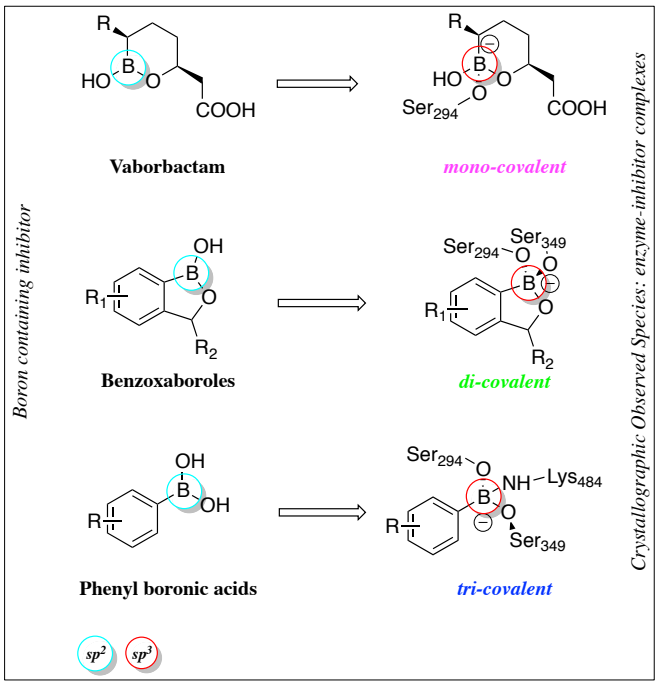

Figure 21. Different complexes between boronic compounds and PBPs (modified from *Journal of Medicinal Chemistry*, **2021**, *64*, 11379-11394).[87]

A series of bis(indolyl)methane boronic acid derivatives was tested for the treatment of methicillin-resistant *Staphilococcus aureus* (MRSA). The boronic acid was attached either to the aryl or to the indole moiety and it was discovered that, when it is on the aryl moiety (as in compound **24**, Figure 22), the activity against MRSA increases and no toxicity is observed. The mechanism of action of these compounds is related to the inhibition of bacterial leucyl-tRna synthetase, which causes, as seen above, the blockage of bacterial protein synthesis. The chelation of glycans in the bacterial cell wall by boronic acid can be implicated in the inhibition too. In 2021, Hao et al. reported the synthesis and crystal structures of a series of benzhydrol-oxaboroles hybrid compounds as inhibitors of leucyl-tRNA synthetase of *Streptococcus pneumonia*. The best compounds of the series were **25** and **26** (Figure 22) with a substituted or a free SH group as substituent on the phenyl ring (**25**, IC_{50} = 0.950 μM; MIC= 6 μg/mL; **26**, IC_{50} = 0.368 μM; MIC= 8 μg/mL).[88]

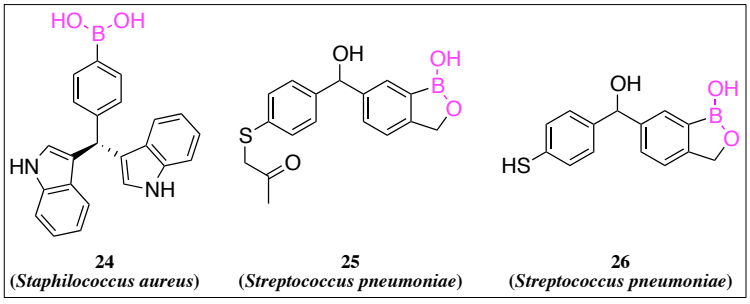

24 (*Staphilococcus aureus*) **25** (*Streptococcus pneumoniae*) **26** (*Streptococcus pneumoniae*)

Figure 22. Leucyl-tRNA inhibitors.

1.3.5.2 Adjuvants of antibiotics

Three factors are involved in the emergence of resistance: (i) overproduction or mutations of PBPs (*i.e* target amplification or target site alterations), which can become less sensitive to antibiotics or more able to deliver the enzyme after the antibiotic attack; (ii) changes in the permeability of the bacterial membrane to antibiotic compounds (decreased influx) or development of efflux pumps which can eliminate the molecule from the bacterial cell; (iii) reduction in drugs uptake or bacterial production of β-lactamases, enzymes able to hydrolyse the β-lactam ring of antibiotics and inactivate them.

Inhibitors of efflux pumps

Boronic acid derivatives can be inhibitors of chromosomal NorA efflux pump of *Staphylococcus aureus*: heterocyclic boronic acids (general structure **27**, Figure 23) demonstrated to be efficient in inhibiting this mechanism of resistance. They have no intrinsic antibacterial activity, so they are supposed to be used in combination with quinolones antibiotics, such as ciprofloxacin or norfloxacin in order to overcome resistance to these molecules.

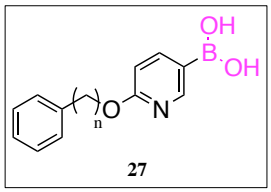

27

Figure 23. Inhibitors of efflux pump.

β-lactamases inhibition

β-Lactamases are bacterial enzymes able to hydrolyse the β-lactam ring of antibiotics and inactivate them. The classification of β-lactamases is made on the basis of their molecular structure and amino acid sequence (Ambler classification[90]) or on functional basis (Bush-Medeiros-Jacoby system[91]). The Ambler classification divides β-lactamases into four classes: class A, C and D enzymes are serine β-lactamases (SBLs), where a serine residue catalyse β-lactams hydrolysis; class B enzymes are metallo-β-lactamases (MBLs) and the hydrolysis is mediated by the presence of one or two zinc ions in the catalytic pocket. The functional classification is based on substrate and inhibitor profiles and includes group 1 cephalosporinases (corresponding to Ambler class C), group 2 inhibitor resistant broad- and extended-spectrum β-lactamases and serine carbapenemases (Ambler class A and D) and group 3

metallo β-lactamases (Ambler class B).[92] Table 1 gives a summary of enzyme types in different classes of β-lactamases with host organisms and substrates.

Table 1. Classification of β-lactamases enzymes (from *Current Clinical Pharmacology*, **2014**, *9*, 27-38 modified).[92,93]

Ambler Class	Bush-Jacoby-Medeiros Group	Active Site	Enzyme Type	Host Organisms	Substrates
A	2a	Serine	PC1	*Enterobacteriaceae*	Ampicillin; cephalotin; penicillins; 3rd-generation cephalosporins
A	2b	Serine	TEM-1; TEM-2; SHV-1		
A	2be	Serine	TEM-3; SHV-2; CTX-M 15; PER-1; VEB-1		
A	2br	Serine	TEM-30; SHV-10		
A	2ber	Serine	TEM-50		
A	2c	Serine	PSE-1; CARB-3		
A	2ce	Serine	RTG-4		
A	2e	Serine	Cep-A	*Enterobacteriaceae* and *Pseudomonas aeruginosa*	Extended-spectrum cephalosporins
A	2f	Serine	KPC-2; IMI-1; SME-1, GES, SFC		Carbapenems
B(1)	3a	Zinc-binding thiol group	IMP-1; VIM-1; CcrA; IND-1, NDM-1	*Enterobacteriaceae, Pseudomonas aeruginosa and Acinetobacter baumannii*	All β-lactams
B(3)	3a	Zinc-binding thiol group	L1; CAU-1; GOB-1; FEZ-1		
B(2)	3b	Zinc-binding thiol group	CphA, Sfh-1		
C	1	Serine	AmpC cephamycinases (AmpC)	*Enterobacter* spp.; *Citrobacter* spp.	Cephamycins; 3rd-generation cephalosporins
C	1	Serine	ACT-1, DHA-1, CMY-2, CMY-10	*Enterobacteriaceae*	Carbapenems
D	2d	Serine	OXA-1; OXA-10	*Enterobacteriaceae* and *Acinetobacter baumannii*	Cloxacillin
D	2de	Serine	OXA-11; OXA-15		Extended-spectrum cephalosporins
D	2df	Serine	OXA-23; OXA-48		Carbapenems

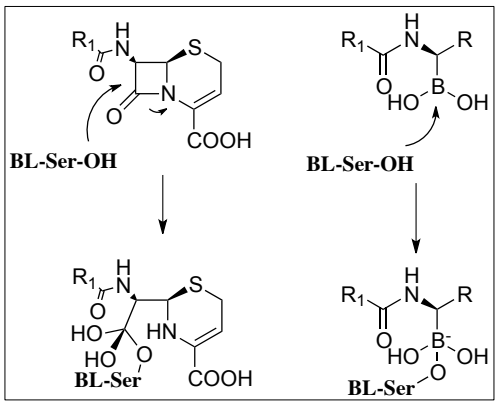

Scheme 5. β-Lactamases attack on β-lactam rings and on boronic acids.

Boronic acid-containing compounds have been widely used in the development of β-lactamase inhibitors: the boron atom is a bioisoster and at the same time it mimics the carbonyl carbon of the β-lactam ring. The catalytic serine of serine β-lactamases attacks the boron atom and a tetrahedral sp^3 intermediate is formed. This intermediate mimics the low energy transition state formed after the attack of the catalytic serine on the β-lactam ring of

antibiotics (Scheme 5). However, in this case de-acylation can't occur and the enzyme is, therefore, inhibited. Because boron-based β-lactamases inhibitors are non β-lactams, bacteria are less able to develop resistance against this kind of inhibitors, although some cases are reported.

The last boronic compound on the market to be cited is **vaborbactam** (Figure 24): in combination with meropenem, it has been approved in 2017 by FDA for the treatment of urinary tract infections. Moreover, it is now in phase III clinical trials for the treatment of pneumonia. Meropenem is a carbapenem, while **vaborbactam** is a monocyclic boronic acid active as β-lactamases inhibitor. It was designed to inhibit *K. pneumonia* carbapenemases (class A), but it demonstrated to be active also against other enzymes (class A and class C): it is, therefore, used for infections caused by several pathogens, such as *Klebsiella spp.*, *Enterobacter spp.*, *Citrobacter spp.*, *E. Coli*. However, **vaborbactam** doesn't inhibit class B and class D β-lactamases and it's not so effective against *A. baumannii* or *P. aeruginosa*. Another limit of **vaborbactam** is that it has less activity in strains that lack a specific porin (needed for drug intake) or that overexpress efflux pumps.[94]

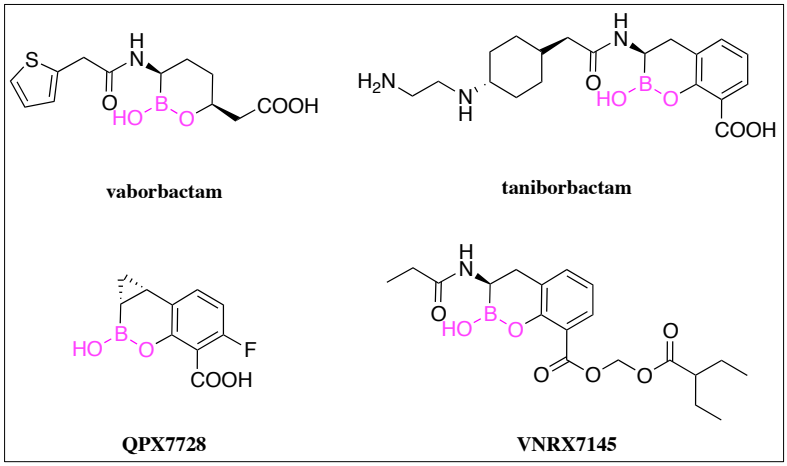

Figure 24. Boronic acids as β-lactamases inhibitors on the market (vaborbactam) or in clinical development.

Three boronic drugs are in clinical development as β-lactamases inhibitors (Figure 24). VNRX-5133 or **taniborbactam** is in phase III clinical trial in combination with cefepime for the treatment of urinary tract infections. It is a bicyclic boronate and it inhibits all classes of β-lactamases, included NDM-1 (IC_{50}= 0.01 μM) and VIM-2 (IC_{50}= 0.0005 μM) MBLs.[95] It is less potent against IMP-1 (IC_{50}= 2.51 μM) and a recent study reported that it is weakly active against B2 MBLs, such as CphA (IC_{50}= 2.51 μM) and it doesn't inhibit B3 (IC_{50} >10 μM) MBLs. Moreover, lower inhibition was observed on OXA-48 class D SBLs (IC_{50}= 2.39 μM).[96] It was discovered after the synthesis of several bicyclic compounds, aiming to improve the ability to overcome the outer membrane of Gram-negative bacteria.[95] This ability is fundamental for β-lactamase inhibitors to be classified as effective therapeutic agents: high-molecular-weight molecules, with clogP < 1 and polar surface area > 150 $Å^2$ have preferred access into Gram-negative bacteria.[97]

QPX7728 is in phase I clinical trial with the general indication of bacterial infections. It is a small bicyclic boronic compound with a spectrum of activity extended to all four classes of β-lactamases and good oral bioavailability. Its K_i values are < 100 nM for all enzymes except IMP-1 (K_i = 220 nM). It was tested in microbiological assays in combination with cefepime, ceftolozane or meropenem and all combinations demonstrated to be effective against *Enterobacteriaceae,* against strains expressing KPC and OXA-48 carbapenemases and against *P. aeruginosa.* Against strains expressing MBLs the best combination was with cefepime, while only meropenem potency demonstrated to be improved in *A. baumannii* strains.[98]

The last compound to enter clinical trials in phase I in 2021 is **VNRX 7145**. It was designed to balance the need for bacterial cell penetration with the attributes necessary for oral absorption in order to obtain an orally bioavailable β-lactamases inhibitor. **VNRX 7145** is a prodrug where the carboxylic group is protected with a 3-pentylacyloxy chain and it demonstrated an oral absolute bioavailability F (%) = 82% in rats and good results also in other animal species.[99]

A long experience against β-lactamases

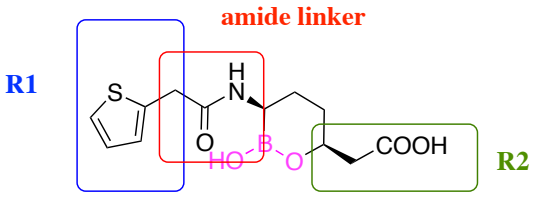

vaborbactam

As described above, **vaborbactam** was the first boronic acid to be approved and to reach the market in 2017. When I joined the research group of prof. Prati for my PhD, his team was working on boronic acids for more than 15 years and the results obtained as β-lactamases transition state inhibitors (BATSIs) contributed to the discovery of this successful compound. In fact, besides the boronic group, in **vaborbactam** there are several other recognition motives: an **R_1** side chain, an **amide linker** and an **R_2** chain. Starting in 2000, Prati and colleagues published several works highlighting the importance and the possible changes of these three elements.

***R1:** starting from β-lactamases substrates*

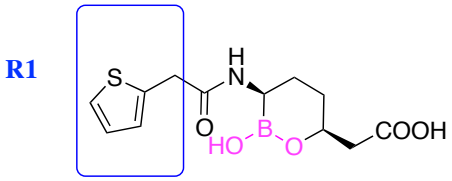

vaborbactam

Starting from acylglycineboronic acids with the same side chains of penicillins and cephalosporins achiral α-amidoboronic acids were tested on TEM-1 and AmpC β-lactamases to measure binding constants and the best compound against both the enzymes was the ceftazidime analogue **LP06** (Figure 26, AmpC K_i = 0.020 μM, TEM-1 K_i = 0.39 μM). **LP06** was further investigated and its crystal structure in complex with AmpC was obtained: the ceftazidime side chain made only few interactions with the enzyme, but if this side chain was removed the activity became 15-fold worse.[100] Even if **LP06** was so potent in this first study, the cephalotin R_1 chain (compound **28**, Figure 25) demonstrated to be the best compromise between contribution to recognition and steric hindrance. Actually, cephalotin R_1 chain is able to interact with different β-lactamases, especially when associated with the *m*-carboxyphenyl R_2 chain (see below). Other substituents were tested during years, but none of them proved to be more useful for the interaction with β-lactamases and, in particular, against class A and class C enzymes.[101,102]

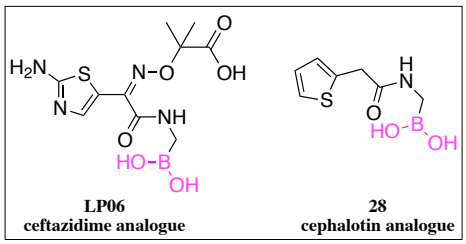

Figure 25. Boronic acids with R_1 chains of β-lactam antibiotics.

R2: a carboxylate important for recognition

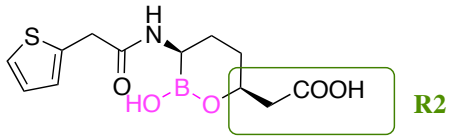

vaborbactam

All β-lactams antibiotics possess a carboxylic at position C3 or C4 (a sulfonic group in monobactams, like aztreonam). Therefore, the importance of a negatively charged group in this position was investigated by the team. Initially, structure-based approach was followed (Figure 26): starting from the cephalotin analogue **28**, the structure of the inhibitor was gradually increased by the stereoselective insertion of a phenyl ring, that was intent to mimic the dihydrotiazine ring of cephalotin (increasing one order of magnitude the affinity) and then the *m*-carboxyphenyl group (**SM23**), where the –COOH group corresponded to the ubiquitous C4 carboxylate in cephalosporins; **SM23** inhibited AmpC β-lactamases with K_i = 1 nM, representing the most potent inhibitor synthesised until that moment.[103]

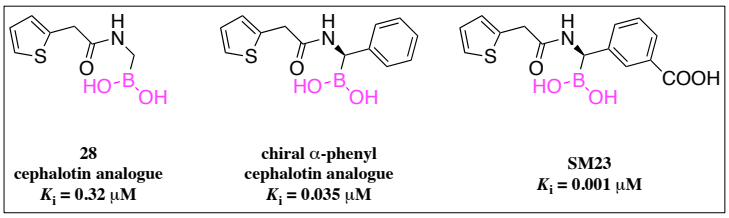

Figure 26. From achiral to chiral *m*-carboxyphenyl substituted boronic acids: improvement in activity.

Against TEM-1 enzymes (class A) **SM23** increased by 100-fold the activity of compound **28** (SM23, K_i = 64 nM)[104] and it demonstrated to be a good inhibitor also against class A CTX-M-9 (K_i = 0.578 μM), CTX-M-14 (K_i =0.423 μM)[105] and SHV-1 (K_i = 0.68 μM).[106] In CTX-M enzymes **SM23** was 10-fold more potent than the corresponding achiral compound **28** (K_i of **28** against CTX-M-9 = 5.5 μM, against CTX-M-14 K_i = 2.8 μM), while against SHV-1 it was 62-fold more potent than **28** (K_i of **28** against SHV-1= 42 μM). When tested against *Acinetobacter* derived cephalosporinases (ADCs), a family of class C β-lactamases responsible for resistance to penicillins, cephalosporins and β-lactam-β-lactamase inhibitor combinations, **SM23** demonstrated the best activity also against these enzymes with K_i = 11 nM.[101]

A series of analogues of **SM23** was synthesised to see if it was possible to increase its activity by interacting with different residues of the enzymes. Two different strategies were applied: 1) the substitution of the carboxylate with the bioisosteric tetrazole (**29a**, Figure 27), a more lipophilic substituent, which should increase the distance between the anionic charge and the phenyl ring; 2) the insertion of different spacers between the carboxylate and the phenyl ring, such as a methylene (**29b**) or a vinyl group (**29c**). Compound **29c** (K_i = 1 nM) was the best inhibitor, but it didn't improve the activity of **SM23**.[107]

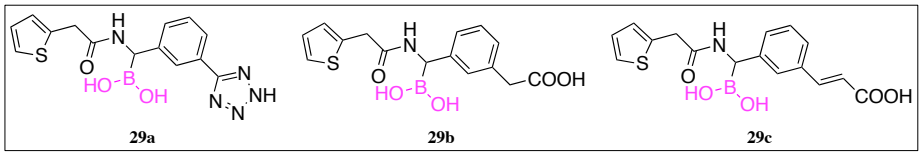

Figure 27. Analogues of **SM23** with different substituent on the phenyl ring.

Finally, **SM23** was used for a molecular modelling study in which the importance of the C3/C4 carboxylate in the recognition of substrates by PDC-3 (*P. aeruginosa* AmpC β-lactamases) enzymes was investigated. The conclusion of this work was that there are several possible binding modes for the recognition of the carboxylate moiety by the enzyme and different residues are involved. In any case, this study showed the inhibitory activity of **SM23** to be in the nanomolar range also against PDC-3 enzymes (K_i = 0.22 μM).[108] All the results obtained with **SM23** are summarized in Table 2.

Table 2. SM23 activity towards class A and C β-lactamases (K_is).

	AmpC	*TEM-1*	*CTX-M-9*	*CTX-M-14*	*SHV-1*	*ADC*	*ADC-7*	*PDC-3*
SM23	0.001 μM	0.064 μM	0.578 μM	0.423 μM	0.68 μM	0.011 μM	0.021 μM	0.22 μM

S02030 (Figure 28) was synthesised as carboxytriazole analogue of **SM23**, where instead of the phenyl there is a triazole ring, more easily synthesised.[109] Indeed, the synthesis of **S02030** exploited the CuAAC click reaction, a synthetic method, which proceeds in mild conditions, with inexpensive reagents and easy isolation of the product. ADC-7 was identified as the target against which **SM23** and **S02030** were tested and compared. In kinetic analysis both compounds had high binding affinity (**SM23**, K_i = 0.021 μM; **S02030**, K_i = 0.044 μM). The lower value for **SM23** was explained by the major distance between the carboxylate group of this compound and Arg340 if compared with **S02030** where the presence of a methylene bridge makes the carboxylate closer to this residue. Arg340 is a residue that distinguishes ADC-7 from other AmpCs, responsible for the recognition of the carboxylate.

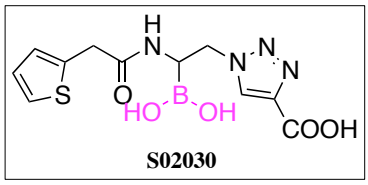

S02030

Figure 28. Boronic acid where the phenyl ring was substituted with a triazole ring.

To elucidate the role of Arg340 and the recognition of carboxylate in ADC-7 a more recent study was conducted with some **S02030** derivatives. This study demonstrated that class C enzymes possess a high degree of plasticity and different residues can take part in recognition and interactions with substrates and inhibitors even if they are not conserved among different enzyme subclasses. The presence of a negative charge in R_2 position improves both enzyme affinity and cell penetration, but a wider choice of R_2 negatively charged groups is allowed.[110] The improvement of affinity obtained with the insertion of a triazole ring revealed the potency of this heterocycle; not only as a phenyl bioisoster, but also for direct interactions it creates with the enzyme catalytic pocket. Indeed, triazoles are frequently present in drug molecules (for example in tazobactam, a classical β-lactamases inhibitor on the market) thanks to their stability to acid and base hydrolysis and reductive and oxidative conditions, as well as metabolic degradation. The results obtained with **S02030** are summarized in Table 3.

Table 3. Activity of **S02030** on different β-lactamases (K_is).

	ADC-7	*CTX-M-96*	*SHV-1*	*KPC-2*	*PDC-3*	*P99*
S02030	0.044 μM	0.002 μM	0.130 μM	0.080 μM	0.004 μM	0.023 μM

Amide linker: interesting changes

amide linker

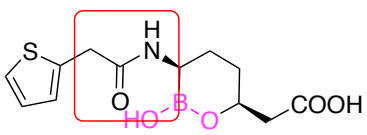

vaborbactam

The α-acylamido group, that is meant to mimic the amido group in position 6/7 of penicillins/cefalosporins, is crucial for β-lactamases recognition, displaying several interactions with highly conserved aminoacidic residues, such as, for instance, Gln120 and Asn237 in Ampc.

Inspired by the work of Tan et al.[111] the α-acylamido chain was replaced with a sulphonamide chain and 10 compounds were synthesised and tested against AmpC β-lactamases (general structure Figure 29). Both achiral and chiral compounds bearing a phenyl or a carboxyphenyl R_2 chain were synthesised and all of them retained activity as inhibitors of β-lactamases, but the structure-activity relationship was quite different for these compounds when compared to the acylamido analogues. Indeed, chiral compounds demonstrated less potency than achiral sulphonamides. The best compound of the series was the achiral compound **30a** (Figure 29), which showed inhibitory activity in the nanomolar range (K_i = 0.025 μM).[112] Starting from these results a fragment-guide design of achiral sulphonamide containing boronic acids permitted to identify subnanomolar inhibitors of AmpC. Compound **30b** (Figure 29), where the carboxylate is in *meta*- instead of the *orto*- position, showed a 10-fold increased activity (K_i = 0.0012 μM). The most potent inhibitor was **30c** (Figure 29) with a K_i = 0.05 nM.[113]

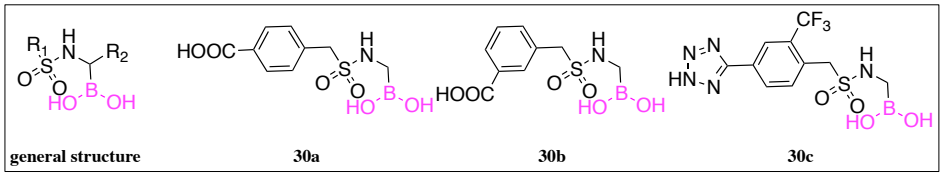

Figure 29. Sulphonamidoboronic acids where the α-amide chain commonly present in antibiotics was substituted with the bioisosteric sulphonamide.

The 1,2,3-triazole ring is also described as a non-classical amide bioisoster, and was therefore considered for the bio-isosteric substitution in glycylboronic inhibitors. Similarly to the amide group the triazole is planar, displays a similar dipole moment, hydrogen bond forming capabilities and almost the same size as the amide group. On the other hand, it is a cycle, less flexible than the amide chain and it is also more stable against oxidation and hydrolysis. For these reasons the feasibility to synthesise α-triazolyl boronic acids bearing a triazole instead of the classical α-amide chain of antibiotics was successfully tested and a little library of [(1,2,3-triazol-1-yl)-methyl]-boronic acid was synthesised (Scheme 6).[114]

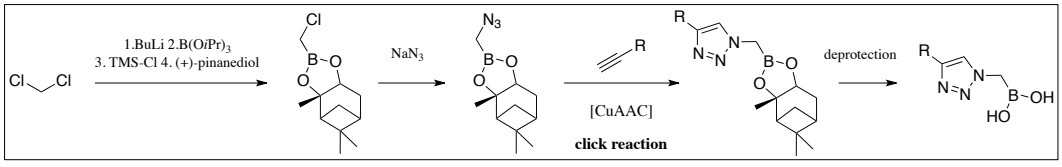

Scheme 6. Synthesis of α-triazolylboronic acids. CuAAC conditions: $CuSO_4$, NaAsc, *t*ButOH/H_2O 1:1

In 2016, an important study on class A β-lactamases was published in which, starting from a reference compound with only an amide group, three regions of the molecule were modified: R_1, R_2 and the amide (Figure 30).[102] The compounds were tested against KPC and SHV-1 enzymes. The addition of

the cephalotin R_1 side chain (**28**) improved the activity 200-fold for KPC and 3-fold for SHV-1. Chiral cephalotin analogues with an amide group and various R_2 chains demonstrated greater affinity for both the enzymes, with some of them in the nanomolar range: the most potent inhibitors were **31**, **32**, **S02030** and **33**. The substitution of the tiophene ring with a phenyl ring didn't affect the activity (compound **34** is very similar to compound **31**) and when the amide group was replaced with a urea (**35**) or a thiourea (**36**) a loss of activity was observed. The activity of **S02030** was confirmed thanks to the crystal structure of the inhibitor in complex with both the enzymes.[115]

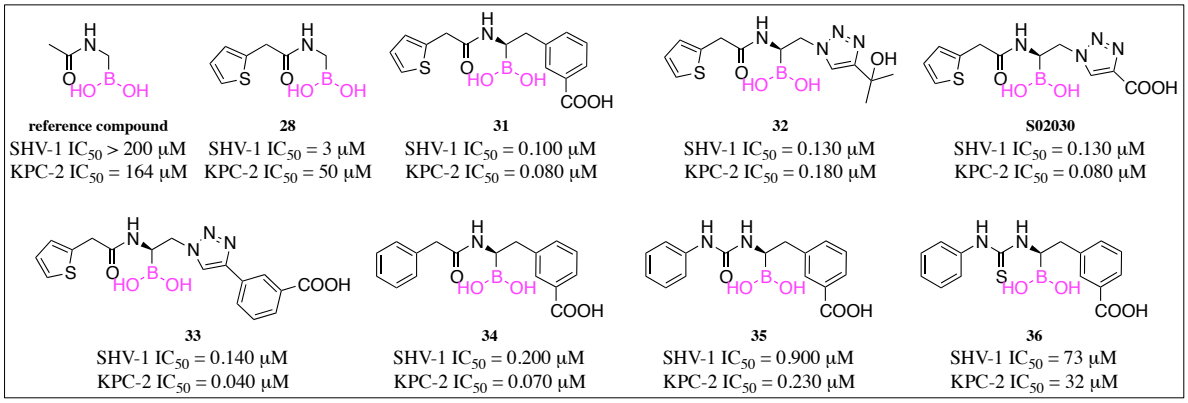

Figure 30. Boronic acids tested on class A β-lactamases.

In conclusion, when I joined Prof. Fabio Prati's lab in 2019, a lot had already been done in order to improve the activity of boronic acids as β-lactamases inhibitors and two main compounds had become leads for further development: **SM23** and **S02030**. Several studies confirmed the potency of both these compounds as inhibitors against class A and class C β-lactamases, but there was a lack of activity against other classes of enzymes. At the moment I started my doctoral project, none of the compounds synthesised by the group had proved activity against class B and/or class D β-lactamases. That was my starting point.

References

(1) Argust, P. Distribution of Boron in the Environment. *Biol. Trace Elem. Res.* **1998**, *66* (1–3), 131–143. https://doi.org/10.1007/BF02783133.

(2) Benderdour, M.; Bui-Van, T.; Dicko, A.; Belleville, F. In Vivo and in Vitro Effects of Boron and Boronated Compounds. *J. Trace Elem. Med. Biol.* **1998**, *12* (1), 2–7. https://doi.org/10.1016/S0946-672X(98)80014-X.

(3) Mäder, P. Boron in Medicinal Chemistry: Powerful, but Neglected. *Chimia (Aarau).* **2019**, *73* (7–8), 637–638. https://doi.org/10.2533/chimia.2019.637.

(4) Plescia, J.; Moitessier, N. Design and Discovery of Boronic Acid Drugs. *Eur. J. Med. Chem.* **2020**, *195*, 112270. https://doi.org/10.1016/j.ejmech.2020.112270.

(5) Chen, T. S. S.; Chang, C.; Floss, H. g. Biosynthesis of Boromycin. *J. Org. Chem.* **1981**, *46* (13), 2661–2665.

(6) Brenchley, W. E. The Effect of Boron on Plant Growth. *Br. Med. J.* **1924**, *2* (3314), 9–10. https://doi.org/10.1136/bmj.2.3314.9.

(7) Howe, P. D. A Review of Boron Effects in the Environment. *Biol. Trace Elem. Res.* **1998**, *66* (1–3), 153–166. https://doi.org/10.1007/BF02783135.

(8) Geneva: World Health Organization. *Trace Elements in Human Nutrition and Health*; 1967.

(9) Diaz, D. B.; Yudin, A. K. The Versatility of Boron in Biological Target Engagement. *Nat. Chem.* **2017**, *9* (8), 731–742. https://doi.org/10.1038/NCHEM.2814.

(10) Hall, D. G. *Structure, Properties, and Preparation of Boronic Acid Derivatives. Overview of Their Reactions and Applications*; 2006. https://doi.org/10.1002/3527606548.ch1.

(11) Beenen, M. A.; An, C.; Ellman, J. A. Asymmetric Copper-Catalyzed Synthesis of α-Amino Boronate Esters from N-Tert-Butanesulfinyl Aldimines. *J. Am. Chem. Soc.* **2008**, *130* (22), 6910–6911. https://doi.org/10.1021/ja800829y.

(12) Buesking, A. W.; Bacauanu, V.; Cai, I.; Ellman, J. A. Asymmetric Synthesis of Protected α-Amino Boronic Acid Derivatives with an Air- and Moisture-Stable Cu(II) Catalyst. *J. Org. Chem.* **2014**, *79* (8), 3671–3677. https://doi.org/10.1021/jo500300t.

(13) Li, C.; Wang, J.; Barton, L. M.; Yu, S.; Tian, M.; Peters, D. S.; Kumar, M.; Yu, A. W.; Johnson, K. A.; Chatterjee, A. K.; et al. Decarboxylative Borylation. *Science (80-.).* **2017**, *356* (6342). https://doi.org/10.1126/science.aam7355.

(14) Wang, J.; Shang, M.; Lundberg, H.; Feu, K. S.; Hecker, S. J.; Qin, T.; Blackmond, D. G.; Baran, P. S. Cu-Catalyzed Decarboxylative Borylation. *ACS Catal.* **2018**, *8* (10), 9537–9542. https://doi.org/10.1021/acscatal.8b02928.

(15) Matteson, D. S.; Sadhu, K. M. No Title. *Organometallics 3* **1984**, 614–618.

(16) Matteson, D. S.; Majumdar, D. No Title. *Organometallics 2* **1983**, 1529–1535.

(17) Gorovoy, A. S.; Gozhina, O. V.; Svendsen, J. S.; Domorad, A. A.; Tetz, G. V.; Tetz, V. V.; Lejon, T. Boron-Containing Peptidomimetics - A Novel Class of Selective Anti-Tubercular Drugs. *Chem. Biol. Drug Des.* **2013**, *81* (3), 408–413. https://doi.org/10.1111/cbdd.12091.

(18) Gorovoy, A. S.; Gozhina, O.; Svendsen, J.-S.; Tetz, G. V; Domorad, A.; Tetz, V. V; Lejon, T. Syntheses and Anti-

Tubercular Activity of β-Substituted and A,β-Disubstituted Peptidyl β-Aminoboronates and Boronic Acids. *J. Pept. Sci.* **2013**, *19* (10), 613–618. https://doi.org/https://doi.org/10.1002/psc.2537.

(19) Torssell, K. Arylboronic Acids III. Bromination of Tolylboronic Acids according to Wohl-Ziegler. *ArK Kemi* **1957**, *10*, 507–511.

(20) Ji, L.; Zhou, H. Recent Developments in the Synthesis of Bioactive Boron-Containing Compounds. *Tetrahedron Lett.* **2021**, No. xxxx, 153411. https://doi.org/10.1016/j.tetlet.2021.153411.

(21) Adamczyk-Woźniak, A.; Madura, I.; Velders, A. H.; Sporzyński, A. Diverse Reactivity of 2-Formylphenylboronic Acid with Secondary Amines: Synthesis of 3-Amino-Substituted Benzoxaboroles. *Tetrahedron Lett.* **2010**, *51* (47), 6181–6185. https://doi.org/https://doi.org/10.1016/j.tetlet.2010.09.091.

(22) Adamczyk-Woźniak, A.; Borys, K. M.; Sporzyński, A. Recent Developments in the Chemistry and Biological Applications of Benzoxaboroles. *Chem. Rev.* **2015**, *115* (11), 5224–5247. https://doi.org/10.1021/cr500642d.

(23) Wienhold, F.; Claes, D.; Graczyk, K.; Maison, W. Synthesis of Functionalized Benzoxaboroles for the Construction of Boronolectins. *Synthesis (Stuttg)*. **2011**, *24*, 4059–4067.

(24) Dąbrowski, M.; Kurach, P.; Luliński, S.; Serwatowski, J. An Ortho-Lithiated Derivative of Protected Phenylboronic Acid: An Approach to Ortho-Functionalized Arylboronic Acids and 1,3-Dihydro-1-hydroxybenzo[c][2,1]oxaboroles. *Appl. Organomet. Chem.* **2007**, *21* (4), 234–238. https://doi.org/https://doi.org/10.1002/aoc.1217.

(25) Ishiyama, T.; Murata, M.; Miyaura, N. Palladium(0)-Catalyzed Cross-Coupling Reaction of Alkoxydiboron with Haloarenes: A Direct Procedure for Arylboronic Esters. *J. Org. Chem.* **1995**, *60* (23), 7508–7510. https://doi.org/10.1021/jo00128a024.

(26) Yamamoto, Y.; Ishii, J.; Nishiyama, H.; Itoh, K. Cp*RuCl-Catalyzed Formal Intermolecular Cyclotrimerization of Three Unsymmetrical Alkynes through a Boron Temporary Tether: Regioselective Four-Component Coupling Synthesis of Phthalides. *J. Am. Chem. Soc.* **2005**, *127* (26), 9625–9631. https://doi.org/10.1021/ja051377d.

(27) Baker, S. J.; Ding, C. Z.; Akama, T.; Zhang, Y. K.; Hernandez, V.; Xia, Y. Therapeutic Potential of Boron-Containing Compounds. *Future Med. Chem.* **2009**, *1* (7), 1275–1288. https://doi.org/10.4155/fmc.09.71.

(28) Plescia, J.; Moitessier, N. Design and Discovery of Boronic Acid Drugs. *Eur. J. Med. Chem.* **2020**, *195*. https://doi.org/10.1016/j.ejmech.2020.112270.

(29) Draganov, A.; Wang, D.; Wang, B. The Future of Boron in Medicinal Chemistry: Therapeutic and Diagnostic Applications. In *Topics in Medicinal Chemistry*; Springer-Verlag Berlin Heidelberg 2014, 2014. https://doi.org/10.1007/7355_2014_65.

(30) ADAMS, J.; BEHNKE, M.; CHEN, S.; CRUICKSHANK, A. A.; DICK, L. R.; GRENIER, L.; KLUNDER, J. M.; MA, Y.-T.; PLAMONDON, L.; STEIN, R. L. Potent and Selective Inhibitors of the Proteasome: Dipeptidyl Boronic Acids. *Bioorganic Med. Chem. Lett.* **1998**, *8*, 333–338. https://doi.org/10.1002/chin.199821191.

(31) Russo, A.; Fratto, M. E.; Bazan, V.; Schiró, V.; Agnese, V.; Cicero, G.; Vincenzi, B.; Tonini, G.; Santini, D. Targeting Apoptosis in Solid Tumors: The Role of Bortezomib from Preclinical to Clinical Evidence. *Expert Opin. Ther. Targets* **2007**, *11* (12), 1571–1586. https://doi.org/10.1517/14728222.11.12.1571.

(32) Richardson, P. G.; Sonneveld, P.; Schuster, M. W.; Stadtmauer, E. A.; Facon, T.; Harousseau, J. L.; Ben-Yehuda, D.; Lonial, S.; Goldschmidt, H.; Reece, D.; et al. Reversibility of Symptomatic Peripheral Neuropathy with Bortezomib in the

Phase III APEX Trial in Relapsed Multiple Myeloma: Impact of a Dose-Modification Guideline. *Br. J. Haematol.* **2009**, *144* (6), 895–903. https://doi.org/10.1111/j.1365-2141.2008.07573.x.

(33) Shirley, M. Ixazomib: First Global Approval. *Drugs* **2016**, *76* (3), 405–411. https://doi.org/10.1007/s40265-016-0548-5.

(34) Vogl, D. T.; Martin, T. G.; Vij, R.; Hari, P.; Mikhael, J. R.; Siegel, D.; Wu, K. L.; Delforge, M.; Gasparetto, C. Phase I/II Study of the Novel Proteasome Inhibitor Delanzomib (CEP-18770) for Relapsed and Refractory Multiple Myeloma. *Leuk. Lymphoma* **2017**, *58* (8), 1872–1879. https://doi.org/10.1080/10428194.2016.1263842.

(35) Han, L.; Wen, Y.; Li, R.; Xu, B.; Ge, Z.; Wang, X.; Cheng, T.; Cui, J.; Li, R. Synthesis and Biological Activity of Peptide Proline-Boronic Acids as Proteasome Inhibitors. *Bioorg. Med. Chem.* **2017**, *25* (15), 4031–4044. https://doi.org/https://doi.org/10.1016/j.bmc.2017.05.049.

(36) Zhang, W.; Bai, H.; Han, L.; Zhang, H.; Xu, B.; Cui, J.; Wang, X.; Ge, Z.; Li, R. Synthesis and Biological Evaluation of Curcumin Derivatives Modified with α-Amino Boronic Acid as Proteasome Inhibitors. *Bioorg. Med. Chem. Lett.* **2018**, *28* (14), 2459–2464. https://doi.org/https://doi.org/10.1016/j.bmcl.2018.06.004.

(37) Han, L.-Q.; Yuan, X.; Wu, X.-Y.; Li, R.-D.; Xu, B.; Cheng, Q.; Liu, Z.-M.; Zhou, T.-Y.; An, H.-Y.; Wang, X.; et al. Urea-Containing Peptide Boronic Acids as Potent Proteasome Inhibitors. *Eur. J. Med. Chem.* **2017**, *125*, 925–939. https://doi.org/https://doi.org/10.1016/j.ejmech.2016.10.023.

(38) Cunningham, C. C. Talabostat. *Expert Opin. Investig. Drugs* **2007**, *16* (9), 1459–1465. https://doi.org/10.1517/13543784.16.9.1459.

(39) Poplawski, S. E.; Lai, J. H.; Sanford, D. G.; Sudmeier James L., W. W.; Bachovchin, W. W. Pro-Soft Val-boroPro: A Strategy for Enhancing in Vivo Performance of Boronic Acid Inhibitors of Serine Proteases. *J. Med. Chem.* **2011**, *54* (7), 2022–2028. https://doi.org/10.1021/jm100972f.

(40) Kikuchi, J.; Wada, T.; Shimizu, R.; Izumi, T.; Akutsu, M.; Mitsunaga, K.; Noborio-Hatano, K.; Nobuyoshi, M.; Ozawa, K.; Kano, Y.; et al. Histone Deacetylases Are Critical Targets of Bortezomib-Induced Cytotoxicity in Multiple Myeloma. *Blood* **2010**, *116* (3), 406–417. https://doi.org/10.1182/blood-2009-07-235663.

(41) Zhou, Y.; Liu, X.; Xue, J.; Liu, L.; Liang, T.; Li, W.; Yang, X.; Hou, X.; Fang, H. Discovery of Peptide Boronate Derivatives as Histone Deacetylase and Proteasome Dual Inhibitors for Overcoming Bortezomib Resistance of Multiple Myeloma. *J. Med. Chem.* **2020**, *63* (9), 4701–4715. https://doi.org/10.1021/acs.jmedchem.9b02161.

(42) Liu, J.; Zheng, S.; Akerstrom, V. L.; Yuan, C.; Ma, Y.; Zhong, Q.; Zhang, C.; Zhang, Q.; Guo, S.; Ma, P.; et al. Fulvestrant-3 Boronic Acid (ZB716): An Orally Bioavailable Selective Estrogen Receptor Downregulator (SERD). *J. Med. Chem.* **2016**, *59* (17), 8134–8140. https://doi.org/10.1021/acs.jmedchem.6b00753.

(43) Kong, Y.; Grembecka, J.; Edler, M. C.; Hamel, E.; Mooberry, S. L.; Sabat, M.; Rieger, J.; Brown, M. L. Structure-Based Discovery of a Boronic Acid Bioisostere of Combretastatin A-4. *Chem. Biol.* **2005**, *12* (9), 1007–1014. https://doi.org/https://doi.org/10.1016/j.chembiol.2005.06.016.

(44) Kumar, S. K.; Hager, E.; Pettit, C.; Gurulingappa, H.; Davidson, N. E.; Khan, S. R. Design, Synthesis, and Evaluation of Novel Boronic-Chalcone Derivatives as Antitumor Agents. *J. Med. Chem.* **2003**, *46* (14), 2813–2815. https://doi.org/10.1021/jm030213+.

(45) Albers, H. M. H. G.; van Meeteren, L. A.; Egan, D. A.; van Tilburg, E. W.; Moolenaar, W. H.; Ovaa, H. Discovery and Optimization of Boronic Acid Based Inhibitors of Autotaxin. *J. Med. Chem.* **2010**, *53* (13), 4958–4967.

https://doi.org/10.1021/jm1005012.

(46) Peiró Cadahía, J.; Previtali, V.; Troelsen, N. S.; Clausen, M. H. Prodrug Strategies for Targeted Therapy Triggered by Reactive Oxygen Species. *Medchemcomm* **2019**, *10* (9), 1531–1549. https://doi.org/10.1039/C9MD00169G.

(47) Chen, W.; Balakrishnan, K.; Kuang, Y.; Han, Y.; Fu, M.; Gandhi, V.; Peng, X. Reactive Oxygen Species (ROS) Inducible DNA Cross-Linking Agents and Their Effect on Cancer Cells and Normal Lymphocytes. *J. Med. Chem.* **2014**, *57* (11), 4498–4510. https://doi.org/10.1021/jm401349g.

(48) Wang, L.; Xie, S.; Ma, L.; Chen, Y.; Lu, W. 10-Boronic Acid Substituted Camptothecin as Prodrug of SN-38. *Eur. J. Med. Chem.* **2016**, *116*, 84–89. https://doi.org/https://doi.org/10.1016/j.ejmech.2016.03.063.

(49) Bielec, B.; Poetsch, I.; Ahmed, E.; Heffeter, P.; Keppler, B. K.; Kowol, C. R. Reactive Oxygen Species (ROS)-Sensitive Prodrugs of the Tyrosine Kinase Inhibitor Crizotinib. *Molecules* . 2020. https://doi.org/10.3390/molecules25051149.

(50) Li, X.; Zhang, Y.-K.; Liu, Y.; Ding, C. Z.; Li, Q.; Zhou, Y.; Plattner, J. J.; Baker, S. J.; Qian, X.; Fan, D.; et al. Synthesis and Evaluation of Novel α-Amino Cyclic Boronates as Inhibitors of HCV NS3 Protease. *Bioorg. Med. Chem. Lett.* **2010**, *20* (12), 3550–3556. https://doi.org/https://doi.org/10.1016/j.bmcl.2010.04.129.

(51) Li, X.; Zhang, Y.-K.; Liu, Y.; Ding, C. Z.; Zhou, Y.; Li, Q.; Plattner, J. J.; Baker, S. J.; Zhang, S.; Kazmierski, W. M.; et al. Novel Macrocyclic HCV NS3 Protease Inhibitors Derived from α-Amino Cyclic Boronates. *Bioorg. Med. Chem. Lett.* **2010**, *20* (19), 5695–5700. https://doi.org/https://doi.org/10.1016/j.bmcl.2010.08.022.

(52) Wilfret, D. A.; Walker, J.; Voitenleitner, C.; Baptiste-Brown, S.; Lovern, M.; Kim, J.; Adkison, K.; Shotwell, B.; Mathis, A.; Moss, L.; et al. A Randomized, Double Blind, Dose Escalation, First Time in Human Study to Assess the Safety, Tolerability, Pharmacokinetics, and Antiviral Activity of Single Doses of GSK2485852 in Chronically Infected Hepatitis C Subjects. *Clin. Pharmacol. Drug Dev.* **2014**, *3* (6), 439–448. https://doi.org/https://doi.org/10.1002/cpdd.142.

(53) Chong, P. Y.; Shotwell, J. B.; Miller, J.; Price, D. J.; Maynard, A.; Voitenleitner, C.; Mathis, A.; Williams, S.; Pouliot, J. J.; Creech, K.; et al. Design of N-Benzoxaborole Benzofuran GSK8175—Optimization of Human Pharmacokinetics Inspired by Metabolites of a Failed Clinical HCV Inhibitor. *J. Med. Chem.* **2019**, *62* (7), 3254–3267. https://doi.org/10.1021/acs.jmedchem.8b01719.

(54) Ghosh, A. K.; Xia, Z.; Kovela, S.; Robinson, W. L.; Johnson, M. E.; Kneller, D. W.; Wang, Y.-F.; Aoki, M.; Takamatsu, Y.; Weber, I. T.; et al. Potent HIV-1 Protease Inhibitors Containing Carboxylic and Boronic Acids: Effect on Enzyme Inhibition and Antiviral Activity and Protein-Ligand X-Ray Structural Studies. *ChemMedChem* **2019**, *14* (21), 1863–1872. https://doi.org/https://doi.org/10.1002/cmdc.201900508.

(55) Wang, W.; Yin, R.; Zhang, M.; Yu, R.; Hao, C.; Zhang, L.; Jiang, T. Boronic Acid Modifications Enhance the Anti-Influenza A Virus Activities of Novel Quindoline Derivatives. *J. Med. Chem.* **2017**, *60* (7), 2840–2852. https://doi.org/10.1021/acs.jmedchem.6b00326.

(56) Nitsche, C.; Zhang, L.; Weigel, L. F.; Schilz, J.; Graf, D.; Bartenschlager, R.; Hilgenfeld, R.; Klein, C. D. Peptide-Boronic Acid Inhibitors of Flaviviral Proteases: Medicinal Chemistry and Structural Biology. *J. Med. Chem.* **2017**, *60* (1), 511–516. https://doi.org/10.1021/acs.jmedchem.6b01021.

(57) Markham, A. Tavaborole: First Global Approval. *Drugs* **2014**, *74* (13), 1555–1558. https://doi.org/10.1007/s40265-014-0276-7.

(58) Li, X.; Hernandez, V.; Rock, F. L.; Choi, W.; Mak, Y. S. L.; Mohan, M.; Mao, W.; Zhou, Y.; Easom, E. E.; Plattner, J. J.; et

al. Discovery of a Potent and Specific M. Tuberculosis Leucyl-tRNA Synthetase Inhibitor: (S)-3-(Aminomethyl)-4-Chloro-7-(2-hydroxyethoxy)benzo[c][1,2]oxaborol-1(3H)-Ol (GSK656). *J. Med. Chem.* **2017**, *60* (19), 8011–8026. https://doi.org/10.1021/acs.jmedchem.7b00631.

(59) Sonoiki, E.; Palencia, A.; Guo, D.; Ahyong, V.; Dong, C.; Li, X.; Hernandez, V. S.; Zhang, Y.-K.; Choi, W.; Gut, J. Antimalarial Benzoxaboroles Target Plasmodium Falciparum Leucyl-tRNA Synthetase. *Antimicrob. Agents Chemother.* **2016**, *60* (8), 4886–4895.

(60) Sonoiki, E.; Ng, C. L.; Lee, M. C. S.; Guo, D.; Zhang, Y.-K.; Zhou, Y.; Alley, M. R. K.; Ahyong, V.; Sanz, L. M.; Lafuente-Monasterio, M. J.; et al. A Potent Antimalarial Benzoxaborole Targets a Plasmodium Falciparum Cleavage and Polyadenylation Specificity Factor Homologue. *Nat. Commun.* **2017**, *8* (1), 14574. https://doi.org/10.1038/ncomms14574.

(61) Kurz, S. G.; Hazra, S.; Bethel, C. R.; Romagnoli, C.; Caselli, E.; Prati, F.; Blanchard, J. S.; Bonomo, R. A. Inhibiting the β-Lactamase of Mycobacterium Tuberculosis (Mtb) with Novel Boronic Acid Transition-State Inhibitors (BATSIs). *ACS Infect. Dis.* **2016**, *1* (6), 234–242. https://doi.org/10.1021/acsinfecdis.5b00003.

(62) Xie, S. C.; Gillett, D. L.; Spillman, N. J.; Tsu, C.; Luth, M. R.; Ottilie, S.; Duffy, S.; Gould, A. E.; Hales, P.; Seager, B. A.; et al. Target Validation and Identification of Novel Boronate Inhibitors of the Plasmodium Falciparum Proteasome. *J. Med. Chem.* **2018**, *61* (22), 10053–10066. https://doi.org/10.1021/acs.jmedchem.8b01161.

(63) Zhang, Y.-K.; Plattner, J. J.; Easom, E. E.; Jacobs, R. T.; Guo, D.; Freund, Y. R.; Berry, P.; Ciaravino, V.; Erve, J. C. L.; Rosenthal, P. J.; et al. Benzoxaborole Antimalarial Agents. Part 5. Lead Optimization of Novel Amide Pyrazinyloxy Benzoxaboroles and Identification of a Preclinical Candidate. *J. Med. Chem.* **2017**, *60* (13), 5889–5908. https://doi.org/10.1021/acs.jmedchem.7b00621.

(64) Akama, T.; Zhang, Y.-K.; Freund, Y. R.; Berry, P.; Lee, J.; Easom, E. E.; Jacobs, R. T.; Plattner, J. J.; Witty, M. J.; Peter, R.; et al. Identification of a 4-Fluorobenzyl L-Valinate Amide Benzoxaborole (AN11736) as a Potential Development Candidate for the Treatment of Animal African Trypanosomiasis (AAT). *Bioorg. Med. Chem. Lett.* **2018**, *28* (1), 6–10. https://doi.org/https://doi.org/10.1016/j.bmcl.2017.11.028.

(65) Zhang, Y. K.; Plattner, J. J.; Easom, E. E.; Zhou, Y.; Akama, T.; Bu, W.; White, W. H.; Defauw, J. M.; Winkle, J. R.; Balko, T. W.; et al. Discovery of an Orally Bioavailable Isoxazoline Benzoxaborole (AN8030) as a Long Acting Animal Ectoparasiticide. *Bioorganic Med. Chem. Lett.* **2015**, *25* (23), 5589–5593. https://doi.org/10.1016/j.bmcl.2015.10.044.

(66) Akama, T.; Baker, S. J.; Zhang, Y.-K.; Hernandez, V.; Zhou, H.; Sanders, V.; Freund, Y.; Kimura, R.; Maples, K. R.; Plattner, J. J. Discovery and Structure–activity Study of a Novel Benzoxaborole Anti-Inflammatory Agent (AN2728) for the Potential Topical Treatment of Psoriasis and Atopic Dermatitis. *Bioorg. Med. Chem. Lett.* **2009**, *19* (8), 2129–2132. https://doi.org/https://doi.org/10.1016/j.bmcl.2009.03.007.

(67) Dong, C.; Virtucio, C.; Zemska, O.; Baltazar, G.; Zhou, Y.; Baia, D.; Jones-Iatauro, S.; Sexton, H.; Martin, S.; Dee, J.; et al. Treatment of Skin Inflammation with Benzoxaborole Phosphodiesterase Inhibitors: Selectivity, Cellular Activity, and Effect on Cytokines Associated with Skin Inflammation and Skin Architecture Changes. *J. Pharmacol. Exp. Ther.* **2016**, *358* (3), 413 LP-422. https://doi.org/10.1124/jpet.116.232819.

(68) António, J. P. M.; Gonçalves, L. M.; Guedes, R. C.; Moreira, R.; Gois, P. M. P. Diazaborines as New Inhibitors of Human Neutrophil Elastase. *ACS Omega* **2018**, *3* (7), 7418–7423. https://doi.org/10.1021/acsomega.8b00702.

(69) Kraljić, K.; Jelić, D.; Žiher, D.; Cvrtila, A.; Dragojević, S.; Sinković, V.; Mesić, M. Benzoxaboroles—Novel Autotaxin Inhibitors. *Molecules* . 2019. https://doi.org/10.3390/molecules24193419.

(70) Baldwin, A. G.; Tapia, V. S.; Swanton, T.; White, C. S.; Beswick, J. A.; Brough, D.; Freeman, S. Design, Synthesis and Evaluation of Oxazaborine Inhibitors of the NLRP3 Inflammasome. *ChemMedChem* **2018**, *13* (4), 312–320. https://doi.org/10.1002/cmdc.201700731.

(71) Maeda, D. Y.; Peck, A. M.; Schuler, A. D.; Quinn, M. T.; Kirpotina, L. N.; Wicomb, W. N.; Auten, R. L.; Gundla, R.; Zebala, J. A. Boronic Acid-Containing CXCR1/2 Antagonists: Optimization of Metabolic Stability, in Vivo Evaluation, and a Proposed Receptor Binding Model. *Bioorg. Med. Chem. Lett.* **2015**, *25* (11), 2280–2284. https://doi.org/https://doi.org/10.1016/j.bmcl.2015.04.041.

(72) Lu, C.-J.; Hu, J.; Wang, Z.; Xie, S.; Pan, T.; Huang, L.; Li, X. Discovery of Boron-Containing Compounds as Aβ Aggregation Inhibitors and Antioxidants for the Treatment of Alzheimer's Disease. *Medchemcomm* **2018**, *9* (11), 1862–1870. https://doi.org/10.1039/C8MD00315G.

(73) Tapparelli, C.; Metternich, R.; Ehrhardt, C.; Zurini, M.; Claeson, G.; Scully, M. F.; Stone, S. R. In Vitro and in Vivo Characterization of a Neutral Boron-Containing Thrombin Inhibitor. *J. Biol. Chem.* **1993**, *268* (7), 4734–4741. https://doi.org/https://doi.org/10.1016/S0021-9258(18)53458-X.

(74) Quan, M. L.; Wityak, J.; Dominguez, C.; Duncia, J. V; Kettner, C. A.; Ellis, C. D.; Liauw, A. Y.; Park, J. M.; Santella, J. B.; Knabb, R. M.; et al. Biaryl Substituted Alkylboronate Esters as Thrombin Inhibitors. *Bioorg. Med. Chem. Lett.* **1997**, *7* (13), 1595–1600. https://doi.org/https://doi.org/10.1016/S0960-894X(97)00254-0.

(75) Coutts, S. J.; Kelly, T. A.; Snow, R. J.; Kennedy, C. A.; Barton, R. W.; Adams, J.; Krolikowski, D. A.; Freeman, D. M.; Campbell, S. J.; Ksiazek, J. F.; et al. Structure−Activity Relationships of Boronic Acid Inhibitors of Dipeptidyl Peptidase IV. 1. Variation of the P2 Position of Xaa-boroPro Dipeptides. *J. Med. Chem.* **1996**, *39* (10), 2087–2094. https://doi.org/10.1021/jm950732f.

(76) von Lewinski, D.; Selvanayagam, J. B.; Schatz, R. A.; Jilma, B.; Kubica, J.; Povsik, T. J.; Nix, D.; Henauer, S.; Wallner, M.; Group, R.-D. study. Protocol for a Phase II, Randomized, Double-Blind, Placebo-Controlled, Safety and Efficacy Study of Dutogliptin in Combination with Filgastrim in Early Recovery Post-Myocardial Infarction: Study Protocol for a Rondomized Controlled Trial. *Trials* **2020**, *21* (1), 744.

(77) IGO.., G. W. H. O. 2017(WHO/EMP/IAU/2017. 12). (L. C. B.-N.-S. 3. .; Cataloguing-in-Publication. *PRIORITIZATION OF PATHOGENS TO GUIDE DISCOVERY, RESEARCH AND DEVELOPMENT OF NEW ANTIBIOTICS FOR DRUG-RESISTANT BACTERIAL INFECTIONS, INCLUDING TUBERCULOSIS*; 2017.

(78) Rice, L. B. Federal Funding for the Study of Antimicrobial Resistance in Nosocomial Pathogens: No ESKAPE. *J. Infect. Dis.* **2008**, *197* (8), 1079–1081. https://doi.org/10.1086/533452.

(79) Ma, Y. X.; Wang, C. Y.; Li, Y. Y.; Li, J.; Wan, Q. Q.; Chen, J. H.; Tay, F. R.; Niu, L. N. Considerations and Caveats in Combating ESKAPE Pathogens against Nosocomial Infections. *Adv. Sci.* **2020**, *7* (1). https://doi.org/10.1002/advs.201901872.

(80) Michaelis, A.; Becker, P. Ueber Monophenylborchlorid Und Einige Derivate Desselben. *Ber Dtsch Chem Ges* **1882**, *15*, 180–185.

(81) NIH. http://clinicaltrials.gov/ct2/results?cond=&term=boric+acid&cntry=&state=&city=&dist.

(82) Pechenov, A.; Stefanova, M. E.; Nicholas, R. A.; Peddi, S.; Gutheil, W. G. Potential Transition State Analogue Inhibitors for the Penicillin-Binding Proteins. *Biochemistry* **2003**, *42* (2), 579–588. https://doi.org/10.1021/bi026726k.

(83) Nicola, G.; Peddi, S.; Stefanova, M.; Nicholas, R. A.; Gutheil, W. G.; Davies, C. Crystal Structure of Escherichia Coli Penicillin-Binding Protein 5 Bound to a Tripeptide Boronic Acid Inhibitor: A Role for Ser-110 in Deacylation. *Biochemistry* **2005**, *44* (23), 8207–8217. https://doi.org/10.1021/bi0473004.

(84) Woon, E. C. Y.; Zervosen, A.; Sauvage, E.; Simmons, K. J.; Živec, M.; Inglis, S. R.; Fishwick, C. W. G.; Gobec, S.; Charlier, P.; Luxen, A.; et al. Structure Guided Development of Potent Reversibly Binding Penicillin Binding Protein Inhibitors. *ACS Med. Chem. Lett.* **2011**, *2* (3), 219–223. https://doi.org/10.1021/ml100260x.

(85) Inglis, S. R.; Zervosen, A.; Woon, E. C. Y.; Gerards, T.; Teller, N.; Fischer, D. S.; Luxen, A.; Schofield, C. J. Synthesis and Evaluation of 3-(Dihydroxyboryl)benzoic Acids as D,d-Carboxypeptidase R39 Inhibitors. *J. Med. Chem.* **2009**, *52* (19), 6097–6106. https://doi.org/10.1021/jm9009718.

(86) Zervosen, A.; Bouillez, A.; Herman, A.; Amoroso, A.; Joris, B.; Sauvage, E.; Charlier, P.; Luxen, A. Synthesis and Evaluation of Boronic Acids as Inhibitors of Penicillin Binding Proteins of Classes A, B and C. *Bioorg. Med. Chem.* **2012**, *20* (12), 3915–3924. https://doi.org/https://doi.org/10.1016/j.bmc.2012.04.018.

(87) Newman, H.; Krajnc, A.; Bellini, D.; Eyermann, C. J.; Boyle, G. A.; Paterson, N. G.; McAuley, K. E.; Lesniak, R.; Gangar, M.; Von Delft, F.; et al. High-Throughput Crystallography Reveals Boron-Containing Inhibitors of a Penicillin-Binding Protein with Di- And Tricovalent Binding Modes. *J. Med. Chem.* **2021**, *64* (15), 11379–11394. https://doi.org/10.1021/acs.jmedchem.1c00717.

(88) Hao, G.; Li, H.; Yang, F.; Dong, D.; Ding, Y.; Pan, W.; Wang, E.; Liu, R.; Zhou, H. Discovery of Benzhydrol-Oxaborole Derivatives as Streptococcus Pneumoniae Leucyl-tRNA Synthetase Inhibitors. *Bioorg. Med. Chem.* **2021**, *29*, 115871.

(89) Alav, I.; Sutton, J. M.; Rahman, K. Role of Bacterial Efflux Pumps in Biofilm Formation. *J. Antimicrob. Chemother.* **2018**, *73*. https://doi.org/10.1093/jac/dky042.

(90) Ambler, R. P. The Structure of Beta-Lactamases. *Philos. Trans. R. Soc. Lond. B. Biol. Sci.* **1980**, *289* (1036), 321–331. https://doi.org/10.1098/rstb.1980.0049.

(91) Bush, K.; Jacoby, G. A.; Medeiros, A. A. A Functional Classification Scheme for β-Lactamases and Its Correlation with Molecular Structure. *Antimicrob. Agents Chemother.* **1995**, *39* (6), 1211–1233. https://doi.org/10.1128/AAC.39.6.1211.

(92) Curcio, D. Multidrug-Resistant Gram-Negative Bacterial Infections: Are You Ready for the Challenge? *Curr. Clin. Pharmacol.* **2014**, *9* (1), 27–38. https://doi.org/10.2174/15748847113089990062.

(93) Jeon, J. H.; Lee, J. H.; Lee, J. J.; Park, K. S.; Karim, A. M.; Lee, C. R.; Jeong, B. C.; Lee, S. H. Structural Basis for Carbapenem-Hydrolyzing Mechanisms of Carbapenemases Conferring Antibiotic Resistance. *Int. J. Mol. Sci.* **2015**, *16* (5), 9654–9692. https://doi.org/10.3390/ijms16059654.

(94) Lomovskaya, O.; Sun, D.; Rubio-Aparicio, D.; Nelson, K.; Tsivkovski, R.; Griffith, D. C.; Dudley, M. N. Vaborbactam: Spectrum of Beta-Lactamase Inhibition and Impact of Resistance Mechanisms on Activity in Enterobacteriaceae. *Antimicrob. Agents Chemother.* **2017**, *61* (11), 1–15. https://doi.org/10.1128/AAC.01443-17.

(95) Liu, B.; Trout, R. E. L.; Chu, G. H.; Mcgarry, D.; Jackson, R. W.; Hamrick, J. C.; Daigle, D. M.; Cusick, S. M.; Pozzi, C.; De Luca, F.; et al. Discovery of Taniborbactam (VNRX-5133): A Broad-Spectrum Serine- And Metallo-β-Lactamase Inhibitor for Carbapenem-Resistant Bacterial Infections. *J. Med. Chem.* **2020**, *63* (6), 2789–2801. https://doi.org/10.1021/acs.jmedchem.9b01518.

(96) Krajnc, A.; Brem, J.; Hinchliffe, P.; Calvopiña, K.; Panduwawala, T. D.; Lang, P. A.; Kamps, J. J. A. G.; Tyrrell, J. M.;

Widlake, E.; Saward, B. G.; et al. Bicyclic Boronate VNRX-5133 Inhibits Metallo- And Serine-β-Lactamases. *J. Med. Chem.* **2019**, *62* (18), 8544–8556. https://doi.org/10.1021/acs.jmedchem.9b00911.

(97) O'Shea, R.; Moser, H. E. Physicochemical Properties of Antibacterial Compounds: Implications for Drug Discovery. *J. Med. Chem.* **2008**, *51* (10), 2871–2878. https://doi.org/10.1021/jm700967e.

(98) Hecker, S. J.; Reddy, K. R.; Lomovskaya, O.; Griffith, D. C.; Rubio-Aparicio, D.; Nelson, K.; Tsivkovski, R.; Sun, D.; Sabet, M.; Tarazi, Z.; et al. Discovery of Cyclic Boronic Acid QPX7728, an Ultrabroad-Spectrum Inhibitor of Serine and Metallo-β-Lactamases. *J. Med. Chem.* **2020**, *63* (14), 7491–7507. https://doi.org/10.1021/acs.jmedchem.9b01976.

(99) Trout, R. E.; Zulli, A.; Mesaros, E.; Jackson, R. W.; Boyd, S.; Liu, B.; Hamrick, J.; Daigle, D.; Chatwin, C. L.; John, K.; et al. Discovery of VNRX-7145 (VNRX-5236 Etzadroxil): An Orally Bioavailable β-Lactamase Inhibitor for Enterobacterales Expressing Ambler Class A, C, and D Enzymes. *J. Med. Chem.* **2021**, *64* (14), 10155–10166. https://doi.org/10.1021/acs.jmedchem.1c00437.

(100) Powers, R. A.; Caselli, E.; Focia, P. J.; Prati, F.; Shoichet, B. K. Structures of Ceftazidime and Its Transition-State Analogue in Complex with AmpC β-Lactamase: Implications for Resistance Mutations and Inhibitor Design. *Biochemistry* **2001**, *40* (31), 9207–9214. https://doi.org/10.1021/bi0109358.

(101) Drawz, S. M.; Babic, M.; Bethel, C. R.; Taracila, M.; Distler, A. M.; Ori, C.; Caselli, E.; Prati, F.; Bonomo, R. A. Inhibition of the Class C β-Lactamase from Acinetobacter Spp.: Insights into Effective Inhibitor Design. *Biochemistry* **2010**, *49* (2), 329–340. https://doi.org/10.1021/bi9015988.

(102) Rojas, L. J.; Taracila, M. A.; Papp-Wallace, K. M.; Bethel, C. R.; Caselli, E.; Romagnoli, C.; Winkler, M. L.; Spellberg, B.; Prati, F.; Bonomoa, R. A. Boronic Acid Transition State Inhibitors Active against KPC and Other Class a β-Lactamases: Structure-Activity Relationships as a Guide to Inhibitor Design. *Antimicrob. Agents Chemother.* **2016**, *60* (3), 1751–1759. https://doi.org/10.1128/AAC.02641-15.

(103) Caselli, E.; Shoichet, B. K.; Morandi, S.; Morandi, F.; Focia, P. J.; Prati, F.; Blázquez, J. Nanomolar Inhibitors of AmpC β-Lactamase. *J. Am. Chem. Soc.* **2003**, *125* (3), 685–695. https://doi.org/10.1021/ja0288338.

(104) Wang, X.; Minasov, G.; Blázquez, J.; Caselli, E.; Prati, F.; Shoichet, B. K. Recognition and Resistance in TEM β-Lactamase. *Biochemistry* **2003**, *42* (28), 8434–8444. https://doi.org/10.1021/bi034242y.

(105) Chen, Y.; Shoichet, B.; Bonnet, R. Structure, Function, and Inhibition along the Reaction Coordinate of CTX-M β-Lactamases. *J. Am. Chem. Soc.* **2005**, *127* (15), 5423–5434. https://doi.org/10.1021/ja042850a.

(106) Drawz, S. M.; Bethel, C. R.; Hujer, K. M.; Hurless, K. N.; Distler, A. M.; Caselli, E.; Prati, F.; Bonomo, R. A. The Role of a Second-Shell Residue in Modifying Substrate and Inhibitor Interactions in the SHV β-Lactamase: A Study of Ambler Position Asn276. *Biochemistry* **2009**, *48* (21), 4557–4566. https://doi.org/10.1021/bi9003292.

(107) Morandi, S.; Morandi, F.; Caselli, E.; Shoichet, B. K.; Prati, F. Structure-Based Optimization of Cephalothin-Analogue Boronic Acids as β-Lactamase Inhibitors. *Bioorganic Med. Chem.* **2008**, *16* (3), 1195–1205. https://doi.org/10.1016/j.bmc.2007.10.075.

(108) Drawz, S. M.; Taracila, M.; Caselli, E.; Prati, F.; Bonomo, R. A. Exploring Sequence Requirements for C3/C4 Carboxylate Recognition in the Pseudomonas Aeruginosa Cephalosporinase: Insights into Plasticity of the AmpC β-Lactamase. *Protein Sci.* **2011**, *20* (6), 941–958. https://doi.org/10.1002/pro.612.

(109) Powers, R. A.; Prati, F.; Bonomo, R. A.; Romagnoli, C.; Taracila, M. A.; Swanson, H. C.; Wallar, B. J.; Florek, N. W.;

Caselli, E. Biochemical and Structural Analysis of Inhibitors Targeting the ADC-7 Cephalosporinase of Acinetobacter Baumannii . *Biochemistry* **2014**, *53* (48), 7670–7679. https://doi.org/10.1021/bi500887n.

(110) Caselli, E.; Romagnoli, C.; Powers, R. A.; Taracila, M. A.; Bouza, A. A.; Swanson, H. C.; Smolen, K. A.; Fini, F.; Wallar, B. J.; Bonomo, R. A.; et al. Inhibition of Acinetobacter -Derived Cephalosporinase: Exploring the Carboxylate Recognition Site Using Novel β-Lactamase Inhibitors. *ACS Infect. Dis.* **2018**, *4* (3), 337–348. https://doi.org/10.1021/acsinfecdis.7b00153.

(111) Tan, Q.; Ogawa, A. M.; Painter, R. E.; Park, Y.-W.; Young, K.; DiNinno, F. P. 4,7-Dichloro Benzothien-2-Yl Sulfonylaminomethyl Boronic Acid: First Boronic Acid-Derived Beta-Lactamase Inhibitor with Class A, C, and D Activity. *Bioorg. Med. Chem. Lett.* **2010**, *20* (8), 2622–2624. https://doi.org/https://doi.org/10.1016/j.bmcl.2010.02.065.

(112) Eidam, O.; Romagnoli, C.; Caselli, E.; Babaoglu, K.; Pohlhaus, D. T.; Karpiak, J.; Bonnet, R.; Shoichet, B. K.; Prati, F. Design, Synthesis, Crystal Structures, and Antimicrobial Activity of Sulfonamide Boronic Acids as β-Lactamase Inhibitors. *J. Med. Chem.* **2010**, *53* (21), 7852–7863. https://doi.org/10.1021/jm101015z.

(113) Caselli, E.; Bonnet, R.; Prati, F.; Dalmasso, G.; Barelier, S.; Eidam, O.; Shoichet, B. K.; Romagnoli, C. Fragment-Guided Design of Subnanomolar -Lactamase Inhibitors Active in Vivo. *Proc. Natl. Acad. Sci.* **2012**, *109* (43), 17448–17453. https://doi.org/10.1073/pnas.1208337109.

(114) Romagnoli, C.; Caselli, E.; Prati, F. Synthesis of [(1,2,3-Triazol-1-Yl)methyl]boronic Acids through Click Chemistry: Easy Access to a Potential Scaffold for Protease Inhibitors. *European J. Org. Chem.* **2015**, *2015* (5), 1075–1083. https://doi.org/10.1002/ejoc.201403408.

(115) Nguyen, N. Q.; Krishnan, N. P.; Rojas, L. J.; Prati, F.; Caselli, E.; Romagnoli, C.; Bonomo, R. A.; Van Den Akker, F. Crystal Structures of KPC-2 and SHV-1 β-Lactamases in Complex with the Boronic Acid Transition State Analog S02030. *Antimicrob. Agents Chemother.* **2016**, *60* (3), 1760–1766. https://doi.org/10.1128/AAC.02643-15.

2 Aims and structure of the work

Boron chemistry is a fascinating and emerging field of research: it combines advanced knowledge on (stereo)selective synthesis of boron containing molecules with the search for possible pharmaceutical applications, designing genuinely new molecules with therapeutic potentialities. Since the first boron containing drug approved in 2003 (bortezomib), boronic acids has been regarded with growing interest by both academic and industrial drug discovery groups, as pointed out by the number of patents or articles containing the word "boronic acids" in SciFinder (Chart 1). The aim of my doctoral research was to contribute to the identification of boronic acids as effective tool to contrast the word wide alarming problem of antibiotic resistance, developing new boron-containing scaffolds able to inhibit β-lactamases, the main resistance mechanism to β-lactam antibiotics.

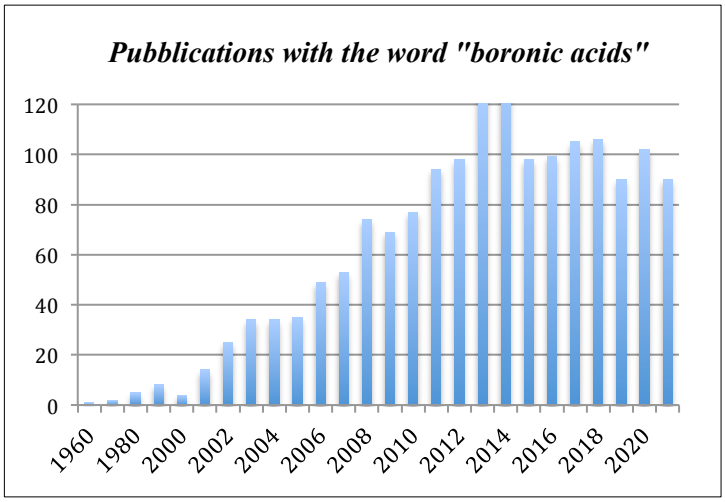

Chart 1. Number of pubblications containing the word "boronic acids" reported on Scifinder from 1960s to 2021.

This research encompasses design, stereoselective synthesis, X-ray diffraction analysis, kinetic and microbiological studies. This multidisciplinary approach afforded the identification of several potent inhibitors of β-lactamases capable to restore *in vitro* and *in vivo* the activity of β-lactams.

When I joined the research group of Prof. Fabio Prati, a lot had already been done in order to improve the activity of boronic acids as β-lactamases inhibitors. They started from the similarity in reactivity between the electrophilic boron atom and the carbonyl carbon of the β-lactam ring (Figure 31) and developed several boronic acids bearing similar properties and structures with β-lactams.[1] Initially achiral α-amidoboronic acids with the same R_1 side chains of β-lactam antibiotics were synthesised. The cephalotin R_1 chain (compound **28**, Figure 32) demonstrated to be the best compromise between contribution to recognition and steric hindrance. Actually, cephalotin R_1 chain is able to interact with different β-lactamases, especially when associated with the *m*-carboxyphenyl R_2 chain. Indeed, the activity of **28** was improved by 300-fold with the introduction of the R_2 *m*-carboxyphenyl side chain and the compound obtained (**SM23**,

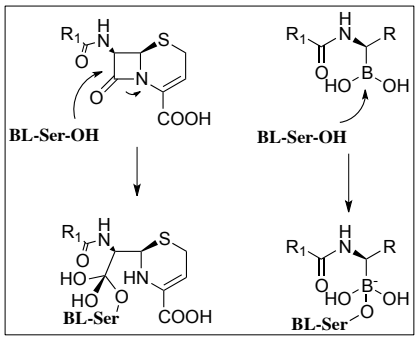

Figure 31. Similarity between the boronic acid and the carboxyl of β-lactam rings.

Figure 32) inhibited AmpC β-lactamases with K_i = 1 nM.[2] Subsequently, a new class of compounds bearing a triazole instead of the phenyl ring in R_2 position was synthesised.[3] This aromatic scaffold aimed to simplify the synthesis, to improve the biochemical affinity, to increase the accessibility to the target and to enhance chemical diversity. The synthetic approach applied relied on the well-known "Copper Catalyzed Azide Alkyne Cycloaddition" (CuAAC) reaction where the boronic scaffold, containing a properly inserted alpha- or beta- azide group, can react with a terminal alkyne in mild conditions, with high yields and easy isolation of the product.[4] Although the 1,4-disubstituted 1,2,3-triazole ring replaces the *m*-carboxybenzyl group preserving its aromatic character, it exploits a stronger dipole moment, thus potentially acting as an active linker, and allows a large variability of the R groups. The β-triazolylethaneboronic acids showed potent activity against clinically relevant class C and A β-lactamases, and compound **S02030** (Figure 32) was the best compound with K_i as low as 80 nM for KPC-2 and 44 nM for ADC-7.[5,6] Several studies confirmed the potency of **S02030** as inhibitor against class A and class C β-lactamases, but there was a lack in activity against other classes of enzymes. At the moment I started my doctoral project, none of the compounds synthesised by the group had proved activity against class B and/or class D β-lactamases. That was my starting point.

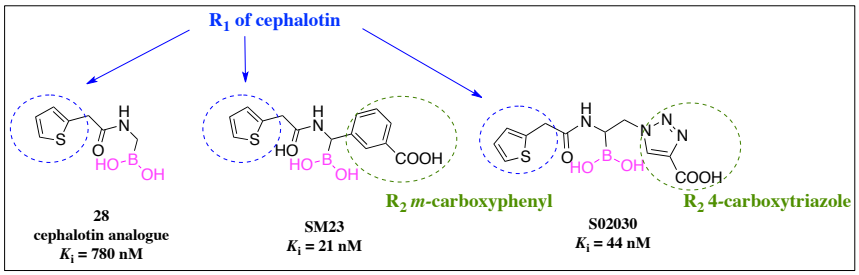

Figure 32. Research pathways in prof. Prati's laboratory: from α-amidoboronic acids with β-lactam side chains (**28**) to α-amido-β-tryazolylboronic acids (**S02030**). Inhibition constants (K_i) against ADC-7 are reported.

My PhD project involved different modification of **S02030** scaffold with two main objectives: to extend the activity of this BATSI against class D and B β-lactamases and to identify a new BATSI with improved pharmacokinetic properties to be co-administered with a β-lactam to address a specific unmet medical need. To achieve these aims, changes in the three different determinants of **S02030** structure were performed: the amide side chain, the R_1 groups attached to it and the R_2 side chain (Figure 33).

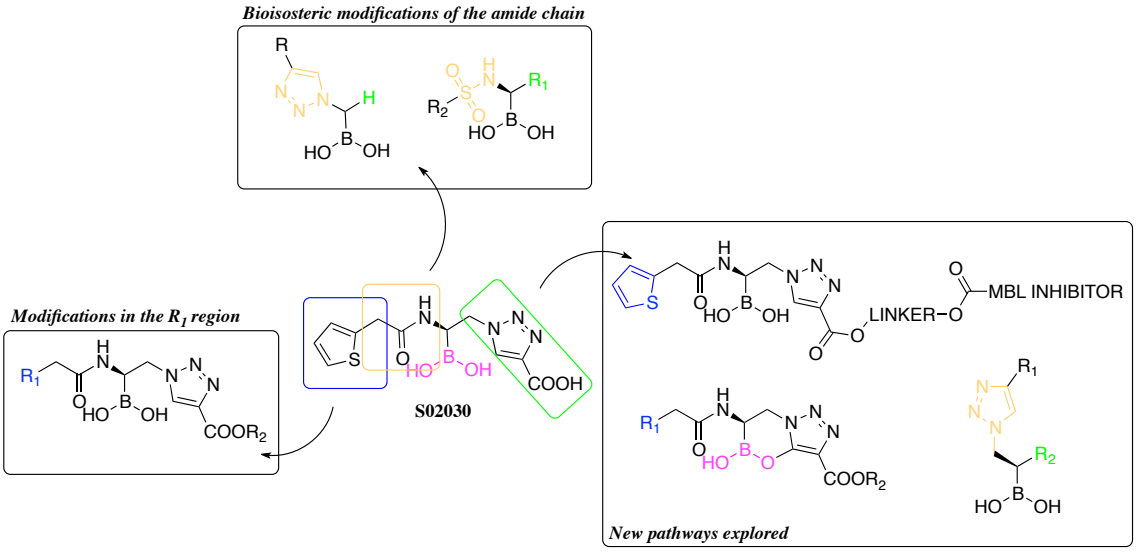

Figure 33. Schematic representation of the aims.

2.1 Bioisosteric modifications of the amide

The amide group, typically present in β-lactam antibiotics, was replaced with different bioisosteres to gain interactions and activity against different β-lactamases. In particular, the triazole ring and the sulphonamide chain were introduced in the BATSIs' structure as bioisosters of the amide group.

The triazole ring is a non-classical amide bioisoster, since both share key physical properties including planarity, size, dipole moment and hydrogen bond forming capabilities. On the other hand, triazole is cyclic, less flexible than the amide and it is also more stable against oxidation and hydrolysis. 1,4-Disubstituted 1,2,3-triazoles are easily accessible through the same CuAAC click reaction employed for the synthesis of **S02030**.[4] In this way a large number of derivatives can be easily obtained: in fact, initially I was able to obtain a library of 24 α-triazolylboronic acids, which were successfully tested against class C and class A β-lactamases, ADC-7 and KPC-2 respectively. They proved able to restore activity of β-lactams against nosocomial bacterial strains: they were not only excellent inhibitors, but also promising hit compounds active *in vitro*.

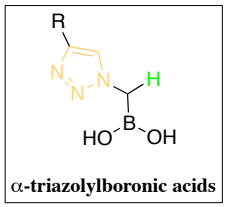

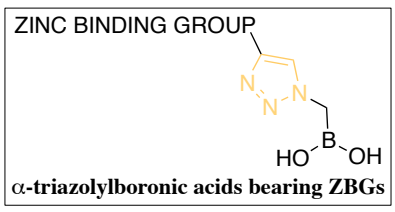

Strengthened by these first results, I planned to extend inhibition capabilities of the α-triazolyl scaffold to class B β-lactamases (MBLs), metallo-hydrolases possessing one or two zinc ions in their catalytic pocket. Looking at the literature, three strategies are taken to inhibit these enzymes: removing the zinc ions through chelating agents; substituting the zinc ions with other atoms (bismuth); binding the zinc ions with zinc binding groups (ZBGs). The third strategy is the most used, inserting different functional groups able to bind zinc ions (such as thiols, carboxylic acids, nitrogen containing heterocycles or hydroxamates).[7] I therefore designed and synthesised an initial series of 8 α-triazolylmethaneboronic acids bearing a

Zinc Binding Group (ZBG) as substituent on the C4 of the triazole ring. These compounds were sent to our collaborators at the Case Western University (Cleveland, US) to be tested against MBLs and preliminary results on VIM-2 enzymes were encouraging.

The second amide bioisoster I introduced in the structure of boronic acids was ***the sulphonamide chain***. Achiral α-sulphonamide boronic acids have been already tested as inhibitors of class C AmpC enzymes.[8] Against this class of enzymes they demonstrated to retain inhibition activity if compared to carboxamide analogues and to rescue antibiotic resistance when used in combination with third generation antibiotics. Moreover, the sulphonamide group was observed to change not only the electronic character of a key interaction, but also the geometry of the inhibitors.[9]

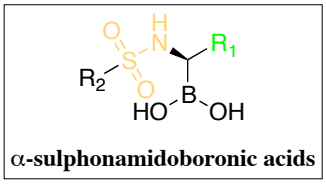

α-sulphonamidoboronic acids

My intent was to extend the inhibition against class D BLs, also known as oxacillinase. OXA enzymes display structural diversities from class A and C Serine β-lactamases: in particular they possess a hydrophobic bridge (formed by a Tyr or Phe on one side, and a Met or Trp on the other) across the top of the active site.[10] Due to this structural "constrain" planar amide side chain do not fit properly in the active site. Therefore, changing the planarity of the amide group to a tetrahedral sulphonamide seemed a good solution to better fit into the OXA catalytic site. Moreover, the study of the crystal structure of doripenem, the carbapenem with the highest affinity towards OXA 24/40, in complex with the class D enzyme provided important insights for the development of new boronic compounds.

A small library of six sulphonamide-BATSIs was synthesised: four of them had the same stereochemistry of the alpha carbon as in doripenem, whereas one compound was synthesised with opposite stereochemistry and one compound was achiral. Methyl and ethyl hydrophobic side chain were introduced and the importance of the terminal carboxylate group on the phenyl ring was explored. Kinetic analysis, crystallographic structures and microbiological assays were developed to better understand the activity of these new molecules, highlighting some interesting results. In particular, the best compound of the series demonstrated activity in the low micromolar range and represented the best inhibitor of class D β-lactamases identified so far in our laboratory.

2.2 *Modifications in the R_1 region*

A different project was focused on substitution in the R_1 side chain of **S02030**. Several heterocycles, different from the tiophene ring, were bound to the amide chain and a series of analogues were synthesised to extend the activity of **S02030** against MBLs (R_1 side chains with groups able to bind zinc ions) and to improve the pharmacokinetic profile of our BATSI. The thiophene ring is in fact known to undergo oxidation in vivo.[11] Seven molecules were synthesised and tested in kinetic and microbiological assays and the X-ray crystal structure of the best inhibitor obtained in complex with KPC-2. The results allowed the identification of **MB076**, a potent BATSI

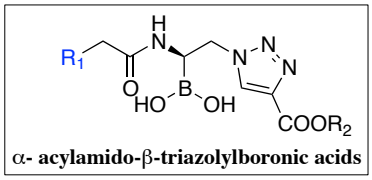

α- acylamido-β-triazolylboronic acids

active against ESBLs and carbapenemases. **MB076** proved impressively active in restoring activity of β-lactams in resistant clinical strains. Its synthesis was scaled up in order to provide the amount requested to perform preclinical tests, such as toxicity, efficacy, PK/PD profile analysis and mice survival experiments. These tests were supported by the NIH/NIAID program for the discovery of anti-infective agents to our collaboration with Prof. Bonomo at the Case Western Reserve University in Cleveland (Ohio, USA). The results obtained with this molecule made it a promising compound to address clinical concerns regarding multi-drug resistant infections. In particular, we focused our attention on complicated urinary tract infections (cUTI) and pyelonephritis for which new treatment are urgently needed. The potency of this compound was confirmed with several studies fostering me to synthesize a related compound suitable for the development of an oral version of the antibiotic drug.

2.3 *Strategies for new inhibitors*

My research path towards boronic compounds included some other projects, which provided new useful synthetic strategies to obtain molecules with interesting structural changes. Even if *in vitro* analyses for such compounds have not been performed yet, some of these projects are currently on going.

All the α-triazolylboronic acids library synthesised showed poor affinity against class D β-lactamases with K_i values > 100 mM. On the basis of crystallographic structures of OXA enzymes, the insertion of one more carbon atom between the boron atom and the triazole was designed to overcome the hydrophobic bridge and to extend the activity of α-triazolylboronic acids towards class D. The synthesis of achiral and chiral β-triazolylboronic acids was developed and a series of ten molecules was successfully obtained and is ready for *in vitro* tests.

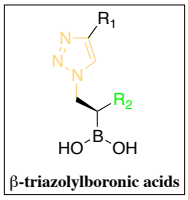

β-triazolylboronic acids

Against MBLs, three directions were followed: (i) α-triazolylmethaneboronic acids with a ZBG as substituent on the triazole ring, as described before; (ii) co-drugs where a known inhibitor of MBLs was bound to **S02030** to have in the same molecule the activity against class A and class C β-lactamases; (iii) the synthesis of cyclic α-amido-β-triazolylboronic acids.

A "co-drug" or "mutual prodrug" is synthesised by attaching directly or *via* a linkage two different pharmacophores with similar or different pharmacological activities. The aim of this approach is to improve physicochemical, biopharmaceutical and drug delivery properties of therapeutic agents.

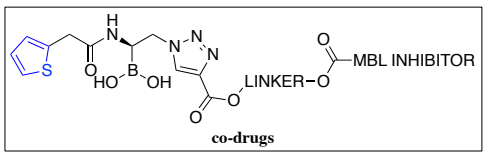

co-drugs

Indeed, the union of two molecules with different pharmacokinetic profile in a single structure allows obtaining an entity with a single pharmacokinetic profile, which can guarantee absorption of the two compounds at the same time and with a constant 1: 1 *ratio*.[12] The rationale I followed was the design

of co-drugs containing **S02030**, which proved to be an excellent inhibitor against SBLs and **L-captopril**, used as an Angiotensin- Converting- Enzyme (ACE) inhibitor and active on some of the most relevant MBLs.[13] The synthesis of two co-drugs was successfully accomplished and, hoping to obtain good microbiological results, this could represent the starting point for a new kind of BATSI: not just one molecule with multiple inhibitory activity, but two molecules with different target bound together in a single co-drug.

In the very recent literature, all the boronic inhibitors of β-lactamases that reached the clinic are cyclic

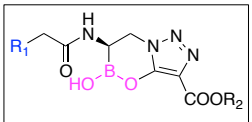

cyclic triazolylboronic acids

boronates. This evidence encouraged my research in the direction of cyclic triazolylboronic compounds. If **S02030**, sulphonamidoboronic acids and also α-tryazolylboronic acids proved to be good inhibitors of class A and class C β-lactamases, their cyclic analogues could be broad spectrum inhibitors of all classes, like **QPX7728**.[14] For this reason, during these three years of PhD I developed different strategies to obtain cyclic triazolylboronic acids. This project is currently on going, but we are now very close to our first final product.

A new target

During my PhD, I worked also in collaboration with the research group of prof. Zambon at the Department of Chemical and Geological Sciences, to find a new target for our boronic acids. Prof. Zambon works in the field of medicinal chemistry and on the synthesis of kinase inhibitors against acute myeloid leukaemia (AML). FLT3 and RET (Figure), in particular, are receptor protein kinases (RTKs), tyrosine kinases incorporated into the cell membrane: they have an extracellular receptor part able to bind specific signal molecules and activate the intracellular catalytic site of the kinase, promoting substrate phosphorylation. FLT3 and RET are simultaneously activated in cases of AML presenting mutated FLT3.[15,16] There is, thus, a strong clinical rationale for the simultaneous inhibition of RET and FLT3 for the treatment of AML. Boronic compounds are attractive scaffolds for the development of new agents due to their favourable physico-chemical properties such as low lipophilicity, water solubility and stability. As kinase-targeting agents, boronic compounds are only scantly reported, thus presenting a relatively unhindered IP landscape. Therefore, a first little series of 20 compounds from different classes of boronic acids (α-acylamido, α-sulphonamido, α and β-triazolylboronic acids) was tested and achiral α-triazolylboronic acids demonstrated to be interesting as inhibitors of RET and FLT3 protein kinases. Subsequently, a docking study was performed to identify the best compounds and a second series of 30 molecules was analysed, obtaining promising results.

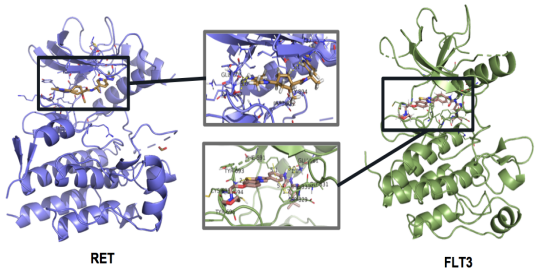

RET and FLT3 in complex with a dual inhibitor.

References

(1) Powers, R. A.; Caselli, E.; Focia, P. J.; Prati, F.; Shoichet, B. K. Structures of Ceftazidime and Its Transition-State Analogue in Complex with AmpC β-Lactamase: Implications for Resistance Mutations and Inhibitor Design. *Biochemistry* **2001**, *40* (31), 9207–9214. https://doi.org/10.1021/bi0109358.

(2) Caselli, E.; Shoichet, B. K.; Morandi, S.; Morandi, F.; Focia, P. J.; Prati, F.; Blázquez, J. Nanomolar Inhibitors of AmpC β-Lactamase. *J. Am. Chem. Soc.* **2003**, *125* (3), 685–695. https://doi.org/10.1021/ja0288338.

(3) Powers, R. A.; Prati, F.; Bonomo, R. A.; Romagnoli, C.; Taracila, M. A.; Swanson, H. C.; Wallar, B. J.; Florek, N. W.; Caselli, E. Biochemical and Structural Analysis of Inhibitors Targeting the ADC-7 Cephalosporinase of Acinetobacter Baumannii . *Biochemistry* **2014**, *53* (48), 7670–7679. https://doi.org/10.1021/bi500887n.

(4) Romagnoli, C.; Caselli, E.; Prati, F. Synthesis of [(1,2,3-Triazol-1-Yl)methyl]boronic Acids through Click Chemistry: Easy Access to a Potential Scaffold for Protease Inhibitors. *European J. Org. Chem.* **2015**, *2015* (5), 1075–1083. https://doi.org/10.1002/ejoc.201403408.

(5) Rojas, L. J.; Taracila, M. A.; Papp-Wallace, K. M.; Bethel, C. R.; Caselli, E.; Romagnoli, C.; Winkler, M. L.; Spellberg, B.; Prati, F.; Bonomoa, R. A. Boronic Acid Transition State Inhibitors Active against KPC and Other Class a β-Lactamases: Structure-Activity Relationships as a Guide to Inhibitor Design. *Antimicrob. Agents Chemother.* **2016**, *60* (3), 1751–1759. https://doi.org/10.1128/AAC.02641-15.

(6) Rojas, L. J.; van den Akker, F.; Prati, F.; Romagnoli, C.; Caselli, E.; Krishnan, N. P.; Nguyen, N. Q.; Bonomo, R. A. Crystal Structures of KPC-2 and SHV-1 β-Lactamases in Complex with the Boronic Acid Transition State Analog S02030. *Antimicrob. Agents Chemother.* **2016**, *60* (3), 1760–1766. https://doi.org/10.1128/aac.02643-15.

(7) Yan, Y.-H.; Li, G.; Li, G.-B. Principles and Current Strategies Targeting Metallo-β-Lactamase Mediated Antibacterial Resistance. *Med. Res. Rev.* **2020**, *40* (5), 1558–1592. https://doi.org/https://doi.org/10.1002/med.21665.

(8) Eidam, O.; Romagnoli, C.; Caselli, E.; Babaoglu, K.; Pohlhaus, D. T.; Karpiak, J.; Bonnet, R.; Shoichet, B. K.; Prati, F. Design, Synthesis, Crystal Structures, and Antimicrobial Activity of Sulfonamide Boronic Acids as β-Lactamase Inhibitors. *J. Med. Chem.* **2010**, *53* (21), 7852–7863. https://doi.org/10.1021/jm101015z.

(9) Eidam, O.; Romagnoli, C.; Caselli, E.; Babaoglu, K.; Pohlhaus, D. T.; Karpiak, J.; Bonnet, R.; Shoichet, B. K.; Prati, F. Design, Synthesis, Crystal Structures, and Antimicrobial Activity of Sulfonamide Boronic Acids as β-Lactamase Inhibitors. *J. Med. Chem.* **2010**, *53* (21), 7852–7863. https://doi.org/10.1021/jm101015z.

(10) Santillana, E.; Beceiro, A.; Bou, G.; Romero, A. Crystal Structure of the Carbapenemase OXA-24 Reveals Insights into the Mechanism of Carbapenem Hydrolysis. *Proc. Natl. Acad. Sci.* **2007**, *104* (13), 5354–5359. https://doi.org/10.1073/pnas.0607557104.

(11) Treiber, A.; Dansette, P. M.; El Amri, H.; Girault, J.-P.; Ginderow, D.; Mornon, J.-P.; Mansuy, D. Chemical and Biological Oxidation of Thiophene: Preparation and Complete Characterization of Thiophene S-Oxide Dimers and Evidence for Thiophene S-Oxide as an Intermediate in Thiophene Metabolism in Vivo and in Vitro. *J. Am. Chem. Soc.* **1997**, *119* (7), 1565–1571. https://doi.org/10.1021/ja962466g.

(12) Das, N.; Dhanawat, M.; Dash, B.; Nagarwal, R. C.; Shrivastava, S. K. Codrug: An Efficient Approach for Drug Optimization. *Eur. J. Pharm. Sci.* **2010**, *41* (5), 571–588. https://doi.org/10.1016/j.ejps.2010.09.014.

(13) Berkel, S. S. Van; Zollman, D.; Lee, S. Y.; Gileadi, O.; Mchugh, P. J.; Walsh, T. R.; Mcdonough, M. A.; Schofield, C. J.

Structural Basis of Metallo-ᴺL-Lactamase Inhibition by Captopril Stereoisomers. *Antimicrob. Agents Chemother.* **2016**, *60* (1), 142–150. https://doi.org/10.1128/AAC.01335-15.Address.

(14) Hecker, S. J.; Reddy, K. R.; Lomovskaya, O.; Griffith, D. C.; Rubio-Aparicio, D.; Nelson, K.; Tsivkovski, R.; Sun, D.; Sabet, M.; Tarazi, Z.; et al. Discovery of Cyclic Boronic Acid QPX7728, an Ultrabroad-Spectrum Inhibitor of Serine and Metallo-β-Lactamases. *J. Med. Chem.* **2020**, *63* (14), 7491–7507. https://doi.org/10.1021/acs.jmedchem.9b01976.

(15) Barabé, F.; Gil, L.; Celton, M.; Bergeron, A.; Lamontagne, V.; Roques, É.; Lagacé, K.; Forest, A.; Johnson, R.; Pécheux, L.; et al. Modeling Human MLL-AF9 Translocated Acute Myeloid Leukemia from Single Donors Reveals RET as a Potential Therapeutic Target. *Leukemia* **2017**, *31* (5), 1166–1176. https://doi.org/10.1038/leu.2016.302.

(16) Rudat, S.; Pfaus, A.; Cheng, Y. Y.; Holtmann, J.; Ellegast, J. M.; Bühler, C.; Marcantonio, D. Di; Martinez, E.; Göllner, S.; Wickenhauser, C.; et al. RET-Mediated Autophagy Suppression as Targetable Co-Dependence in Acute Myeloid Leukemia. *Leukemia* **2018**, *32* (10), 2189–2202. https://doi.org/10.1038/s41375-018-0102-4.

3 Bioisosteric modifications of the amide chain

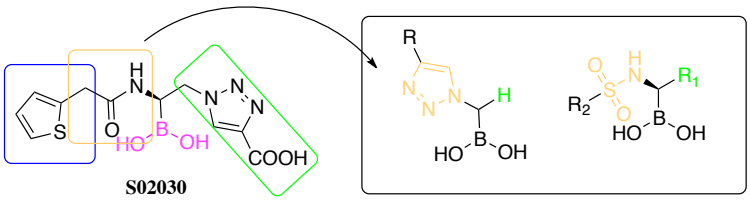

3.1 Triazoles

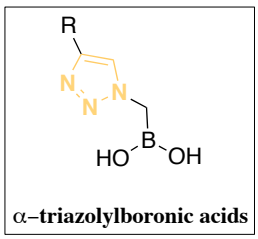

Triazoles are excellent amide bioisoster, due to their size, planarity, dipole moment and hydrogen bond forming capabilities, which make them similar to amide chains. Furthermore, the presence of the triazole ring makes the structure more rigid and reduces its susceptibility to oxidation and hydrolysis. The feasibility to synthesise α-triazolylboronic acids bearing a triazole instead of the classical α-amide chain of antibiotics had been previously tested, allowing to discover that 1,2,3-triazolylboronic compounds are easily accessible through copper-catalysed azide-alkyne cycloaddition (CuAAC) reaction.[1] In this reaction azidemethaneboronate can react with alkynes in mild condition, with inexpensive reagents, high versatility and rapid purification of products. Therefore, a large number of 1,4-disubstituted 1,2,3-triazoles can be easily and rapidly synthesised, allowing the introduction of different substituents to gain interactions with their targets.

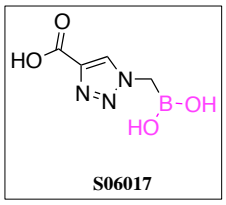

Figure 34. Structure of S06017.

Among the compounds previously synthesised, only compound **S06017** (Figure 34) was tested as inhibitor of β-lactamases: it displayed a lower binding affinity to class C, ADC-7 (K_i = 6.1 μM) if compared to α-acylamide and α-sulphonamide boronic acids, but the structural information from the X-ray crystal structure of the enzyme-inhibitor complex confirmed that the triazole maintained two of the canonical interactions in the amide binding site (two nitrogen atoms form hydrogen bonds with the conserved Gln120 and Asn152 residues), thus behaving as amide bioisoster.[2]

α-Triazolylboronates are the first class of boron-containing compounds I addressed and they proved to be very good inhibitors of class C and class A β-lactamases and promising inhibitors also against class B metallo β-lactamases.

3.1.1 Synthesis of α-triazolylboronic acids

The synthesis of α-triazolylmethaneboronate is described in Scheme 7. The commercially available bromomethanetrifluoroborate was reacted with sodium azide to afford the azidomethanetrifluoroborate

(***1***) in 90% yield. Conversion of the organotrifluoroborate into the (+)-pinanediol α-azidomethaneboronate (***2***) was performed in the presence of silica gel (1.5 eq.) and a stoichiometric amount of (+)-pinanediol (90% yield). The (+)-pinanediol α-azidomethaneboronate is one of the partners of CuAAC; the acetylene counterparts were conveniently purchased or synthesized following literature procedures (see the Experimental section). The azide ***3*** was reacted with an excess of alkyne (1.5 eq.) together with copper sulphate (0.05 eq.), which was reduced *in situ* by sodium ascorbate (0.2 eq.). The expected 1,4-disubstituted triazoles (***4***), differently substituted at the R_1 group, were easily isolated by extraction (85-99% yield) and used as such for the next step. Final deprotection of (+)-pinanediol esters was accomplished by transesterification with isobutylboronic acid (0.95 eq.) and HCl 3 M (3 eq.), allowing one to obtain final boronic acids ***5***.

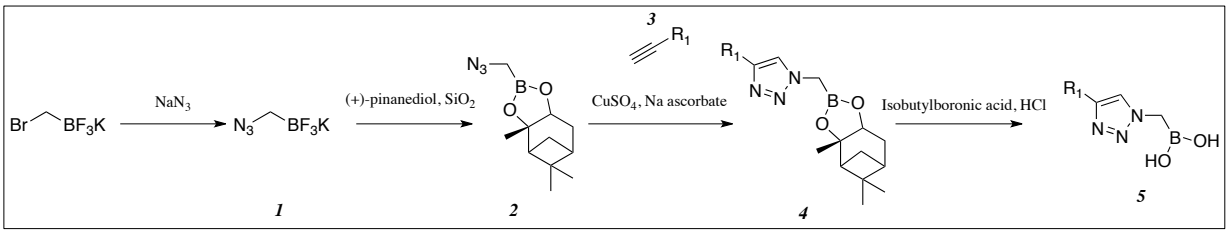

Scheme 7. Synthesis of α-triazolylmethaneboronic acids.

3.1.2 α-Triazolylboronic acids as inhibitors of class C β-lactamases

The WHO priority list assigned *A. baumannii* as a critical priority pathogen due to the high prevalence of cephalosporin and carbapenem resistance and to its ability to survive in adverse environmental conditions, making it one of the most threatening nosocomial pathogens.[3] *A. baumannii* possess many clinically diverse β-lactamases from all four classes, but the most significant portion of β-lactam resistance in this microorganism is expressed by class C *Acinetobacter*-derived cephalosporinases (ADCs), chromosomally encoded β-lactamases responsible for resistance to advanced generation cephalosporins. The importance of identifying β-lactamases inhibitors active against these enzymes, encouraged the synthesis and assays of α-triazolylboronic acids against ADC-7. A series of 24 4-substituted [(1,2,3-triazol-1-yl)-methyl]-boronic acids were synthesised and characterized via kinetic analysis and microbiological assays. Moreover, the X-ray crystal structures of ADC-7 in complex with 5 of these compounds were determined.

The compounds synthesised are represented in Figure 35. Four compounds (***5a-d***) contain a phenyl ring directly bound to the triazole with a substituent on the aromatic moiety. Three triazoles (***5e-g***) bear electron rich and electron poor heterocyclic rings replacing the phenyl, whereas compounds ***5h-j*** and compounds ***5k-o*** introduce a phenyloxymethyl substituent or a substituted aminomethyl bridge on the triazole in order to confer more flexibility to the structures. Compound ***5o*** proved to be the best compound under both kinetic and microbiological profiles. To further improve the structure of ***5o***, triazoles ***5p-x*** were designed.

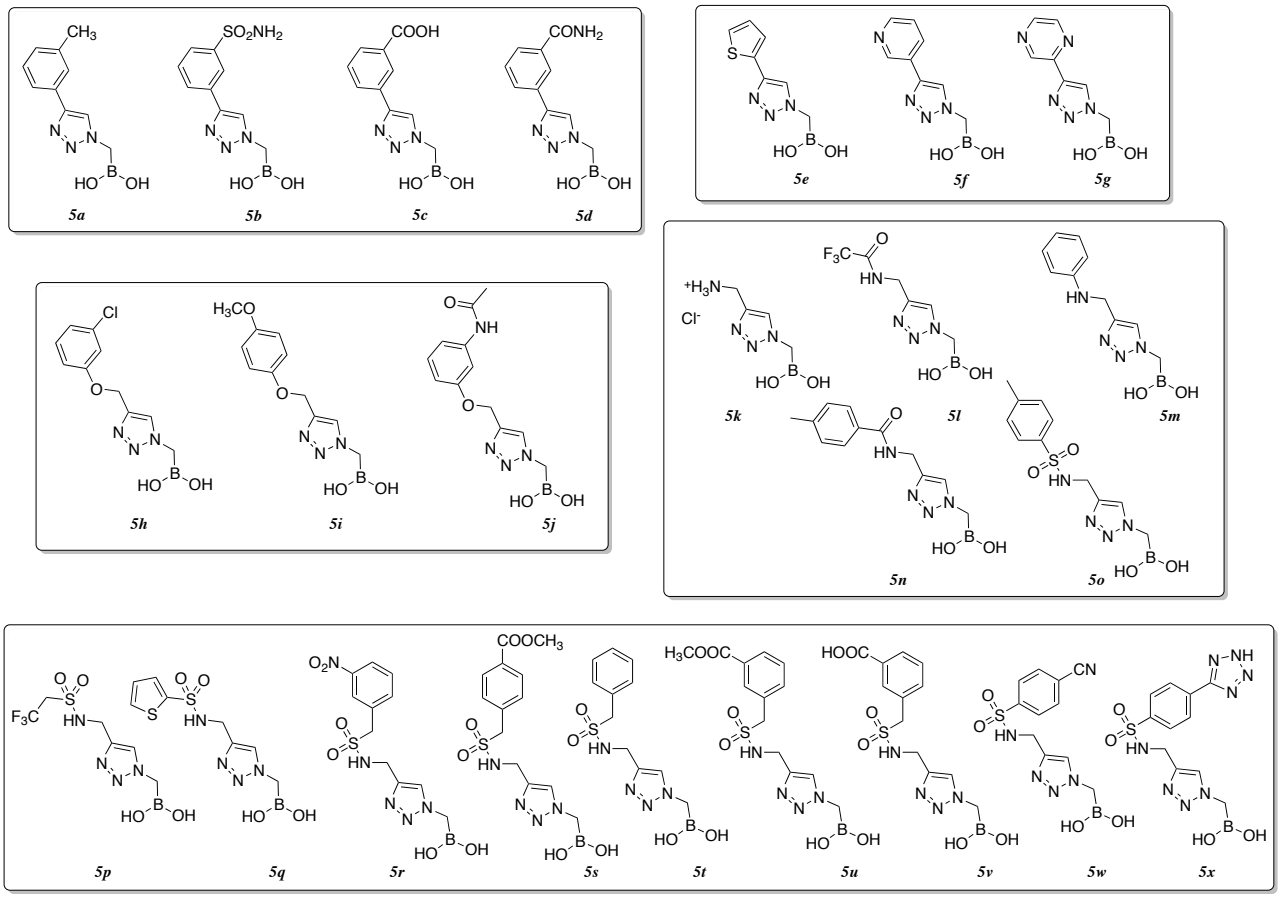

Figure 35. α-Triazolylboronic acids.

Inhibition Kinetics

The binding affinities (K_i) for each of the BATSIs with ADC-7 were determined using competition kinetics with nitrocefin (NCF) used as substrate. The K_i values for all BATSIs, corrected for the NCF affinity, are reported in Chart 2. All compounds showed inhibition of ADC-7 β-lactamase in the low micromolar range. Compounds with an aromatic phenyl ring directly bound to the triazole, exhibit K_i values spanning from 0.2 μM (compound ***5d***) to 1.6 μM (compound ***5b***). When the aromatic moiety is a heterocycle or a substituted benzyloxy group, inhibition remains in the low micromolar range, with the thiophene substituent (***5e***, K_i = 1.0 μM) and the 3-chlorophenyl (***5h***, K_i = 0.98 μM) being the best ones. Compounds ***5k-o*** showed the most surprising results, suggesting that the addition of moieties to the triazole to increase flexibility is not always beneficial: activity varies from 33.8 μM for compound ***5n***, having an amide as a bridge between the triazole and the phenyl ring, down to as low as 90 nM for ***5o***, which replaces the amide of ***5n*** with a sulphonamide. The 300- fold difference in activity between compound ***5n*** and ***5o*** encouraged the synthesis of compounds ***5p-x***, which show nanomolar (***5x***, K_i = 210 nM) to low micromolar (***5p***, K_i =1.46 μM) inhibitory activity against ADC-7 β-lactamase.

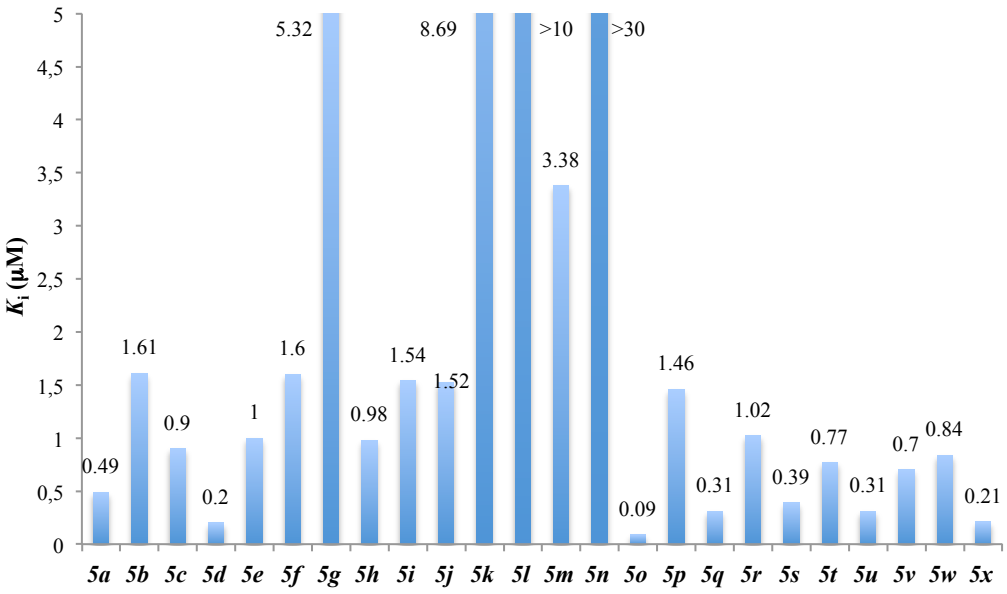

Chart 2. Binding affinities of α-triazolylboronic acids against ADC-7**.**

Analysis of Crystallographic Structures

To identify the structural basis for the observed inhibition of ADC-7 by these novel triazole boronic acids as well as to confirm the triazole functionality as a bioisoster for the R_1 amide group found in the natural β-lactam substrates, X-ray crystal structures of five ADC-7/BATSI complexes were determined (compounds ***5c***, ***5d***, ***5e***, ***5o*** and ***5p***). The stereoview of interactions in the ADC-7/***5o*** complex is reported in Figure 36.

The ADC-7/BATSI complexes were determined to resolutions ranging from 1.80 to 2.04 Å. The boronic acid moiety interacts as expected with the enzyme in most of the complexes. The O_1 hydroxyl group is observed to hydrogen bond with residues that comprise the oxyanion hole (main chain nitrogens of Ser64 and Ser315 and the main chain carbonyl oxygen of Ser315), while the O_2 atom of the boronic acid is modified with a covalently bound phosphate ion, as has been observed in several other ADC-7/BATSI complexes where the BATSI lacks an R_2 group.[2] All complexes exhibited the expected hydrogen bonds between the two lone pairs nitrogens of the triazole ring and the side chain nitrogens of Gln120 and Asn152. Overall, these five structures confirm that, in ADC-7, the triazole is an effective amide bioisoster.

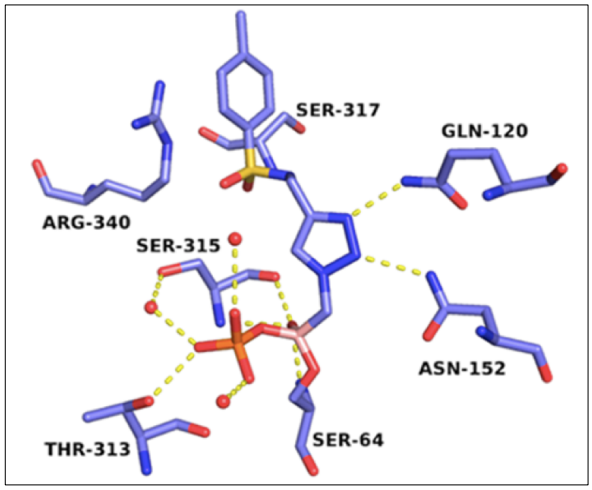

Figure 36. Stereoview of the hydrogen bonding interactions in the ADC-7/***5o*** complex.

Crystallographic structure can be used to explain binding affinities and highlight some differences between the compounds. Where a substituted phenyl ring is directly attached to the triazole (compounds ***5a-d***) K_i values were from 200 nM to 1.61 μM. The benzamide carbonyl oxygen of ***5d*** (K_i = 200 nM), makes a hydrogen bond with Arg340, suggesting the role that interactions with Arg340 may play in increasing binding affinity. Indeed, in ***5c***, where the carboxylate group is flipped ~180° from the benzamide and the negatively charged group is positioned away from Arg340 and oriented toward the solvent, the activity decreased by 4.5 fold (K_i = 900 nM). The role of Arg340 is confirmed comparing the structure of the enzyme in complex with ***5e*** with the ADC-7/***5d*** complex (Figure 37). The two compounds have a 5-fold difference in activity (K_i of 1 μM for ***5e*** *vs* 200 nM for ***5d***): the thiophene ring is placed in the same position as the phenyl ring and does not take advantage of any specific interaction with the enzyme. The most distinctive difference between the two structures is the positioning of Arg340, which is oriented toward the active site in ADC-7/***5e*** complex and away from the active site in the ADC-7/***5d*** complex.

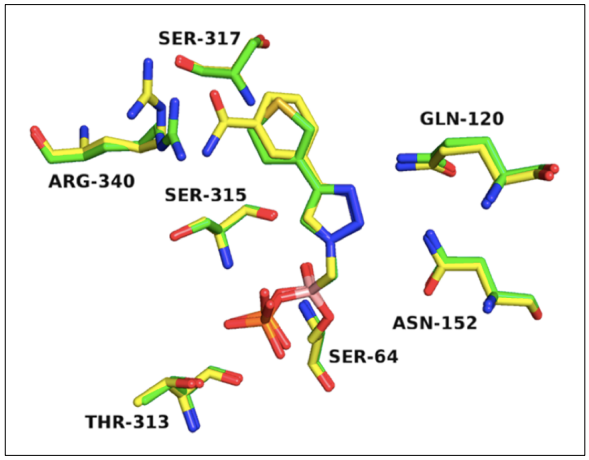

Figure 37. Superposition of ADC-7 in complex with ***5d*** (yellow) and ***5e*** (green).

Significant differences appeared when a substituted aminomethyl bridge was inserted as in compounds

5k-o. Activity, in fact, dramatically dropped when a protonated aminomethyl (compound ***5k***) or acylamino side chain (compounds ***5l*** and ***5n***) was introduced (K_i from 8.7 to 33.8 μM). In contrast, compound ***5o*** with a *p*-tolylsulphonylamino substituent displayed the best activity among all the α-triazolyl BATSIs (K_i = 90 nM), pointing to ***5o*** as one of the best achiral inhibitors of class C β-lactamases. The analysis of the ADC-7/***5o*** complex revealed how the tetrahedral geometry of the sulphonamide allows for cation−π interactions with Arg340, which is probably not reached when a planar geometry is introduced through an amide linker as in ***5n***.

None of compounds ***5p-x*** improved the activity toward ADC-7 with K_i spanning from 0.21 to 1.46 μM. This is probably due to the absence of new favourable interactions and a loss of interaction with Arg340, a residue that is unique to the ADC enzymes as compared to other class C β-lactamases. Compound ***5p*** was the worst one. Its crystallographic structure show that the trifluoroethyl group is unable to make the cation−π interaction seen in the ADC-7/***5o*** complex: Arg340 in fact points away, likely resulting in lower binding affinity of the compound. Compounds ***5r-v*** all contain a methylene linker that may extend the distal group away from Arg340 and prevent this interaction. Compounds ***5w*** and ***5x*** lack this flexible methylene linker: ***5w*** contains a cyano group as compared to the tetrazole of ***5x***, which might impact the ability of the aryl rings to form cation−π interactions with Arg340.

Microbiological assays

The minimum inhibitory concentrations (MICs) data for all the compounds are reported in Table 4. The microdilution MICs were performed in 200 μL wells, with BATSI concentrations maintained at 4 μg/mL. The antibiotic partner for class C β-lactamase strains (*E. coli* DH10B carrying bla_{ADC-7}) was ceftazidime (CAZ) with increasing concentrations from 0.12 to 128 μg/mL. For compounds ***5a-o*** data show a good agreement between kinetic and antimicrobial activity: the lower the MIC, the higher the affinity of the compound. Compound ***5o*** proved to be the best compound under both kinetic and microbiological profile, but also compounds ***5c*** and ***5d*** lowered the MIC value for CAZ from 16 to 2 μg/mL, proving the importance of a carboxylate for cell penetration. For the second series, ***5p-x***, the addition of boronic acid inhibitors decreased the CAZ MIC for *E. coli* DH10B bla_{ADC-7} from 16 to 2 μg/mL for all the compounds with the only exception of compound ***5p***, the only one without an aromatic ring.

Table 4. Cellular assays for compounds ***5a-x***.

Compound	E. coli DH10B bla_{ADC-7}	Compound	E. coli DH10B bla_{ADC-7}
CAZ	16	CAZ	16
5a	4	*5m*	8

5b	4	*5n*	8
5c	*2*	*5o*	*2*
5d	*2*	*5p*	4
5e	8	*5q*	*2*
5f	4	*5r*	*2*
5g	4	*5s*	*2*
5h	4	*5t*	*2*
5i	4	*5u*	*2*
5j	8	*5v*	*2*
5k	8	*5w*	*2*
5l	8	*5x*	*2*

Conclusions

Twenty-four 4-substituted [(1,2,3-triazol-1-yl)-methyl]-boronic acids have been synthesised exploiting the efficient CuAAC click reaction. They were characterized via kinetic analysis, X-ray crystal structures and microbiological assays. All 24 BATSIs displayed K_i values spanning from low micromolar to nanomolar values, with compound ***5o*** being among the best achiral inhibitors of class C β-lactamases.

Crystallographic analyses highlighted Arg340 as a key residue to discriminate the activity of these compounds. Known to be a contributor to protein− protein and protein−ligand interactions, the cation−π interaction observed in these ADC-7/inhibitor complexes suggests that it is important for the design of future series. Arg340 may be important to target as it is unique to this class of enzymes and has shown the ability to interact with a variety of different functional groups (amide, carboxylate, trifluoromethyl, phenyl) in a variety of different interactions, such as Coulombic, ionic, hydrogen bond, and cation−π.

Furthermore, α-triazolylboronic acids proved to be able to restore CAZ activity in *E. coli* DH10B cells carrying $bla_{ADC\text{-}7}$.

3.1.3 α-Triazolylboronic acids as inhibitors of class A β-lactamases

Together with *A. baumannii*, *K. pneumoniae* is among the most clinically- relevant pathogens to be addressed. A meta-analysis published in 2020 confirmed that the trend in the isolation rate of *K. pneumoniae* is increasing and there is a rapid global emergence of strains of this organism resistant to almost all antibiotics, including carbapenems.[4] The main resistance mechanism responsible for antibiotic resistance is the production of *Klebsiella pneumoniae* carbapenemases (KPCs), β-lactamases belonging to class A. To date, at least 54 variants of KPC have been identified, although KPC-2 and KPC-3 are the most common.[5] Encouraged by the results obtained on ADC-7, 14 α-triazolylmethaneboronic acids (compounds ***5k-x***) were tested against KPC-2 in kinetic and microbiological assays. Moreover, docking studies were performed to rationalize the structure-activity relationship.

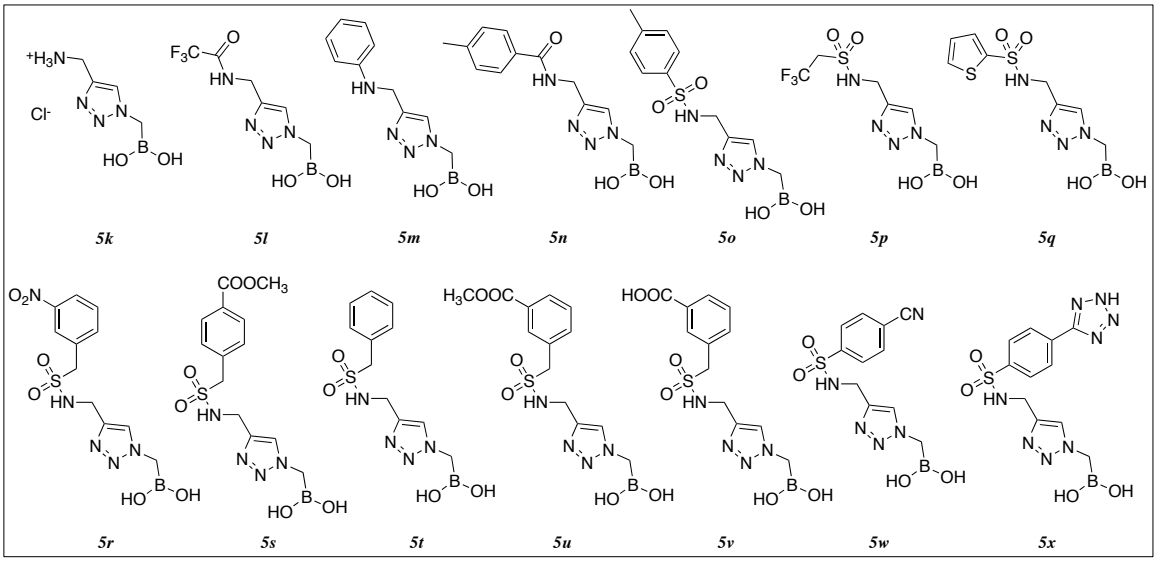

Figure 38. α-Triazolylboronic acids tested against KPC-2.

Inhibition Kinetics

Also in this case, the binding affinities for each compound ***5k-x*** with KPC-2 enzyme were determined using competition assays with NCF as substrate. The K_i values for all BATSIs, corrected for the NCF affinity are reported in Chart 3. Compounds ***5o-x*** with the methylsulphonamide chain performed better (K_is from 1 nM to 92 nM) than the planar substituted carboxamides ***5l*** (K_i = 1.28 μM) and ***5n*** (K_i = 0.196 μM). The only exception was compound ***5x*** (K_i = 0.295 μM), which, besides the phenylsulphonamide side chain, bears a tetrazole ring on the phenil *para* position, thus suggesting that a negative charge in this position is detrimental for affinity. This observation is corroborated by the affinities detected for compound ***5u***, bearing a methoxycarbonyl substituent (K_i = 10 nM), and compound ***5v***, bearing a carboxylate (K_i = 42 nM).

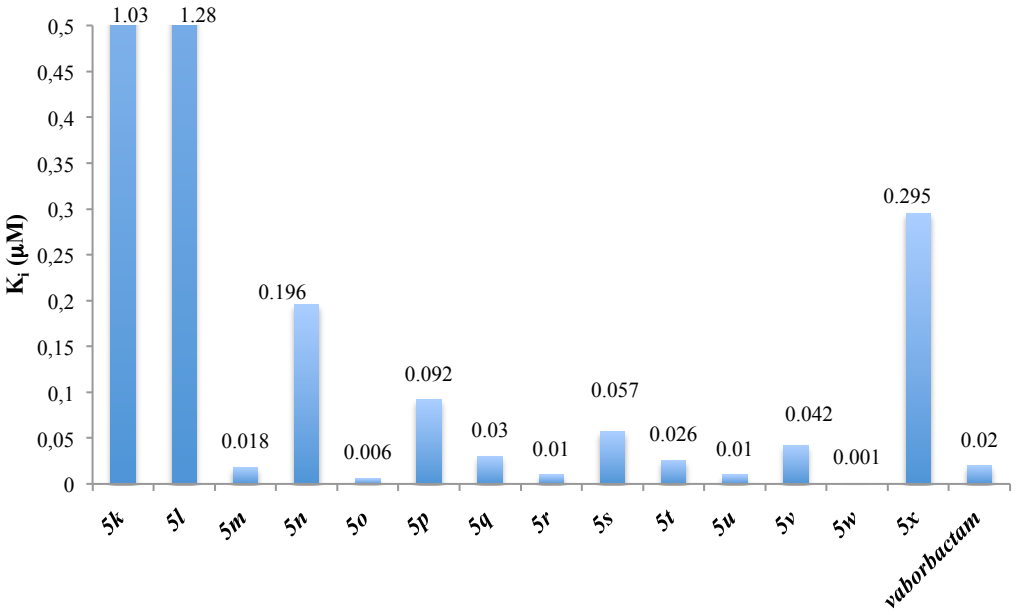

Chart 3. Binding affinities against KPC-2 of compounds ***5k-x***.

Both series of compounds bearing a carboxamide and a sulphonamide point to an enhancement of activity when an aromatic ring is inserted. Comparison of compounds ***5l*** with ***5n*** and ***5p*** with ***5t*** demonstrated a gain in affinity for KPC-2 enzyme by more than 6 times in acylamido compounds (***5l***, K_i = 1.28 μM *vs* ***5n***, K_i = 0.196 μM) and by 4 times in sulphonamido compounds (***5p***, K_i = 92 nM *vs* ***5t***, K_i = 26 nM).

Molecular docking

Aiming to rationalize the relationship between structure and affinity, docking studies were performed. The crystal structures of KPC-2 *apo*-enzyme (PDB ID: 2OV5) and KPC-2 in complex with vaborbactam (PDB ID: 6TD0) showed that Trp105 side chain, positioned at the entrance of the active site is changing its position more than 90° (Figure 39). The molecular modeling based on KPC-2 *apo*-enzyme is consistent with the crystal structures, showing that the flexibility of Trp105 changes in the active-site cavity, and the receptor-ligand interaction surface.

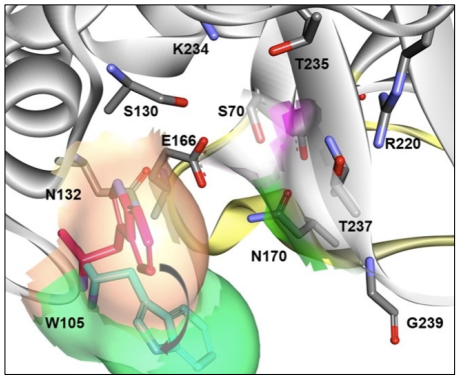

Figure 39. KPC-2 serine β-lactamases active site with important catalytic residue labeled.

The molecular docking for compounds ***5w*** and ***5q*** suggests that the α-triazolylboronic acids are accommodated very well into the active site of the KPC-2 enzyme. In particular the triazole ring makes favorable π–π stacking interaction with Trp105, thus allowing the best positioning of the boronic group (Figure 40). We caution that docking studies only provide hypothesis to assist in the interpretation of K_i values for such very active compounds, and further crystallographic experiment are needed. However, these results highlight the potential offered by α-triazolylboronate in KPC mediated resistance.

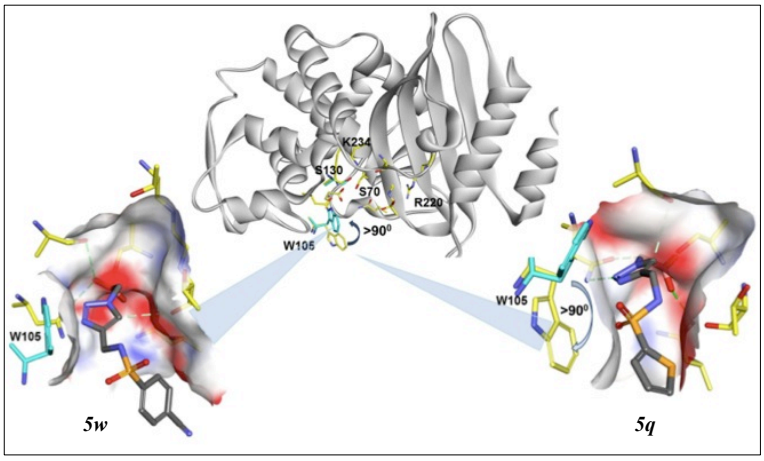

Figure 40. Molecular modeling of ***5w*** and ***5q*** into the active site of KPC-2 (PDB ID: 2OV5)

Microbiological assays

The activity of compounds ***5k-x*** in combination with cefepime (FEP) against *Klebsiella bla*$_{KPC-2}$ and KPC-Kpn cells was also determined (Table 5). Cefepime was chosen as partner as it exhibits rapid cell penetration and it is stable to AmpC cephalosporinases. The compounds (with the only exception of ***5s***) lowered the MIC for cefepime in both strains. However, the trend of antimicrobial activities was not always correlated with K_i values. Although the presence of a negative charge was detrimental for affinity, it improved MICs: compound ***5v*** had MICs of 1 μg/mL in KPC-Kpn strain and 2 μg/mL in *Klebsiella bla*$_{KPC-2}$, values 3 fold higher than the structurally related compound ***5u***. Comparison between compounds bearing the cyano group ***5w*** and the tetrazole ring ***5x*** confirmed that whereas the negative charge lowered activity by 300 times (***5w***, K_i = 1 nM *vs* ***5x***, K_i = 295 nM), MICs lower 1 fold. The presence of a phenyl ring on the triazole substituent had opposite effect on MICs in respect to K_i values, given the decrease of MICs from compounds ***5l*** to ***5n*** and from ***5p*** to ***5t***. The compound with the best affinity for KPC-2 was ***5w***, with a K_i as low as 1 nM. This compound bears a *p*-cyanophenyl substituent on the sulphonamide, and it exhibits good microbiological activity (MIC = 4 μg/mL for both strains). However, the compound with the best effect in restoring antibiotic susceptibility associated with β-lactamase inhibition is ***5q*** (K_i = 30 nM, MIC in KPC-Kpn = 0.5 μg/mL) with a thiophene replacing the phenyl ring. Many factors must be considered with interpreting MIC and kinetic differences, such as the complexity of β-lactamase background, cell entry, efflux, time

dependence of inhibition, etc. The data for compound ***5q*** is closely comparable with those obtained for the commercially available cyclic boronate vaborbactam (K_i = 20 nM, MIC in KPC-Kpn = 0.5 μg/mL). This is remarkable considering that vaborbactam has two stereocenters and a more complex synthetic access and at the same time, it underlines the potential offered by the triazoleboronates as bioisosters of amidoboronates.

Table 5. Cellular assays for compounds ***5k-x***.

Compound	MIC KPC-Kpn	MIC *K.pneum.* bla_{KPC-2}	Compound	MIC KPC-Kpn	MIC *K.pneum.* bla_{KPC-2}
FEP	32	32	***5r***	4	16
5k	4	4	***5s***	16	32
5l	4	2	***5t***	2	16
5m	2	4	***5u***	8	16
5n	8	16	***5v***	1	2
5o	4	4	***5w***	4	4
5p	1	2	***5x***	8	8
5q	0.5	2	**vaborbactam**	0.5	1

Conclusions

From the 24 4-substituted [(1,2,3-triazol-1-yl)-methyl]-boronic acids, synthesised exploiting the efficient CuAAC click reaction and successfully tested on ADC-7, 14 compounds were tested on KPC-2. Kinetic analysis, molecular docking and microbiological assays were performed to fully characterize the activity of these compounds. They emerged as a new promising scaffold for *K. pneumoniae* carbapenemases inhibition. In particular, compound ***5q*** bearing a sulphonamide substituted by a tiophene ring proved to be an excellent KPC-2 inhibitor (K_i = 30 nM) and it restores cefepime susceptibility in KPC-Kpn cells. These values are comparable to the commercially available vaborbactam, which is prescribed for *Klebsiella* infections. More experiments are needed to determine the exact binding mode of these molecules and to investigate their cross class activity. However, the results obtained are very promising in the fight against KPC-mediated resistance.

3.1.4 α-Triazolylboronic acids as inhibitors of class B β-lactamases

Class B β-lactamases are metallo- hydrolases that require one or two zinc ions to catalyse the hydrolysis of substrates (Scheme 8). They are active against all types of β-lactams, except for aztreonam (however, it is attacked by some SBLs) and traditional β-lactamases inhibitors, such as clavulanic acid, sulbactam or tazobactam are not able to inhibit them.

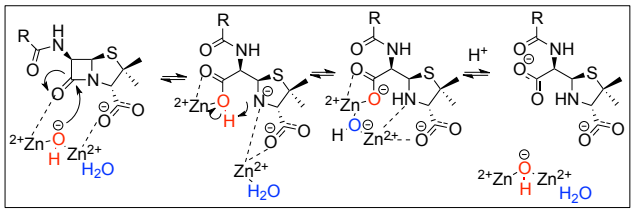

Scheme 8. Mechanism of action of MBLs.

MBLs are sorted in three classes on the basis of their primary structure and number of zinc ions required: B1, B2 and B3. B1 and B3 MBLs possess two zinc ions in their catalytic site and they have a larger spectrum of action if compared with B2 enzymes, where only one zinc ion is present. In B1 and B3 enzymes one zinc ion is tetrahedrally coordinated by some residues of the enzyme, while the other one has a trigonal-planar coordination and there is one water molecule or hydroxide (OH^-) which coordinates both the zinc ions (Figure 41). In B2 enzymes, on the other hand, there is only one zinc ion, which coordinates three amino acid residues in the active site and a water molecule or hydroxide (Figure 41).

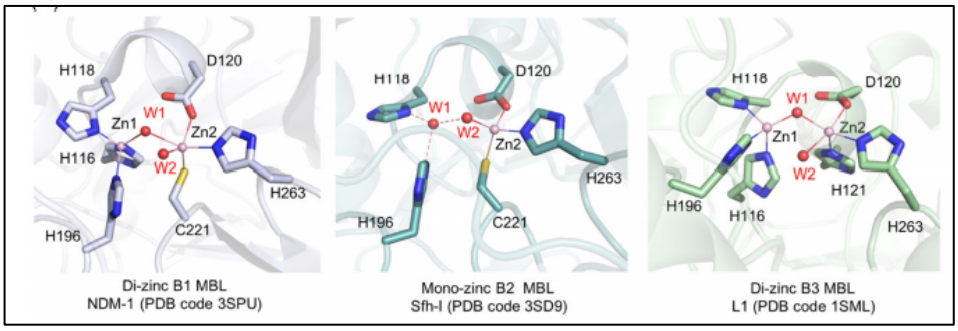

Figure 41. MBLs active sites (from *Medicinal Research Review*, **2020**, *40*, 1558-1592).[6]

Previously described α-triazolylboronic acids ***5a-o*** were tested in disc assays against *E.coli* NDM-1, in combination with imipenem. Compounds ***5b***, ***5c***, ***5d*** and ***5f*** (reported in Figure 42), all containing an aromatic ring directly bound to the triazole were the best performing compounds, but they demonstrated only a low microbiological activity.

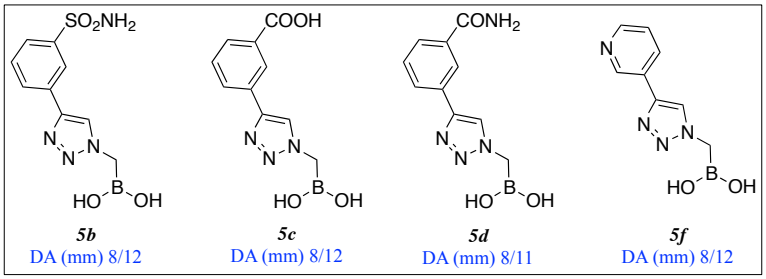

Figure 42. α-Triazolylboronic acids which demonstrated good results in disk assays against NDM-1. Disks were performed with 10 μg of inhibitor and 10 μg of partner antibiotic, imipenem. The diameter (mm) of inhibition was recovered and compared with that of imipenem alone (8 mm).

Therefore, a new strategy was followed to obtain α-triazolylboronic acids, which could inhibit not only class C and class A β-lactamases, as described in previous chapters, but also class B MBLs. To do this, the general structure of 1,4-disubstituted triazoles should be decorated with groups able to interact with zinc ions (Figure 43).

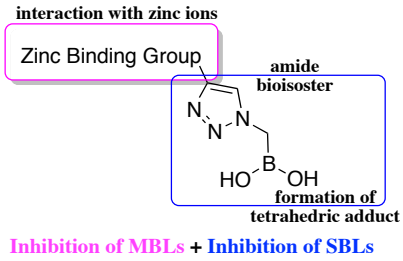

Figure 43. Schematic rappresentation of dual inhibitors of SBLs and MBLs.

Looking at the literature, three strategies are commonly pursued to inhibit zinc-containing enzymes: removing the zinc ions through chelating agents; substituting the zinc ions with other atoms (bismuth); binding the zinc ions with zinc binding groups (ZBGs). The third strategy is the most used, inserting different functional groups able to bind zinc ions (such as thiols, carboxylic acids, nitrogen containing heterocycles or hydroxamates).[6] Therefore, 8 ZBGs were selected and inserted on α-triazolylboronic acids (Figure 44) to bind zinc ions and inhibit MBLs. Synthesis of compounds ***6a-h*** followed the same synthetic procedure reported in section 3.1.1 and in scheme 7 for compounds ***5a-x***.

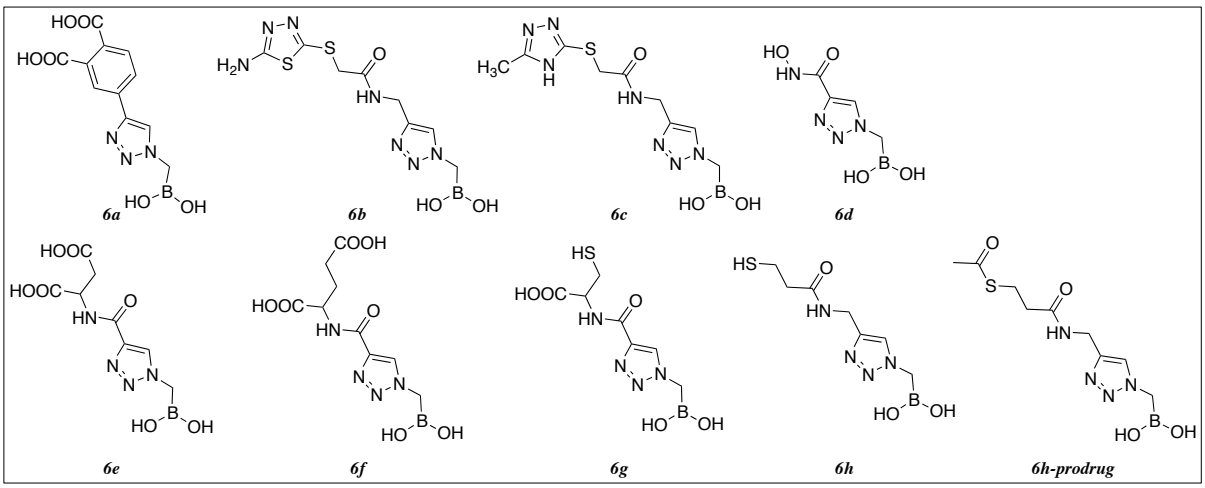

Figure 44. α-Triazolylboronic acids containing zinc binding groups.

Preliminary in vitro tests

The binding affinity of six α-triazolylboronic acids with ZBGs was determined in competition assays after 5 min incubation with VIM-2 periplasmic extract and using NCF as reporter substrate. K_is for ***6d*** and ***6g*** were not measured because of paucity of material obtained.

Compound ***6h*** was tested also in its protected form (Figure 44), to avoid the easy oxidation of the –SH and formation of disulphide bridges. The protected form was tested, considering that the hydrolysis of the thioester, known to be more reactive than esters, could take place in the experiment media. In any case, ***6h*** was the only compound able to decrease the speed of the reaction when tested at 50 μM (IC_{50} = 7.7 μM). All other molecules were inactive against VIM-2 β-lactamase.

Conclusions

Eight α-triazolylboronic acids decorated with zinc binding groups were designed. The synthesis of all compounds was successfully achieved and all compounds were tested in preliminary assays on VIM-2, class B β-lactamase. Compound ***6h*** was the only ZBG bearing α-triazolylboronic acid that demonstrated to inhibit VIM-2, with a K_i value of 7.7 μM. More experiments are needed to determine the binding mode of this compound and to understand why other ZBGs are not effective in inhibit MBLs. Probably, the synthesis of new chiral compounds will optimize the activity of these α-triazolylboronic acids. Even if the results were disappointing, the discovery of a triazolylboronic acid able to interact with MBLs is a positive and encouraging step towards the inhibition of this class of enzyme. As described below, this was only one of the strategy targeting MBLs we are following (see chapter 5).

3.2 Sulphonamides

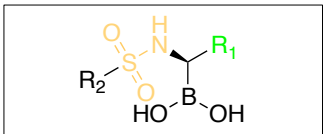

α-sulphonamidoboronic acids

The results obtained with α-triazolylboronic acids against class C and class A β-lactamases encouraged the search for new broad spectrum compounds active also against class D enzymes. Very little is described in the literature regarding the inhibition of this class by boronic acids.[7] In particular, vaborbactam has no inhibitory activity against OXA β-lactamases. However, taniborbactam and QPX7728 are boronic acid inhibitors in clinical development, which exhibited activity against all classes of β-lactamases. All the α-triazolylboronic acids library described in 3.1.2 showed poor affinity against class D β-lactamases with K_i values > 100 mM. For this reason a different class of amide bioisosters, namely sulphonamides, was explored. Achiral α-sulphonamide boronic acids have been already tested as inhibitors of class C AmpC enzymes.[8] Against this class of enzymes they demonstrated to retain inhibition activity if compared to carboxamide analogues and to rescue antibiotic resistance when used in combination with third generation antibiotics. X-ray crystal structures of AmpC in complex with these compounds confirmed that the sulphonamide group maintained two of the canonical interactions in the amide binding site

(the two oxygen atoms of sulphonamide form hydrogen bonds with the conserved Gln120 and Asn152 residues), thus behaving as amide bioisoster. However, the presence of the sulphonamide moiety was observed to change the geometry of the inhibitors: the sulphonamide possesses a tetrahedric structure, which changes the way of inhibitor interactions and the structure activity relationship. The substituent bound to the sulphonamide is positioned on the R_2 side, where the presence of a carboxylate mimics the C3/C4 carboxylate of β-lactams[9]; while the carbon α to the boron points where the R_1 side chain of β-lactams is positioned.

Therefore, α-sulphonamidoboronic acids with a benzyl or *m*-carboxybenzyl group as R_2 substituent were designed (Figure 45). The benzylic linker between the sulphonamide and the –COOH increases the flexibility and the conformational freedom of the R_2 side chain. On the other side, an H or a little hydrophobic substituent was introduced as R_1, based on the analysis of crystal structures of class D enzymes in complex with carbapenems.

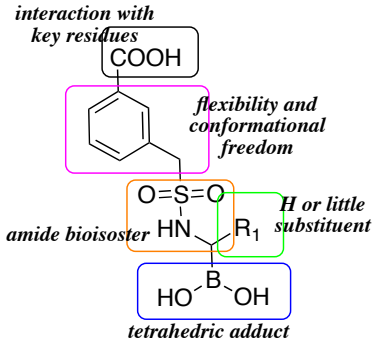

Figure 45. Schematic representation of the structure of α-sulphonamidoboronic acids designed as inhibitors of class A, C and D β-lactamases.

3.2.1 Synthesis of α-sulphonamidoboronic acids

The synthetic process to obtain α-sulphonamidoboronic acids is summarized in Scheme 9. Commercially available alkylboronic acids were converted in corresponding pinanendiol esters. (+)- or (-)- pinanendiol were used as chiral auxiliary for stereoselective insertion of the halogenated and asymmetrically substituted carbon atom in the pre-existing C-B bond through homologation. The conversion of compounds ***7*** in the corresponding α-chloroboronates was carried out at -100°C in anhydrous THF where dichloromethylithium is formed *in situ* starting from distilled CH_2Cl_2 (2 eq.) and *n*-BuLi (1.2 eq.). α-Chloro alkylboronates ***8*** were obtained in 90-97% yield and then reacted in a nucleophilic substitution with lithium bis(trimethylsilyl)amide (1.1 eq.) in dry THF to synthesise compounds **9** (63% yield). The hydrolysis to the corresponding hydrochloride salts ***10*** (90% yield) was accomplished using HCl 4 M in dioxane (3.5 eq.). Two different commercially available sulphonyl chlorides (benzylsulphonyl chloride and *m*-carboxybenzylsulphonyl chloride) were used to obtain α-sulphonamidoboronates (80% yield). Final deprotection of the pinanendiol ester was accomplished by transesterification with isobutylboronic acid (0.95 eq.) and HCl 3 M (3 eq.), allowing

one to obtain final boronic acids ***12***.

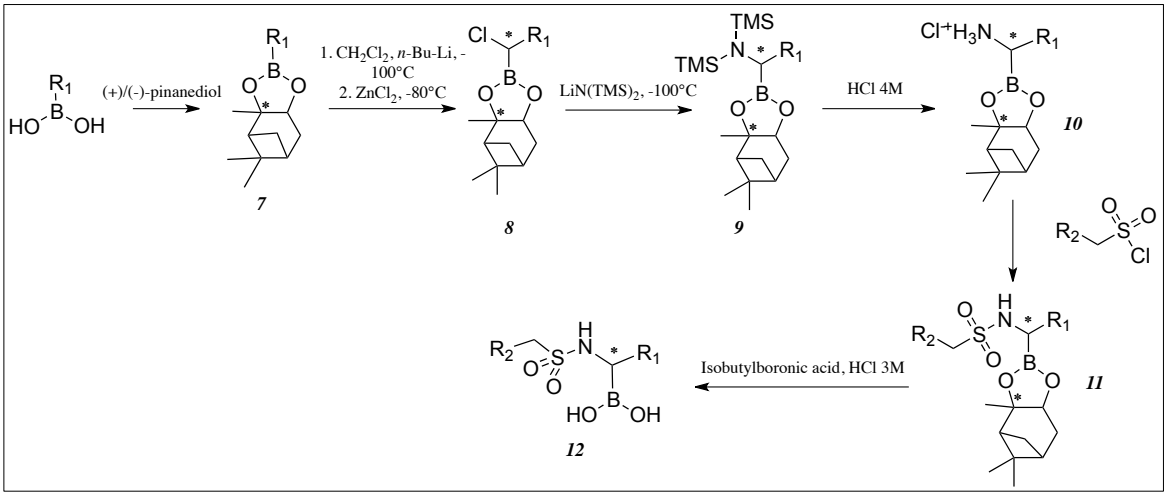

Scheme 9. Synthesis of chiral α-sulphonamidoboronic acids.

3.2.2 α-Sulphonamidoboronic acids as inhibitors of class D β-lactamases

Class D β-lactamases are different from other SBLs in their structure and behaviour. They can be differentiated into 14 families and OXA enzymes represent the largest family. OXA enzymes are named also oxacillinases for their ability to hydrolyse this class of antibiotics and they are classified into subfamilies on the basis of the substrates they are able to hydrolyse (OXA-23, OXA24/40, OXA-48, OXA-51, OXA-58, OXA-134a, OXA-143, OXA-211, OXA-213, OXA-214, OXA-229 and OXA-235). These enzymes were initially isolated from *A. baumannii*, but later they were identified also in other *Acinetobacter spp*., in *P. aeruginosa* and in *K. pneumoniae* strains. OXA enzymes are able to hydrolyze penicillins but have also shown activity towards cephalosporins and carbapenems; in particular, OXA 24/40 is the most active subclass enzyme towards carbapenems.

The most important feature, which differentiates class D β-lactamases from others, is the presence of a tunnel-like entrance to the active site, first identified in OXA 24/40 enzymes, where it is formed through the specific arrangement of Tyr112 and Met223 side chains. These residues create a barrier, which avoids the entrance of antibiotics with bulky substituents, while little substituents, such as the hydroxyethyl side chains of carbapenems, are easily accommodated under the barrier (Figure 46).[10]

Doripenem is the carbapenem with the highest affinity towards OXA 24/40 and the study of its structure in complex with the enzyme (Figure 46) provided important insights for the development of new boronic compounds.

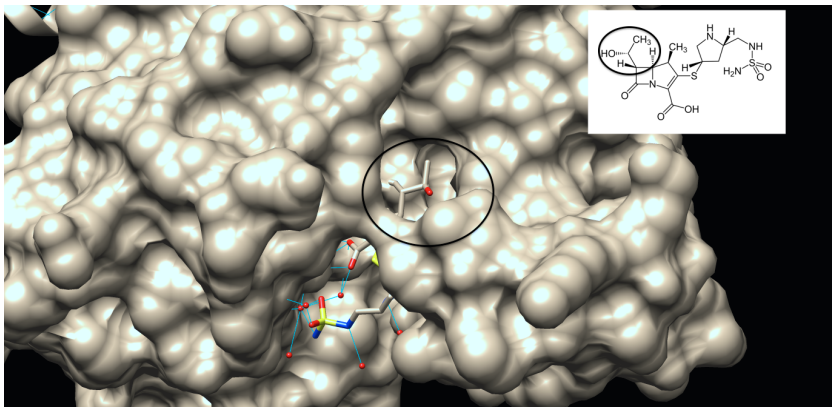

Figure 46. Doripenem in the active site of OXA 24/40.

The opened β-lactam ring of doripenem is positioned behind the bridge formed by Tyr112 and Met223 side chains. The carboxylate interacts with Arg261, which is the conserved recognition residue. The planar position of the sulphur atom that bridges the pyrroline and the pyrrolidine rings forces the pyrrolidine in a hydrophobic pocket composed of Met114, Tyr112, Met223 and Trp221. Therefore, the R_2 site, where the carbapenem "tail" is located, is relatively open and offers a lot of space. On the other hand, the site where the hydroxyethyl chain binds does not offer much space to expand. It is important to notice also the different conformation of the R_1 side chain between carbapenems and other β-lactam antibiotics. In fact, the stereochemistry at C(7) in cephalosporins is *opposite* with respect to C(6) in carbapenems (Figure 47). Therefore, even if the hydroxyethyl chain occupies a little binding site, trajectory can be changed > 90° to occupy the R_1 binding site, where there is more space and lots of hydrophobic side chains (Val130, Trp167, Leu168, Val169).

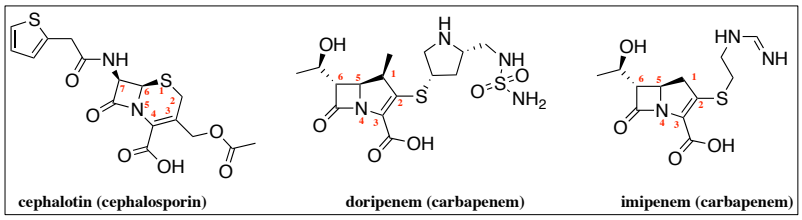

Figure 47. Comparison between β-lactam antibiotics.

Starting from the knowledge about OXA 24/40 structure, a series of α-sulphonamidoboronic acids were synthesised where a little hydrophobic substituent was inserted in position R_1 (compounds ***12a-f***, Figure 48). The only exception was compound ***12f***, the only achiral compound where R_1= H. In all other compounds an ethyl or methyl group was added to mimic the hydroxyethyl group of carbapenems and improve affinity for class D enzymes. Corresponding compounds that lacked the terminal carboxylate group were also synthesized. The goal was i) to explore whether there was a preference for one chiral orientation over another, ii) to see if there was space to accommodate either a methyl or ethyl group, and iii) to test the importance of the carboxylate group. To verify all these information, chiral sulphonamide BATSI where tested in kinetic and microbiological assays. Moreover, crystal structures of compounds ***12d***, ***12e*** and ***12f*** in complex with OXA-24/40 were

performed. These three compounds were chosen because they differ only in the chirality of the α carbon to the boron (R, S, achiral respectively).

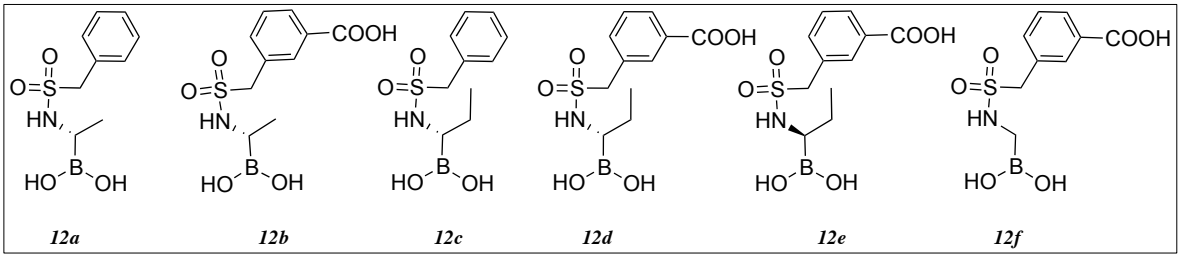

Figura 48. α-Sulphonamidoboronic acids (***12a-f***).

Inhibition Kinetics

The binding affinities for each compound ***12a-f*** with OXA-24/40 enzyme were determined after a 3 min pre-incubation of drug and enzyme, using competition assays with NCF as substrate. The K_i values for all BATSIs, corrected for the NCF affinity are reported in Chart 4.

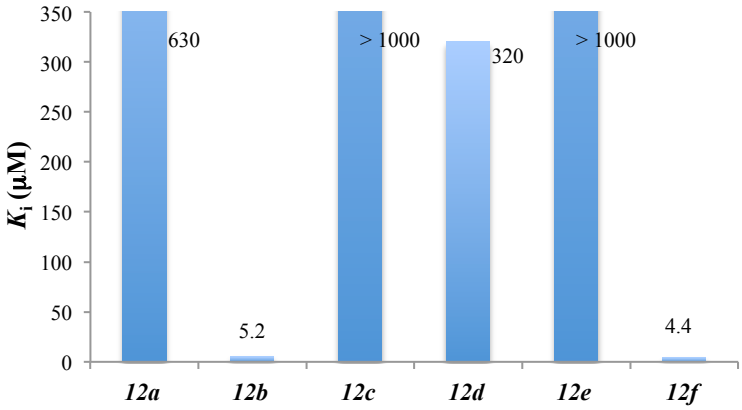

Chart 4. Binding affinities against OXA 24/40 of compounds ***12a-f***.

The best inhibitors of the group are ***12f*** (K_i = 4.4 μM) and ***12b*** (K_i = 5.2 μM). At the same time, the worst inhibitors are ***12c*** (K_i > 1000 μM) and ***12e*** (K_i *vs* > 1000 μM). The bests and the worsts differ by three structural characteristics: chirality at the α carbon, the presence of the *m*-carboxylate on the aromatic ring and the number of carbons attached to the chiral centre. The R configuration is preferred than the S configuration, as confirmed by the different affinity between compounds ***12d*** (K_i = 320 μM) and ***12e*** (K_i > 1000 μM) which differ only for this characteristic. The *m*-carboxylate is important for the inhibition and the fewer carbons attached in R_1 position, the better the affinity: in compound ***12f*** R_1 = H and in compound ***12b*** R_1 = CH_3.

Analysis of crystallographic structures

Compounds ***12d***, ***12e*** and ***12f*** were crystallized in complex with OXA-24/40 enzyme. The analysis of X-ray crystal structures confirmed the results obtained in kinetic assays. The chirality in ***12d*** was

confirmed to be preferred over that in ***12e***, as ***12d*** maintains the interaction with Arg261, fundamental in doripenem binding and present also in ***12f***. Indeed, the inhibitors bind away from the Tyr112/Met223 bridge, allowing the terminal carboxylate group to form a key ionic interaction with the class D carboxylate recognition residue Arg261 in the same way as the –COOH in doripenem. In ***12f*** the carbon α to the boron is in the same position where the hydroxyethyl side chain of doripenem is pointing. The ethyl substituent of ***12e*** is well accommodated in this position, while the substituent of ***12d*** clashes with the main chain carbonyl O of Trp221 and it is in close contact with Leu168. Interestingly in both complexes with chiral compounds, Val130 adopts 2 conformers, which is not the case in the OXA-24/40/***12f*** complex. For ***12e***, the carboxylate group clashes with Val130 in its "open" conformation and it is in close contact with the main chain carbonyl O of Ser128.

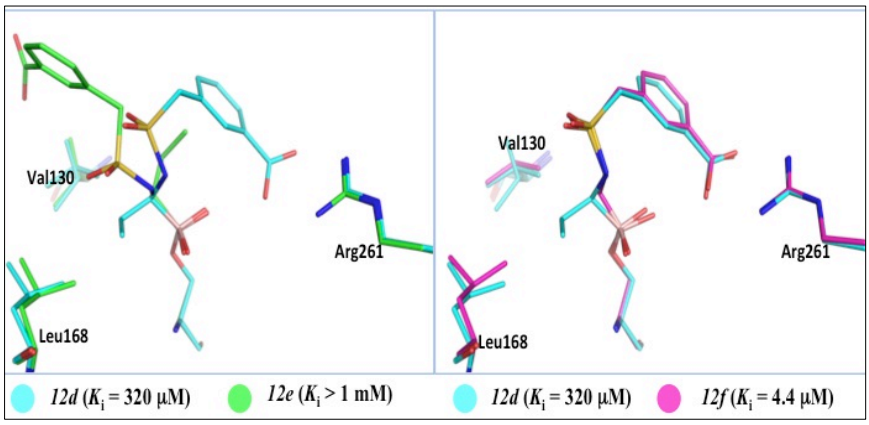

Figure 49. Stereoview of the main interactions of compounds ***12d***, ***12e*** and ***12f*** with OXA-24/40.

Microbiological assays

α-Sulphonamidoboronic acids ***12a-e*** were tested against two bacterial strains expressing class D OXA-23 and OXA 24/40 β-lactamases respectively and MIC values were evaluated (Table 6). The experiments on the class D *A. baumannii* pWH1266/OXA-23 strain were performed with ceftazidime (CAZ), cefepime (FEP) and imipenem (IMI) as antibiotic partners and the same was carried out for class D *A. baumannii* pWH1266/OXA-24/40 strain. In according with kinetic analysis and X-ray crystal structure, the most potent inhibitor was ***12b***, decreasing the MICs for FEP from 32 µg/mL to 8 µg/mL in both experiments and the MICs for IMI from 64 to 32 µg/mL for OXA-23 and from 128 to 64 µg/mL for OXA 24/40. All the other BATSIs were not so good inhibitors in OXA assays. Unfortunately, compound ***12f*** was not included in these assays.

Table 6. Cellular assays for compounds ***12a-e***.

Compound	MIC *A. baumannii*, pWH1266/OXA-23			MIC *A. baumannii*, pWH1266/OXA-24/40		
	CAZ	FEP	IMI	CAZ	FEP	IMI

/	4	32	64	4	16	128
12a	2	16	32	4	16	64
12b	4	8	32	2	8	64
12c	4	16	32	2	16	64
12d	4	16	32	4	16	64
12e	4	16	32	4	8	128

Conclusions

Six α-sulphonamideboronic acids were synthesised and tested in an attempt to gain activity against class D OXA β-lactamases. Their structure was designed on the basis of previously obtained sulphonamidoboronic acids and taking into account the crystallographic structure of doripenem in complex with OXA-24/40 enzyme. Therefore, a benzylic or *m*-carboxybenzylic substituent on the sulphonamide chain was inserted, while H or a little hydrophobic substituent was inserted in R_1 position. The best compound of the series was ***12f***, the only achiral α-sulphonamidoboronic acid, where R_1 = H.

Analysing all data collected it is possible to highlight that i) one chiral orientation is better than the other (***12d*** is better than ***12e***) and the preferred R configuration is *opposite* than the configuration commonly adopted for inhibition of class C enzymes; ii) the fewer carbons attached to the carbon next to the boron, the better the binding (***12f*** is better than ***12b***, which is better than ***12d***). This can be explained by slight steric interactions between both the carbons of the ethyl group in ***12d*** and the side chain of Leu168 and the carbonyl oxygen of Trp221. iii) The carboxylate group contributes to binding affinity making a good ionic interaction with the active site Arg261.

All the results obtained encourage the development of new compounds to improve inhibitory activity, starting from compound ***12f***, which is the best inhibitor of class D β-lactamases identified so far.

Experimental section

General synthetic information

Reactions were monitored by thin layer chromatography (TLC), which were visualized by UV fluorescence and by Hanessian's cerium molybdate stain. Deoxygenated water was obtained through sonication. Melting points were measured in open capillary tubes on a Stuart SMP30 Melting Point apparatus. ^{1}H and ^{13}C NMR spectra were recorded on a Bruker Avance-400 MHz spectrometer. Chemical shifts (δ) are reported in ppm and were calibrated to the residual signals of the deuterated solvent. Multiplicity is given as s = singlet, d = doublet, t = triplet, q = quartet, m = multiplet; coupling constants (J) are given in Hz. Two-dimensional NMR techniques (COSY, HMBC, HSQC) were used to aid in the assignment of signals in ^{1}H and ^{13}C spectra. Particularly, in the ^{13}C spectra, the signal of the boron-bearing carbon atom, which tend to be broadened, and the signal of the quaternary triazole carbon (when present) are often beyond the detection limit, but their resonances were unambiguously determined by HSQC and HMBC. Mass spectra were determined on an Agilent Technologies LC-MS (n) Ion Trap 6310A (ESI, 70 eV). High-resolution mass spectra were recorded on an Agilent Technologies 6520 Accurate-Mass Q-TOF LC/MS.

Synthesis of 1,4-disubstituted 1,2,3-triazolylboronic acids

Synthesis of (+)-pinanediol α-azidomethaneboronate (2)

Two strategies were applied to synthesise compound ***2*** starting from potassium (bromomethyl)trifluoroborate or from triisopropylborate.

Synthesis from potassium (bromomethyl)trifluoroborate

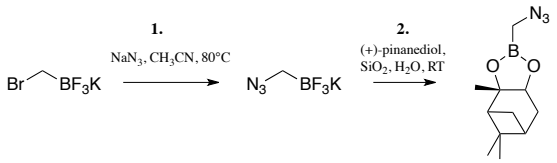

1. The commercially available potassium (bromomethyl)trifluoroborate (14.9 mmol) and sodium azide (17.9 mmol) were suspended in 30 mL CH_3CN and refluxed (80°C) for 4 hours. The reaction was allowed to reach room temperature and the solid (NaBr) was filtered over a celite pad and abundantly washed with CH_3CN (30 mL). The filtered solution was concentrated under vacuum to afford ***1*** as a white solid, which was triturated with Et_2O.

2. Compound ***1*** (14.11 mmol), (+)-pinanediol (14.11 mmol) and silica flash (SiO_2, 21.17 mmol) were suspended in deoxygenated water (15 mL) at room temperature for 16 hours. The suspension was filtered on a celite pad and washed with abundant ethyl acetate. The two phases were separated and the organic phase washed with water, brine and dried with Na_2SO_4, filtered and concentrated in *vacuo*. The crude residue was purified through chromatography (SiO_2, petroleum ether /diethyl ether 7:3).

Synthesis from triisopropylborate

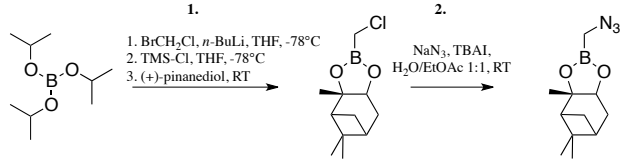

1. Triisopropyl-borate (12.99 mmol) and chloro-bromo-methane (15.07 mmol) were dissolved in dry THF (8 mL) under argon. The temperature was cooled to -78°C. *n*-Butyl-lithium (13.63 mmol) was added dropwise (45 min).

The mixture was stirred for 1h, then trimethyl-silyl-chloride (TMS-Cl, 15.07 mmol) was added. The mixture was allowed to reach room temperature slowly overnight, under vigorous stirring. The formation of a white precipitate was observed. Solid (+)-pinandiol (12.99 mmol) was added. The precipitate disappeared and the mixture was stirred for two more hours. The volume of the reaction mixture was concentrated and 50 mL of ethyl acetate and 20 mL of H_2O were added. The two phases were separated; the aqueous one was re-extracted with ethyl acetate (2 x 25 mL) and the combined organic phases were washed with 25 mL of brine, dried with Na_2SO_4, filtered and evaporated.

2. (+)-pinanediol α-chloromethaneboronate (0.012 mmol), NaN_3 (0.12 mmol) and *tert*-butylammonium iodide (6 mmol) were solubilized in 16.21 mL of ethyl acetate and 40 mL of H_2O were added. The reaction mixture was stirred overnight. Petroleum ether (90 mL) and H_2O / $NH_4Cl_{(sat)}$ 1: 1 (40 mL) were added and the two phases were separated. The aqueous one was re-extracted with petroleum ether (2 x 90 mL) and the combined organic phases were dried with Na_2SO_4, filtered and evaporated. The crude was purified by column chromatography (eluent phase: petroleum / ether 8: 2).

Potassium (azidomethyl)trifluoroborate (1)

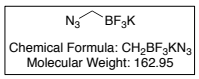

White solid (90%). ^{1}H NMR (500 MHz, DMSO-d6): δ 2.03 (s, 2H). ^{13}C NMR (125.8 MHz, DMSO-d6): δ no peaks. ^{19}F (470.8 MHz, Acetone-d6): δ -146.4. ^{11}B NMR (128.4 MHz, Acetone-d6): δ 3.48. MS: m/z $[M-K]^-$ theo.124.0294; found, 124.0296.

(+)-pinanediol α-chloromethaneboronate

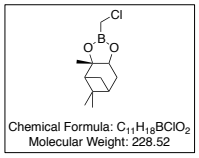

Pale yellow oil (93%). ^{1}H NMR (400 MHz, $CDCl_3$) δ 4.49 (dd, J = 8.7, 2.0 Hz, 1H, CHO_{pin}), 3.01 (s, 2H, CH_2B), 1.92- 2.42 (m, 5H, pinanediol), 1.47 (s, 3H, $CH_{3\text{-}pin}$), 1.34 (s, 3H, $CH_{3\text{-}pin}$), 1.15 (d, J = 10.8 Hz, d, 1H, $CH_{2\text{-}pin}$), 0.88 (s, 3H, $CH_{3\text{-}pin}$).

(+)-pinanediol α-azidomethaneboronate (2)

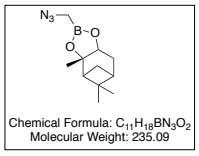

Viscous colourless oil (50% and 78%). ^{1}H NMR (400 MHz, $CDCl_3$) δ 4.49 (dd, J = 8.7, 2.0 Hz, 1H, CHO_{pin}), 3.01 (s, 2H, CH_2B), 1.92- 2.42 (m, 5H, pinanediol), 1.47 (s, 3H, $CH_{3\text{-}pin}$), 1.34 (s, 3H, $CH_{3\text{-}pin}$), 1.15 (d, J = 10.8 Hz, 1H, $CH_{2\text{-}pin}$), 0.88 (s, 3H, $CH_{3\text{-}pin}$). ^{13}C NMR (100 MHz, $CDCl_3$) δ 87.0, 78.6, 51.5, 39.5, 38.1, 35.9 (CH_2B), 35.2, 28.5, 27.0, 26.5, 23.9. MS-GC: m/z 235 (M+), 220, 206, 192, 179, 166, 150, 138, 125, 110, 93, 67, 55. $[\alpha]^{20}_D$: + 26.5.

Synthesis of alkynes

Alkynes ***3a***, ***3c***, ***3e–3g***, ***3k*** were purchased from Merck. Alkynes ***3b***,[11] ***3d***,[12] ***3h*** **and** ***3i***,[13] ***3j***,[14] ***3l***,[15] ***3m***,[16] ***3n***,[17] ***3o***,[18] ***3u***[19] were synthesized according to literature and the spectroscopic data were coherent to what previously describe.

General procedure for the synthesis of N-allylsulphonamides (3p-x)

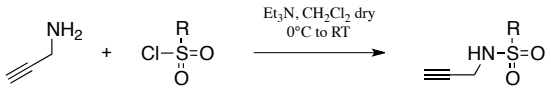

To a stirred solution of allyl amine (0.1 mmol) and Et_3N (0.12 mmol) in anhydrous CH_2Cl_2 (5 mL) at 0°C the proper sulfonyl chloride (0.11 mmol) in anhydrous CH_2Cl_2 (3 mL) was slowly added. After stirring for 4 hours at room temperature, the reaction was quenched with saturated aqueous NH_4Cl (4 mL) and the resulting mixture was extracted with CH_2Cl_2 (3 x 10

mL). The organic extract was washed with brine (5 mL), dried over $MgSO_4$, filtered, and concentrated *in vacuo*. The residue was purified by column chromatography (petroleum ether /ethyl acetate 7:3) affording the desired sulfonamide.

2,2,2-trifluoro-N-(prop-2-yn-1-yl)ethanesulfonamide (3p)

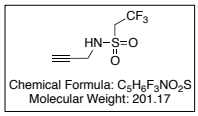

Yellowish crystals (89%), m.p. 49-52 °C. ^{1}H NMR (400 MHz $CDCl_3$): δ 5.00 (t, J = 6.2 Hz, 1H, CH), 4.03 (dd, J = 6.2, 2.5 Hz, 2H, CH_2SO_2), 3.98 (q, J = 8.9 Hz, 2H, CH_2NH), 2.44 (t, J = 2.5 Hz, 1H, NH). ^{13}C NMR (100 MHz, $CDCl_3$): δ 122.86 (q, J = 277.5), 77.76, 74.14, 55.33 (q, J = 31.1), 32.92. MS: LC-MS (ESI Ion Trap) m/z $[M - H]^-$ 199.7.

N-(prop-2-yn-1-yl)-1-(thiophen-2-yl)methanesulfonamide (3q)

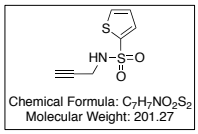

White solid (79%), m.p. 70-72 °C. ^{1}H NMR (400 MHz, $CDCl_3$): δ 7.66 (dd, J = 3.8, 1.3 Hz, 1H, CH_{tioph}), 7.62 (dd, J = 5.0, 1.3 Hz, 1H, CH_{tioph}), 7.10 (dd, J = 5.0, 3.8 Hz, 1H, CH_{tioph}), 4.82 (t, J = 6.0 Hz, 1H, CH), 3.91 (dd, J = 6.0, 2.5 Hz, 2H, CH_2), 2.15 (t, J = 2.5 Hz, 1H, NH). ^{13}C NMR (100 MHz, $CDCl_3$): δ 140.4, 133.0, 132.6, 127.6, 77.7, 73.2, 33.3. MS: LC-MS (ESI Ion Trap) m/z $[M - H]^-$ 199.8.

1-(3-nitrophenyl)-N-(prop-2-yn-1-yl)methanesulfonamide (3r)

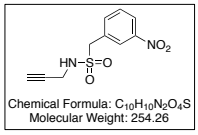

Yellow solid (77%), m.p. 123-125 °C. ^{1}H NMR (400 MHz, $CDCl_3$) δ 8.38 (t, J = 1.9 Hz, 1H, CH_{phen}), 8.28 – 8.23 (m, 1H, CH_{phen}), 7.86 – 7.80 (m, 1H, CH_{phen}), 7.60 (t, J = 8.0 Hz, 1H, CH_{phen}), 4.51 (t, J = 6.1 Hz, 1H, CH), 4.47 (s, 2H, CH_2SO_2), 3.97 (dd, J = 6.1, 2.5 Hz, 2H, CH_2NH), 2.50 (t, J = 2.5 Hz, 1H, NH). ^{13}C NMR (100 MHz, $CDCl_3$) δ 148.6, 137.1, 131.2, 130.0, 126.1, 124.0, 79.0, 74.1, 59.0, 33.1. MS: LC-MS (ESI Ion Trap) m/z $[M - H]^-$ 252.8.

methyl 4-((N-(prop-2-yn-1-yl)sulfamoyl)methyl)benzoate (3s)

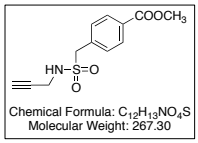

Yellowish solid (64%), m.p. 75-77 °C. ^{1}H NMR (400 MHz, $CDCl_3$) δ 8.04 (d, J = 8.3 Hz, 2H, CH_{phen}), 7.54 (d, J = 8.3 Hz, 2H, CH_{phen}), 4.65 (t, J = 6.0 Hz, 1H, CH), 4.41 (s, 2H, CH_2SO_2), 3.92 (s, 3H, CH_3), 3.89 (dd, J = 6.0, 2.5 Hz, 2H, CH_2NH), 2.43 (t, J = 2.5 Hz, 1H, NH). ^{13}C NMR (100 MHz, $CDCl_3$): δ 166.7, 134.0, 131.1, 130.7, 130.1, 79.1, 73.7, 59.6, 52.4, 33.1. LC-MS (ESI Ion Trap) m/z $[M - H]^-$ 265.8.

1-phenyl-N-(prop-2-yn-1-yl)methanesulfonamide (3t)

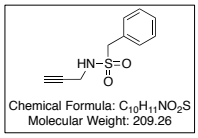

Yellowish solid (76%), m.p. 56-59 °C. ^{1}H NMR (400 MHz, $CDCl_3$): δ 7.50-7.35 (m, 5H, CH_{phen}), 4.50 (t, J = 6.1, 1H, CH), 4.37 (s, 2H, CH_2SO_2), 3.88 (dd, J = 6.1, 2.4, 2H, CH_2NH), 2.44 (t, J = 2.4 Hz, 1H, NH). ^{13}C NMR (100 MHz, DMSO): δ 130.8, 130.2, 128.3, 127.9, 79.2, 73.9, 58.8, 52.6, 32.7. MS: LC-MS (ESI Ion Trap) m/z $[M - H]^-$ 207.8.

methyl 3-((N-(prop-2-yn-1-yl)sulfamoyl)methyl)benzoate (3u)

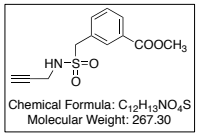

Yellowish solid (64%). ^{1}H NMR (400 MHz, $CDCl_3$) δ 8.14 (t, J = 1.4 Hz, 1H, CH_{phen}), 8.03 (dt, J = 7.8, 1.4 Hz, CH_{phen}), 7.65 (dt, J = 7.6, 1.4 Hz, 1H, CH_{phen}), 7.44 (t, J = 7.8 Hz, 1H, CH_{phen}), 4.98 (t, J = 6.0 Hz, 1H, CH), 4.38 (s, 2H, CH_2SO_2), 3.89 - 3.85 (m, 2H, CH_2NH), 3.87 (s, 3H, CH_3), 2.44 (t, J = 2.5 Hz, 1H, NH). ^{13}C NMR (100 MHz, $CDCl_3$): δ 166.6, 135.5, 132.1, 130.7, 130.0, 129.6, 129.0, 79.2, 73.6, 59.2, 52.4, 32.9. MS: LC-MS (ESI Ion Trap) m/z $[M - H]^-$ 265.9.

4-cyano-N-(prop-2-yn-1-yl)benzenesulfonamide (3w)

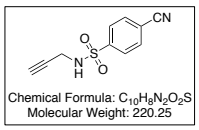

Chemical Formula: $C_{10}H_8N_2O_2S$
Molecular Weight: 220.25

White solid (48%), m.p. 125-128 °C. ^{1}H NMR (400 MHz, $CDCl_3$) δ 8.02 (d, J = 8.5 Hz, 2H, CH_{phen}), 7.83 (d, J = 8.5 Hz, 2H, CH_{phen}), 4.86 (t, J = 6.2 Hz, 1H, CH), 3.84 (dd, J = 6.2, 2.7 Hz, 2H, CH_2NH), 2.08 (t, J = 2.5 Hz, 1H, NH). ^{13}C NMR (100 MHz, $CDCl_3$): δ 144.4 , 133.0 , 128.2 , 117.4 , 116.9 , 73.7 , 33.1. MS: LC-MS (ESI Ion Trap) m/z $[M - H]^-$ 218.7.

Synthesis of alkyne 2-chloro-N-(prop-2-yn-1-yl)acetamide

Substituents in compounds ***6b*** and ***6c*** were not inserted as alkynes. The azidomethaneboronate was reacted first with 2-chloro-*N*-(prop-2-yn-1-yl)acetamide and then the compound obtained was reacted with the two different heterocycles.

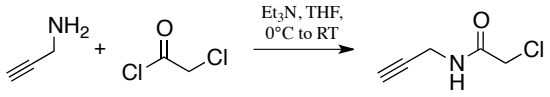

Propargylamine (1 eq.) was dissolved in THF dry under argon and the mixture was cooled to 0°C. Et_3N (1 eq.) and 2-chloroacetyl-chloride (1 eq.) were dissolved in THF and then added to the mixture. The mixture turned from yellow to dark orange and a brown precipitate was observed. The reaction mixture was left 45 min under vigorous stirring at 0°C, then at room temperature for a further 2h. The mixture was concentrated, DCM + 10% HCl were added and the two phases were separated. The organic phase was washed with H_2O and the aqueous phase was re-extracted with DCM. The organic phase was dried with Na_2SO_4, filtered and concentrated *in vacuo* to obtain the desired product.

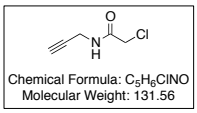

Chemical Formula: C_5H_6ClNO
Molecular Weight: 131.56

Yellowish solid (63%). ^{1}H NMR (400 MHz, $CDCl_3$) δ 6.76 (s, 1H, NH), 4.11 (dd, J = 5.4, 2.6 Hz, 2H, CH_2CCH), 4.07 (s, 2H, CH_2Cl), 2.28 (t, J = 2.6 Hz, 1H, HCC). ^{13}C NMR (101 MHz, $CDCl_3$) δ 165.76, 78.66, 72.37, 42.50, 29.73. MS: LC-MSQO m/z $[M-H]^-$ theo. 131.0142; found. 131.0132.

Synthesis of alkyne N-hydroxypropiolamide (d)

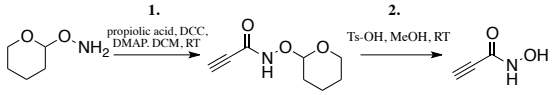

1. Propiolic acid (1 eq.) was dissolved in DCM and cooled to 0°C. Tetrahydropyranyl-hydroxamate (1 eq.) and DMAP (0.05 eq.) were added. DCC (1 eq.) was dissolved in DCM and added dropwise to the reaction mixture, which was left under vigorous magnetic stirring for 3h, at room temperature. The mixture was concentrated, filtered on celite and the filtrate was evaporated. The crude was purified by column chromatography (eluent phase: DCM / ethyl ether 8: 2).

2. *N*-((tetrahydro-2*H*-pyran-2-yl)oxy)propiolamide (1 eq.) was dissolved in methanol and *p*-toluene-sulfonic acid (0.1 eq.) was added. The reaction mixture was left under vigorous magnetic stirring for 30 hours and followed by TLC. The crude product was recovered after evaporation of the solvent and purified by column chromatography (eluent phase: DCM / ether 8: 2).

N-((tetrahydro-2H-pyran-2-yl)oxy)propiolamide

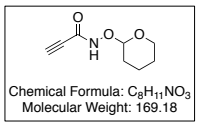

Chemical Formula: $C_8H_{11}NO_3$
Molecular Weight: 169.18

Yellowish oil (74%). ^{1}H NMR (400 MHz, $CDCl_3$) δ 8.60 (s, 1H, NH), 4.99 (d, J = 3.1 Hz, 1H, OCHO), 3.95 (t, J = 10.7 Hz, 1H, CH_2O), 3.67 (dtd, J = 11.3, 4.0, 2.1 Hz, 1H, CH_2O), 2.88 (s, 1H, CHC), 1.89 –1.62 (m, 6H, THP). ^{13}C NMR (101 MHz, $CDCl_3$) δ 149.88, 103.02, 76.07, 74.61, 62.82, 27.95, 25.01, 18.50. MS: LC-MSQO m/z $[M-H]^-$ theo 168.06552 found 168.6658.

N-hydroxypropiolamide

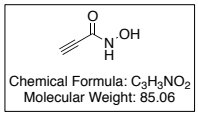

White solid (47%). ^{1}H NMR (400 MHz, DMSO-d_6) δ 11.22 (s, 1H, OH), 9.26 (s, 1H, NH), 4.15 (s, 1H, CHC). ^{13}C NMR (101 MHz, DMSO-d_6) δ 149.28, 77.44, 76.16. MS: LC-MSQO m/z $[M-H]^-$ theo 85.0160; found 85.0159

Synthesis of alkyne e-f

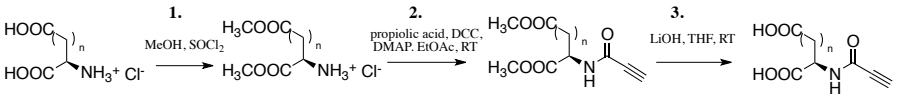

1. D-amino acids (1 eq.) were suspended in methanol. The temperature was cooled to 0°C and thionyl chloride (1.5 eq.) was added dropwise. The temperature was left at 0°C for 10 min, then it was allowed to reach room temperature and subsequently heated to 70°C. The mixture was vigorously stirred for 4h and a change in the appearance was observed: from a white suspension, it became a colourless solution. The mixture was concentrated and it was obtained an oil which was purified by trituration with dry ethyl ether.

2. Dimethyl amino acids (1 eq.) were dissolved in a saturated solution of K_2CO_3 (pH = 12) and extracted with ethyl acetate (2 x 5 ml). The organic phases were dried with Na_2SO_4 and filtered. DMAP (0.05 eq.), propiolic acid (1 eq.) and DCC (1 eq.) were added to the filtrate at -10°C. The mixture was allowed to reach room temperature and left under vigorous magnetic stirring overnight. The formation of a white precipitate (DCU) was observed. The solid was removed by filtration. The filtrate was concentrated and it was obtained an oil; the crude was purified by column chromatography (eluent phase: petroleum ether/ ethyl acetate 7: 3, 6: 4, 1: 1).

3. The protected alkynes (1 eq.) were dissolved in THF and LiOH 0.5M (4 eq.) was added. The reaction mixture was left under vigorous stirring for 2 hours at room temperature. Ethyl acetate and 10% HCl were added. The two phases were separated and the aqueous one was re-extracted with ethyl acetate (2 x 5 ml). The organic phase was dried with Na_2SO_4, filtered and evaporated.

Dimethyl-D-aspartic acid

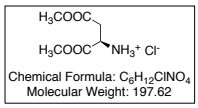

Colourless oil (96%). ^{1}H NMR (400 MHz, MeOD) δ 4.48 (t, J = 5.4 Hz, 1H, CH), 3.90 (s, 3H, CH_3), 3.80 (s, 3H, CH_3), 3.19 – 3.13 (m, 2H, CH_2). ^{13}C NMR (101 MHz, MeOD) δ 171.37, 169.56, 54.03, 53.04, 50.39, 34.76. MS: LC-MSQO m/z $[M+H]^+$ theo 162.076108 found 162.0761. $[\alpha]^{20}_D$= +22.0

Dimethyl-D-glutamic acid

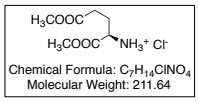

Colourless oil (100%). **1**H NMR (400 MHz, MeOD) δ 4.13 (t, J = 6.8 Hz, 1H, CH), 3.84 (s, 3H, CH_3), 3.70 (s, 3H, CH_3), 2.58 (td, J = 7.3, 3.7 Hz, 2H, $CH_2\beta$), 2.32 – 2.08 (m, 2H, $CH_2\gamma$). ^{13}C NMR (101 MHz, MeOD) δ 174.03, 170.54, 53.74, 53.22, 52.42, 30.14, 26.56. MS: LC-MSQO m/z $[M+H]^+$ theo. 176.09173, found 176.0917. $[\alpha]^{20}_D$= +24.53.

(R)-dimethyl 2-propiolamidosuccinate

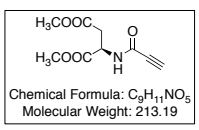

Yellow oil (60%). ^{1}H NMR (400 MHz, $CDCl_3$): δ 6.96-6.98 (d, J = 7.2, 1H, NH), 4.82-4.86 (m, 1H, CH), 3.76 (s, 3H, CH_3), 3.68 (s, 3H, CH_3), 3.01 (dd, J = 17.4, J = 4.3 Hz, 1H, $CH_2\beta$), 2.86 (s, 1H, CHC), 2.83 (dd, J =17.4 Hz, J = 4.3 Hz, 1H, $CH_2\beta$). ^{13}C NMR (100MHz, $CDCl_3$) δ: 171.2, 170.2, 151.67, 76.65, 74.48, 53.03, 52.55, 48.60, 35.8. MS: (ESI-TOF) $[M+H]^+$ 214.07 MS/MS 214.07 m/z 182.046(27), 158.03(4), 154.05(100), 123.02(2), 122.024(33), 112.02(5). $[\alpha]^{20}_D$= +27.90.

(R)-dimethyl 2-propiolamidopentanedioate

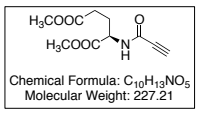

Yellow oil (35%). ^{1}H NMR (400 MHz, $CDCl_3$) δ 6.68 (t, *J* = 18.5 Hz, 1H, NH), 4.66 (td, *J* = 7.8, 5.2 Hz, 1H, CH), 3.76 (s, 3H, CH_3), 3.68 (s, 3H, CH_3), 2.85 (s, 1H, CHC), 2.49 – 2.30 (m, 2H, $CH_2\gamma$), 2.31 – 1.96 (m, 2H, $CH_2\beta$). ^{13}C NMR (101 MHz, $CDCl_3$) δ 173.23, 171.50, 151.90, 74.36, 52.91, 52.03, 52.06, 30.01, 27.25. MS LC-MSQO m/z: $[M+H]^+$ theo. 228.08665; found 228.0866. $[\alpha]^{20}_D$= -26.87.

(R)-2-propiolamidosuccinic acid

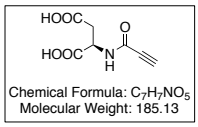

White solid (75%). ^{1}H NMR (400 MHz, MeOD): δ 5.05 (s, 1H, NH), 4.75 (m, 1H, CH), 3.59 (s, 1H, CHC), 2.85 (dd, *J* = 16.9 Hz, *J* = 5.2 Hz, 1H, $CH_2\beta$), 2.76 (dd, *J* = 16.9 Hz, *J* = 5.2 Hz, 1H, $CH_2\beta$).^{13}C NMR (100MHz, MeOD) δ 173.38, 172.87, 154.15, 77.68, 76.53, 50.26, 36.54. MS: LC-MSQO m/z $[M-H]^-$ theo. 184.02405, found 184.0244. $[\alpha]^{20}_D$ = + 10.0.

(R)-2-propiolamidopentanedioic acid

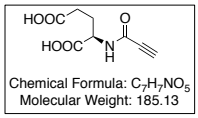

White solid (61%). ^{1}H NMR (400 MHz, MeOD) δ 4.43 (dd, *J* = 9.2, 5.1 Hz, 1H, CH), 3.59 (s, 1H, CHC), 2.38 (t, *J* = 7.5 Hz, 2H, CH_2 g), 2.16 (dtd, *J* = 15.6, 7.8, 5.1 Hz, 1H, CH_2b), 1.93 (ddd, *J* = 14.1, 8.2, 5.0 Hz, 1H, CH_2b). ^{13}C NMR (101 MHz, Methanol-d_4) δ 175.92, 173.84, 154.50, 77.64, 76.25, 53.09, 30.91, 27.33. MS: LC-MSQO m/z $[M-H]^-$ theo. 198.03970, found 198.0402. $[\alpha]^{20}_D$ = -18.51.

Synthesis of alkyne tert-butyl 2-propiolamido-3-(tritylthio)propanoate

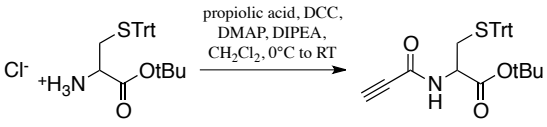

1-(*tert*-butoxy)-1-oxo-3-(tritylthio)propan-2-aminium chloride (0.85 mmol) was solubilized in dry DCM (3.6 mL) and the temperature was cooled to 0°C. Propiolic acid (0.85 mmol), DMAP (0.042 mmol) and DCC (0.85 mmol) were added. DIPEA (1.7 mmol) was solubilized in dry CH_2Cl_2 and added dropwise. After 10 min. the ice bath was removed. After 1h, the formation of an orange suspension was observed. The reaction mixture was vigorously stirred for 15h. The mixure was filtered on celite twice to eliminate DCU. The filtrate was concentrated and a spongy orange solid was obtained; the crude was purified by column chromatography (eluent phase: petroleum / ethyl acetate 8: 2).

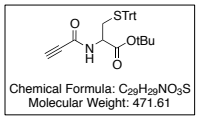

Spongy white solid (47%). ^{1}H-NMR (400Hz, $CDCl_3$): δ 7.11-7.37 (m, 15H, Trt), 6.34 (d, 1H, *J* = 7.78, NH), 4.43 (m, 1H, CH), 2.75 (s, 1H, CHC), 2.63 (m, 2H, CH_2), 1.37 (s, 9H, tBu). ^{13}C-NMR (100Hz, $CDCl_3$) δ 28.3, 33.9, 51.8, 66.9, 74.06, 77.3, 83.3, 144.0, 151.5, 168.8, 127-129.5. MS: ESI-TOF $[M+23]^+$ 494.176 MS/MS 494.176 m/z 437.19 (14), 415.215 (46), 243.124 (100), 227.082 (11), 125.98 (9). $[\alpha]^{20}_D$ = - 17.5.

Synthesis of alkyne S-(3-oxo-3-(prop-2-yn-1-ylamino)propyl) ethanethioate

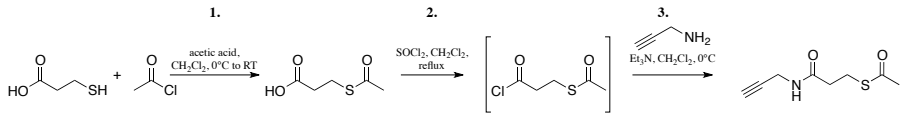

1. 3-mercaptopropanoic acid (2.83 mmol) was dissolved in CH_2Cl_2 (4 mL) and glacial acetic acid (4 mL). The temperature was cooled to 0°C and acetyl chloride (11.32 mmol) was slowly added dropwise. The mixture was allowed to warm to room temperature and stirred for two days. The solution turned pink. CH_2Cl_2 (20 mL) + H_2O (10 mL) were added and the two phases were separated: the aqueous one was re-extracted with CH_2Cl_2 (2 x14 mL). The organic phase was

washed first with 10 mL of H_2O and then with 20 mL of saturated NaCl. It was dried with Na_2SO_4, filtered and concentrated.

2. 3-(acetylthio)propanoic acid (2.83 mmol) was dissolved in DCM dry and thionyl chloride (3.11 mmol) was added. The formation of a dark red solution was observed and the mixture was refluxed for 90 min. under vigorous stirring. The reaction product was not isolated but directly used for next reaction.

3. Propargylamine (3.39 mmol) was dissolved in DCM (2.3 mL) under argon and Et_3N (3.68 mmol) was added. The reaction mixture was cooled to 0°C and the mixture containing *S*-(3-chloro-3-oxopropyl) ethanethioate (2.83 mmol) was added dropwise. The formation of fumes was observed and the reaction mixture became orange-brown with the presence of a precipitate. It was stirred for 2 h. CH_2Cl_2 (25 mL) and H_2O (15 mL) were added and the two phases were separated. The aqueous one was re-extracted with DCM (2 x 25 mL). The organic phases were washed with $NaHCO_3$, anhydrified with Na_2SO_4, filtered and evaporated. An orange solid was recovered and purified by silica gel column chromatography (eluent phase = petroleum / ethyl acetate 1: 1).

3-(acetylthio)propanoic acid

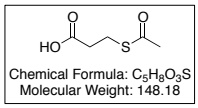

Chemical Formula: $C_5H_8O_3S$
Molecular Weight: 148.18

Dusty pink solid (100%). ^{1}H-NMR (400 MHz, $CDCl_3$) δ 3.11 (t, *J* = 6.9 Hz, 2H, SCH_2), 2.69 (t, *J* = 6.9 Hz, 2H, CH_2), 2.34 (s, 3H, CH_3).^{13}C-NMR (101 MHz, $CDCl_3$) δ 195.29, 177.08, 33.93, 30.36, 23.66.

S-(3-oxo-3-(prop-2-yn-1-ylamino)propyl) ethanethioate (6h)

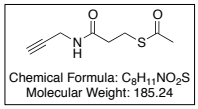

Chemical Formula: $C_8H_{11}NO_2S$
Molecular Weight: 185.24

Yellowish solid (69%).^{1}H NMR (400 MHz, $CDCl_3$) δ 5.81 (s, 1H, NH), 4.05 (dd, *J* = 5.2, 2.6 Hz, 2H, CH_2S), 3.14 (t, *J* = 7.0 Hz, 2H, CH_2), 2.51 (t, *J* = 7.0 Hz, 2H, CH_2NH), 2.33 (s, 3H, CH_3), 2.24 (t, *J* = 2.6 Hz, 1H, CHC).^{13}C NMR (101 MHz, $CDCl_3$) δ 196.26, 170.35, 79.44, 71.90, 36.23, 30.73, 29.42, 24.90. MS: LC-MSQO m/z $[M+H]^+$ theo. 186.05833, found 186.0583

General procedure for CuAAC between azidomethylboronate and terminal alkynes

Azidomethaneboronate ***2*** (1.00 mmol), the selected terminal alkyne (1.1 mmol), copper sulfate (aqueous solution 30 mg/mL, 0.03 mmol) and sodium ascorbate (0.20 mmol) were dissolved in a 1:1 mixture of *tert*-Butanol and water (2.0 mL each). The reaction was magnetically stirred at room temperature for the proper time (2-16 hours as specified in each case), until disappearance of the azido boronate (TLC). The mixture was then partitioned between ethyl acetate (20 mL), water (5 mL) and saturated NaCl (5 mL); the aqueous phase extracted with ethyl acetate (2 x 20 mL). The pooled organic phases were washed with brine (15 mL), dried over Na_2SO_4, filtered and concentrated *in vacuo*, affording the expected 1,2,3-triazol-1-yl-methaneboronate ***4***.

(+)-Pinanediyl [(4-(m-tolyl)-1H-1,2,3-triazol-1-yl)methyl]boronate (4a)

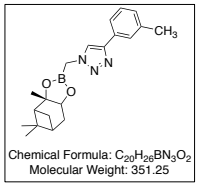

Chemical Formula: $C_{20}H_{26}BN_3O_2$
Molecular Weight: 351.25

Yellow oil (91%). ^{1}H NMR (400 MHz, $CDCl_3$) *d* 7.88 (s, 1H, CH_{triaz}), 7.69 (s, 1H, CH_{phen}), 7.59 (d, *J* = 7.7 Hz, 1H, CH_{phen}), 7.29 (t, *J* = 7.6 Hz, 1H, CH_{phen}), 7.14 (t, *J* = 8.5 Hz, 1H, CH_{phen}), 4.40 (dd, *J* = 8.8, 1.8 Hz, 1H, CH_{pin}), 4.26 (s, 2H, CH_2B), 2.38 (s, 3H, CH_3), 2.38 – 2.31 (m, 1H, $CH_{2\text{-}pin}$), 2.31- 2.23 (m, 1H, CH_{pin}), 2.11 – 2.07 (m, 1H, CH_{pin}), 1.97 – 1.87 (m, 2H, $CH_{2\text{-}pin}$), 1.45 (s, 3H, $CH_{3\text{-}pin}$), 1.30 (s, 3H, $CH_{3\text{-}pin}$), 1.17 (d, *J* = 11.1 Hz, 1H, $CH_{2\text{-}pin}$), 0.85 (s, 3H, $CH_{3\text{-}pin}$).^{13}C NMR (101 MHz, $CDCl_3$) *δ* 147.8, 138.5, 131.0, 128.8, 128.7, 126.5, 123.0, 121.0, 87.6, 79.0, 51.2, 39.5, 38.3, 35.8 (CB), 35.2, 28.7, 27.2, 26.6, 24.1, 21.6. HRMS (ESI-QTOF) m/z $[M+H]^+$ theo. 352.2194, found 352.2201. $[\alpha]^{20}_D$ = – 2.1 ($CHCl_3$).

(+)-Pinanediyl [(4-(3-sulfamoylphenyl)-1H-1,2,3-triazol-1-yl)methyl]boronate (4b)

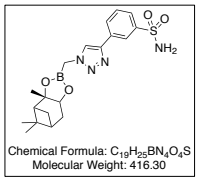

Yellow solid (75%). ^{1}H NMR (400 MHz, $CDCl_3$) δ 8.30 (t, J = 1.6 Hz, 1H, CH_{phen}), 8.06 (d, J = 7.8 Hz, 1H, CH_{phen}), 8.00 (s, 1H, CH_{triaz}), 7.85 – 7.83 (m, 1H, CH_{phen}), 7.53 (t, J = 7.8 Hz, 1H, CH_{phen}), 4.42 (dd, J = 8.8, 1.9 Hz, 1H, CH_{pin}), 4.27 (s, 2H, CH_2B), 2.40 – 2.33 (m, 1H, $CH_{2\text{-}pin}$), 2.31 – 2.25 (m, 1H, $CH_{2\text{-}pin}$), 2.11 – 2.08 (m, 1H, CH_{pin}), 1.97 – 1.93 (m, 1H, CH_{pin}), 1.92 – 1.85 (m, 1H, $CH_{2\text{-}pin}$), 1.45 (s, 3H, $CH_{3\text{-}pin}$), 1.30 (s, 3H, $CH_{3\text{-}pin}$), 1.15 (d, J = 11.1 Hz, 1H, $CH_{2\text{-}pin}$), 0.84 (s, 3H, $CH_{3\text{-}pin}$). ^{13}C NMR (101 MHz, $CDCl_3$) δ 146.0, 142.8, 132.3, 129.8, 129.7, 125.6, 123.6, 121.9, 87.8, 79.1, 51.2, 39.5, 38.3, 35.8 (*C*B), 35.2, 28.6, 27.1, 26.6, 24.10. HRMS (ESI-QTOF) m/z $[M+H]^+$ theo. 417.1865, found 417.1871. $[\alpha]^{20}_D$ = + 10.5 ($CHCl_3$).

(+)-Pinanediyl ((4-(3-carboxyphenyl)-1H-1,2,3-triazol-1-yl)methyl)boronate (4c)

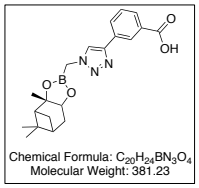

Yellow solid (94%). m.p. 48.1-50.8°C. ^{1}H NMR (400 MHz, $CDCl_3$) δ 8.50 (s, 1H, CH_{phen}), 8.19 (dt, J = 7.7, 1.3 Hz, 1H, CH_{phen}), 8.07 (dt, J = 7.7, 1.3 Hz, 1H, CH_{phen}), 8.02 (s, 1H, CH_{triaz}), 7.54 (t, J = 7.7 Hz, 1H, CH_{phen}), 4.43 (dd, J = 8.8, 1.8 Hz, 1H, CH_{pin}), 4.30 (s, 2H, CH_2B), 2.41 – 2.34 (m, 1H, $CH_{2\text{-}pin}$), 2.32 – 2.26 (m, 1H, $CH_{2\text{-}pin}$), 2.11 (t, J = 5.5 Hz, 1H, CH_{pin}), 1.99 – 1.94 (m, 1H, CH_{pin}), 1.94 – 1.89 (m, 1H, $CH_{2\text{-}pin}$), 1.46 (s, 3H, $CH_{3\text{-}pin}$), 1.31 (s, 3H, $CH_{3\text{-}pin}$), 1.17 (d, J = 11.1 Hz, 1H, $CH_{2\text{-}pin}$), 0.86 (s, 3H, $CH_{3\text{-}pin}$). ^{13}C NMR (101 MHz, $CDCl_3$) δ 171.1, 146.7, 131.5, 131.0, 130.1, 129.7, 129.2, 127.5, 121.6, 87.8, 79.1, 51.2, 39.5, 38.3, 36.1 (br, *C*B), 35.3, 28.6, 27.1, 26.7, 24.1. HRMS (ESI-QTOF) m/z $[M+H]^+$ theo. 382.1936, found 382.1938. $[\alpha]^{20}_D$ = - 2.1 ($CHCl_3$).

(+)-Pinanediyl [(4-(3-carbamoylphenyl)-1H-1,2,3-triazol-1-yl)methyl]boronate (4d)

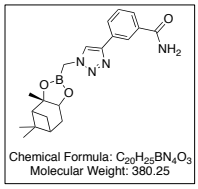

White hygroscopic solid (92%). ^{1}H NMR (400 MHz, $CDCl_3$) δ 8.29 (s, 1H, CH_{phen}), 8.03 – 7.96 (m, 2H, CH_{triaz} + CH_{phen}), 7.78 (d, J = 7.7 Hz, 1H, CH_{phen}), 7.49 (t, J = 7.7 Hz, 1H, CH_{phen}), 6.48 (s, 1H), 5.97 (s, 1H), 4.41 (dd, J = 8.8, 1.7 Hz, 1H, CH_{pin}), 4.28 (s, 2H, CH_2B), 2.42 – 2.32 (m, 1H, $CH_{2\text{-}pin}$), 2.32 – 2.24 (m, 1H, $CH_{2\text{-}pin}$), 2.09 (t, J = 5.5 Hz, 1H, CH_{pin}), 1.99 – 1.93 (m, 1H, CH_{pin}), 1.93 – 1.87 (m, 1H, $CH_{2\text{-}pin}$), 1.45 (s, 3H, $CH_{3\text{-}pin}$), 1.30 (s, 3H, $CH_{3\text{-}pin}$), 1.15 (d, J = 11.1 Hz, 1H, $CH_{2\text{-}pin}$), 0.85 (s, 3H, $CH_{3\text{-}pin}$). ^{13}C NMR (101 MHz, $CDCl_3$) δ 169.3, 146.7, 133.9, 131.5, 129.3, 129.21, 127.0, 124.7, 121.6, 87.8, 79.1, 51.2, 39.5, 38.3, 36.1 (*C*B), 35.2, 28.6, 27.1, 26.7, 24.1. HRMS (ESI-QTOF) m/z $[M+H]^+$ theo. 381.2096, found 381.2103. $[\alpha]^{20}_D$ = + 10.1 ($CHCl_3$).

(+)-Pinanediyl [(4-(pyridin-3-yl)-1H-1,2,3-triazol-1-yl)methyl]boronate (4f)

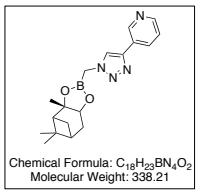

White solid (81%). m.p. 138.2-140.7 °C. ^{1}H NMR (400 MHz, $CDCl_3$) δ 8.98 (s, 1H, CH_{pyr}), 8.54 (s, 1H, CH_{pyr}), 8.22 (d, J = 7.9 Hz, 1H, CH_{pyr}), 7.99 (s, 1H, CH_{triaz}), 7.36 (dd, J = 7.7, 4.9 Hz, 1H, CH_{pyr}), 4.39 (dd, J = 8.7, 1.7 Hz, 1H, CH_{pin}), 4.26 (s, 2H, CH_2B), 2.40 – 2.31 (m, 1H, $CH_{2\text{-}pin}$), 2.31 – 2.23 (m, 1H, $CH_{2\text{-}pin}$), 2.08 (t, J = 5.5 Hz, 1H, CH_{pin}), 1.97 – 1.89 (m, 2H, $CH_{2\text{-}pin}$ + CH_{pin}), 1.42 (s, 3H, $CH_{3\text{-}pin}$), 1.29 (s, 3H, $CH_{3\text{-}pin}$), 1.16 (d, J = 11.3 Hz, 1H, $CH_{2\text{-}pin}$), 0.84 (s, 3H, $CH_{3\text{-}pin}$). ^{13}C NMR (101 MHz, $CDCl_3$) δ 148.7, 146.8, 144.4, 133.2, 127.4, 123.9, 121.4, 87.6, 78.9, 51.2, 39.5, 38.2, 36.1 (br, *C*B), 35.3, 28.5, 27.1, 26.6, 24.0. HRMS (ESI-QTOF) m/z $[M+H]^+$ theo. 339.1990, found 339.1995. $[\alpha]^{20}_D$ = + 11.9 ($CHCl_3$).

(+)-Pinanediyl [(4-(pyrazin-2-yl)-1H-1,2,3-triazol-1-yl)methyl]boronate (4g)

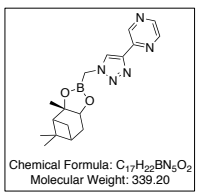

Yellow oil (100%). ^{1}H NMR (400 MHz, $CDCl_3$) δ 9.43 (s, 1H, CH_{pyr}), 8.54 (s, 2H, CH_{pyr}), 8.30 (s, 1H, CH_{triaz}), 4.41 (dd, J = 8.8, 1.6 Hz, 1H, CH_{pin}), 4.30 (s, 2H, CH_2B), 2.39 – 2.32 (m, 1H, $CH_{2\text{-}pin}$), 2.30 – 2.25 (m, 1H, $CH_{2\text{-}pin}$), 2.09 (t, J = 5.5 Hz, 1H, CH_{pin}), 1.97 – 1.87 (m, 2H, CH_{pin} + $CH_{2\text{-}pin}$), 1.45 (s, 3H, $CH_{3\text{-}pin}$), 1.30 (s, 3H, $CH_{3\text{-}pin}$), 1.15 (d, J = 11.1 Hz, 1H, $CH_{2\text{-}pin}$), 0.84 (s, 3H, $CH_{3\text{-}pin}$). ^{13}C NMR (101 MHz, $CDCl_3$) δ 146.5, 145.8, 144.0, 143.4, 142.3, 124.4, 87.8, 79.1, 51.2, 39.5, 38.3, 35.2, 35.8 (br, *C*B), 28.6, 27.1, 26.6, 24.1. HRMS (ESI-QTOF) m/z $[M+H]^+$ theo. 340.1942, found 340.1953. $[\alpha]^{20}_D$ = + 11.7 ($CHCl_3$)

(+)-Pinanediyl [(4-((3-chlorophenoxy)methyl)-1H-1,2,3-triazol-1-yl)methyl]boronate (4h)

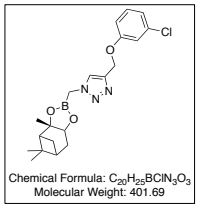

Yellow oil (98%). ^{1}H NMR (400 MHz, $CDCl_3$) δ 7.76 (s, 1H, CH_{triaz}), 7.19 (t, J = 8.2 Hz, 1H, CH_{phen}), 7.00 – 6.98 (m, 1H, CH_{phen}), 6.96 – 6.92 (m, 1H, CH_{phen}), 6.90 – 6.87 (m, 1H, CH_{phen}), 5.19 (s, 2H, CH_2O), 4.39 (dd, J = 8.8, 1.9 Hz, 1H, CH_{pin}), 4.22 (s, 2H, CH_2B), 2.39 – 2.31 (m, 1H, $CH_{2\text{-}pin}$), 2.29 – 2.22 (m, 1H, $CH_{2\text{-}pin}$), 2.09 – 2.05 (m, 1H, CH_{pin}), 1.97 – 1.83 (m, 2H, CH_{pin} + $CH_{2\text{-}pin}$), 1.43 (s, 3H, $CH_{3\text{-}pin}$), 1.30 (s, 3H, $CH_{3\text{-}pin}$), 1.11 (d, J = 11.1 Hz, 1H, $CH_{2\text{-}pin}$), 0.84 (s, 3H, $CH_{3\text{-}pin}$). ^{13}C NMR (101 MHz, $CDCl_3$) δ 159.0, 143.2, 134.8, 130.2, 124.1, 121.3, 115.4, 113.2, 87.5, 78.9, 62.3, 51.0, 39.3, 38.2, 35.7 (br, *C*B), 35.1, 28.4, 27.0, 26.5, 23.9. HRMS (ESI-QTOF) m/z $[M+H]^+$ theo. 402.1754, found 402.1745. $[\alpha]^{20}_D$ = +14.8 ($CHCl_3$).

(+)-Pinanediyl ((4-((4-methoxyphenoxy)methyl)-1H-1,2,3-triazol-1-yl)methyl)boronate (4i)

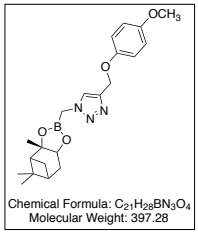

Yellow oil (98%). ^{1}H NMR (400 MHz, $CDCl_3$) δ 7.75 (s, 1H, CH_{triaz}), 6.97 – 6.89 (m, 2H, CH_{phen}), 6.86 – 6.78 (m, 2H, CH_{phen}), 5.15 (s, 2H, CH_2O), 4.39 (dd, J = 8.8, 1.9 Hz, 1H, CH_{pin}), 4.21 (s, 2H, CH_2B), 3.76 (s, 3H, CH_3), 2.38 – 2.32 (m, 1H, $CH_{2\text{-}pin}$), 2.28 – 2.22 (m, 1H, $CH_{2\text{-}pin}$), 2.08 – 2.05 (m, 1H, CH_{pin}), 1.98 – 1.84 (m, 2H, CH_{pin} + $CH_{2\text{-}pin}$), 1.43 (s, 3H, $CH_{3\text{-}pin}$), 1.30 (s, 3H, $CH_{3\text{-}pin}$), 1.12 (d, J = 11.1 Hz, 1H, $CH_{2\text{-}pin}$), 0.84 (s, 3H, $CH_{3\text{-}pin}$). ^{13}C NMR (101 MHz, $CDCl_3$) δ 154.23, 152.6, 144.3, 124.1, 116.0, 114.8, 87.7, 79.0, 63.0, 55.8, 51.2, 39.5, 38.3, 35.8 (br, *C*B), 35.2, 28.6, 27.1, 26.6, 24.1. HRMS (ESI-QTOF) m/z $[M+H]^+$ theo. 398.2249, found 398.2257. $[\alpha]^{20}_D$ = + 12.7 ($CHCl_3$)

(+)-Pinanediyl ((4-((3-acetamidophenoxy)methyl)-1H-1,2,3-triazol-1-yl)methyl)boronate (4j)

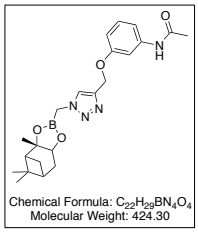

Yellow oil (100%). ^{1}H NMR (400 MHz, $CDCl_3$) δ 7.78 (s, 1H, CH_{triaz}), 7.51 (s, 1H, CH_{phen}), 7.27 (s, 1H, CH_{phen}), 7.18 (t, J = 8.1 Hz, 1H, CH_{phen}), 7.08 (d, J = 7.9 Hz, 1H, CH_{phen}), 6.72 (dd, J = 8.2, 2.0 Hz, 1H), 5.18 (s, 2H, CH_2O), 4.39 (dd, J = 8.8, 1.8 Hz, 1H, CH_{pin}), 4.21 (s, 2H, CH_2B), 2.39 – 2.30 (m, 1H, $CH_{2\text{-}pin}$), 2.28 – 2.22 (m, 1H, $CH_{2\text{-}pin}$), 2.15 (s, 3H, CH_3), 2.08 – 2.05 (m, 1H, CH_{pin}), 1.95 – 1.85 (m, 2H, CH_{pin} + $CH_{2\text{-}pin}$), 1.43 (s, 3H, $CH_{3\text{-}pin}$), 1.29 (s, 3H, $CH_{3\text{-}pin}$), 1.12 (d, J = 11.1 Hz, 1H, $CH_{2\text{-}pin}$), 0.84 (s, 3H, $CH_{3\text{-}pin}$). ^{13}C NMR (101 MHz, $CDCl_3$) δ 168.4, 158.7, 143.6, 139.1, 129.7, 124.5, 112.5, 110.8, 106.4, 87.5, 78.8, 61.9, 51.0, 39.3, 38.2, 35.7 (br, *C*B) ,35.0, 28.4, 27,3, 26.5, 25.0, 23.9. HRMS (ESI-QTOF) m/z $[M+H]^+$ theo. 425.2359, found 425.2354. $[\alpha]^{20}_D$ = + 11.4 ($CHCl_3$).

(+)-Pinanediyl((4-(3-((tert-butoxycarbonyl)amino)phenyl)-1H-1,2,3-triazol-1-yl)methyl)boronate (4k)

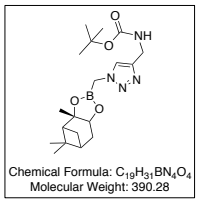

Pale yellow oil (96%). ^{1}H NMR (400 MHz, $CDCl_3$) δ 7.63 (s, 1H, CH_{triaz}), 5.17 (br, s, 1H, NH), 4.48 – 4.31 (m, 3H, CH_{pin} + CH_2NH_3), 4.18 (s, 2H, CH_2B), 2.37 – 2.31(m, 1H, $CH_{2\text{-}pin}$), 2.28 – 2.22 (m, 1H, $CH_{2\text{-}pin}$), 2.06 (t, J = 5.5 Hz, 1H, CH_{pin}), 1.96 – 1.84 (m, 2H, CH_{pin} + $CH_{2\text{-}pin}$), 1.43 (s, 9H, tBu), 1.42 (s, 3H, $CH_{3\text{-}pin}$), 1.29 (s, 3H, $CH_{3\text{-}pin}$), 1.12 (d, J = 11.1 Hz, 1H, $CH_{2\text{-}pin}$), 0.84 (s, 3H, $CH_{3\text{-}pin}$). ^{13}C NMR (101 MHz, $CDCl_3$) δ 156.0, 145.1, 123.3, 87.6, 79.7, 79.0, 51.2, 39.5, 38.3, 36.3, 36.1 (br, *C*B), 35.2, 28.6, 28.5 (3C), 27.1, 26.6, 24.1. ^{11}B NMR (128 MHz, $CDCl_3$) δ 31.8. HRMS (ESI-QTOF) m/z $[M+H]^+$ theo. 391.2515, found 391.2527. $[\alpha]^{20}_D$ = + 12.2 ($CHCl_3$)

(+)-Pinanediyl ((4-((2,2,2-trifluoroacetamido)methyl)-1H-1,2,3-triazol-1-yl)methyl)boronate (4l)

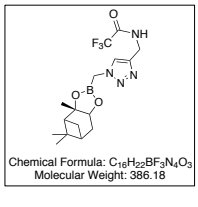

Yellow solid (100%). m.p. 102.3-105.9 °C. ^{1}H NMR (400 MHz, $CDCl_3$) δ 7.73 (s, 1H, CH_{triaz}), 7.69 (br, s, 1H, NH), 4.59 (d, J = 5.7 Hz, 2H, CH_2NH), 4.39 (dd, J = 8.8, 1.7 Hz, 1H, CH_{pin}), 4.21 (s, 2H, CH_2B), 2.41 – 2.31 (m, 1H, $CH_{2\text{-}pin}$), 2.31 – 2.23 (m, 1H, $CH_{2\text{-}pin}$), 2.07 (t, J = 5.5 Hz, 1H, CH_{pin}), 1.97 – 1.84 (m, 2H, CH_{pin} + $CH_{2\text{-}pin}$), 1.43 (s, 3H, $CH_{3\text{-}pin}$), 1.30 (s, 3H, $CH_{3\text{-}pin}$), 1.11 (d, J = 11.1 Hz, 1H, $CH_{2\text{-}pin}$), 0.84 (s, 3H, $CH_{3\text{-}pin}$). ^{13}C NMR (101 MHz, $CDCl_3$) δ 157.4 (q, J = 37.4 Hz), 142.3, 124.0,

115.9 (q, *J* = 287.6 Hz), 87.8, 79.1, 51.2, 39.5, 38.3, 36.2 (br, *C*B), 35.2, 35.2, 28.6, 27.1, 26.6, 24.1. ^{11}B NMR (128 MHz, $CDCl_3$) δ 30.4. HRMS (ESI-QTOF) m/z $[M+H]^+$ theo. 387.1813, found 387.1805. $[\alpha]^{20}_D$ = + 13.1 ($CHCl_3$).

(+)-Pinanediyl ((4-((phenylamino)methyl)-1H-1,2,3-triazol-1-yl)methyl)boronate (4m)

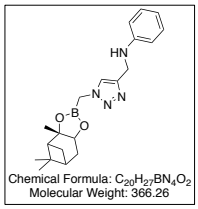

Yellow solid (95%). ^{1}H NMR (400 MHz, $CDCl_3$) δ 7.58 (s, 1H, CH_{triaz}), 7.20 – 7.14 (m, 2H, CH_{phen}), 6.75 – 6.72 (m, 1H, CH_{phen}), 6.69 – 6.67 (m, 2H, CH_{phen}), 4.44 (s, 2H, CH_2NH), 4.37 (dd, *J* = 8.8, 1.9 Hz, 1H, CH_{pin}), 4.18 (s, 2H, CH_2B), 2.37 – 2.31 (m, 1H, $CH_{2\text{-}pin}$), 2.28 – 2.20 (m, 1H, $CH_{2\text{-}pin}$), 2.08 – 2.03 (m, 1H, CH_{pin}), 1.96 – 1.90 (m, 1H, CH_{pin}), 1.88 – 1.82 (m, 1H, $CH_{2\text{-}pin}$), 1.42 (s, 3H, $CH_{3\text{-}pin}$), 1.32 (s, 3H, $CH_{3\text{-}pin}$), 1.10 (d, *J* = 11.1 Hz, 1H, $CH_{2\text{-}pin}$), 0.84 (s, 3H, $CH_{3\text{-}pin}$). ^{13}C NMR (101 MHz, $CDCl_3$) δ 147.7, 145.8, 129.4123.0, 118.1, 113.4, 87.6, 79.0, 51.2, 40.2, 39.5, 38.3, 35.9 (br, *C*B), 35.2, 28.6, 27.1, 26.6, 24.1. ^{11}B NMR (128 MHz, $CDCl_3$) δ 30.8. HRMS (ESI-QTOF) m/z $[M+H]^+$ theo. 367.2303, found 367.2315. $[\alpha]^{20}_D$ = + 13.5 ($CHCl_3$).

(+)-Pinanediyl ((4-((4-methylbenzamido)methyl)-1H-1,2,3-triazol-1-yl)methyl)boronate (4n)

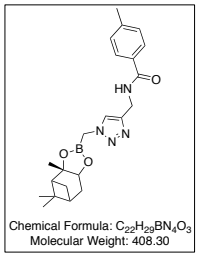

Yellow solid (100%). ^{1}H NMR (400 MHz, $CDCl_3$) δ 7.72 (s, 1H, CH_{triaz}), 7.68 (d, *J* = 8.0 Hz, 2H, CH_{phen}), 7.21 (d, *J* = 8.0 Hz, 2H, CH_{phen}), 7.00 – 6.94 (m, 1H, NH), 4.69 (d, *J* = 5.5 Hz, 2H, CH_2NH), 4.38 (dd, *J* = 8.8, 1.8 Hz, 1H, CH_{pin}), 4.19 (s, 2H, CH_2B), 2.37 (s, 3H, CH_3), 2.37 – 2.31 (m, 1H, $CH_{2\text{-}pin}$), 2.29 – 2.22 (m, 1H, $CH_{2\text{-}pin}$), 2.07 (t, *J* = 5.5 Hz, 1H, CH_{pin}), 1.96 – 1.90 (m, 1H, CH_{pin}), 1.90 – 1.84 (m, 1H, $CH_{2\text{-}pin}$), 1.43 (s, 3H, $CH_{3\text{-}pin}$), 1.29 (s, 3H, $CH_{3\text{-}pin}$), 1.12 (d, *J* = 11.1 Hz, 1H, $CH_{2\text{-}pin}$), 0.84 (s, 3H, $CH_{3\text{-}pin}$). ^{13}C NMR (101 MHz, $CDCl_3$) δ 167.4, 144.4, 142.1, 131.4, 129.3, 127.1, 123.7, 87.7, 79.0, 51.2, 39.5, 38.3, 35.9 (br, *C*B), 35.5, 35.2, 28.6, 27.1, 26.6, 24.1, 21.6. ^{11}B NMR (128 MHz, $CDCl_3$) δ 31.2. HRMS (ESI-TOF) m/z $[M+H]^+$ theo. 409.2409, found 409.2421. $[\alpha]^{20}_D$ = + 11.9 ($CHCl_3$).

(+)-Pinanediyl ((4-((4-methylphenylsulfonamido)methyl)-1H-1,2,3-triazol-1-yl)methyl)boronate (4o)

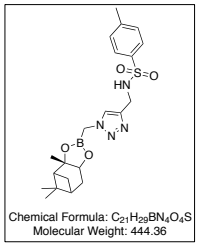

White oil (100%). ^{1}H NMR (400 MHz, $CDCl_3$) δ 7.73 (d, *J* = 8.1 Hz, 2H, CH_{phen}), 7.58 (s, 1H, CH_{triaz}), 7.29 (d, *J* = 8.1 Hz, 2H, CH_{phen}), 5.18 (t, *J* = 5.9, 1H, NH), 4.38 (dd, *J* = 8.8, 1.7 Hz, 1H, CH_{pin}), 4.23 (d, *J* = 6.1 Hz, 2H, CH_2NH), 4.14 (s, 2H, CH_2B), 2.42 (s, 3H, CH_3), 2.38 – 2.32 (m, 1H, $CH_{2\text{-}pin}$), 2.30 – 2.24 (m, 1H, $CH_{2\text{-}pin}$), 2.08 (t, *J* = 5.5 Hz, 1H, CH_{pin}), 1.97 – 1.92 (m, 1H, CH_{pin}), 1.89 – 1.84 (m, 1H, $CH_{2\text{-}pin}$), 1.43 (s, 3H, $CH_{3\text{-}pin}$), 1.30 (s, 3H, $CH_{3\text{-}pin}$), 1.10 (d, *J* = 11.1 Hz, 1H, $CH_{2\text{-}pin}$), 0.85 (s, 3H, $CH_{3\text{-}pin}$). ^{13}C NMR (101 MHz, $CDCl_3$) δ 143.7, 143.2, 136.7, 129.9, 127.3, 123.6, 87.7, 79.0, 51.2, 39.5, 39.0, 38.3, 35.8 (br, *C*B), 35.2, 28.6, 27.1, 26.6, 24.1, 21.7. ^{11}B NMR (128 MHz, $CDCl_3$) δ 31.6. HRMS (ESI-QTOF) m/z $[M+H]^+$ theo. 445.2079, found 445.2100. $[\alpha]^{20}_D$ = + 10.3 ($CHCl_3$).

(+)-Pinanediyl((4-((2,2,2-trifluoroethylsulfonamido)methyl)-1H-1,2,3-triazol-1-yl)methyl)boronate (4p)

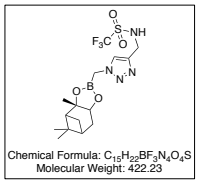

White viscous oil (98%). ^{1}H NMR (400 MHz, Acetone-d_6): δ 7.90 (s, 1H, CH_{triaz}), 7.15 (t, *J* = 6.07 Hz, 1H, NH), 4.53 – 4.38 (m, 3H, CH_{pin} + CH_2NH), 4.36 – 4.15 (m, 4H, CH_2CF_3 + CH_2B), 2.45 – 2.33 (m, 1H, $CH_{2\text{-}pin}$), 2.29 – 2.17 (m, 1H, $CH_{2\text{-}pin}$), 2.00 – 1.94 (m, 1H, CH_{pin}), 1.95 – 1.86 (m, 1H, CH_{pin}), 1.86 – 1.76 (m, 1H, $CH_{2\text{-}pin}$), 1.41 (s, 3H, $CH_{3\text{-}pin}$), 1.29 (s, 3H, $CH_{3\text{-}pin}$), 1.23 (d, *J* = 11.0 Hz, 1H, $CH_{2\text{-}pin}$), 0.87 (s, 3H, $CH_{3\text{-}pin}$). ^{13}C NMR (100 MHz, Acetone-d_6): δ 130.7, 122.9, 102.3, 88.1, 82.5, 70.7, 55.7, 41.1, 40.6, 39.8, 38.8, 35.3 (CB, br), 25.1, 24.4, 21.9. ^{11}B NMR (128 MHz, $CDCl_3$) δ 31.4. MS: LC-MS (ESI Ion Trap) m/z $[M + H]^+$ 437.4. $[\alpha]^{20}_D$ = + 8.3 ($CHCl_3$).

(+)-Pinanediyl ((4-((thiophene-2-sulfonamido)methyl)-1H-1,2,3-triazol-1-yl)methyl)boronate (4q)

Orange viscous oil (98%). ^{1}H NMR (400 MHz, Acetone-d_6): δ 7.75 (dt, J = 5.0, 1.1 Hz, 1H, CH_{thioph}), 7.65 (s, 1H, CH_{triaz}), 7.54 – 7.52 (m, 1H, CH_{thioph}), 7.08 (dd, J = 5.0, 3.8 Hz, 1H, CH_{thioph}), 6.99 (t, J = 6.1 Hz, 1H, NH), 4.36 (dd, J = 8.8, 1.9 Hz, 1H, CH_{pin}), 4.18 (d, J = 6.1 Hz, 2H, CH_2NH), 4.08 (d, J = 1.8 Hz, 2H, CH_2B), 2.45 – 2.34 (m, 1H, $CH_{2\text{-}pin}$), 2.29 – 2.19 (m, 1H, $CH_{2\text{-}pin}$), 1.97 – 1.95 (m, 1H, CH_{pin}), 1.95 – 1.88 (m, 1H, CH_{pin}), 1.86 – 1.78 (m, 1H, $CH_{2\text{-}pin}$), 1.41 (s, 3H, $CH_{3\text{-}pin}$), 1.29 (s, 3H, $CH_{3\text{-}pin}$), 1.26 (d, J = 10.4 Hz, 1H, $CH_{2\text{-}pin}$), 0.87 (s, 3H, $CH_{3\text{-}pin}$). ^{13}C NMR (100 MHz, Acetone-d_6): δ 170.9, 142.8, 132.8, 132.7, 124.5, 128.3, 87.8, 79.2, 60.5, 52.1, 40.3, 39.8, 38.9, 36.5 (CB, br), 28.7, 27.3, 26.9, 24.1. ^{11}B NMR (128 MHz, $CDCl_3$) δ 31.4. MS: LC-MS (ESI Ion Trap) m/z $[M + H]^+$ 437.3. MS/MS (ESI Ion Trap, *m/z*): 273.2 (40), 135.3 (96), 112.3 (55). $[\alpha]^{20}_D$ = + 9.2 ($CHCl_3$).

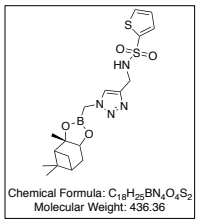

(+)-Pinanediyl ((4-(((3-nitrophenyl)methylsulfonamido)methyl)-1H-1,2,3-triazol-1-yl)methyl)boronate (4r)

Orange viscous oil (76%). ^{1}H NMR (400 MHz, Acetone-d_6): δ 8.27 – 8.11 (m, 2H, CH_{phen}), 7.91 (s, 1H, CH_{triaz}), 7.78 (dt, J = 7.7, 1.3 Hz, 1H, CH_{phen}), 7.65 (t, J = 7.9 Hz, 1H, CH_{phen}), 6.67 (t, J = 5.7 Hz, 1H, NH), 4.52 (s, 2H, CH_2SO_2), 4.44 (dd, J = 8.7, 2.0 Hz, 1H, CH_{pin}), 4.40 (d, J = 5.7 Hz, 2H, CH_2NH), 4.27 (d, J = 2.1 Hz, 2H, CH_2B), 2.42 – 2.15 (m, 1H, $CH_{2\text{-}pin}$), 2.25 – 2.16 (m, 1H, $CH_{2\text{-}pin}$), 2.01 – 1.94 (m, 1H, CH_{pin}), 1.93 – 1.74 (m, 1H, CH_{pin}), 1.83 – 1.74 (m, 1H, $CH_{2\text{-}pin}$), 1.39 (s, 3H, $CH_{3\text{-}pin}$), 1.27 (s, 3H, $CH_{3\text{-}pin}$), 1.23 (d, J = 10.9 Hz, 1H, $CH_{2\text{-}pin}$), 0.85 (s, 3H, $CH_{3\text{-}pin}$). ^{13}C NMR (100 MHz, Acetone-d_6): δ 171.0, 149.2, 145.2, 138.4, 133.9, 130.6, 126.5, 123.9, 88.0, 79.4, 60.7, 58.5, 52.2, 40.4, 39.3, 39.0, 36.7 (CB) 28.8, 27.4, 27.1, 24.2. ^{11}B NMR (128 MHz, CDCl3) δ 31.3. MS: LC-MS (ESI Ion Trap) m/z $[M + H]^+$, 490.4. MS/MS (ESI Ion Trap, *m/z*): 273.2 (98), 255.3 (52), 135.3 (55). $[\alpha]^{20}_D$ = + 6.3 ($CHCl_3$).

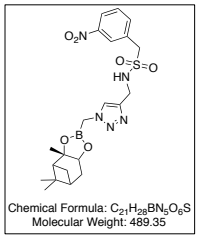

(+)-Pinanediyl((4-(((4-(methoxycarbonyl)phenyl)methylsulfonamido)methyl)-1H-1,2,3-triazol-1-yl)methyl)boronate (4s)

White viscous oil (89%). ^{1}H NMR (400 MHz, Acetone-d_6): δ 7.96 (d, J = 8.6 Hz, 2H, CH_{phen}), 7.87 (s, 1H, CH_{triaz}), 7.45 (d, J = 8.2 Hz, 2H, CH_{phen}), 6.56 (t, J = 6.1 Hz, NH), 4.45 (dd, J = 8.8, 2.0 Hz, CH_{pin}), 4.41 (s, 2H, CH_2SO_2), 4.35 (d, 2H, J = 4.62 Hz, CH_2NH), 4.26 (d, J = 2.1 Hz, CH_2B), 3.89 (s, CH_3), 2.43 – 2.29 (m, 1H, $CH_{2\text{-}pin}$), 2.29 – 2.15 (m, 1H, $CH_{2\text{-}pin}$), 2.02 – 1.94 (m, 1H, CH_{pin}), 1.93 – 1.84 (m, 1H, CH_{pin}), 1.85 – 1.75 (m, 1H, $CH_{2\text{-}pin}$), 1.40 (s, 3H, $CH_{3\text{-}pin}$), 1.27 (s, 3H, $CH_{3\text{-}pin}$), 1.23 (d, J = 11.1 Hz, 1H, $CH_{2\text{-}pin}$), 0.86 (s, 3H, $CH_{3\text{-}pin}$). ^{13}C NMR (100 MHz, Acetone-d_6): δ 167.0, 145.1, 136.7, 132.0, 130.8, 130.1, 124.7, 87.9, 79.3, 59.1, 52.4, 52.1, 40.3, 39.2, 38.9, 36.7, (CB), 35.8, 28.7, 27.3, 27.0, 24.1. ^{11}B NMR (128 MHz, $CDCl_3$) δ 31.6. MS: LC-MS (ESI Ion Trap) m/z $[M + H]^+$, 503.4. $[\alpha]^{20}_D$ = + 8.7 ($CHCl_3$).

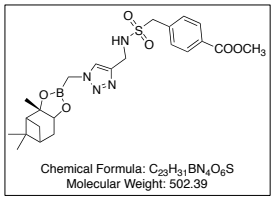

(+)-Pinanediyl ((4-((phenylmethylsulfonamido)methyl)-1H-1,2,3-triazol-1-yl)methyl)boronate (4t)

Yellow/orange viscous oil (98%). ^{1}H NMR (400 MHz, Acetone-d_6): δ 7.86 (s, 1H, CH_{triaz}), 7.43 – 7.14 (m, 5H, CH_{phen}), 6.46 (t, J = 6.1 Hz, 1H, NH), 4.44 (dd, J = 8.8, 2.0 Hz, CH_{pin}), 4.33 – 4.28 (m, 4H, CH_2SO_2 + CH_2NH), 4.24 (d, J = 1.9 Hz, 2H, CH_2B), 2.43 – 2.30 (m, 1H, $CH_{2\text{-}pin}$), 2.28 – 2.16 (m, 1H, $CH_{2\text{-}pin}$), 2.02 – 1.94 (m, 1H, CH_{pin}), 1.93 – 1.86 (m, 1H, CH_{pin}), 1.86 – 1.73 (m, 1H, $CH_{2\text{-}pin}$), 1.39 (s, 3H, $CH_{3\text{-}pin}$), 1.27 (s, 3H, $CH_{3\text{-}pin}$), 1.23 (d, J = 10.3 Hz, 1H, $CH_{2\text{-}pin}$), 0.85 (s, 3H, $CH_{3\text{-}pin}$). ^{13}C NMR (100 MHz, Acetone-d_6): δ 145.5, 132.0, 131.6, 129.3, 129.0, 124.8, 87.9, 79.4, 60.7, 59.6, 52.2, 40.4, 39.6, 38.9, 35.9 (CB), 28.9, 27.5, 27.1, 24.3. ^{11}B NMR (128 MHz, $CDCl_3$) δ 31.3. MS: LC-MS (ESI Ion Trap) m/z $[M + H]^+$, 445,4. $[\alpha]^{20}_D$ = + 11.7 ($CHCl_3$).

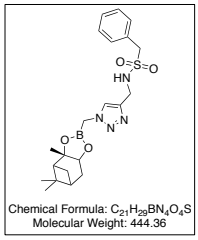

(+)-Pinanediyl((4-(((3-(methoxycarbonyl)phenyl)methylsulfonamido)methyl)-1H-1,2,3-triazol-1-yl)methyl)boronate (4u)

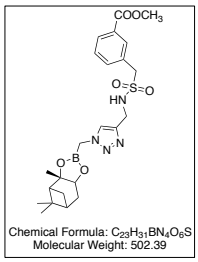

White viscous oil (98%). ^{1}H NMR (400 MHz, Acetone-d_6): δ 8.02 – 7.94 (m, 2H, CH_{phen}), 7.88 (s, 1H, CH_{triaz}), 7.60 (d, J = 7.6 Hz, 1H, CH_{phen}), 7.49 (t, J = 7.7, 0.6 Hz, 1H, CH_{phen}), 6.57 (t, J = 6.2 Hz, 1H, NH), 4.44 (dd, J = 8.8, 2.0 Hz, 1H, CH_{pin}), 4.41 (s, 2H, CH_2SO_2), 4.35 (d, J = 6.2 Hz, 2H, CH_2NH), 4.26 (d, J = 1.7 Hz, 2H, CH_2B), 3.90 (s, 3H, CH_3), 2.39 – 2.31 (m, 1H, $CH_{2\text{-}pin}$), 2.26 – 2.15 (m, 1H, $CH_{2\text{-}pin}$), 2.01 – 1.94 (m, 1H, CH_{pin}), 1.92 – 1.85 (m, 1H, CH_{pin}), 1.83 – 1.73 (m, 1H, $CH_{2\text{-}pin}$), 1.39 (s, 3H, $CH_{3\text{-}pin}$), 1.27 (s, 3H, $CH_{3\text{-}pin}$), 1.23 (d, J = 9.5 Hz, 1H, $CH_{2\text{-}pin}$), 0.85 (s, 3H, $CH_{3\text{-}pin}$). ^{13}C NMR (100 MHz, Acetone-d_6): δ 168.5, 144.5, 136.2, 132.9, 132.0, 131.8, 130.1, 129.3, 124.3, 88.2, 78.9, 58.7, 52.8, 52.3, 40.3, 39.2, 38.9, 36.4 (CB), 35.8, 28.7, 27.3, 27.0, 24.1. ^{11}B NMR (128 MHz, $CDCl_3$) δ 31.6. MS: LC-MS (ESI Ion Trap) m/z $[M + H]^+$, 503.4. $[\alpha]^{20}_D$ = + 7.5 ($CHCl_3$).

((+)-Pinanediyl ((4-((4-cyanophenylsulfonamido)methyl)-1H-1,2,3-triazol-1-yl)methyl)boronate (4w)

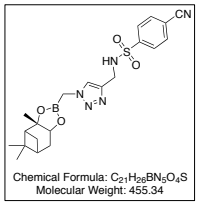

White solid (93%). m.p. 142-145°C. ^{1}H NMR (400 MHz, Acetone-d_6): δ 8.01 (d, J = 8.5 Hz, 2H, CH_{phen}), 7.97 (d, J = 8.4 Hz, 2H, CH_{phen}), 7.72 (s, 1H, CH_{triaz}), 7.24 (t, J = 5.9 Hz, 1H, NH), 4.46 (dd, J = 8.8, 1.9 Hz, 1H, CH_{pin}), 4.27 (s, 2H, CH_2NH), 4.15 (d, J = 3.0 Hz, 2H, CH_2B), 2.44 – 2.32 (m, 1H, $CH_{2\text{-}pin}$), 2.30 – 2.17 (m, 1H, $CH_{2\text{-}pin}$), 2.08 – 2.03 (m, 1H, CH_{pin}), 1.95 – 1.88 (m, 1H, CH_{pin}), 1.42 (s, 3H, $CH_{3\text{-}pin}$), 1.30 (s, 3H, $CH_{3\text{-}pin}$), 1.22 (d, J = 11.1 Hz, 1H, $CH_{2\text{-}pin}$), 0.87 (s, 3H, $CH_{3\text{-}pin}$). ^{13}C NMR (100 MHz, Acetone-d_6): δ 146.2, 146.1, 133.9, 128.6, 124.5, 118.3, 116.5, 87.8, 79.2, 52.1, 39.5, 39.4, 38.9, 35.9 (CB), 35.8, 28.7, 27.3, 26.9, 24.1. ^{11}B NMR (128 MHz, $CDCl_3$) δ 31.2. MS: LC-MS (ESI Ion Trap) m/z $[M + H]^+$, 456.4. $[\alpha]^{20}_D$ = +12.7° ($CHCl_3$, c = 1.10 g/100mL).

(+)-Pinanediyl((4-((((4-(1H-tetrazol-5-yl)phenyl)methylsulfonamido)methyl)-1H-1,2,3-triazol-1-yl)methyl)boronate (4x)

Compound ***4x*** was obtained from ***4w*** according to the following procedure: compound ***4w*** (0.17 mmol) was dissolved in THF (0.2 mL) in a microwave cuvette. TBAF (0.17mmol) and $TMSN_3$ (0.76 mmol) were added and the reaction was conducted at 110 °C for 20 min. The mixture was partitioned between ethyl acetate and water and the organic phase washed with saturated ammonium chloride. The organic phase was extracted twice with ethyl acetate, dried over Na_2SO_4, filtered and concentrated under *vacuum* to give ***4x***.

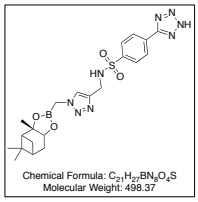

Yellow/white solid (65%). m.p. 130-132°C. ^{1}H NMR (400 MHz, Acetone-d_6): δ 8.30 (d, J = 8.4 Hz, 2H, CH_{phen}), 8.05 (d, J = 8.4 Hz, 2H, CH_{phen}), 7.71 (s, 1H, CH_{triaz}), 7.13 (t, J = 6.2 Hz, 1H, NH), 4.41 (dd, J = 8.8, 1.9 Hz, 1H, CH_{pin}), 4.28 (d, J = 6.2 Hz, 2H, CH_2NH), 4.12 (d, J = 2.3 Hz, 2H, CH_2B), 2.44 – 2.30 (m, 1H, $CH_{2\text{-}pin}$), 2.26 – 2.16 (m, 1H, $CH_{2\text{-}pin}$), 2.04 – 1.97 (m, 1H, CH_{pin}), 1.94 – 1.85 (m, 1H, CH_{pin}), 1.82 – 1.71 (m, 1H, $CH_{2\text{-}pin}$), 1.38 (s, 3H, $CH_{3\text{-}pin}$), 1.28 (s, 3H, $CH_{3\text{-}pin}$), 1.18 (d, J = 11.0 Hz, 1H, $CH_{2\text{-}pin}$), 0.86 (s, 3H, $CH_{3\text{-}pin}$), N–H tetrazole not seen. ^{13}C NMR (101 MHz, Acetone-d_6): δ 157.8, 144.1, 144.0, 128.80, 128.79, 128.5, 124.5, 87.8, 79.2, 52.0, 40.3, 39.5, 38.9, 36.9 (*C*B), 35.8, 28.7, 27.3, 26.9, 24.1. ^{11}B NMR (128 MHz, $CDCl_3$) δ 31.4. MS: LC-MS (ESI Ion Trap) m/z $[M + H]^+$, 365.1. $[\alpha]^{20}_D$ = +2.30° (CH_3OH, c = 1.3 g/100mL).

4-(1-(((3aS)-3a,5,5-trimethylhexahydro-4,6-methanobenzo[d][1,3,2]dioxaborol-2-yl)methyl)-1H-1,2,3-triazol-4-yl)phthalic acid

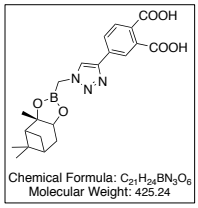

Yellowish solid (70%). ^{1}H NMR (400 MHz, MeOD) δ 8.38 (s, 1H, CH_{triaz}), 8.15 (d, J = 1.8 Hz, 1H, CH_{phen}), 7.99 (dd, J = 8.0, 1.7 Hz, 1H, CH_{phen}), 7.85 (d, J = 8.1 Hz, 1H, CH_{phen}), 4.43 (dd, J = 8.7, 1.9 Hz, 1H, CH_{pin}), 4.28 (s, 2H, CH_2B), 2.45 – 1.78 (m, 6H, $CH_{2\text{-}pin}$ + CH_{pin}), 1.42 (s, 3H, $CH_{3\text{-}pin}$), 1.28 (s, 3H, $CH_{3\text{-}pin}$), 1.23 (d, J = 3.4 Hz, 1H, $CH_{2\text{-}pin}$), 0.84 (s, 3H, $CH_{3\text{-}pin}$). ^{13}C NMR (101 MHz, MeOD) δ 146.60, 134.68, 130.89, 128.14, 126.40, 124.16, 88.43, 79.81, 52.28, 40.56, 39.03, 35.86 (CB), 28.56,

27.23, 27.01, 24.06. ^{11}B NMR (128 MHz, MeOD) δ 31.51. MS: LC-MSQO m/z $[M+H]^+$ theo. 292.07354; found 292.0735 (- pinanediol). $[\alpha]^{20}_D$ = + 9.00.

(2R)-2-(1-(((3aS)-3a,5,5-trimethylhexahydro-4,6-methanobenzo[d][1,3,2]dioxaborol-2-yl)methyl)-1H-1,2,3-triazole-4-carboxamido)succinic acid

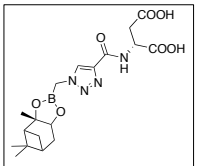

White solid (60%). ^{1}H NMR (400 MHz, MeOD) δ 8.37 (s, 1H, CH_{triaz}), 4.97 (t, *J* = 5.5 Hz, 1H, CH), 4.46 (dd, *J* = 8.7, 1.9 Hz, 1H, CH_{pin}), 4.31 (d, *J* = 1.0 Hz, 2H, CH_2B), 2.99 (t, *J* = 5.4 Hz, 2H, CH_2-b), 2.40 – 1.84 (m, 5H, $CH_{2\text{-pin}}$ + CH_{pin}), 1.44 (s, 3H, $CH_{3\text{-pin}}$), 1.32 (s, 3H, $CH_{3\text{-pin}}$), 0.88 (s, 3H, $CH_{3\text{-pin}}$). ^{13}C NMR (101 MHz, MeOD) δ 174.15, 173.72, 162.27, 143.20, 128.36, 88.67, 80.05, 52.52, 40.79, 39.26 (CB), 36.88, 36.07, 28.74, 27.44, 27.22, 24.27, 15.43. ^{11}B NMR (128 MHz, MeOD) δ 31.54. MS: LC-MSQO m/z $[M-H]^-$ theo. 285.06371 found 285.0651 (- pinanediol). $[\alpha]^{20}_D$ = +1.1527.

(2R)-2-(1-(((3aS)-3a,5,5-trimethylhexahydro-4,6-methanobenzo[d][1,3,2]dioxaborol-2-yl)methyl)-1H-1,2,3-triazole-4-carboxamido)pentanedioic acid

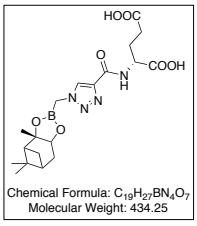

White solid (60%). ^{1}H NMR (400 MHz, MeOD) δ 8.37 (s, 1H, CH_{triaz}), 4.68 (dd, *J* = 8.9, 4.9 Hz, 1H, CH), 4.47 (dd, *J* = 8.8, 1.9 Hz, 1H, CH_{pin}), 4.31 (s, 2H, CH_2B), 2.54 – 1.81 (m, $CH_{2\text{-pin}}$ + CH_{pin} + CH_2 – b + CH_2 -g), 1.45 (s, 3H, $CH_{3\text{-pin}}$), 1.33 (s, 3H, $CH_{3\text{-pin}}$), 1.26 (d, *J* = 5.5 Hz, 1H, $CH_{2\text{-pin}}$), 0.89 (s, 3H, $CH_{3\text{-pin}}$). ^{13}C NMR (101 MHz, MeOD) δ 176.36, 174.58, 162.62, 143.26, 128.37, 88.65, 80.04, 52.53, 40.80, 39.26, 36.09 (CB), 31.24, 28.75, 27.98, 27.45, 27.22, 24.28. ^{11}B NMR (128 MHz, MeOD) δ 30.37. MS: LC-MSQO m/z $[M-H]^-$ theo. 299.07936, found 299.0805(- pinanediol) e 281.07 (- H_2O). $[\alpha]^{20}_D$ = + 4.91132.

2-chloro-N-((1-(((3aS)-3a,5,5-trimethylhexahydro-4,6-methanobenzo[d][1,3,2]dioxaborol-2-yl)methyl)-1H-1,2,3-triazol-4-yl)methyl)acetamide

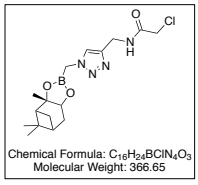

White solid (45%). ^{1}H NMR (400 MHz, $CDCl_3$) δ 7.67 (s, 1H, CH_{triaz}), 4.57 (d, *J* = 5.6 Hz, 2H, CH_2NH), 4.39 (dd, *J* = 8.7, 1.9 Hz, 1H, CH_{pin}), 4.20 (s, 2H, CH_2B), 4.05 (s, 2H, CH_2Cl), 2.41 – 2.22 (m, 2H, $CH_{2\text{-pin}}$), 2.08 (t, *J* = 5.5 Hz, 1H, CH_{pin}), 1.97 – 1.84 (m, 2H, CH_{pin} + $CH_{2\text{-pin}}$), 1.44 (s, 3H, $CH_{3\text{-pin}}$), 1.30 (s, 3H, $CH_{3\text{-pin}}$), 1.12 (d, *J* = 11.1 Hz, 1H, $CH_{2\text{-pin}}$), 0.85 (s, 3H, $CH_{3\text{-pin}}$). ^{13}C NMR (101 MHz, $CDCl_3$) δ 166.14, 123.66, 87.73, 79.03, 51.21, 42.63, 39.50, 38.32, 35.42, 35.22 (CB), 28.59, 27.11, 26.64, 24.09. ^{11}B NMR (128 MHz, $CDCl_3$) δ 31.23. MS: LC-MSQO m/z $[M+H]^+$ theo. 233.06072, found 233.0607 (- pinanediol). $[\alpha]^{20}_D$ = + 8.69130.

Synthesis of esters of compounds 6b and 6c

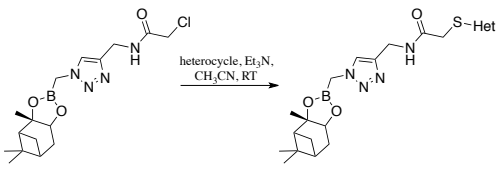

2-chloro-N-((1-(((3aS)-3a,5,5-trimethylhexahydro-4,6-methanobenzo[d][1,3,2]dioxaborol-2-yl)methyl)-1H-1,2,3-triazol-4-yl)methyl)acetamide (1 eq.) and the desired substituted heterocycle (1 eq.) were dissolved in dry acetonitrile. Dry Et_3N (1.02 eq.) was added dropwise and the mixture was stirred vigorously at room temperature for 4h. The volume was concentrated. CH_2Cl_2 (20 mL) and H_2O (15 mL) were added and the two phases were separated. The aqueous phase was re-extracted with CH_2Cl_2 and the organic phase was washed with water. The organic phase was dried with Na_2SO_4, filtered and evaporated. The crude product was purified by trituration with dry diethyl ether.

2-((5-amino-1,3,4-thiadiazol-2-yl)thio)-N-((1-(((3aS)-3a,5,5-trimethylhexahydro-4,6-methanobenzo[d][1,3,2]dioxaborol-2-yl)methyl)-1H-1,2,3-triazol-4-yl)methyl)acetamide

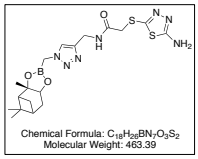

White solid (35%). ^{1}H NMR (400 MHz, MeOD) δ 7.80 (s, 1H, CH_{triaz}), 4.45 (s, 2H, CH_2NH), 4.42 (dd, J = 8.7, 2.0 Hz, 1H, CH_{pin}), 4.21 (s, 2H, CH_2B), 3.80 (s, 2H, CH_2S), 2.45 – 1.81 (m, 5H, $CH_{2\text{-}pin}$ + CH_{pin}), 1.41 (s, 3H, $CH_{3\text{-}pin}$), 1.30 (s, 3H, $CH_{3\text{-}pin}$), 1.21 (d, J = 11.0 Hz, 1H, $CH_{2\text{-}pin}$), 0.87 (s, 3H, $CH_{3\text{-}pin}$). ^{13}C NMR (101 MHz, MeOD) δ 170.40, 145.92, 125.63, 88.72, 80.15, 52.75, 41.00, 39.46, 38.83, 36.37 (CB), 36.30, 28.99, 27.66, 27.45, 24.49. ^{11}B NMR (128 MHz, MeOD) δ 30.67. MS: LC-MSQO m/z: $[M+H]^+$ theo. 330.06089 found 330.0607 (- pinanediol) e 312.0502 (-H_2O). $[\alpha]^{20}_D$ = + 5.769230.

2-((5-methyl-4H-1,2,4-triazol-3-yl)thio)-N-((1-(((3aS)-3a,5,5-trimethylhexahydro-4,6-methanobenzo[d][1,3,2]dioxaborol-2-yl)methyl)-1H-1,2,3-triazol-4-yl)methyl)acetamide

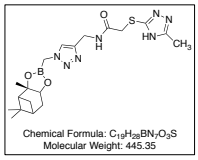

White solid (32%). ^{1}H NMR (400 MHz, MeOD) δ 7.83 (s, 1H, CH_{triaz}), 4.47 (s, 2H, CH_2NH), 4.40 (m, 1H, CH_{pin}), 4.21 (s, 2H, CH_2B), 3.85 (m, 2H, CH_2S), 2.44 – 2.20 (m, 5H, CH_3 + $CH_{2\text{-}pin}$), 2.02 (t, J = 5.6 Hz, 1H, CH_{pin}), 1.95 – 1.78 (m, 3H, CH_{pin} + $CH_{2\text{-}pin}$), 1.42 (s, 3H, $CH_{3\text{-}pin}$), 1.30 (s, 3H, $CH_{3\text{-}pin}$), 1.19 (d, J = 11.0 Hz, 1H, $CH_{2\text{-}pin}$), 0.87 (s, 3H, $CH_{3\text{-}pin}$). ^{13}C NMR (101 MHz, MeOD) δ 170.66, 157.78, 156.45, 125.48, 88.56, 79.97, 52.50, 40.77, 39.79, 39.25, 36.07, 28.77, 27.44, 27.22, 24.27, 11.46. ^{11}B NMR (128 MHz, MeOD) δ 30.98. MS: LC-MSQO m/z: $[M+H]^+$ theo. 312.0447; found 312.1043 (- pinanediol); 2540674 (- H_2O). $[\alpha]^{20}_D$ = + 0.0115.

N-hydroxy-1-(((3aS)-3a,5,5-trimethylhexahydro-4,6-methanobenzo[d][1,3,2]dioxaborol-2-yl)methyl)-1H-1,2,3-triazole-4-carboxamide

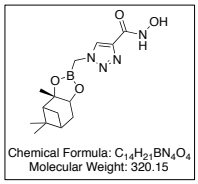

White solid (60%). ^{1}H-NMR (400 MHz, $CDCl_3$) δ 8.30 (s, 1H, CH_{triaz}), 4.39 (dd, J = 8.8, 1.9 Hz, 1H, CH_{pin}), 4.24 (s, 2H, CH_2B), 2.40 – 2.22 (m, 2H, $CH_{2\text{-}pin}$), 2.08 (t, J = 5.5 Hz, 1H, CH_{pin}), 1.98 – 1.83 (m, 2H, CH_{pin} + $CH_{2\text{-}pin}$), 1.43 (s, 3H, $CH_{3\text{-}pin}$), 1.29 (s, 3H, $CH_{3\text{-}pin}$), 1.09 (d, J = 11.1 Hz, 1H, $CH_{2\text{-}pin}$), 0.84 (s, 3H, $CH_{3\text{-}pin}$). ^{13}C NMR (101 MHz, $CDCl_3$) δ 158.63, 129.88, 127.18, 88.01, 78.87, 51.17, 39.48, 38.31, 36.45 (CB), 35.15, 28.55, 27.09, 26.64, 24.07. ^{11}B NMR (128 MHz, $CDCl_3$) δ 31.22. MS: LC-MSQO $[M-H]^-$ theo. 185.04766; found 185.0481 (- pinanediol). $[\alpha]^{20}_D$ = + 0.0116.

S-(3-oxo-3-(((1-(((3aS)-3a,5,5-trimethylhexahydro-4,6-methanobenzo[d][1,3,2]dioxaborol-2-yl)methyl)-1H-1,2,3-triazol-4-yl)methyl)amino)propyl) ethanethioate

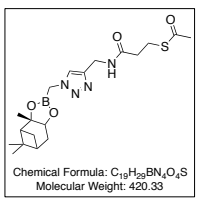

Yellow oil (87%). ^{1}H NMR (400 MHz, $CDCl_3$) δ 7.64 (s, 1H, CH_{triaz}), 6.22 (s, 1H, NH), 4.51 (d, J = 5.6 Hz, 2H, CH_2NH), 4.39 (dd, J = 8.8, 1.9 Hz, 1H, CH_{pin}), 4.19 (s, 2H, CH_2B), 3.14 (t, J = 7.0 Hz, 2H, CH_2CO), 2.49 (t, J = 6.9 Hz, 2H, CH_2S), 2.40 – 2.34 (m, 1H, $CH_{2\text{-}pin}$), 2.31 (s, 3H, CH_3), 2.26 (m, 1H, $CH_{2\text{-}pin}$), 2.08 (t, J = 5.5 Hz, 1H, CH_{pin}), 1.97 – 1.92 (m, 1H, CH_{pin}), 1.88 (m, 1H, $CH_{2\text{-}pin}$), 1.44 (s, 3H, $CH_{3\text{-}pin}$), 1.30 (s, 3H, $CH_{3\text{-}pin}$), 1.13 (d, J = 11.1 Hz, 1H, $CH_{2\text{-}pin}$), 0.85 (s, 3H, $CH_{3\text{-}pin}$). ^{13}C-NMR (100 MHz, $CDCl_3$) δ 195.7, 170.9, 144.4, 123.7, 87.5, 78.8, 51.0, 39.3, 38.1, 35.7, 35.0, 34.7 (CB), 30.5, 28.4, 26.9, 26.4, 24.8, 23.9. MS: LC-MS: m/z 421 $[M+H]^+$, 379 (base peak), 345 (8%), 245 (6%). $[\alpha]^{20}_D$ = - 4.71 ($CHCl_3$).

tert-butyl 2-(1-(((3aS)-3a,5,5-trimethylhexahydro-4,6-methanobenzo[d][1,3,2]dioxaborol-2-yl)methyl)-1H-1,2,3-triazole-4-carboxamido)-3-(tritylthio)propanoate

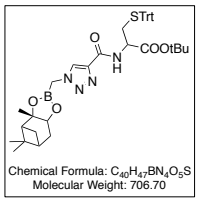

White solid (80%). ^{1}H NMR (400 MHz, $CDCl_3$) δ 8.19 (s, 1H, CH_{triaz}), 7.62 (d, J = 8.4 Hz, 1H, NH), 7.42 – 7.38 (m, 7H, Trt), 7.24 – 7.16 (m, 8H, Trt), 4.64 (m, J = 8.5, 1.4 Hz, 1H, CH), 4.40 (dd, J = 8.8, 1.9 Hz, 1H, CH_{pin}), 4.27 (s, 2H, CH_2B), 2.73 - 2.51 (m, 2H, CH_2S), 2.40 – 2.32 (m, 1H, $CH_{2\text{-}pin}$), 2.31 – 2.24 (m, 1H, $CH_{2\text{-}pin}$), 2.08 (t, J = 5.5 Hz, 1H, CH_{pin}), 1.95 (m, 1H, CH_{pin}), 1.89 (m, 1H, $CH_{2\text{-}pin}$), 1.44 (m, 13H, $CH_{3\text{-}pin}$ e tBu), 1.30 (s, 3H, $CH_{3\text{-}pin}$), 1.11 (d, J = 11.1 Hz, 1H, $CH_{2\text{-}pin}$), 0.85 (s, 3H, $CH_{3\text{-}pin}$). ^{13}C NMR (101 MHz, $CDCl_3$) δ 169.20, 159.95, 144.57,142.73, 129.72, 128.09, 126.86, 87.92, 82.68, 79.14, 66.96, 51.65, 51.22, 39.52, 38.33, 35.19, 34.61, 28.59, 28.11, 27.13, 26.67, 24.10. ^{11}B NMR (128 MHz, $CDCl_3$) δ 31.85. MS: LC-MSQO m/z $[M\text{-}H]^-$ theo. 617.22, found 617.22 (- pinanediol; + formic acid). $[\alpha]^{20}_D$ = - 6.00.

General procedure for deprotection of pinanedyl boronates through transesterification

To a solution of 1,2,3-triazol-1-yl-methaneboronate (0.50 mmol) in CH_3CN (3 mL), HCl (3M aqueous solution, 1.50 mmol), isobutylboronic acid (0.50 mmol) and *n*-hexane (3 mL) were sequentially added and the resulting biphasic solution was vigorously stirred. After 30 min the *n*-hexane layer, containing the pinanediol isobutylboronate, was removed and fresh *n*-hexane (3 mL) was added. The last procedure was repeated several times until the disappearance of isobutylboronate from the *n*-hexane layer, monitored by TLC analysis (total reaction time 3-6 hours). The acetonitrile phase was then concentrated and the crude recrystallized to afford the 1,2,3-triazol-1-yl-methaneboronic acid.

[(4-(m-tolyl)-1H-1,2,3-triazol-1-yl)methyl]boronic acid (5a)

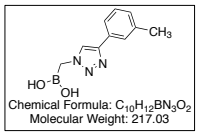

Yellow solid (100%). ^{1}H NMR (400 MHz, MeOD) δ 8.75 (s, 1H, CH_{triaz}), 7.77 – 7.50 (m, 2H, CH_{phen}), 7.50 – 7.12 (m, 2H, CH_{phen}), 4.49 (s, 2H, CH_2B), 2.44 (s, 3H, CH_3). ^{13}C NMR (100 MHz, MeOD): δ 144.9, 141.0, 132.8, 130.7, 128.1, 126.9, 125.7, 124.7, 42.7 (*C*B), 21.4. ^{11}B NMR(128 MHz, MeOD) δ 27.4. MS: HRMS (ESI-QTOF) m/z $[M + H]^+$ theo. 218.1097, found 218.1089.

[(4-(3-sulfamoylphenyl)-1H-1,2,3-triazol-1-yl)methyl]boronic acid (5b)

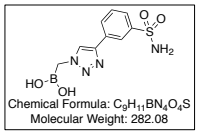

Yellow solid (82%). ^{1}H NMR (400 MHz, MeOD) δ 8.64 (s, 1H, CH_{triaz}), 8.35 (t, J = 1.8 Hz, 1H, CH_{phen}), 8.05-7.97 (m, 2H, CH_{phen}), 7.70 (t, J = 7.8 Hz, 1H, CH_{phen}), 4.44 (s, 2H, CH_2B). ^{13}C NMR (100 MHz, MeOD): δ 146.4, 144.8, 131.2, 130.6, 129.4, 128.1, 126.2, 124.6, 41.5 (CB). ^{11}B NMR(128 MHz, MeOD) δ 27.9. MS: HRMS (ESI-QTOF) m/z $[M + H]^+$ theo. 283.0669, found 283.0676.

((4-(3-carboxyphenyl)-1H-1,2,3-triazol-1-yl)methyl)boronic acid (5c)

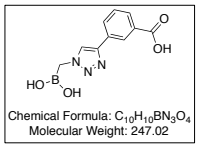

Yellow solid (99%). ^{1}H NMR (400 MHz, MeOD) δ 8.61 (s, 1H, CH_{triaz}), 8.47 (d, J = 1.9 Hz, 1H, CH_{phen}), 8.13 – 8.01 (m, 2H, CH_{phen}), 7.64 (t, J = 7.8 Hz, 1H, CH_{phen}), 4.43 (s, 2H, CH_2B). ^{13}C NMR (100 MHz, MeOD) δ 168.8, 145.4, 133.2, 131.7, 131.4, 130.7, 128.2, 127.9, 125.9, 41.1 (CB). ^{11}B NMR (128 MHz, MeOD) δ 27.7. MS: HRMS (ESI-QTOF) $[M + H]^+$ m/z theo. 246.0693, found 246.0687.

[(4-(3-carbamoylphenyl)-1H-1,2,3-triazol-1-yl)methyl]boronic acid (5d)

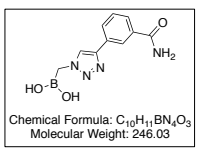

White solid (88%). ^{1}H NMR (400 MHz, MeOD) δ 8.73 (s, 1H, CH_{triaz}), 8.34 (t, J = 1.8 Hz, 1H, CH_{phen}), 8.03 – 7.97 (m, 2H, CH_{phen}), 7.66 (t, J = 7.8 Hz, 1H, CH_{phen}), 4.49 (s, 2H, CH_2B). ^{13}C NMR (100 MHz, MeOD) δ 171.3, 144.8, 136.5, 131.0, 130.6, 130.3, 127.8, 127.0, 126.8, 42.1 (CB). ^{11}B NMR (128 MHz, MeOD) δ 27.6. MS: HRMS (ESI-QTOF) m/z $[M + H]^+$ theo. 247.0999, found 247.1010.

((4-(pyridin-3-yl)-1H-1,2,3-triazol-1-yl)methyl)boronic acid (5f)

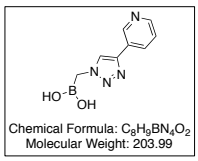

Yellow hygroscopic solid (95%). ^{1}H NMR (400 MHz, MeOD) δ 9.34 (s, 1H, CH_{triaz}), 9.04 (dt, J = 8.3, 1.6 Hz, 1H, CH_{pyr}), 8.81 (d, J = 5.7 Hz, 1H, CH_{pyr}), 8.62 (s, 1H, CH_{pyr}), 8.18 (dd, J = 8.3, 5.7 Hz, 1H, CH_{pyr}), 4.35 (s, 2H,).^{13}C NMR (100 MHz, MeOD) δ 143.4, 141.9, 141.3, 139.3, 133.0, 129.0, 126.1, 39.4 (CB). ^{11}B NMR (128 MHz, MeOD) δ 28.4. MS: HRMS (ESI-QTOF) m/z $[M + H]^+$ theo. 205.0893, found 205.0901.

[(4-(pyrazin-2-yl)-1H-1,2,3-triazol-1-yl)methyl]boronic acid (5g)

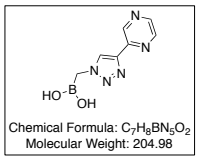

Yellow hygroscopic solid (96%). ^{1}H NMR (400 MHz, MeOD) δ 9.32 (s, 1H, CH_{triaz}), 8.72 (m, 4H, CH_{pyraz}), 4.42 (s, 2H, CH_2B).^{13}C NMR (100 MHz, MeOD): δ 146.5, 143.8, 143.2, 141.1, 127.6, 117.6, 40.6 (CB). ^{11}B NMR (128 MHz, MeOD) δ 28.0. MS: HRMS (ESI-QTOF) m/z $[M + H]^+$ theo. 206.0845, found 206.0839.

((4-((3-chlorophenoxy)methyl)-1H-1,2,3-triazol-1-yl)methyl)boronic acid (5h)

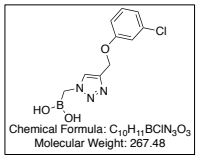

White solid (83%) ^{1}H NMR (400 MHz, MeOD) δ 8.42 (s, 1H, CH_{triaz}), 7.30 (t, J = 8.2 Hz, 1H, CH_{phen}), 7.10 (t, J = 2.2 Hz, 1H, CH_{phen}), 7.07 – 6.96 (m, 2H, CH_{phen}), 5.32 (s, 2H, CH_2O), 4.43 (s, 2H, CH_2B). ^{13}C NMR (101 MHz, MeOD) δ 159.9, 141.4, 136.1, 131.8, 128.7, 123.0, 116.4, 114.5, 60.9, 41,9 (CB). ^{11}B NMR (128 MHz, MeOD) δ 27.6. MS: HRMS (ESI-QTOF) m/z $[M + H]^+$ theo. 268.0657, found 268.0656.

((4-((4-methoxyphenoxy)methyl)-1H-1,2,3-triazol-1-yl)methyl)boronic acid (5i)

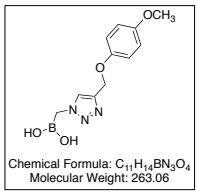

White hygroscopic solid (88%). ^{1}H NMR (400 MHz, MeOD) δ 8.30 (s, 1H, CH_{triaz}), 7.01 – 6.92 (m, 2H, CH_{phen}), 6.91 – 6.82 (m, 2H, CH_{phen}), 5.21 (s, 2H, CH_2O), 4.40 (s, 2H, CH_2B), 3.74 (s, 3H, CH_3). ^{13}C NMR (100 MHz, MeOD): δ 156.3, 153.1, 142.1, 128.6, 117.3, 115.8, 61.5, 56.1, 42.0 (CB). ^{11}B NMR (128 MHz, MeOD) δ 27.4. MS: HRMS (ESI-QTOF) m/z $[M + H]^+$ theo. 264.1152, found 264.1143.

((4-((3-acetamidophenoxy)methyl)-1H-1,2,3-triazol-1-yl)methyl)boronic acid (5j)

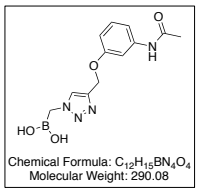

Yellow hygroscopic solid (90%). ^{1}H NMR (400 MHz, MeOD) δ 8.28 (s, 1H, CH_{triaz}), 7.47 (t, J = 2.2 Hz, 1H, CH_{phen}), 7.23 (t, J = 8.2 Hz, 1H, CH_{phen}), 7.07-7.02 (m, 1H, CH_{phen}), 6.80- 6.75 (m, 1H, CH_{phen}), 5.26 (s, 2H, CH_2O), 4.39 (s, 2H, CH_2B), 2.12 (s, 3H, CH_3). ^{13}C NMR (100 MHz, MeOD):) δ 171.7, 159.6, 141.2, 130.7, 128.2, 116.5, 114.3, 111.5, 108.0, 61.2, 41.2 (CB), 23.9. ^{11}B NMR (128 MHz, MeOD) δ 27.4. MS: HRMS (ESI-QTOF) m/z $[M + H]^+$ theo. 291.1261, found 291.1260.

((4-(3-ammoniophenyl)-1H-1,2,3-triazol-1-yl)methyl)boronic acid, chloride salt (5k)

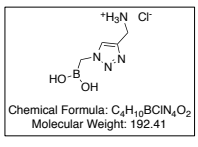

Brown hygroscopic solid (99%). ^{1}H NMR (400 MHz, MeOD) δ 8.11 (s, 1H, CH_{triaz}), 4.29 (s, 2H, CH_2NH_3), 4.26 (s, 2H, CH_2B). ^{13}C NMR (100 MHz, MeOD): δ 127.4, 77.6, 41.0 (CB, br), 35.3. ^{11}B NMR (128 MHz, MeOD) δ 27.8. MS: HRMS (ESI-QTOF) m/z $[M + H]^+$ theo. 157.0898, found 157.0886.

((4-((2,2,2-trifluoroacetamido)methyl)-1H-1,2,3-triazol-1-yl)methyl)boronic acid (5l)

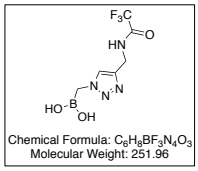

Yellow hygroscopic solid (83%). ^{1}H NMR (400 MHz, MeOD) δ 8.25 (s, 1H, CH_{triaz}), 4.65 (s, 2H, CH_2B), 3.12 (s, 2H, CH_2NH). ^{13}C NMR (100 MHz, MeOD) δ 159.3 (q, J = 37.7) 141.1, 128.4, 117.2

(q, J = 285.0), 41.3 (CB), 34.3. ^{11}B NMR (128 MHz, MeOD) δ 27.5. MS: HRMS (ESI-QTOF) m/z $[M + H]^+$ theo. 253.0715, found 253.0723.

((4-((phenylamino)methyl)-1H-1,2,3-triazol-1-yl)methyl)boronic acid (5m)

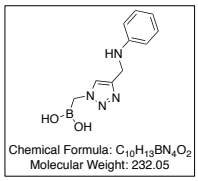

Yellow hygroscopic solid (95%). ^{1}H NMR (400 MHz, MeOD) δ 7.97 (s, 1H, CH_{triaz}), 7.60 – 7.47 (m, 3H, CH_{phen}), 7.40 (d, J = 7.7 Hz, 2H, CH_{phen}), 4.78 – 4.67 (m, 2H, CH_2NH), 4.26 (s, 2H, CH_2B). ^{13}C NMR (101 MHz, MeOD) δ 136.4, 131.44, 131.37, 130.7, 128.5, 124.0, 123.9, 47.1, 39.7 (CB). ^{11}B NMR (128 MHz, MeOD) δ 28.0. MS: HRMS (ESI-TOF) m/z $[M + H]^+$ theo. 233.1206, found 233.1213.

((4-((4-methylbenzamido)methyl)-1H-1,2,3-triazol-1-yl)methyl)boronic acid (5n)

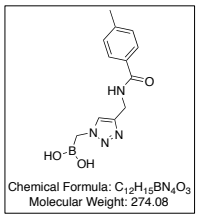

Yellow hygroscopic solid (86%). ^{1}H NMR (400 MHz, MeOD) δ 8.27 (s, 1H, CH_{triaz}), 7.77 (d, J = 7.9 Hz, 2H, CH_{phen}), 7.29 (d, J = 7.8 Hz, 2H, CH_{phen}), 4.70 (s, 2H, CH_2NH), 4.38 (s, 2H, CH_2B), 2.40 (s, 3H, CH_3). ^{13}C NMR (100 MHz, MeOD) δ 143.9, 132.1, 130.3, 130.2, 128.51, 128.46, 119.1, 42.8 (CB), 34.9, 21.4. ^{11}B NMR (128 MHz, MeOD) δ 27.2. MS: HRMS (ESI-QTOF) m/z $[M + H]^+$ theo. 275.1312, found 275.1300.

((4-((4-methylphenylsulfonamido)methyl)-1H-1,2,3-triazol-1-yl)methyl)boronic acid (5o)

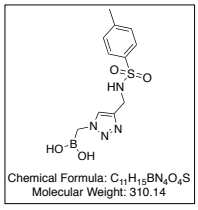

White hygroscopic solid (100%). ^{1}H NMR (400 MHz, MeOD) δ 8.23 (s, 1H, CH_{triaz}), 7.72 (t, J = 7.6 Hz, 2H, CH_{phen}), 7.36 (dd, J = 15.4, 8.0 Hz, 2H, CH_{phen}), 4.35 (s, 2H, CH_2NH), 4.24 (s, 2H, CH_2B), 2.40 (d, J = 7.2 Hz, 3H, CH_3). ^{13}C NMR (101 MHz, MeOD) δ 143.9, 141.2, 136.5, 129.6, 127.5, 126.8, 40.1, 35.6 (br, *C*B), 20.12. ^{11}B NMR (128 MHz, MeOD) δ 27.21. MS: HRMS (ESIQTOF) m/z $[M + H]^+$ theo. 311.0982, found 311.0995.

((4-((2,2,2-trifluoroethylsulfonamido)methyl)-1H-1,2,3-triazol-1-yl)methyl)boronic acid (5p)

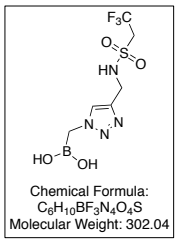

Orange hygroscopic solid (69%). ^{1}H NMR (400 MHz, MeOD) δ 8.34 (s, 1H, CH_{triaz}), 4.54 (s, 2H, CH_2NH), 4.43 (s, 2H, CH_2B), 4.26 (q, J = 9.5 Hz, 2H, CH_2CF_3). ^{13}C NMR (100 MHz, MeOD): δ 142.1, 128.05, 122.7 (q, J = 277.6), 53.9 (q, J = 30.7), 41.2 (CB), 36.4. ^{11}B NMR (128 MHz, MeOD) δ 27.6 MS: HRMS (ESI-QTOF) m/z $[M + H]^+$ theo. 303.0542, found 303.0547.

((4-((thiophene-2-sulfonamido)methyl)-1H-1,2,3-triazol-1-yl)methyl)boronic acid (5q)

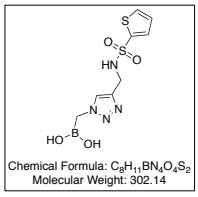

Yellow hygroscopic solid (98%), mp 68-70 °C. ^{1}H NMR (400 MHz, MeOD) δ 8.29 (s, 1H, CH_{triaz}), 7.84 (dd, J = 5.0, 1.3 Hz, 1H, CH_{thio}), 7.67 (dd, J = 3.7, 1.3 Hz, 1H, CH_{thio}), 7.18 (dd, J = 5.0, 3.8 Hz, 1H, CH_{thio}), 4.41 (s, 2H, CH_2NH), 4.35 (s, 2H, CH_2B). ^{13}C NMR (100 MHz, MeOD): δ 143.9, 141.8, 133.8, 133.7, 128.8, 128.5, 41.9 (CB), 37.9. ^{11}B NMR (128 MHz, MeOD) δ 27.3 MS: HRMS (ESI-QTOF) m/z $[M + H]^+$ theo. 303.0389, found 303.0387.

((4-(((3-nitrophenyl)methylsulfonamido)methyl)-1H-1,2,3-triazol-1-yl)methyl)boronic acid (5r)

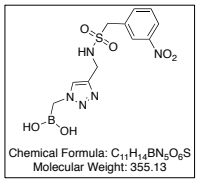

Orange hygroscopic solid (96%). ^{1}H NMR (400 MHz, MeOD) δ 8.34 (s, 1H, CH_{triaz}), 8.31 (t, J = 1.7 Hz, 1H, CH_{phen}), 8.29-8.27 (m, 1H, CH_{phen}), 7.86 (d, J = 7.8 Hz, 1H, CH_{phen}), 7.67 (t, J = 8.2 Hz, 1H, CH_{phen}), 4.60 (s, 2H, CH_2SO_2), 4.46 (s, 4H, CH_2NH + CH_2B). ^{13}C NMR (100 MHz, MeOD): δ 149.9, 138.5, 133.6, 131.1, 130.9, 129.3, 126.9, 124.6, 58.6, 42.3 (CB), 37.6. ^{11}B NMR (128 MHz, MeOD) δ

27.6. MS: HRMS (ESI-QTOF) m/z $[M + H]^+$ theo. 356.0833, found 356.0826.

((4-(((4-(methoxycarbonyl)phenyl)methylsulfonamido)methyl)-1H-1,2,3-triazol-1-yl)methyl)boronic acid (5s)

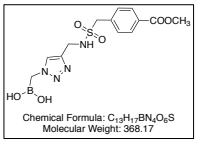

Yellow hygroscopic solid (98%). ^{1}H NMR (400 MHz, MeOD) δ 8.27 (s, 1H, CH_{triaz}), 8.02 (d, J = 8.3 Hz, 2H, CH_{phen}), 7.54 (d, J = 8.3 Hz, 2H, CH_{phen}), 4.50 (s, 2H, CH_2SO_2), 4.42 (s, 2H, CH_2NH), 4.36 (s, 2H, CH_2B), 3.91 (s, 3H, CH_3). ^{13}C NMR (100 MHz, MeOD): δ 168.1, 136.2, 132.2, 131.5, 130.7, 130.6, 128.9, 59.3, 52.8, 42.4 (CB), 37.4. ^{11}B NMR (128 MHz, MeOD) δ 27.7. MS: HRMS (ESI-QTOF) m/z $[M + H]^+$ theo. 369.1037, found 369.1047.

((4-((phenylmethylsulfonamido)methyl)-1H-1,2,3-triazol-1-yl)methyl)boronic acid (5t)

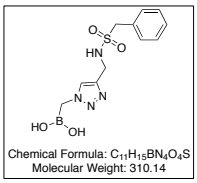

Yellow hygroscopic solid (59%). ^{1}H NMR (400 MHz, MeOD) δ 8.25 (s, 1H, CH_{triaz}), 7.51 – 7.23 (m, 5H, CH_{phen}), 4.40 (s, 2H, CH_2SO_2), 4.39 (s, 2H, CH_2NH), 4.29 (s, 2H, CH_2B). ^{13}C NMR (100 MHz, MeOD): δ 144.2, 132.0, 130.9, 129.69, 129.65, 129.0, 59.7, 42.2 (CB), 37.6. ^{11}B NMR (128 MHz, MeOD) δ 27.5. MS: HRMS (ESI-QTOF) m/z $[M + H]^+$ theo. 311.0982, found 311.0986.

((4-(((3-(methoxycarbonyl)phenyl)methylsulfonamido)methyl)-1H-1,2,3-triazol-1-yl)methyl)boronic acid (5u)

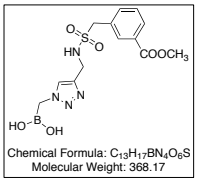

Yellow hygroscopic solid (95%). ^{1}H NMR (400 MHz, MeOD) δ 8.14 (s, 1H, CH_{triaz}), 8.04 - 8.00 (m, 2H, CH_{phen}), 7.65 (d, J = 7.8Hz, 1H, CH_{phen}), 7.51 (t, J = 7.6 Hz, 1H, CH_{phen}), 4.45 (s, 2H, CH_2SO_2), 4.33 (s, 4H, CH_2NH + CH_2B), 3.92 (s, 3H, CH_3). ^{13}C NMR (100 MHz, MeOD): δ 168.2, 144.2, 136.8, 133.1, 132.0, 131.9, 130.7, 130.1, 128.1, 59.3, 52.9, 41.7 (CB), 38.0. ^{11}B NMR (128 MHz, MeOD) δ 27.7. MS: HRMS (ESI-QTOF) m/z $[M + H]^+$ theo. 369.1037, found 369.1044.

((4-(((3-carboxyphenyl)methylsulfonamido)methyl)-1H-1,2,3-triazol-1-yl)methyl)boronic acid (5v)

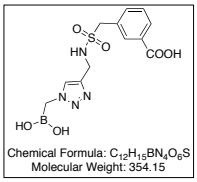

Deprotection of methyl ester and pinanediol auxiliary was performed by treatment of **4u** (0.36 mmol) with HCl in degassed water (3N, 4mL) under reflux for 3 h.

Grey hygroscopic solid (67%). ^{1}H NMR (400 MHz, MeOD) δ 8.33 (s, 1H, CH_{triaz}), 8.07 (s, 1H, CH_{phen}), 8.03 (dt, J = 7.8, 1.3 Hz, 1H, CH_{phen}), 7.68 (d, J = 7.6 Hz, 1H, CH_{phen}), 7.51 (t, J = 7.7 Hz, 1H, CH_{phen}), 4.50 (s, 2H, CH_2SO_2), 4.44 (s, 2H, CH_2NH), 4.38 (s, 2H, CH_2B). ^{13}C NMR (100 MHz, MeOD): δ 169.3, 143.1, 136.7, 133.3, 132.6, 131.7, 130.9, 130.1, 129.3, 59.2, 43.0 (CB), 37.3. ^{11}B NMR (128 MHz, MeOD) δ 27.4. MS: HRMS (ESI-QTOF) m/z $[M - H]^-$ theo. 352.0769, found 352.0771.

((4-((((4-cyanophenyl)methylsulfonamido)methyl)-1H-1,2,3-triazol-1-yl)methyl)boronic acid (5w)

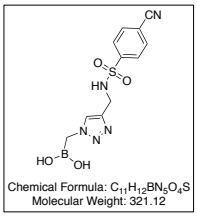

White hygroscopic solid (96%). ^{1}H NMR (400 MHz, MeOD) δ 8.27 (s, 1H, CH_{triaz}), 8.03 (dd, J = 8.64, 1.94 Hz, 2H, CH_{phen}), 7.97 (dd, J = 8.64, 1.94 Hz, 2H, CH_{phen}), 4.41 (s, 2H, CH_2B), 4.33 (d, J = 6.3 Hz, 2H, CH_2NH).^{13}C NMR (100 MHz, MeOD): δ 145.5, 134.4, 129.6, 128.9, 128.3, 118.4, 117.6, 42.2 (CB), 37.3. ^{11}B NMR (128 MHz, MeOD) δ 27.3. MS: HRMS (ESI-QTOF) m/z $[M + H]^+$ theo. 322.0778, found 322.0774.

((4-((((4-(1H-tetrazol-5-yl)phenyl)methylsulfonamido)methyl)-1H-1,2,3-triazol-1-yl)methyl)boronic acid (5y)

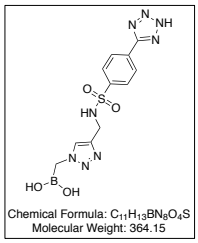

White hygroscopic solid (30%). ^{1}H NMR (400 MHz, MeOD) δ 8.38 (s, 1H, CH_{triaz}), 8.27 (d, J = 8.3 Hz, 2H, CH_{phen}), 8.08 (d, J = 8.4 Hz, 2H, CH_{phen}), 4.41 (s, 2H, CH_2SO_2), 4.39 (s, 2H, CH_2B). ^{13}C NMR (100 MHz, MeOD): δ 157.9, 143.3, 142.1, 130.5, 129.4, 129.2, 129.1, 43.0 (CB), 37.1. ^{11}B NMR (128 MHz, MeOD) δ 27.2. MS: HRMS (ESI-QTOF) m/z $[M + H]^+$ theo. 365.0948, found 365.094.

4-(1-(boronomethyl)-1H-1,2,3-triazol-4-yl)phthalic acid (6a)

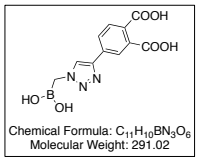

Yellowish solid (99%). ^{1}H NMR (400 MHz, MeOD): δ 8.60 (s, 1H, CH_{triaz}), 8.15 (d, J = 1.7 Hz, 1H, CH_{phen}), 7.99 (dd, J = 8.0, 1.8 Hz, 1H, CH_{phen}), 7.85 (d, J = 8.1 Hz, 1H, CH_{phen}), 4.39 (s, 2H, CH_2B).^{13}C NMR (101 MHz, MeOD): δ 170.98, 170.40, 135.54, 133.21, 131.33, 130.96, 128.64, 126.66, 125.32. ^{11}B NMR (128 MHz, MeOD): δ 28.39. MS: LC-MSQO m/z: $[M-H]^-$ theo. 290.05789, found 290.0592

((4-((2-((5-amino-1,3,4-thiadiazol-2-yl)thio)acetamido)methyl)-1H-1,2,3-triazol-1-yl)methyl)boronic acid (6b)

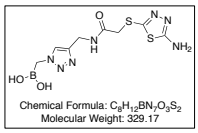

Yellow solid (100%). ^{1}H NMR (400 MHz, MeOD) δ 8.26 (s, 1H, CH_{triaz}), 4.57 (s, 2H, CH_2NH), 4.44 (s, 2H, CH_2B), 4.02 (s, 2H, CH_2S). ^{13}C NMR (101 MHz, MeOD) δ 172.39, 169.82, 156.18, 142.15, 128.69, 42.94 (CB), 37.46, 34.53. ^{11}B NMR (128 MHz, MeOD) δ 27.54. MS: LC-MSQO m/z: $[M+H]^+$ theo. 328.04524, found 328.0467

((4-((2-((5-methyl-4H-1,2,4-triazol-3-yl)thio)acetamido)methyl)-1H-1,2,3-triazol-1-yl)methyl)boronic acid (6c)

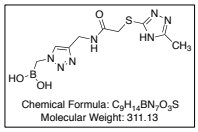

Yellow solid (99%). ^{1}H NMR (400 MHz, MeOD) δ 8.28 (s, 1H, CH_{triaz}), 4.50 (s, 2H, CH_2NH), 4.38 (s, 2H, CH_2B), 3.99 (s, 2H, CH_2S), 2.58 (s, 3H, CH_3). ^{13}C NMR (400 MHz, MeOD) δ 170.20, 155.38, 154.12, 142.53, 129.64, 43.33 (CB), 36.73, 34.54, 10.72. ^{11}B NMR (128 MHz, MeOD) δ 27.63. MS: LC-MSQO m/z: $[M+H]^+$ theo. 312.1045, found 312.10447.

((4-(hydroxycarbamoyl)-1H-1,2,3-triazol-1-yl)methyl)boronic acid (6d)

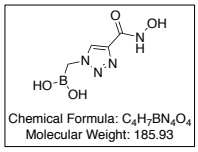

White solid. ^{1}H-NMR (400 MHz, DMSO-d_6): δ11.3 (s, 1H, OH), 8.5 (s, 1H, NH), 7.75 (s, 1H, CH_{triaz}), 4.01 (s, 2H, CH_2B). ^{13}C-NMR (101 MHz, DMSO-d_6) δ 173.87, 155.52, 122.10, 38.11 (CB).

2-(1-(boronomethyl)-1H-1,2,3-triazole-4-carboxamido)succinic acid (38e)

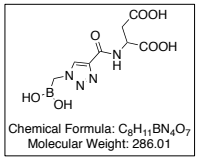

Yellow solid (100%). ^{1}H NMR (400 MHz, MeOD) δ 8.40 (s, 1H, CH_{triaz}), 5.00 – 4.91 (m, 1H, CH), 4.27 (s, 2H, CH_2B), 3.03 – 2.90 (m, 2H, CH_2-β). ^{13}C NMR (101 MHz, MeOD) δ 172.71, 172.44, 162.39, 142.89, 128.69, 39.76 (CB) 36.79. ^{11}B NMR (128 MHz, MeOD) δ 28.64. MS: LC-MSQO m/z $[M-H]^-$ theo. 285.0648, found 299.06506. $[\alpha]^{20}_D$ = - 2.68.

2-(1-(boronomethyl)-1H-1,2,3-triazole-4-carboxamido)pentanedioic acid (6f)

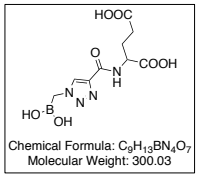

Yellowish solid (90%). ^{1}H NMR (400 MHz, MeOD) δ 8.26 (s, 1H, CH_{triaz}), 4.54 (dt, J = 9.9, 4.9 Hz, 1H, CH), 4.16 (s, 2H, CH_2B), 2.47 – 2.30 (m, 2H, CH_2-γ), 2.28 – 1.90 (m, 2H, CH_2-β). ^{13}C NMR (101 MHz, MeOD) δ 173.49, 173.41, 172.93, 171.88, 127.48, 52.63, 38.57 (CB), 31.22, 27.72. ^{11}B NMR (128 MHz, MeOD) δ 28.94. MS: LC-MSQO m/z $[M-H]^-$ theo. 299.0794, found 299.07936. $[\alpha]^{20}_D$ = - 7.86.

((4-((1-(tert-butoxy)-1-oxo-3-(tritylthio)propan-2-yl)carbamoyl)-1H-1,2,3-triazol-1-yl)methyl)boronic acid (6g)

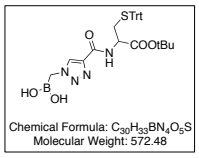

Yellow solid (64%). ^{1}H NMR (400 MHz, DMSO-d_6) δ 8.57 (d, J = 8.2 Hz, 1H, OH), 8.39 (s, 1H, CH_{triaz}), 7.36 – 7.22 (m, 15H, Trt), 4.23 (td, J = 8.7, 4.4 Hz, 1H, CH), 4.05 (s, 2H; CH_2B), 2.85 (dd, J = 12.5, 9.2 Hz, 1H, CH_2-β), 2.42 (dd, J = 12.4, 4.5 Hz, 1H, CH_2-β), 1.30 (s, 9H, tBu). ^{13}C NMR (101 MHz, DMSO-d_6) δ 169.23, 160.05, 144.44, 141.76, 129.30, 128.27, 127.53, 127.04, 81.37, 66.63, 52.29, 33.05, 27.73. $[\alpha]^{20}_{D}$ = - 4.80

((4-((3-(acetylthio)propanamido)methyl)-1H-1,2,3-triazol-1-yl)methyl)boronic acid (6h prodrug)

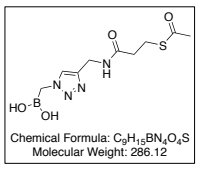

White solid (100%). ^{1}H NMR (400 MHz, MeOD) δ 8.31 (s, 1H, CH_{triaz}), 4.57 (s, 2H, CH_2B), 3.17 (s, 2H, CH_2NH), 2.98 (t, J = 7.3 Hz, 2H; CH_2S), 2.45 (t, J = 7.2 Hz, 2H; CH_2CO), 2.30 (s, 3H; CH_3). ^{13}C NMR (101 MHz, MeOD) δ 197.21, 142.49, 128.52, 36.41, 34.19 (CB), 30.61, 25.56.^{11}B NMR (128 MHz, MeOD) δ 27.80. MS: LC-MSQO m/z $[M+H]^+$ theo. 287.097, found 287.0980.

((4-((3-mercaptopropanamido)methyl)-1H-1,2,3-triazol-1-yl)methyl)boronic acid (6h)

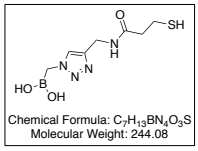

Compounds **6h** was obtained from **6h-prodrug** through hydrolysis in HCl / MeOH. 6h-prodrug was dissolved in a solution of HCl 0.1 M in MeOH. The reaction mixture was heated to 70°C and was stirred vigorously for 4h. A white solid was obtained (100%).

Synthesis of sulphonamidoboronic acids

Synthesis of pinanediol alkyl boronates (7)

(+)- or (-)- pinanediol (16.7 mmol, 1 eq.) was added to a solution of alkylboronic acids (16.7 mmol, 1 eq.) in dry THF (15 mL). The mixture was stirred at room temperature for 5h. The THF was evaporated *in vacuo*. The crude was re-solubilized in CH_2Cl_2 and Na_2SO_4 was added. The solution was dried over Na_2SO_4 for 20-30min then it was filtered and evaporated. The crude product was purified by column chromatography (petroleum ether /diethyl ether 95:5).

(3aR)-2,3a,5,5-tetramethylhexahydro-4,6-methanobenzo[d][1,3,2]dioxaborole (***7a***)

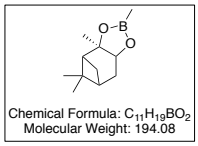

Colourless oil (68%). ^{1}H NMR (400 MHz, $CDCl_3$) δ 4.25 (dd, J = 8.7, 1.8 Hz, 1H, CH_{pin}), 2.39 – 2.28 (m, 1H, $CH_{2\text{-pin}}$), 2.27 – 2.16 (m, 1H, $CH_{2\text{-pin}}$), 2.04 (t, J = 5.5 Hz, 1H, CH_{pin}), 1.91 (dt, J = 8.6, 4.5 Hz, 1H, CH_{pin}), 1.87 – 1.81 (m, 1H, $CH_{2\text{-pin}}$), 1.54 (s, 3H, CH_3), 1.39 (s, 3H, $CH_{3\text{-pin}}$), 1.29 (s, 3H, $CH_{3\text{-pin}}$), 1.13 (d, J = 10.9 Hz, 1H, $CH_{2\text{-pin}}$), 0.84 (s, 3H, $CH_{3\text{-pin}}$).^{13}C NMR (101 MHz, $CDCl_3$) δ 85.56, 77.81, 51.49, 39.70, 38.29, 35.63, 28.83, 27.25, 26.60, 24.14. ^{11}B NMR (400 MHz, $CDCl_3$) δ 33.42.

(3aR)-2-ethyl-3a,5,5-trimethylhexahydro-4,6-methanobenzo[d][1,3,2]dioxaborole (***7b***)

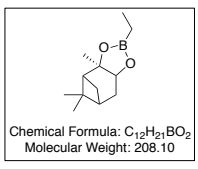

Colourless oil (54%). ^{1}H NMR (400 MHz, $CDCl_3$) δ 4.25 (dd, J = 8.7, 1.9 Hz, 1H, CH_{pin}), 2.39 – 2.28 (m, 1H, $CH_{2\text{-pin}}$), 2.21 (m, 1H, $CH_{2\text{-pin}}$), 2.04 (t, J = 5.6 Hz, 1H, CH_{pin}), 1.91 (dt, J = 5.6, 2.9 Hz, 1H, CH_{pin}), 1.88 – 1.79 (m, 1H, $CH_{2\text{-pin}}$), 1.38 (s, 3H, $CH_{3\text{-pin}}$), 1.29 (s, 3H, $CH_{3\text{-pin}}$), 1.11 (d, J = 10.9 Hz, 1H, $CH_{2\text{-pin}}$), 0.97 (t, J = 7.8 Hz, 3H, CH_3), 0.84 (s, 3H, $CH_{3\text{-pin}}$), 0.82 – 0.74 (m, 2H, CH_2B).^{13}C NMR (101 MHz, CDCl3) δ 85.46, 77.74, 51.48, 39.69, 38.28, 35.70, 28.83, 27.24, 26.57, 24.14, 8.01. ^{11}B NMR (400 MHz, $CDCl_3$) δ 33.94.

(3aS)-2-ethyl-3a,5,5-trimethylhexahydro-4,6-methanobenzo[d][1,3,2]dioxaborole (***7c***)

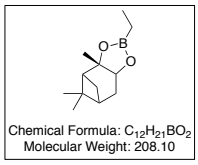

Colourless oil (91%). ^{1}H NMR (400 MHz, $CDCl_3$) δ 4.25 (dd, *J* = 8.7, 1.9 Hz, 1H, CH_{pin}), 2.39 – 2.28 (m, 1H, $CH_{2\text{-}pin}$), 2.21 (m, 1H, $CH_{2\text{-}pin}$), 2.04 (t, *J* = 5.6 Hz, 1H, CH_{pin}), 1.91 (dt, *J* = 5.6, 2.9 Hz, 1H, CH_{pin}), 1.88 – 1.79 (m, 1H, $CH_{2\text{-}pin}$), 1.38 (s, 3H, $CH_{3\text{-}pin}$), 1.29 (s, 3H, $CH_{3\text{-}pin}$), 1.11 (d, *J* = 10.9 Hz, 1H, $CH_{2\text{-}pin}$), 0.97 (t, *J* = 7.8 Hz, 3H, CH_3), 0.84 (s, 3H, $CH_{3\text{-}pin}$), 0.82 – 0.74 (m, 2H, CH_2B).^{13}C NMR (101 MHz, CDCl3) δ 85.46, 77.74, 51.48, 39.69, 38.28, 35.70, 28.83, 27.24, 26.57, 24.14, 8.01. ^{11}B NMR (400 MHz, $CDCl_3$) δ 33.94.

Synthesis of α-chloroalkylboronates (8)

Freshly distilled CH_2Cl_2 (8.24 mmol, 2 eq.) and dry THF (11 mL) were added in a four-necked flask under argon. The temperature was cooled to -100°C using a 1:1 EtOH/MeOH bath and liquid N_2. *n*-Butyllithium (4.94 mmol, 1.2 eq.) was added dropwise and the mixture was stirred at -100°C. After 20min the selected pinanediol alkylboronate ***7*** (4.12 mmol, 1 eq.) was dissolved in dry THF and added dropwise to the mixture. The temperature was allowed to reach -80°C and $ZnCl_2$ (3.3 mmol, 0.8 eq.) was added dropwise. The temperature was allowed to warm overnight, then the EtOH/MeOH bath was removed and the mixture was stirred for 1h at room temperature. The mixture was partitioned between saturated NH_4Cl (20 mL) and petroleum ether (70 mL). The organic phase was washed twice with saturated NH_4Cl (2 x 20 mL), then dried over Na_2SO_4, filtered and evaporated *in vacuo*. The crude product was not purified and used directly in the next reaction.

General procedure for the substitution of the chloro atom with lithium bis-trimethylsilylamide

The selected α-chloroboronate ***8*** (1.47 mmol, 1 eq.) was dissolved in dry THF (4.40 mL) under Ar. The solution was cooled to -100°C using a 1:1 EtOH/MeOH bath and liquid N_2. Lithium bis-trimethylsilylamide (1.61 mmol, 1.1 eq.) was added dropwise. The temperature was allowed to warm overnight, then the bath was removed and the mixture was stirred at room temperature for 1h. The mixture was partitioned between H_2O (4 mL) and petroleum ether (15 mL). The aqueous phase was re-extracted twice with petroleum ether (2 x 10 mL), then the organic phases were washed with saturated NaCl, dried over Na_2SO_4, filtered and evaporated *in vacuo*.

*1,1,1-trimethyl-N-((1S)-1-((3aR)-3a,5,5-trimethylhexahydro-4,6-methanobenzo[d][1,3,2]dioxaborol-2-yl)ethyl)-N-(trimethylsilyl)silanamine (**9a**)*

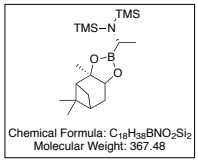

Yellow oil (56%). ^{1}H NMR (400 MHz, $CDCl_3$) δ 4.33 (d, *J* = 3.6 Hz, CH_{pin}), 2.39-1.86 (m, 5H, pinanediol), 1.42 (s, 3H, $CH_{3\text{-}pin}$), 1.31 (s, 3H, $CH_{3\text{-}pin}$), 1.22 (d, *J* = 7.5 Hz, 3H, CH_3), 1.17 (d, *J* = 10.9 Hz, 1H, $CH_{2\text{-}pin}$), 0.87 (s, 3H, $CH_{3\text{-}pin}$), 0.13 (s, 18H, TMS_2). ^{13}C NMR (101 MHz, $CDCl_3$) δ 85.68, 78.32, 51.47, 39.50, 38.20, 37.00 (CB), 35.45, 28.41, 27.08, 26.28, 24.02, 21.28, 2.67.

*1,1,1-trimethyl-N-((1S)-1-((3aR)-3a,5,5-trimethylhexahydro-4,6-methanobenzo[d][1,3,2]dioxaborol-2-yl)propyl)-N-(trimethylsilyl)silanamine (**9b**)*

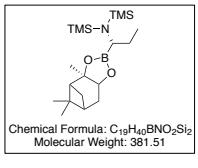

Yellow oil (85%). ^{1}H NMR (400 MHz, $CDCl_3$) δ 4.23 (dd, *J* = 8.6, 1.8 Hz, 1H, CH_{pin}), 2.71 (t, *J* = 7.1 Hz, 1H, CHB), 2.36 – 2.27 (m, 1H, $CH_{2\text{-}pin}$), 2.26 – 2.15 (m, 1H, $CH_{2\text{-}pin}$), 2.02 (dd, *J* = 10.3, 5.1 Hz, 1H, CH_{pin}), 1.90 (dd, *J* = 5.6, 2.6 Hz, 1H, CH_{pin}), 1.87 – 1.78 (m, 1H, $CH_{2\text{-}pin}$), 1.52 (dd, *J* = 14.5, 7.2 Hz, 2H, CH_2), 1.38 (s, 3H, $CH_{3\text{-}pin}$), 1.32 (s, 3H, $CH_{3\text{-}pin}$), 1.22 (d, *J* = 10.9 Hz, 1H, $CH_{2\text{-}pin}$), 0.93 (td, *J* = 7.4, 2.2 Hz, 3H, CH_3), 0.83 (s, 3H, $CH_{3\text{-}pin}$), 0.18 (s, 9H, TMS), 0.15 (s, 9H, TMS). ^{13}C NMR (101 MHz, $CDCl_3$) δ 83.71, 78.34, 51.60, 44.35, 40.08, 38.50, 35.58, 28.75, 28.57, 28.49, 27.28, 26.56, 24.15, 12.68, 1.49, 1.01.

*1,1,1-trimethyl-N-((1R)-1-((3aS)-3a,5,5-trimethylhexahydro-4,6-methanobenzo[d][1,3,2]dioxaborol-2-yl)propyl)-N-(trimethylsilyl)silanamine (**9c**)*

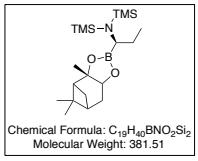

Yellow oil (81%) ^{1}H NMR (400 MHz, $CDCl_3$) δ 4.23 (dd, *J* = 8.6, 1.8 Hz, 1H, CH_{pin}), 2.71 (t, *J* = 7.1 Hz, 1H, CHB), 2.36 – 2.27 (m, 1H, $CH_{2\text{-}pin}$), 2.26 – 2.15 (m, 1H, $CH_{2\text{-}pin}$), 2.02 (dd, *J* = 10.3, 5.1 Hz, 1H, CH_{pin}), 1.90 (dd, *J* = 5.6, 2.6 Hz, 1H, CH_{pin}), 1.87 – 1.78 (m, 1H, $CH_{2\text{-}pin}$), 1.52 (dd, *J* = 14.5, 7.2 Hz, 2H, CH_2), 1.38 (s, 3H, $CH_{3\text{-}pin}$), 1.32 (s, 3H, $CH_{3\text{-}pin}$), 1.22 (d, *J* = 10.9 Hz, 1H, $CH_{2\text{-}pin}$), 0.93 (td, *J* = 7.4, 2.2 Hz, 3H, CH_3), 0.83 (s, 3H, $CH_{3\text{-}pin}$), 0.18 (s, 9H, TMS), 0.15 (s, 9H, TMS). ^{13}C NMR (101 MHz, $CDCl_3$) δ 83.71, 78.34, 51.60, 44.35, 40.08, 38.50, 35.58, 28.75, 28.57, 28.49, 27.28, 26.56, 24.15, 12.68, 1.49, 1.01.

General procedure for the synthesis of hydrochlorides (10)

The selected bis-trimethylsilylamide ***9*** (0.69 mmol, 1 eq.) was dissolved in dry THF (4.1 mL) under Ar. The temperature was cooled to 0°C with an ice bath and HCl 4 M in dioxane (0.6 mL) was slowly added. The reaction was allowed to reach room temperature and stirred under Ar for 4h. The mixture was evaporated to dryness *in vacuo*. The crude product was purified by trituration with dry Et_2O.

(1S)-1-((3aR)-3a,5,5-trimethylhexahydro-4,6-methanobenzo[d][1,3,2]dioxaborol-2-yl)ethan-1-aminium chloride ***(10a)***

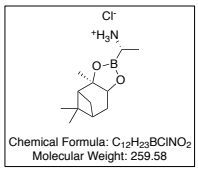

White solid (100%). ^{1}H NMR (400 MHz, DMSO-d_6) δ 7.82 (s, 3H, NH_3), 4.46 (dd, *J* = 8.7, 1.8 Hz, 1H, CH_{pin}), 2.87 (dd, *J* = 7.4, 5.9 Hz, 1H, CHB), 2.39 – 2.26 (m, 1H, $CH_{2\text{-}pin}$), 2.20 (ddd, *J* = 10.8, 6.2, 2.0 Hz, 1H, $CH_{2\text{-}pin}$), 2.01 (t, *J* = 5.5 Hz, 1H, CH_{pin}), 1.91 – 1.81 (m, 1H, CH_{pin}), 1.81 – 1.73 (m, 1H, $CH_{2\text{-}pin}$), 1.38 (s, 3H, $CH_{3\text{-}pin}$), 1.30 (s, 3H, $CH_{3\text{-}pin}$), 1.23 (d, *J* = 7.7 Hz, 3H, CH_3), 1.17 – 1.10 (m, 1H, $CH_{2\text{-}pin}$), 0.86 (s, 3H, $CH_{3\text{-}pin}$). ^{13}C NMR (101 MHz, DMSO-d_6) δ 86.72, 77.67, 51.21, 50.70, 37.90, 35.54, 34.59 (CB), 28.45, 26.88, 25.89, 23.62, 14.53.

(1S)-1-((3aR)-3a,5,5-trimethylhexahydro-4,6-methanobenzo[d][1,3,2]dioxaborol-2-yl)propan-1-aminium chloride ***(10b)***

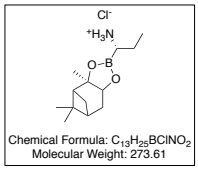

White solid (91%). ^{1}H NMR (400 MHz, DMSO-d_6) δ 7.91 (s, 3H, NH_3); 4.45 (dd, *J* = 8.8, 2.0 Hz, 1H, CH_{pin}); 2.72 (m, 1H, CHB); 2.30 - 1.77 (m, 5H, pinanediol), 1.67 (p, *J* = 7.4 Hz, 2H, CH_2); 1.38 (s, 3H, $CH_{3\text{-}pin}$); 1.27 (s, 3H, $CH_{3\text{-}pin}$); 1.14 (d, *J* = 10.8 Hz, 1H, $CH_{2\text{-}pin}$); 0.95 (t, *J* = 7.5 Hz, 3H, CH_3); 0.83 (s, 3H, $CH_{3\text{-}pin}$). ^{13}C NMR (101 MHz, DMSO-d_6) δ 86.74, 77.56, 50.67, 38.93, 38.82, 37.83 (CB), 34.65, 28.21, 26.80, 25.92, 23.59, 22.46, 10.93. ^{11}B NMR (400 MHz, DMSO-d_6) δ 33.71. $[\alpha]^{20}_D$ = -16.46 (MeOH).

(1R)-1-((3aS)-3a,5,5-trimethylhexahydro-4,6-methanobenzo[d][1,3,2]dioxaborol-2-yl)propan-1-aminium chloride ***(10c)****.*

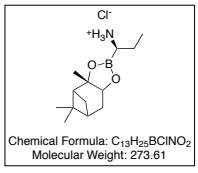

White solid (100%). ^{1}H NMR (400 MHz, DMSO-d_6) δ 7.91 (s, 3H, NH_3); 4.45 (dd, *J* = 8.8, 2.0 Hz, 1H, CH_{pin}); 2.72 (m, 1H, CHB); 2.30 - 1.77 (m, 5H, pinanediol), 1.67 (p, *J* = 7.4 Hz, 2H, CH_2); 1.38 (s, 3H, $CH_{3\text{-}pin}$); 1.27 (s, 3H, $CH_{3\text{-}pin}$); 1.14 (d, *J* = 10.8 Hz, 1H, $CH_{2\text{-}pin}$); 0.95 (t, *J* = 7.5 Hz, 3H, CH_3); 0.83 (s, 3H, $CH_{3\text{-}pin}$). ^{13}C NMR (101 MHz, DMSO-d_6) δ 86.74, 77.56, 50.67, 38.93, 38.82, 37.83 (CB), 34.65, 28.21, 26.80, 25.92, 23.59, 22.46, 10.93. ^{11}B NMR (400 MHz, DMSO-d_6) δ 33.71. $[\alpha]^{20}_D$ = +15.32 (MeOH).

General procedure for the synthesis of pinanendiol sulphonamidoboronates (11)

The selected sulphonyl chloride (1.46 mmol, 2 eq.) was added to a solution of the desired hydrochloride ***10*** (0.73 mmol, 1 eq.) in dry CH_2Cl_2 (11 mL) under Ar. DIPEA (1.60 mmol, 2.2 eq.) was solubilized in dry CH_2Cl_2 (2 mL) and added dropwise to the mixture. The reaction was stirred at room temperature for 4h. CH_2Cl_2 (15 mL) and water (5 mL) were added to the mixture. The two phases were separated and the aqueous phase was re-extracted with CH_2Cl_2 (2 x 10 mL). The organic phases were washed with saturated NaCl, dried over Na_2SO_4, filtered and evaporated under reduced pressure. The crude was purified by column chromatography on silica gel (petroleum ether / diethyl ether 7:3), affording the desired product.

*1-phenyl-N-((1S)-1-((3aR)-3a,5,5-trimethylhexahydro-4,6-methanobenzo[d][1,3,2]dioxaborol-2-yl)ethyl)methanesulfonamide (**11a**)*

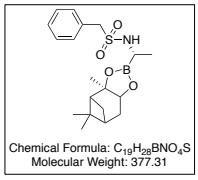

Yellowish solid (56%). ^{1}H NMR (400 MHz, $CDCl_3$) δ 7.45 – 7.31 (m, 5H, CH_{phen}), 4.29 (d + t, *J* = 23.1, 11.3 Hz, 3H, CH_{pin} + CH_2SO_2), 3.16 – 3.02 (m, 1H, CHB), 2.38 – 2.30 (m, 1H, $CH_{2\text{-}pin}$), 2.29 – 2.20 (m, 1H, $CH_{2\text{-}pin}$), 2.04 (q, *J* = 5.1 Hz, 1H, CH_{pin}), 1.92 (d, *J* = 12.3 Hz, 1H, CH_{pin}), 1.84 (d, *J* = 14.8 Hz, 1H, $CH_{2\text{-}pin}$), 1.41 (s, 3H, $CH_{3\text{-}pin}$), 1.29 (d, *J* = 7.6, 4.7 Hz + s, 6H, CH_3 + $CH_{3\text{-}pin}$), 1.09 (d, *J* = 11.0 Hz, 1H, $CH_{2\text{-}pin}$), 0.84 (d, *J* = 4.2 Hz, 3H, $CH_{3\text{-}pin}$).^{13}C NMR (101 MHz, $CDCl_3$) δ 130.91, 129.90, 128.80, 128.68, 87.21, 78.80, 59.55, 51.30, 39.53, 38.34, 35.85 (CB), 35.35, 28.63, 27.15, 26.46, 24.09, 18.89. ^{11}B NMR (400 MHz, $CDCl_3$) δ 32.67. $[\alpha]^{20}_D$ = - 3.61 (MeOH).

*methyl-3-((N-((1S)-1-((3aR)-3a,5,5-trimethylhexahydro-4,6-methanobenzo[d][1,3,2]dioxaborol-2-yl)ethyl)sulfamoyl)methyl)benzoate (**11b**)*

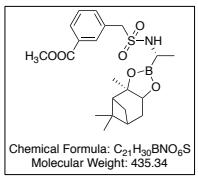

Yellowish solid (52%). ^{1}H NMR (400 MHz, $CDCl_3$) δ 8.08 (s, 1H, CH_{phen}), 8.04 (d, *J* = 7.8 Hz, 1H, CH_{phen}), 7.64 (d, *J* = 7.5 Hz, 1H, CH_{phen}), 7.45 (t, *J* = 7.7 Hz, 1H, CH_{phen}), 4.32 (td, *J* = 14.0, 6.3 Hz, 3H, CH_{pin} + CH_2SO_2), 3.92 (s, 3H, OCH_3), 3.15 (dd, *J* = 13.3, 7.1 Hz, 1H, CHB), 2.34 (dd, *J* = 14.6, 8.9 Hz, 1H, $CH_{2\text{-}pin}$), 2.25 (dd, *J* = 11.4, 6.8 Hz, 1H, $CH_{2\text{-}pin}$), 2.04 (d, *J* = 6.6 Hz, 1H, CH_{pin}), 1.95-1.90 (m, 1H, CH_{pin}), 1.83 (d, *J* = 14.8 Hz, 1H, $CH_{2\text{-}pin}$), 1.41 (s, 3H, $CH_{3\text{-}pin}$), 1.30 (t, *J* = 7.5 Hz, 6H, $CH_{3\text{-}pin}$ + CH_3), 1.07 (d, *J* = 11.0 Hz, 1H, $CH_{2\text{-}pin}$), 0.84 (s, 3H, $CH_{3\text{-}pin}$). ^{13}C NMR (101 MHz, $CDCl_3$) δ 166.68, 135.33, 132.05, 130.82, 130.40, 129.90, 128.90, 87.29, 78.80, 59.31, 52.37, 51.29, 39.53 (CB), 38.33, 35.34, 28.57, 27.14, 26.49, 24.09, 18.78. ^{11}B NMR (400 MHz, $CDCl_3$) δ 32.92. $[\alpha]^{20}_D$ = -3.89 (MeOH)

*1-phenyl-N-((1S)-1-((3aR)-3a,5,5-trimethylhexahydro-4,6-methanobenzo[d][1,3,2]dioxaborol-2-yl)propyl)methanesulfonamide (**11c**)*

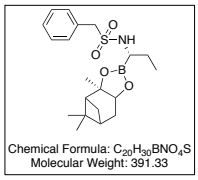

Yellowish solid (76%). ^{1}H NMR (400 MHz, $CDCl_3$) δ 7.41 (dq, *J* = 6.7, 4.1, 3.3 Hz, 2H, CH_{phen}), 7.38 – 7.33 (m, 3H, CH_{phen}), 4.37 (dd, *J* = 8.8, 2.1 Hz, 1H, CH_{pin}), 4.32 (d, *J* = 3.3 Hz, 2H, CH_2SO_2), 4.27 (d, *J* = 6.4 Hz, 1H, NH), 3.05 (q, *J* = 6.0 Hz, 1H, CHB), 2.35 (ddt, *J* = 14.4, 8.9, 2.6 Hz, 1H, $CH_{2\text{-}pin}$), 2.25 (m, 1H, $CH_{2\text{-}pin}$), 2.06 (t, *J* = 5.5 Hz, 1H, CH_{pin}), 1.94 (m, 1H, CH_{pin}), 1.84 (dt, *J* = 14.9, 2.6 Hz, 1H, $CH_{2\text{-}pin}$), 1.74 (dt, *J* = 14.1, 7.1 Hz, 2H, CH_2), 1.41 (s, 3H, $CH_{3\text{-}pin}$), 1.30 (s, 3H, $CH_{3\text{-}pin}$), 1.14 (d, *J* = 10.9 Hz, 1H, $CH_{2\text{-}pin}$), 0.92 (t, *J* = 7.4 Hz, 3H, CH_3), 0.85 (s, 3H, $CH_{3\text{-}pin}$). ^{13}C NMR (101 MHz, $CDCl_3$) δ 130.89, 129.88, 128.78, 128.66, 87.19, 78.71, 59.31, 51.27, 39.57, 38.37, 35.42, 28.80, 27.17, 26.62, 25.95, 24.14, 10.89. ^{11}B NMR (400 MHz, $CDCl_3$) δ 32.59. $[\alpha]^{20}_D$ = - 4.35 (MeOH).

*Methyl-3-((N-((1S)-1-((3aR)-3a,5,5-trimethylhexahydro-4,6-methanobenzo[d][1,3,2]dioxaborol-2-yl)propyl)sulfamoyl)methyl)benzoate (**11d**)*

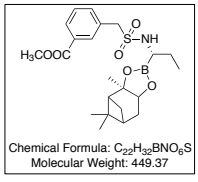

Yellowish solid (56%). ^{1}H NMR (400 MHz, $CDCl_3$) δ 8.08 (s, 1H, CH_{phen}), 8.04 (dt, *J* = 7.8, 1.5 Hz, 1H, CH_{phen}), 7.64 (dt, *J* = 7.7, 1.5 Hz, 1H, CH_{phen}), 7.45 (t, *J* = 7.7 Hz, 1H, CH_{phen}), 4.35 (dd, *J* = 8.8, 2.1 Hz, 1H, CH_{pin}), 4.32 (d, *J* = 3.3 Hz, 2H, CH_2SO_2), 4.27 (d, *J* = 6.4 Hz, 1H, NH), 3.90 (s, 3H, OCH_3), 3.11 (q, *J* = 5.9 Hz, 1H, CHB), 2.42 (m, 1H, $CH_{2\text{-}pin}$), 2.18 (m, 1H, $CH_{2\text{-}pin}$), 2.06 (t, *J* = 5.5 Hz, 1H, CH_{pin}), 1.93 (tt, *J* = 5.7, 3.0 Hz, 1H, CH_{pin}), 1.84 (ddd, *J* = 14.7, 3.4, 2.1 Hz, 1H, $CH_{2\text{-}pin}$), 1.72 (m, 2H, CH_2), 1.41 (s, 3H, $CH_{3\text{-}pin}$), 1.30 (s, 3H, $CH_{3\text{-}pin}$), 1.11 (d, *J* = 11.0 Hz, 1H, $CH_{2\text{-}pin}$), 0.93 (t, *J* = 7.4 Hz, 3H, CH_3), 0.84 (s, 3H, $CH_{3\text{-}pin}$). ^{13}C NMR (101 MHz, $CDCl_3$) δ 166.68, 135.30, 132.04, 130.81, 130.39, 129.89, 128.88, 87.27, 78.71, 59.08, 52.36, 51.25, 39.58, 38.36, 35.41, 28.74, 27.16, 26.59, 25.82, 24.14, 10.93. ^{11}B NMR (400 MHz, $CDCl_3$) δ 32.46. $[\alpha]^{20}_D$ = - 6.87 (MeOH).

*Methyl-3-((N-((1R)-1-((3aS)-3a,5,5-trimethylhexahydro-4,6-methanobenzo[d][1,3,2]dioxaborol-2-yl)propyl)sulfamoyl)methyl)benzoate (**11e**)*

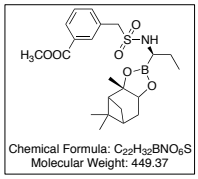

Yellowish solid (61%). ^{1}H NMR (400 MHz, $CDCl_3$) δ 8.08 (s, 1H, CH_{phen}), 8.04 (dt, *J* = 7.8, 1.5 Hz, 1H, CH_{phen}), 7.64 (dt, *J* = 7.7, 1.5 Hz, 1H, CH_{phen}), 7.45 (t, *J* = 7.7 Hz, 1H, CH_{phen}), 4.35 (dd, *J* = 8.8, 2.1 Hz, 1H, CH_{pin}), 4.32 (d, *J* = 3.3 Hz, 2H, CH_2SO_2), 4.27 (d, *J* = 6.4 Hz, 1H, NH), 3.90 (s, 3H, OCH_3), 3.11 (q, *J* = 5.9 Hz, 1H, CHB), 2.42 (m, 1H, $CH_{2\text{-}pin}$), 2.18 (m, 1H, $CH_{2\text{-}pin}$), 2.06 (t, *J* = 5.5 Hz, 1H, CH_{pin}), 1.93 (tt, *J* = 5.7, 3.0 Hz, 1H, CH_{pin}), 1.84 (ddd, *J* = 14.7, 3.4, 2.1 Hz, 1H, $CH_{2\text{-}pin}$), 1.72 (m, 2H, CH_2), 1.41 (s, 3H, $CH_{3\text{-}pin}$), 1.30 (s, 3H, $CH_{3\text{-}pin}$), 1.11 (d, *J* = 11.0 Hz, 1H, $CH_{2\text{-}pin}$), 0.93 (t, *J* = 7.4 Hz, 3H, CH_3), 0.84 (s, 3H, $CH_{3\text{-}pin}$). ^{13}C NMR (101 MHz, $CDCl_3$) δ 166.68, 135.30, 132.04, 130.81, 130.39, 129.89, 128.88, 87.27, 78.71, 59.08, 52.36, 51.25, 39.58, 38.36, 35.41, 28.74, 27.16, 26.59, 25.82, 24.14, 10.93. ^{11}B NMR (400 MHz, $CDCl_3$) δ 32.46. $[\alpha]^{20}_D$ = + 6.22 (MeOH).

General procedure for the transesterification of pinanendiol to obtain boronic acids

Sulphonamidoboronate ***11*** (0.36 mmol, 1 eq.) was dissolved in dry CH_3CN (2 mL). HCl 3M (0.54 mmol, 1.5 eq.) and isobutylboronic acid (0.34 mmol, 0.95 eq.) were added. The mixture was stirred for 5 min, then *n*-hexane (2 mL) was added. The biphasic mixture was vigorously stirred and after 30 min the *n*-hexane layer, containing the pinanediol isobutylboronate, was removed and fresh *n*-hexane (2 mL) was added. The last procedure was repeated several times until the disappearance of isobutylboronate from the *n*-hexane layer, monitored by TLC analysis (total reaction time 3-6 hours). The acetonitrile phase was then concentrated and the crude recrystallized to afford the sulphonamidoboronic acid.

General procedure for deprotection of carboxylic acid

Degassed HCl 3M (3.6 mL) was used to dissolve the sulphonamidoboronic acid (0.33 mmol, 1 eq.). The solution was refluxed for 2-3h. After cooling, the reaction mixture was diluted with water (2 mL) and washed three times with Et_2O (3 × 5 mL). The organic phase was washed twice with water. All the aqueous phase was concentrated *in vacuo* and CH_2Cl_2 was used to eliminate all the water, affording the desired final product.

*(S)-(1-((phenylmethyl)sulfonamido)ethyl)boronic acid (**12a**)*

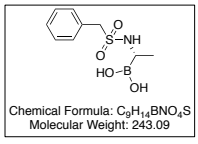

White solid (75%). ^{1}H NMR (400 MHz, MeOD) δ 7.42 – 7.33 (m, 5H, CH_{phen}), 4.39 – 4.23 (m, 2H, CH_2SO_2), 2.86 (d, *J* = 7.6 Hz, 1H, CHB), 1.14 (d, *J* = 7.4 Hz, 3H, CH_3). ^{13}C NMR (101 MHz, MeOD) δ 132.38, 132.05, 129.94, 129.79, 62.06, 60.51 (CB), 18.80.^{11}B NMR (400 MHz, $CDCl_3$) δ 28.82. LC-MSQO m/z $[M-H]^-$ theo. 243.07 found 242.0662. $[\alpha]^{20}_D$ = - 20.03 (MeOH).

*(S)-3-((N-(1-boronoethyl)sulfamoyl)methyl)benzoic acid (**12b**)*

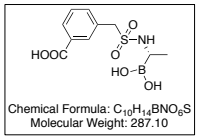

White solid (85%). ^{1}H NMR (400 MHz, MeOD) δ 8.08 (st, *J* = 1.8 Hz, CH_{phen}), 8.02 (dt, *J* = 7.8, 1.5 Hz, CH_{phen}), 7.66 (dt, *J* = 7.8, 1.5 Hz, CH_{phen}), 7.49 (t, *J* = 7.7 Hz, 1H, CH_{phen}), 4.39 - 4.35 (m, 2H, CH_2SO_2), 2.86 (d, *J* = 7.6 Hz, 1H, CHB), 1.14 (d, *J* = 7.4 Hz, 3H, CH_3). ^{13}C NMR (400 MHz, MeOD) δ 169.23, 136.46, 133.20, 132.34, 132.32, 130.59, 129.89, 59.65, 38.28 (CB), 18.41. LC-MSQO m/z $[M-H]^-$ theo. 287.06 found 286.0564. $[\alpha]^{20}_D$ = - 25.16 (MeOH).

*(S)-(1-((phenylmethyl)sulfonamido)propyl)boronic acid (**12c**)*

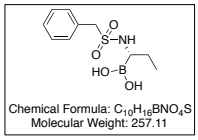

White solid (66%). ^{1}H NMR (400 MHz, MeOD) δ 7.39 (dq, *J* = 17.9, 3.4, 2.9 Hz, 5H, CH_{phen}), 4.38 – 4.22 (m, 2H, CH_2SO_2), 2.79 (t, *J* = 6.6 Hz, 1H, CHB), 1.53 (ddq, *J* = 27.8, 13.8, 7.0 Hz, 2H, CH_2), 0.87 (t, *J* = 7.4 Hz, 3H, CH_3). ^{13}C NMR (101 MHz, MeOD) δ 131.98, 131.63, 129.54, 129.38, 60.08, 44.28

(CB), 26.34, 11.29. ^{11}B NMR (400 MHz, MeOD) δ 29.06. LC-MSQO m/z [M-H]$^-$ theo. 257.09 found 256.0821. $[\alpha]^{20}_D$ = -22.93 (MeOH).

*(S)-3-((N-(1-boronopropyl)sulfamoyl)methyl)benzoic acid (**12d**)*

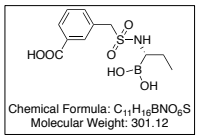

Chemical Formula: $C_{11}H_{16}BNO_6S$
Molecular Weight: 301.12

White solid (42%). ^{1}H NMR (400 MHz, DMSO-d_6) δ 12.97 (s, 1H, COOH), 7.97 (d, *J* = 1.8 Hz, 1H, CH_{phen}), 7.90 (dt, *J* = 7.7, 1.5 Hz, 1H, CH_{phen}), 7.81 (s, 2H, $B(OH)_2$), 7.59 (dt, *J* = 7.7, 1.5 Hz, 1H, CH_{phen}), 7.48 (t, *J* = 7.7 Hz, 1H, CH_{phen}), 6.23 (d, *J* = 6.9 Hz, 1H, NH), 4.38 (s, 2H, CH_2SO_2), 2.78 (q, *J* = 6.3 Hz, 1H, CHB), 1.51 (dt, *J* = 9.7, 6.9 Hz, 2H, CH_2), 0.80 (t, *J* = 7.4 Hz, 3H, CH_3). ^{13}C NMR (101 MHz, DMSO-d_6) δ 166.84, 134.92, 131.47, 131.03, 130.56, 128.50, 128.24, 57.13, 44.55, 24.92, 10.69. ^{11}B NMR (400 MHz, DMSO-d_6) δ 32.90. LC-MSQO m/z [M-H]$^-$ theo. 301.09 found 300.0720. $[\alpha]^{20}_D$ = - 27.58 (MeOH).

*(R)-3-((N-(1-boronopropyl)sulfamoyl)methyl)benzoic acid (**12e**)*

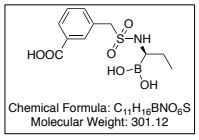

Chemical Formula: $C_{11}H_{16}BNO_6S$
Molecular Weight: 301.12

White solid (52%). ^{1}H NMR (400 MHz, MeOD) δ 8.08 (s, 1H, CH_{phen}), 8.02 (dt, *J* = 7.8, 1.4 Hz, 1H, CH_{phen}), 7.66 (dt, *J* = 7.6, 1.5 Hz, 1H, CH_{phen}), 7.49 (t, *J* = 7.7 Hz, 1H, CH_{phen}), 4.47 – 4.29 (m, 2H, CH_2SO_2), 2.78 (t, *J* = 6.5 Hz, 1H, CHB), 1.54 (ddq, *J* = 27.7, 13.8, 6.9 Hz, 2H, CH_2), 0.86 (t, *J* = 7.5 Hz, 3H, CH_3).^{13}C NMR (101 MHz, MeOD) δ 169.27, 136.46, 133.18, 132.32, 132.26, 130.58, 129.65, 61.18, 59.40 (CB), 26.48, 11.19.^{11}B NMR (400 MHz, MeOD) δ 29.86. LC-MSQO m/z [M-H]$^-$ theo. 301.09 found 300.0722. $[\alpha]^{20}_D$ = + 27.09.

Synthesis of compound 12f

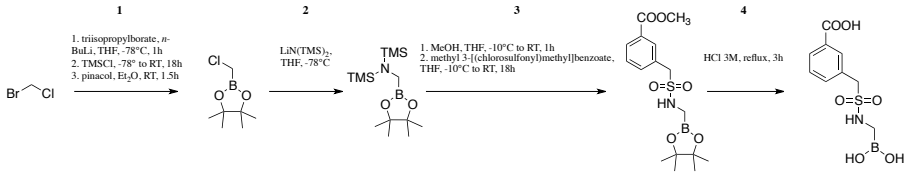

1. Synthesis of pinacol chloromethaneboronate: *n*-butyllithium (2.5 M in hexane, 46.78 mmol, 1 eq.) was added dropwise to a stirred solution of bromochloromethane (46.78 mmol, 1 eq.) and triisopropyl borate (42.53 mmol, 0.9 eq.) in THF (25 mL) at –78 °C. After 1h at –78 °C, trimethylsilyl chloride (TMSCl, 51.04 mmol, 1.1 eq.) was dropped into the reactor. After 2h the temperature was raised to room temperature and the mixture allowed to react overnight. Pinacol (46.78 mmol, 1 eq.) dissolved in diethyl ether (20 mL) was added, and the mixture was stirred for an additional 1.5h. The mixture was partitioned between Et_2O (40 mL) and H_2O (40 mL). The aqueous phase was extracted with Et_2O (3 × 30 mL). The combined organic phases were dried over $MgSO_4$, filtered and concentrated *in vacuo*. The oily residue was distilled *in vacuo* (b.p. 42°C/1 mmHg), recovering the pinacol chloromethaneboronate.

2. Synthesis of pinacol *N*-bis(trimethylsilyl)aminomethaneboronate: a solution of pinacol chloromethaneboronate (28.34 mmol, 1 eq.) in THF (15 mL) was cooled to −78 °C under Ar and lithium bis(trimethylsilyl)amide (1M in THF, 28.34 mmol, 1 eq.) was added dropwise. The reaction mixture was allowed to reach room temperature overnight and then concentrated *in vacuo*. The oily residue was washed with Et_2O, the white precipitate (LiCl) was centrifuged off, the supernatant concentrated, and the residue distilled *in vacuo* (b.p. 72°C/2.5 mmHg), recovering the pinacol *N*-bis(trimethylsilyl)aminomethaneboronate.

3. Synthesis of pinacol [3-(methoxycarbonyl)phenylmethanesulfonylamino]methaneboronate: a solution of pinacol *N*-bis(trimethylsilyl)aminomethaneboronate (1.00 mmol, 1 eq.) in THF (3 mL) was added to a solution of anhydrous methanol in THF (2.5 M, 1.00 mmol, 1 eq.) at −10°C under nitrogen. After stirring for 10 min at −10°C, the cooling bath was removed, and the reaction mixture was stirred for 1h at room temperature. Thereafter, the reaction mixture was once again cooled to −10°C and a solution of methyl 3-[(chlorosulfonyl)methyl]benzoate (1.10 mmol, 1.1 eq.) in THF (2 mL) was slowly added

and allowed to react for 16h. The resulting mixture was allowed to warm to room temperature overnight. The solvent was evaporated *in vacuo* and the residue purified by gradient chromatography (CH_2Cl_2/Et_2O from 8:2 to methanol), affording the pinacol-[3-(methoxycarbonyl)phenylmethanesulfonylamino]methaneboronate.

4. Synthesis of [3-(Carboxyphenyl)methanesulfonylamino]methaneboronic acid (***12f***): a mixture of pinacol [3-(methoxycarbonyl)phenylmethanesulfonylamino]methaneboronate (0.28 mmol, 1 eq.) and HCl 3M degassed (5 mL) was allowed to react at reflux temperature for 3h. After cooling, the reaction mixture was diluted with water (15 mL) and washed twice with Et_2O (2 × 20 mL). Then the aqueous phase was concentrated *in vacuo*, affording ***12f*** .

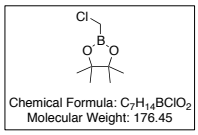

Chemical Formula: $C_7H_{14}BClO_2$
Molecular Weight: 176.45

Colourless liquid (88%). ^{1}H-NMR (200 MHz, $CDCl_3$): δ 2.96 (2H, s, CH_2B), 1.29 (12H, s, pinacol). ^{13}C-NMR (50 MHz, $CDCl_3$): δ 85.30, 29.50 (CB), 25.40. MS (EI): m/z (%) 178-176 (8) [M]+163-161 (100), 136-134 (6), 120-118 (8), 105-103 (5), 85 (44), 59(40).

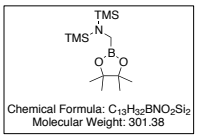

Chemical Formula: $C_{13}H_{32}BNO_2Si_2$
Molecular Weight: 301.38

Colourless liquid (68%). ^{1}H-NMR (200 MHz, $CDCl_3$): δ 2.45 (2H, s, CH_2B), 1.24 (12H, s, pinacol), 0.08 (18H, s, $Si(CH_3)_3$). ^{13}C-NMR (50 MHz, $CDCl_3$): δ 83.2, 29.7 (CB), 24.8, 1.5. MS (EI): m/z (%) 301 [M]+ 286, 228, 186 (100), 170, 112, 73, 59.

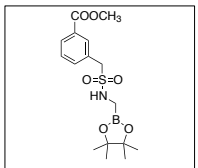

Chemical Formula: $C_{16}H_{24}BNO_6S$
Molecular Weight: 369.24

Yellowish oil (73%). ^{1}H-NMR (400 MHz, $CDCl_3$): δ 8.04-8.09 (2H, m, CH_{phen}), 7.65 (1H, d, J = 7.7, CH_{phen}), 7.47 (1H, t, J = 7.7, CH_{phen}), 4.33 (3H, br, CH_2SO_2 + NH), 3.92 (3H, s, OCH_3), 2.75 (2H, d, J = 2.8, CH_2B), 1.27 (12H, s, pinacol). ^{13}C-NMR (100 MHz, $CDCl_3$): δ 166.50, 135.10, 131.70, 130.80, 130.10, 129.80, 128.90, 84.80, 57.0, 52.20, 28.20 (CB), 24.70. MS (EI): m/z (%) 354 (< 2) [M 15]+160 (43), 150 (20), 146 (100), 119 (14), 104 (20), 91 (14), 90 (16), 74 (26), 59 (16).

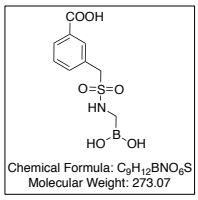

Chemical Formula: $C_9H_{12}BNO_6S$
Molecular Weight: 273.07

Yellow solid (51%). ^{1}H-NMR (400 MHz, MeOD): δ 8.11 (1H, s, CH_{phen}), 8.03 (1H, d, J = 7.7, CH_{phen}), 7.68 (1H, d, J = 7.7, CH_{phen}), 7.50 (1H, t, J = 7.7, CH_{phen}), 4.42 (2H, s, CH_2SO_2), 2.71 (2H, s, CH_2B). ^{13}C-NMR (100 MHz, MeOD): δ 167.90, 135.10, 131.80, 130.90, 130.80, 129.20, 128.30, 55.70, 29.0 (CB). MS (ESI, Ion Trap): m/z (%) 272 [M H]− MS/MS 272: m/z (%) 254 (81), 236 (100).

Purification and Kinetics

ADC-7 β-lactamase was expressed as described in precedent works[20] and purified using cation exchange chromatography. For the purification of ADC-7, cell pellets were suspended in 25 mM 3-(N-morpholino) propane- sulfonic acid (MOPS buffer), pH 6.5, with 1×HALT protease inhibitor cocktail (Sigma) and DNase I (50 Units). The solution was sonicated for 4 × 30 s intervals on ice. The lysate was centrifuged at 15 000 rpm at 4°C for 20 min. The cell-free extract was then loaded onto a carboxymethyl-cellulose column by gravity flow at 4°C (5 mL resin per gram of cell pellet). The column was washed with 100 mL of 25 mM MOPS, pH 6.5, at a flow rate of 0.3 mL/min followed by elution with a linear gradient of 0−0.5 M NaCl in 25 mM MOPS, pH 6.5. The fractions containing ADC-7 were collected, pooled, and then dialyzed in 2 × 5L of 25mM MOPS, pH6.5 at 4°C. The dialyzed ADC-7 was concentrated to at least 10 mg/mL using an Amicon Ultra centrifugal filter unit with Ultra-10 membrane (Millipore). The concentration of ADC-7 was determined using the A280 with an extinction coefficient of 46 300 $M^{-1}cm^{-1}$, as calculated for the expressed residues D24-K383 of ADC-7 by the ProtParam tool on the ExPASy bioinformatics portal.

The inhibition constants (K_i) for each of the BATSIs with ADC-7 were determined using competition kinetics. When nitrocefin (NCF) was utilized as a colorimetric substrate of ADC-7, boronic acids ***5a-o*** were tested as inhibitors of ADC-7 β-lactamase as previously described.[2,20,21] The measurements of the initial velocities were performed with the addition of 100 μM NCF after a 5 min preincubation of the enzyme (2 nM) with increasing concentration of the inhibitor. To determine the average velocities (v_0), data from three experiments were fit to the equation:

$$v_0 = v_u - (v_u [I] / IC_{50} + [I])$$

where v_u represents the NCF uninhibited velocity and IC_{50} represents the inhibitor concentration that results in a 50% reduction of v_u. The K_i values for all BATSIs were corrected for the NCF affinity (Km = 20 μM) with the Cheng-Prusoff equation:

$$K_i = IC_{50} / (1 + [NCF] / K_{mNCF}).$$

The data analysis was performed using EnzFitter and Origin 2019b.

KPC-2 β-lactamase was expressed as previously described[22] and purified using cation exchange chromatography. The inhibition constants (K_i) for each of the boronic acids with KPC-2 were determined using competition kinetics and using, also in this case, nitrocefin (NCF) as a substrate of KPC-2. The measurements of the velocities were performed in the same way performed for ADC-7.

Moreover, also for testing compounds ***12a-f*** on OXA-24/40 the reporter substrate was nitrocefin (NCF) and in this case a 3 min pre-incubation of substrate and enzyme was made. All compounds were 50 mM stocks in 100% DMSO and in some cases a 1:20 dilution in DMSO was made. The buffer used was 50 mM Na_2PO_4, 25 mM Na_2CO_3, pH 7.4.

Crystallization and Structure Determination

Structures of ADC-7 in complexes with the inhibitors were obtained via both soaking and cocrystallization methods. For soaks, ADC- 7 crystals were grown via hanging drop vapor diffusion at room temperature as previously described.[2] Preformed crystals were harvested using a nylon loop and soaked in crystallization buffer containing the BATSI at concentrations ranging from 2 to 16 mM for between 5 and 25 min. Co-crystals were grown in 0.1 M succinate/phosphate/glycine (SPG buffer), pH 5.0, 25% w/v PEG-1500, with 3.5−3.75 mg/mL ADC-7 and 1 mM BATSIs in the initial crystallization buffer. Data for each of the complexes were measured from single crystals at the Advanced Photon Source at Argonne National Laboratory (LS-CAT sector). All diffraction images were processed with XDS25 with the exception of the ADC-7/***5o*** data set, where HKL200026 was used. For the ADC-7/***5p*** data set, additional processing of the structure factors was performed using STARANISO. Structures were determined by molecular replacement with Phaser, using the ADC-7/**S02030** complex (PDB 4U0X), with water, ion, and inhibitor atoms removed, as the starting model. Refinement of the models was done with Refmac5 in the CCP4 suite and model building was done with Coot. The coordinates and structure factors for the ADC-7/ BATSI complexes were deposited in the Protein Data Bank with the following codes: 6TZF (***5c***), 6TZG (***5d***), 6TZH (***5e***), 6TZI (***5p***), and 6TZJ (***5o***).

Microbiology

MICs were performed as described in published articles[23] and according to Clinical and Laboratory Standards Institute (CLSI) guidelines, using a 6 × 104 cfu/mL inoculum. Bacterial cultures were grown overnight in Mueller-Hinton (MH) broth supplemented with 20 μg/mL chloramphenicol. For ADC-7, we employed the *E. Coli* construct that was previously validated as a representative of ADC-7 in a uniform genetic background (bla_{ADC-7} was directionally cloned in pBC SK (−) phagemid vector). Bacterial liquid culture was diluted using MH broth to a 6 × 104 cfu/mL final concentration, and the antibiotic partner, CAZ or FEP, was added at concentrations from 128 to 0.06 μg/ mL. BATSIs were constant at 4 μg/mL. The plates

were incubated at 37 °C overnight, and the results were recorded the next day. For KPC-2, *K. pneumoniae* expressing bla_{KPC-2} was employed. Bacterial liquid culture was then diluted to a McFarland Standard (OD600 0.224). The antibiotic partner cefepime (FEP) was added as serial dilutions, from 128 to 0.12 μg/mL, and the boronic acids were added at a constant 10 μg/mL concentration. The plates were incubated at 37°C overnight, and the results were recorded the next day.

Molecular docking

The crystal structure of KPC-2 (PDB ID: 2OV5) was used for the molecular docking. Using BIOVIA, Discovery Studio, molecular modeling software, the KPC-2 structure was minimized to a RMSD of 0.001 Å. The minimization was done using a Conjugate Gradient algorithm, with Generalized Born with a simple Switching model for solvent. The long-range electrostatics were treated with the particle Mesh Edwald method for periodic boundary condition. The activesite cavity was defined from the known active-site residue, with catalytic serine. The boronic acid compounds were built, minimized and automat docked into the active site of KPC-2 structure using CDOCKER protocol. The protocol uses a CHARMm-based molecular dynamics (MD) scheme to dock ligands into a receptor binding site (KPC-2). Random ligand conformations are generated using high temperature MD. The conformations are then translated into the binding site. Candidate poses are created, using random rigid-body rotations followed by simulated annealing. A final minimization is then used to refine the ligand poses. In addition to the structural information, each record includes the CDOCKER score reported as the negative value (i.e., -CDOCKER_ENERGY), where a higher value indicates a more favourable binding. This enables the energy to be used like a score. This score includes internal ligand strain energy and receptor-ligand interaction energy and is used to sort the poses of each input ligand. The compounds with the best scoring function were analysed, the covalent bond with S70 was form, and the enzyme-ligand complex was future minimized. To assess potential interactions and non bound interactions between the receptor (KPC-2) and boronates, the receptor interaction surface was generated for different compounds.

References

(1) Romagnoli, C.; Caselli, E.; Prati, F. Synthesis of [(1,2,3-Triazol-1-Yl)methyl]boronic Acids through Click Chemistry: Easy Access to a Potential Scaffold for Protease Inhibitors. *European J. Org. Chem.* **2015**, *2015* (5), 1075–1083. https://doi.org/10.1002/ejoc.201403408.

(2) Bouza, A. A.; Swanson, H. C.; Smolen, K. A.; Vandine, A. L.; Taracila, M. A.; Romagnoli, C.; Caselli, E.; Prati, F.; Bonomo, R. A.; Powers, R. A.; et al. Structure-Based Analysis of Boronic Acids as Inhibitors of Acinetobacter -Derived Cephalosporinase-7, a Unique Class C β-Lactamase. *ACS Infect. Dis.* **2018**, *4* (3), 325–336. https://doi.org/10.1021/acsinfecdis.7b00152.

(3) IGO.., G. W. H. O. 2017(WHO/EMP/IAU/2017. 12). (L. C. B.-N.-S. 3. .; Cataloguing-in-Publication. *PRIORITIZATION OF PATHOGENS TO GUIDE DISCOVERY, RESEARCH AND DEVELOPMENT OF NEW ANTIBIOTICS FOR DRUG-RESISTANT BACTERIAL INFECTIONS, INCLUDING TUBERCULOSIS*; 2017.

(4) Effah, C. Y.; Sun, T.; Liu, S.; Wu, Y. Klebsiella Pneumoniae: An Increasing Threat to Public Health. *Ann. Clin. Microbiol. Antimicrob.* **2020**, *19* (1), 1. https://doi.org/10.1186/s12941-019-0343-8.

(5) Stoesser, N.; Sheppard, A. E.; Peirano, G.; Anson, L. W.; Pankhurst, L.; Sebra, R.; Phan, H. T. T.; Kasarskis, A.; Mathers, A. J.; Peto, T. E. A.; et al. Genomic Epidemiology of Global Klebsiella Pneumoniae Carbapenemase (KPC)-Producing Escherichia Coli. *Sci. Rep.* **2017**, *7* (1), 1–11. https://doi.org/10.1038/s41598-017-06256-2.

(6) Yan, Y.-H.; Li, G.; Li, G.-B. Principles and Current Strategies Targeting Metallo-β-Lactamase Mediated Antibacterial Resistance. *Med. Res. Rev.* **2020**, *40* (5), 1558–1592. https://doi.org/https://doi.org/10.1002/med.21665.

(7) Werner, J. P.; Mitchell, J. M.; Taracila, M. A.; Bonomo, R. A.; Powers, R. A. Exploring the Potential of Boronic Acids as Inhibitors of OXA-24/40 β-Lactamase. *Protein Sci.* **2017**, *26* (3), 515–526. https://doi.org/https://doi.org/10.1002/pro.3100.

(8) Eidam, O.; Romagnoli, C.; Caselli, E.; Babaoglu, K.; Pohlhaus, D. T.; Karpiak, J.; Bonnet, R.; Shoichet, B. K.; Prati, F. Design, Synthesis, Crystal Structures, and Antimicrobial Activity of Sulfonamide Boronic Acids as β-Lactamase Inhibitors. *J. Med. Chem.* **2010**, *53* (21), 7852–7863. https://doi.org/10.1021/jm101015z.

(9) Drawz, S. M.; Taracila, M.; Caselli, E.; Prati, F.; Bonomo, R. A. Exploring Sequence Requirements for C3/C4 Carboxylate Recognition in the Pseudomonas Aeruginosa Cephalosporinase: Insights into Plasticity of the AmpC β-Lactamase. *Protein Sci.* **2011**, *20* (6), 941–958. https://doi.org/10.1002/pro.612.

(10) Santillana, E.; Beceiro, A.; Bou, G.; Romero, A. Crystal Structure of the Carbapenemase OXA-24 Reveals Insights into the Mechanism of Carbapenem Hydrolysis. *Proc. Natl. Acad. Sci. U. S. A.* **2007**, *104* (13), 5354–5359. https://doi.org/10.1073/pnas.0607557104.

(11) Schulze Wischeler, J.; Sun, D.; Sandner, N. U.; Linne, U.; Heine, A.; Koert, U.; Klebe, G. Stereo- and Regioselective Azide/Alkyne Cycloadditions in Carbonic Anhydrase II via Tethering, Monitored by Crystallography and Mass Spectrometry. *Chem. – A Eur. J.* **2011**, *17* (21), 5842–5851. https://doi.org/https://doi.org/10.1002/chem.201002437.

(12) Bertrand, H. C.; Schaap, M.; Baird, L.; Georgakopoulos, N. D.; Fowkes, A.; Thiollier, C.; Kachi, H.; Dinkova-Kostova, A. T.; Wells, G. Design, Synthesis, and Evaluation of Triazole Derivatives That Induce Nrf2 Dependent Gene Products and Inhibit the Keap1–Nrf2 Protein–Protein Interaction. *J. Med. Chem.* **2015**, *58* (18), 7186–7194. https://doi.org/10.1021/acs.jmedchem.5b00602.

(13) Munagala, G.; Yempalla, K. R.; Singh, S.; Sharma, S.; Kalia, N. P.; Rajput, V. S.; Kumar, S.; Sawant, S. D.; Khan, I. A.;

Vishwakarma, R. A.; et al. Synthesis of New Generation Triazolyl- and Isoxazolyl-Containing 6-Nitro-2,3-Dihydroimidazooxazoles as Anti-TB Agents: In Vitro, Structure–activity Relationship, Pharmacokinetics and in Vivo Evaluation. *Org. Biomol. Chem.* **2015**, *13* (12), 3610–3624. https://doi.org/10.1039/C5OB00054H.

(14) Miyamoto, Y.; Kalisiak, J.; Korthals, K.; Lauwaet, T.; Cheung, D. Y.; Lozano, R.; Cobo, E. R.; Upcroft, P.; Upcroft, J. A.; Berg, D. E.; et al. Expanded Therapeutic Potential in Activity Space of next-Generation 5-Nitroimidazole Antimicrobials with Broad Structural Diversity. *Proc. Natl. Acad. Sci.* **2013**, *110* (43), 17564 LP-17569. https://doi.org/10.1073/pnas.1302664110.

(15) Sinai, Á.; Vangel, D.; Gáti, T.; Bombicz, P.; Novák, Z. Utilization of Copper-Catalyzed Carboarylation–Ring Closure for the Synthesis of New Oxazoline Derivatives. *Org. Lett.* **2015**, *17* (17), 4136–4139. https://doi.org/10.1021/acs.orglett.5b01860.

(16) Dinges, J.; Albert, D. H.; Arnold, L. D.; Ashworth, K. L.; Akritopoulou-Zanze, I.; Bousquet, P. F.; Bouska, J. J.; Cunha, G. A.; Davidsen, S. K.; Diaz, G. J.; et al. 1,4-Dihydroindeno[1,2-C]pyrazoles with Acetylenic Side Chains as Novel and Potent Multitargeted Receptor Tyrosine Kinase Inhibitors with Low Affinity for the hERG Ion Channel. *J. Med. Chem.* **2007**, *50* (9), 2011–2029. https://doi.org/10.1021/jm061223o.

(17) Stefely, J. A.; Palchaudhuri, R.; Miller, P. A.; Peterson, R. J.; Moraski, G. C.; Hergenrother, P. J.; Miller, M. J. N-((1-Benzyl-1H-1,2,3-Triazol-4-Yl)methyl)arylamide as a New Scaffold That Provides Rapid Access to Antimicrotubule Agents: Synthesis and Evaluation of Antiproliferative Activity Against Select Cancer Cell Lines. *J. Med. Chem.* **2010**, *53* (8), 3389–3395. https://doi.org/10.1021/jm1000979.

(18) Cabrera-Lobera, N.; Quirós, M. T.; Brennessel, W. W.; Neidig, M. L.; Buñuel, E.; Cárdenas, D. J. Atom-Economical Ni-Catalyzed Diborylative Cyclization of Enynes: Preparation of Unsymmetrical Diboronates. *Org. Lett.* **2019**, *21* (16), 6552–6556. https://doi.org/10.1021/acs.orglett.9b02485.

(19) Yoshitomi, Y.; Makino, K.; Hamada, Y. Organocatalytic Synthesis of (2S,3R)-3-Hydroxy-3-Methyl-Proline (OHMePro), a Component of Polyoxypeptins, and Relatives Using OHMePro Itself as a Catalyst. *Org. Lett.* **2007**, *9* (13), 2457–2460. https://doi.org/10.1021/ol0706004.

(20) Caselli, E.; Romagnoli, C.; Powers, R. A.; Taracila, M. A.; Bouza, A. A.; Swanson, H. C.; Smolen, K. A.; Fini, F.; Wallar, B. J.; Bonomo, R. A.; et al. Inhibition of Acinetobacter -Derived Cephalosporinase: Exploring the Carboxylate Recognition Site Using Novel β-Lactamase Inhibitors. *ACS Infect. Dis.* **2018**, *4* (3), 337–348. https://doi.org/10.1021/acsinfecdis.7b00153.

(21) Powers, R. A.; Prati, F.; Bonomo, R. A.; Romagnoli, C.; Taracila, M. A.; Swanson, H. C.; Wallar, B. J.; Florek, N. W.; Caselli, E. Biochemical and Structural Analysis of Inhibitors Targeting the ADC-7 Cephalosporinase of Acinetobacter Baumannii . *Biochemistry* **2014**, *53* (48), 7670–7679. https://doi.org/10.1021/bi500887n.

(22) Papp-Wallace, K. M.; Taracila, M.; Wallace, C. J.; Hujer, K. M.; Bethel, C. R.; Hornick, J. M.; Bonomo, R. A. Elucidating the Role of Trp105 in the KPC-2 β-Lactamase. *Protein Sci.* **2010**, *19* (9), 1714–1727. https://doi.org/https://doi.org/10.1002/pro.454.

(23) Wong, D.; van Duin, D. Novel Beta-Lactamase Inhibitors: Unlocking Their Potential in Therapy. *Drugs* **2017**, *77* (6), 615–628. https://doi.org/10.1007/s40265-017-0725-1.

4 Modifications of the R_1 group

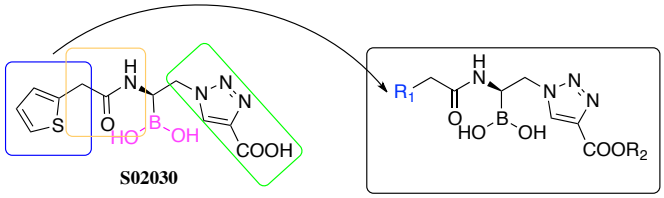

S02030 is a α-amido-β-triazolylboronic acid where the R_1 side chain is the same as the antibiotic cephalothin and the R_2 is a 4-carboxy 1,2,3-triazole which was introduced as an aromatic bioisoster of the phenyl ring inserted in the first series of 1-amido-2-(*m*-carboxyphenyl)ethaneboronic acids as mimic of the dihydrothiazine ring of cephalosporins (Figure 50).

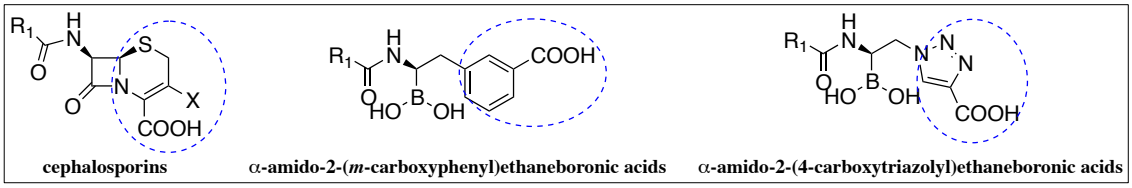

Figure 50. Development of boronic acids from cephalosporins.

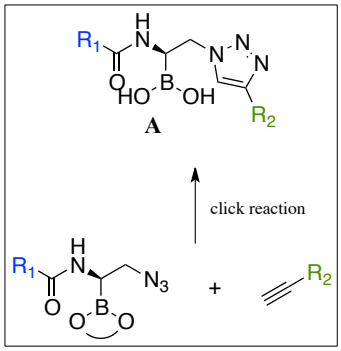

Figure 51. Flexible synthetic accessibility of the triazole ring through click chemistry.

As previously described (see section 1.3.5.3) **S02030** identification was the results of different studies in which several R_1 chains and different substituents on the C4 of the 1,2,3-triazole ring were introduced in the general scaffold A (Figure 51). The flexible synthetic accessibility of the triazole ring through the click reaction (Figure 51) allowed the development of several compounds highly active against clinically relevant class A and C BLs,[1–3] For this class of compounds the improvement in affinity obtained confirmed the usefulness of the triazole ring, which not only behaves as aromatic bioisoster but also actively interacts with enzyme residues. The kinetic analysis and microbiological assays pointed to **S02030** as the best hit for class A and class C β-lactamases inhibition.

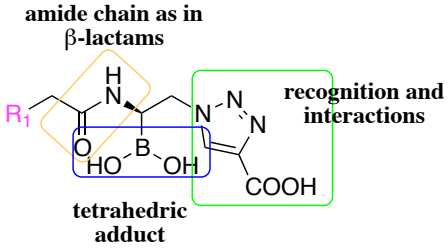

Starting from these results, one of the aims of my PhD programme was to modify **S02030** in order to gain activity against other classes of β-lactamases and to improve its pharmacological profile, since the thiophene ring is known to undergo oxidation *in vivo*.[4] A series of **S02030** derivatives, bearing an extra heteroatom on the R_1 aliphatic side chain directly bound to different heterocycles, was designed (Figure 52). The higher number of heteroatoms can potentially increase the enzyme residues-inhibitor interactions and enhance the *in vivo* stability of the BATSIs. Furthermore, some of these heterocycles are reported as zinc binding groups and might therefore inhibit class B MBLs. Seven molecules were synthesised and tested in kinetic and microbiological assays and the X-ray crystal structure of the best inhibitor was obtained. The results allowed the identification of a potent hit compound ***MB076*** (***19e***), the synthesis of which was scaled up in order to provide the amount needed to perform PK/PD studies and *in vivo* tests.

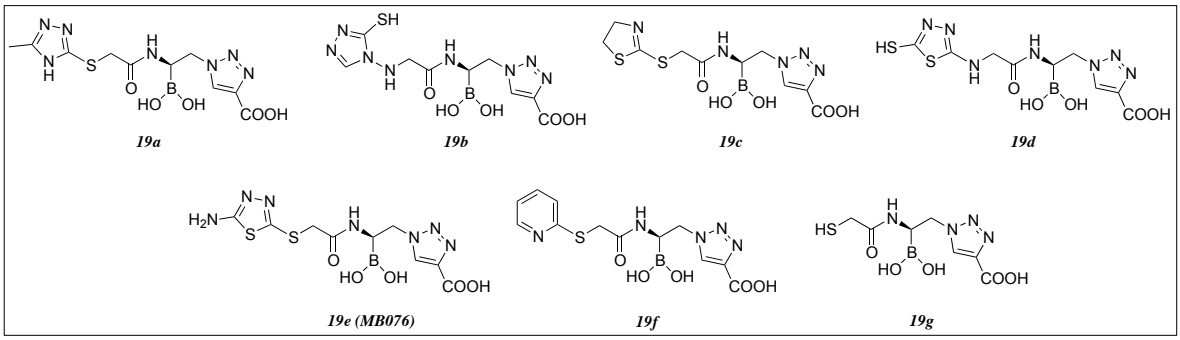

Figure 52. α-Amido-β-triazolylboronic acids (***19a-g***).

4.1 Synthesis of α-amido-β-triazolylboronic acids

The synthesis of α-amido-β-triazolylboronates is described in Scheme 10. Compound ***2*** was synthesised as described before (see section 3.1.1). (+)-Pinanendiol was used as chiral auxiliary for stereoselective insertion of the halogenated and asymmetrically substituted carbon atom in the pre-existing C-B bond through homologation. The conversion of compound ***2*** in the corresponding α-chloroboronate ***13*** was carried out at -100°C in anhydrous THF where dichloromethylithium is formed *in situ* starting from distilled CH_2Cl_2 (2 eq.) and *n*-BuLi (1.2 eq.). Compound ***13*** was obtained in 90% yield and then reacted in a nucleophilic substitution with lithium bis(trimethylsilyl)amide (1.1 eq.) in dry THF to synthesise compound ***14*** (68% yield). The hydrolysis to the corresponding hydrochloride salt ***15*** (99% yield) was accomplished using HCl 4 M in dioxane (3.5 eq.). Chloroacetyl chloride (1.1 eq.) was reacted with the hydrochloride and compound ***16*** was obtained and used directly in the click reaction with *tert*-butylpropiolate (1.05 eq.) affording the β-triazolylboronate ***17*** (95% yield).

Compound ***17*** was the key intermediate, starting from which the different heterocycles were inserted by nucleophilic substitution of the chloro atom with yields ranging from 45 to 95%.

Removal of the *tert*-butyl and the (+)-pinanediol group were finally performed, respectively with

trifluoroacetic acid (13 eq.) in dry CH_2Cl_2 (32 eq.) and by transesterification with isobutylboronic acid (0.95 eq.) and HCl 3 M (3 eq.), to provide the free boronic acids ***19a-g***. For compounds ***19b***, ***19d*** and ***19g*** it was necessary to remove the thioester protective group as final step of the synthesis.

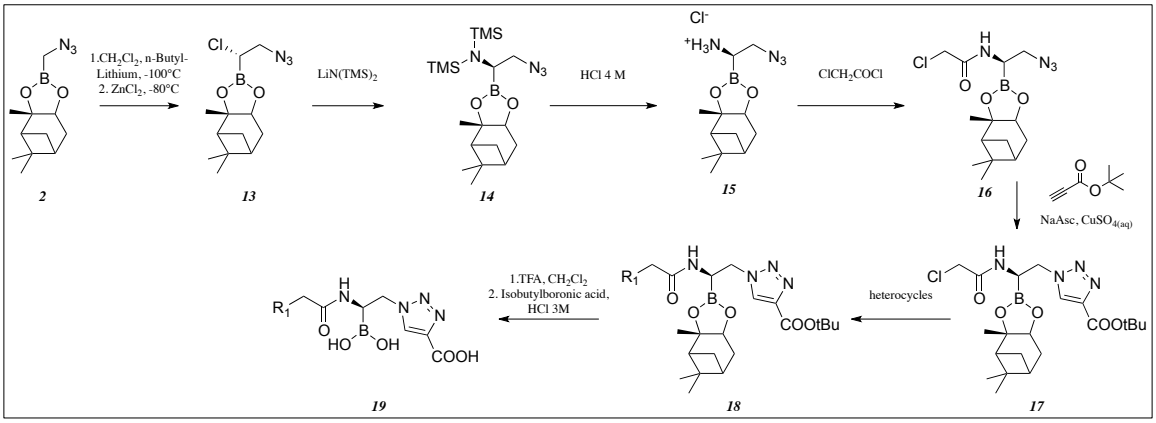

Scheme 10. Synthesis of α-amido-β-triazolylboronic acids (***19a-g***).

4.2 α-Acylamido-β-triazolylboronic acids as inhibitors of β-lactamases

Compounds *19 a-g* were tested as inhibitors of the class A KPC-2 (*K. pneumoniae* carbapenemase -2) and class C PDC-3 (*P. aeruginosa* AmpC -3) β-lactamases, class B VIM-2, IMP-1 and NDM-1 MBLs and class D OXA-23, OXA-24 and OXA-48. Compounds ***19a-g*** proved good inhibitors of PDC-3 with IC_{50} values ranging from 0.02 to 1.43 μM and excellent inhibitors of KPC-2 β-lactamase with IC_{50} values ranging from 0.13 to 0.58 μM. X-ray crystal structure of the best inhibitor ***MB076*** (***19e***) in complex with KPC-2 was obtained. Results obtained against class D and B BLs were not so encouraging. Therefore, we directed our effort in the optimization of this class of compounds as BLs inhibitors from extended-spectrum β-lactamases (ESBL)-producing *Enterobacteriaceae* and carbapenem-resistant *Enterobacteriaceae*.

Inhibition Kinetics

The binding affinities for each compound ***19a-g*** were calculated from competition assays using nitrocefin (NCF) as a reporter substrate. The IC_{50} values for all BATSIs, corrected for the NCF affinity are reported in Chart 5. All compounds (with the only exception of ***19e***) performed better against class A than against class C β-lactamases. Compounds ***19e*** (***MB076***, IC_{50} = 0.13 μM) and ***19g*** (IC_{50} = 0.17 μM) were the best inhibitors of KPC-2, although they are structurally different: ***19e*** possesses a thiadiazole ring and a free $–NH_2$ group, while ***19g*** bears only a little methanethiol chain. In general, compounds where a triazole or a thiadiazole ring was inserted demonstrated to inhibit KPC-2 with higher affinity than other compounds with a lower number of H bond acceptor N atoms (***19a***, ***19b***, ***19d*** and ***19e*** performed better than ***19c*** or ***19f***). The presence of a free –SH group improved the activity

against KPC-2, but if the same group is bound to a heterocycle, the activity decreased (***19g***, IC_{50} = 0.17 μM *vs* ***19b*** IC_{50} = 0.26 μM or ***19d*** IC_{50} = 0.46 μM).

Even if against class C the results were worse, some observations can be done: compound ***19e*** (***MB076***, IC_{50} = 0.02 μM) is the best inhibitor, together with ***19d*** (IC_{50} = 0.63 μM). The two compounds differ for the orientation of the thiadiazole ring. In ***19e*** the ring is bound through the thiol group and there is a free $–NH_2$ residue, while in ***19d*** the amine is bound to the molecule and the thiol group is free. The first orientation is preferred over the second one, where the activity decreases by 30-fold.

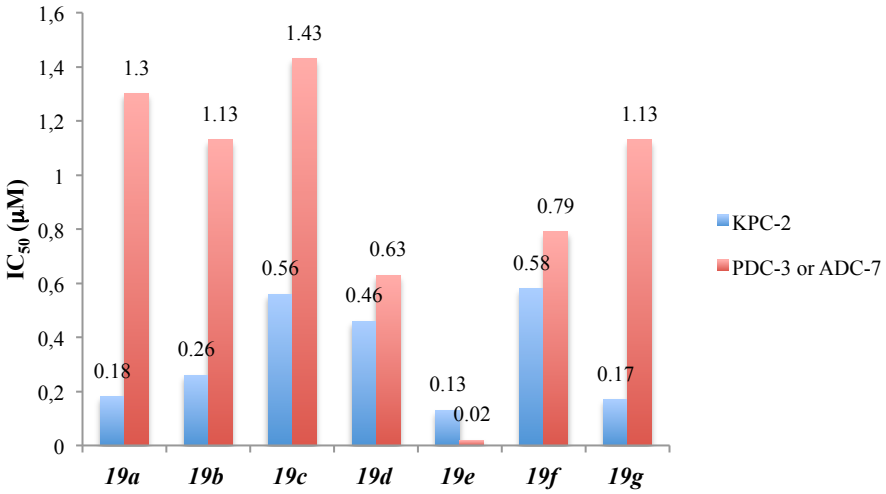

Chart 5. Binding affinities (IC_{50}) for compounds ***19a-g*** against class A, KPC-2 (blue) and class C, PDC-3 or ADC-7 (red) enzymes. ***19e*** was tested on ADC-7, while compounds ***19a-d*** and compounds ***19f-g*** were tested on PDC-3.

The binding affinities against class B, VIM-2, IMP-1 and NDM-1 were performed and the IC_{50} values were all > 20 μM. Compounds ***19a-g*** were tested also against class D, OXA-23, OXA-24 and OXA-48 β-lactamases, but also in this case no inhibition was observed, with IC_{50} values > 10 μM.

X-ray crystal structure of compound 19e (MB076) in complex with KPC-2

The crystal structure of KPC-2 with ***MB076*** **(*19e*)** bound was solved at 1.38Å resolution. The electron density map revealed ***MB076*** being covalently attached to the Oγ atom of the catalytic Ser70 residue (Figure 53). The two boronic acid hydroxyls form stabilizing interactions and occupy the oxyanion hole (formed by backbone nitrogens of Ser70 and Thr237) and the deacylation water pocket (formed by Glu166 and Asn170) of KPC-2.

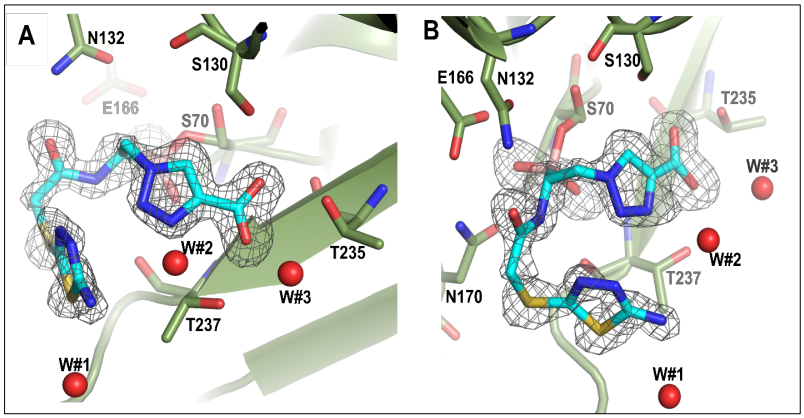

Figure 53. A) The structure and the electron density of ***MB076*** bound covalently in the active site of KPC-2 β-lactamase. B) Same as A, but the view is rotated about 90°.

The carboxylate group of ***MB076*** is placed in the putative β-lactam carboxyl binding pocket and makes hydrogen bonds with Ser130, Thr235, and Thr237. The carbonyl oxygen in ***MB076*** interacts with Asn132. The presence of the aromatic ring with a high dipole moment enhances the polarity of the C-H bond, which was demonstrated to become an efficient hydrogen bond donor. Indeed the CH of the triazole can form a C-H…O hydrogen bond with the hydroxyl of Ser130.

The -CH_2-S-thiadiazole ring- containing portion of ***MB076*** makes hydrophobic interactions with Asn170, the main chain atoms of Cys238, and Thr237. Furthermore, the thiadiazole ring forms intramolecular edge-to-face π-π interactions with the triazolyl moiety of ***MB076.*** The interaction of ***MB076*** binding also involves three water molecules (W#1, W#2, W#3).

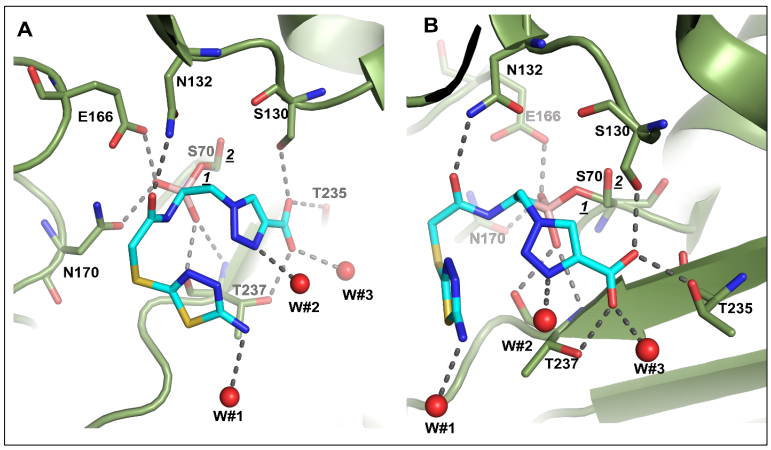

Figure 54. A) ***MB076*** binding in the active site of KPC-2 β-lactamase. B) Same as A, but view is rotated about 90°.

Microbiological assays

The minimum inhibitory concentrations (MICs) data for the α-acylamido-β-triazolylboronic acids ***19a-g*** are reported in Table 7. The agar dilution MICs were performed in combination with cefepime (FEP) on *E. coli* DH10B pBC-SK bla_{KPC-2} strains with BATSI concentrations maintained at 4 μg/mL.

All compounds lowered the MIC value for FEP. Compounds ***19c*** (MIC = 1 μg/mL) and ***19g*** (MIC = 1 μg/mL) reduced the MIC value by only 8-fold, while all the other compounds showed a MIC < 0.25 μg/mL. For ***19c*** the result is in agreement with its binding affinity for KPC-2, while the result is surprising for compound ***19f***, which was among the worst in kinetic analysis. These results demonstrate a potent inhibitory activity of α-acylamido-β-triazolylboronic acids and their ability in cell permeation. Together with kinetic analysis, MICs values point to ***19e (MB076)*** as the most promising compound for further development.

Table 7. Cellular assays for compounds ***19a-g***.

Compound	MIC (μg/mL) *E. coli* DH10B pBC-SK bla_{KPC-2}
FEP	8
19a	< 0.25
19b	< 0.25
19c	1
19d	< 0.25
19e	< 0.25
19f	< 0.25
19g	1

Lead compound assessment

Among the seven α-amido-β-triazolylboronates, designed to improve the activity of **S02030**, ***MB076*** emerged as the best compound in all experiments performed against critical class A and class C β-lactamases. In kinetic analysis, it proved the best inhibitor against both class A and class C enzymes (KPC-2, IC_{50} = 0.13 μM; ADC-7, IC_{50} = 0.02 μM). The X-ray crystal structure of ***MB076*** in complex with KPC-2 confirmed several interactions with the enzyme amino acids. Moreover, all seven α-amido-β-triazolylboronates were able to restore cefepime activity in *E. coli* DH10B pBC-SK bla_{KPC-2} strains, but also in this case ***MB076*** performed better than all the others. The potency of this compound encouraged our research group to continue in the direction of a preclinical development for

this molecule. Therefore, we scaled up the synthesis and produced a larger amount of compound, which was tested in the laboratories of Prof. Robert Bonomo at the Case Western University in Cleveland (Ohio, USA) for further characterization against clinically isolated strains. After that, ***MB076*** entered a program for preclinical development supported by the National Institute for Allergy and Infectious Diseases (NIAID), to assess the toxicity (maximun dose tolerated), the efficacy, the pharmacokinetic and pharmacodynamic profile (PK/PD) and the rate of survival in mice injected with multi-resistant bacterial strains.

4.3 *Preclinical development of MB076 for ESBL and carbapenemase expressing pathogens*

The widespread of multidrug resistant bacterial infections is rapidly becoming a worrisome problem. Extended-spectrum β-lactamases (ESBL) - producing pathogens spread rapidly and cause infection in healthy people, putting at a greater risk those patients with chronic diseases. In particular, Urinary Tract Infections (UTI) cause 1.3 million hospital admission per year. The 30% of these patients need a re-admission caused by multi-resistant UTIs, and among them about 20% of multidrug resistant UTIs are caused by ESBL and KPC- producing bacteria (Figure 55).[5] All these data underline the urgent need for new antimicrobials, and even if the preclinical and clinical pipelines of many pharmaceutical companies are filled by new antimicrobials, the high rate of resistance and the high capabilities of bacteria to develop resistance against new agents encourage the development of new, potent and targeted antimicrobials.

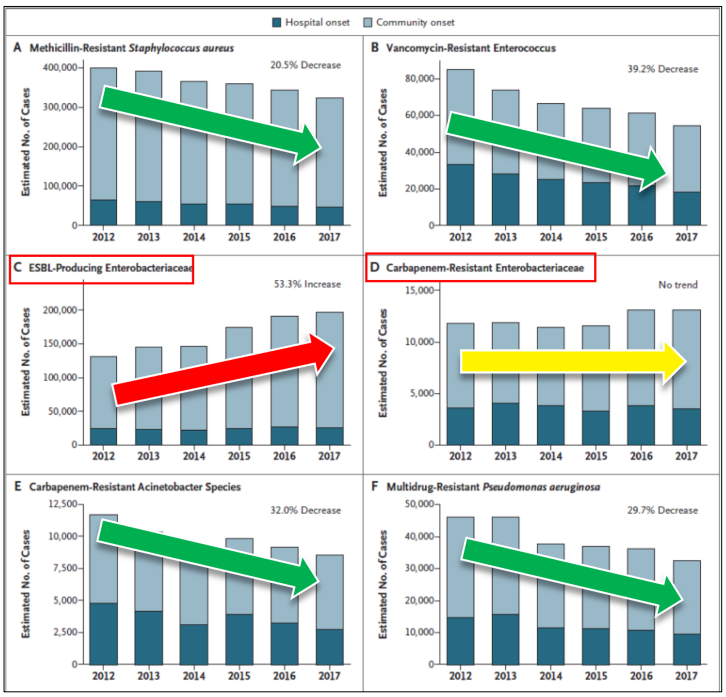

Figure 55. Estimated Number of Cases of Multidrug-Resistant Bacterial Infection in the United States, According to Year and Location Onset, 2012–2017. From *The New England Journal of Medicine*, **2020**, *382* (14), 1309-19 modified.[5]

MB076 emerged as possible lead compound for the treatment of resistant infections in co-administration with a β-lactam. ***MB076*** is a non-cyclic boronic acid, thus representing a new chemical entity in respect to inhibitors under development (see section 1.3.5.2). This new structure should be unlikely to quickly develop mechanism of resistance, and it represents an excellent candidate for the treatment of infections due to extended spectrum β-lactamases (ESBL) and carbapenemases, such as KPCs. Initially, we scaled up the synthesis of such compound and produced the amount needed to perform preclinical studies. ***MB076*** was tested against more resistant clinical strains to better evaluate

its ability to restore antibiotic activity and to select the bacterial strain to be used in efficacy studies. After that, a maximum dose tolerated (MDT) assessment was performed to determine the tolerability and the upper limit of ***MB076*** dosing in combination with meropenem or cilastatin. The MTD assessment was conducted prior to the efficacy study using neutropenic ICR mice; then the efficacy of ***MB076*** with meropenem plus cilastatin in monotherapy and in combination therapy was evaluated in the *K. pneumoniae* AR-BANK#0098 (KPC-2) thigh infection model. The pharmacokinetic profile of the compound was assessed measuring the analyte concentration in plasma and in thigh homogenates. Finally, a study of survival in mice infected IV with *K. pneumoniae* KP1 and treated with FEP alone or in combination with ***MB076*** was performed.

4.3.1 *Optimization of the synthesis of 19e (MB076)*

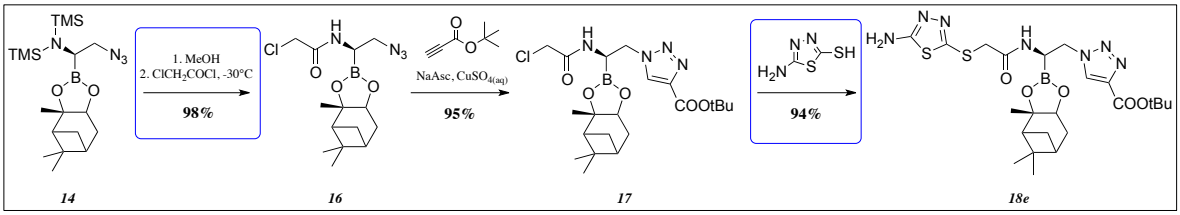

Scheme 11. Synthetic steps optimized for the synthesis of ***19e***.

The synthesis of ***19e*** was optimised changing a couple of synthetic procedures as described in Scheme 11. The first three steps affording the synthesis of compound ***14*** were performed in the same way described before (see section 4.1). A one-pot two-step reaction was performed to convert compound ***14*** into compound ***16***. The first step consisted in the hydrolysis of the bis-trimethylsilylamide performed in THF with dry MeOH (1 eq.). The reaction mixture was then cooled to -30°C and chloroacetyl chloride (1.1 eq.) was added to react with the amine and give compound ***16***. Another important modification was the purification strategy adopted for compound ***16***, which was purified by column chromatography and, thus, obtained in 98% yield. The click reaction with *tert*-butylpropiolate (1.05 eq.) afforded the β-triazolylboronate ***17*** (95% yield). The nucleophilic substitution of the chloro atom with 5-amino-1,3,4-thiadiazole-2-thiol was then performed, and the product was purified by crystallization and obtained in 94% yield. Final deprotections were developed as described before for other α-amido-β-triazolylboronates.

4.3.2 *"In vitro" microbiological assays against more clinical strains*

MIC's were performed on M-H agar plates, with 4 μg/mL of ***MB076*** and increasing concentration of cefepime (FEP). The results are reported in Table 8. The selected boronic acid performed well in all experiments, reducing the MIC value for cefepime with all strains tested. The most potent inhibition effect was observed on KPC-2 strains where MIC value was lowered from 16 to 0.5 μg/mL.

Table 8. Cellular assays of compound 19e against different bacterial strains.

Strains	MIC (µg/mL) FEP	MIC (µg/mL) *19e* + FEP
E-coli DH10B	**0.25**	**≤0.25**
*E-coli S*HV-1_ATCC BAA-202	**8**	**≤0.25**
E.coli DH10B SHV-1_pBC SK (-)	**2**	**≤0.25**
SHV-2_pBCSK	**4**	**≤0.25**
E-coli PBR322 KPC-2	**16**	**1**
K. pneumoniae (5) KPC-2	**16**	**0.5**

Starting from these results the antibacterial efficacy was evaluated against more *K. pneumoniae* strains, comparing the potency of ***MB076*** alone or in combination with FEP or with meropenem (MEM), and the activity of antibiotics alones. The MIC study included tigecycline as the quality control reference (Table 9). The three strains selected are resistant to meropenem and cefepime with a MIC value of greater or equal to 16 µg/mL. The MIC value of ***MB076*** when tested alone was greater than 32 µg/mL. On the contrary, when tested at a fixed concentration of 4 µg/mL in combination therapy with meropenem and cefepime, the MIC values decreased for all three *K. pneumoniae* strains. In particular, against *K. pneumoniae* strain AR-BANK#0098 (KPC-2), the combination therapy resulted in a MIC value of 0.03125 and ≤0.03125 µg/mL with respect to meropenem and cefepime compared to the 16 and 32 µg/mL MIC values of meropenem and cefepime monotherapies. Therefore, this *K. pneumoniae* strain was selected for efficacy study in a thigh infection model.

Table 9. Antimicrobial activity of ***MB076*** alone or in combination with meropenem or cefepime against different strains of *K. pneumoniae.*

Species / Strain ID	MIC, µg/mL					
	MB076	**Meropenem**	**Cefepime**	**Meropenem + *MB076***	**Cefepime + *MB076***	**Tigecycline**
Klebsiella pneumonial BAA-1705	>32	32	>32	**0.06 / 4**	**0.25 / 4**	2
Klebsiella pneumonial FDA-CDC AR-BANK#0097	>32	>32	>32	**1 / 4**	**2 / 4**	4
Klebsiella pneumonial FDA-CDC AR-BANK#0098	>32	16	32	**0.03 / 4**	**≤0.03 / 4**	1

4.3.3 Maximum dose tolerated

A maximum tolerable dose (MTD) assessment was conducted to evaluate the tolerability of ***MB076*** with meropenem and cilastatin combination. Neutropenic uninfected female ICR mice were used. Meropenem combined with cilastatin was subcutaneously (SC) administered followed by intravenous (IV) administration of ***MB076*** within 10 min. Doses were administered four times (QID) with 6 h intervals (q6h) for one day. Animals were monitored for acute symptoms after the first dose administration and cage side observations were recorded for the subsequent QID doses. Moreover, the body weight of each animal was recorded daily. The most significant results are summarized in Table 10. No acute toxicity or mortality was observed in the tested dose groups.

Mild effects were noted in the behavior observations: in particular all dosing groups resulted in slight vocalization and decreased muscle tone of the abdomen and limbs after the first dose administration. For the second to fourth dose administrations, piloerection was observed. No significant change in body weight was observed in the treatment groups compared to the monotherapy of meropenem plus cilastatin. The overall results indicated that the administration of meropenem plus cilastatin SC, followed by additional IV administration of ***MB076*** did not result in acute toxicity.

Table 10. MTD assessment in neutropenic mice. Results are reported as mean of measures on four mice. Only effects where a changement was observed are reported.

Dosage	Body weight after 1° dose	Body weight after 4° dose	Vocalization	Abdominal tone	Limb tone	Piloerection
MEM 1000 mg/Kg + cilastatin 200 mg/Kg (SC) + vehicle (PBS, IV)	23	23	2/4	increased	Mild effect	4/4 after 4° dose
MEM 1000 mg/Kg + cilastatin 200 mg/Kg (SC) + *MB076* 100 mg/Kg (IV)	23	22	0/4	Mild effect	Mild effect/increased	4/4 after 4° dose
MEM 1000 mg/Kg + cilastatin 200 mg/Kg (SC) + *MB076* 50 mg/Kg (IV)	23	22	3/4	Mild effect	Mild effect	4/4 after 4° dose
MEM 1000 mg/Kg + cilastatin 200 mg/Kg (SC) + *MB076* 25 mg/Kg (IV)	23.2	21.7	2/4	Mild effect	Mild effect	4/4 after 4° dose
MEM 500 mg/Kg + cilastatin 200 mg/Kg (SC) + *MB076* 50 mg/Kg (IV)	23	22.2	0/4	increased	Mild effect	4/4 after 4° dose
MEM 500 mg/Kg + cilastatin 200 mg/Kg (SC) + *MB076* 25 mg/Kg (IV)	23	22	1/4	Mild effect	Mild effect	4/4 after 4° dose

4.3.4 Efficacy study

The efficacy of ***MB076*** with meropenem plus cilastatin in monotherapy and in combination therapy was evaluated in the *K. pneumoniae* AR-BANK#0098 (KPC-2) thigh infection model with neutropenic female ICR mice (Table 11). Meropenem was administered with cilastatin to enhance the meropenem efficacy: indeed, cilastatin prolongs the exposure of meropenem in mouse by inhibiting the renal dehydropeptidase I enzyme (mDHPI). The MTD assessment dictated the highest possible dose of ***MB076*** to be tested and tigecycline was used as control reference. The efficacy was measured as reduction of colony forming units (CFU) per gram of tight weight compared to the baseline group and to antibiotics monotherapies. Meropenem at 1000 mg/kg plus cilastatin at 200 mg/kg resulted in modest antibacterial activity and also the monotherapy of ***MB076*** at 100 mg/kg alone had no significant antibacterial effect. On the other hand, the combination of ***MB076*** at 100 mg/kg QID with meropenem at 500 mg/kg plus cilastatin at 200 mg/kg QID resulted in a significant reduction in bacterial counts (0.45-$\log_{10}$ reduction) relative to the meropenem monotherapy at 1000 mg/kg plus cilastatin at 200 mg/kg group. A net static effect was observed with no significant decrease in bacterial counts as compared to baseline group. This dosage combination gave the best result: in fact, all other dosages resulted in no significant reduction in bacterial counts relative to the meropenem monotherapy (Chart 6).

Table 11. Data for efficacy study on ***MB076*** alone and in association with meropenem (MEM) and cilastatin compared to antibiotics monotherapies. All data are reported as mean of measures on five mice. Decrease (%) is the percentage decrease in counts (CFU/g) compared to the vehicle control group.

Dosage	Group	Tight weight (g)	CFU/g Thigh Time post inoculation 2, 26 h	Decrease (%)	Log (CFU/g Thigh) Time post inoculation 2, 26 h
Baseline counts, (2 h PI)	1	0.833	1.68E+05	/	5.10
Vehicle (0.9% NaCl) 10 mL/Kg (SC) + Vehicle (PBS) 6 mL/Kg (IV)	2	0.969	7.27E+07	/	7.65
Tigecycline 50 mg/Kg (SC)	3	0.858	2.13E+04	100	4.22
MEM 1000 mg/Kg + Cilastatin 200 mg/Kg (SC) + Vehicle (PBS) 6 mL/Kg (IV)	4	0.900	4.36E+05	99	5.50
Vehicle (0.9% NaCl) 10 mL/Kg (SC) + *MB076* 100 mg/Kg (IV)	5	0.885	2.87E+07	61	7.01
MEM 1000 mg/Kg + cilastatin 200 mg/Kg (SC) + *MB076* 100 mg/Kg (IV)	6	0.935	1.88E+05	100	5.06
MEM 1000 mg/Kg + cilastatin 200 mg/Kg (SC) + *MB076* 50 mg/Kg (IV)	7	0.958	1.48E+05	100	4.95
MEM 1000 mg/Kg + cilastatin 200 mg/Kg (SC) + *MB076* 25 mg/Kg (IV)	8	0.888	1.30E+05	100	4.98
MEM 1000 mg/Kg + cilastatin 200 mg/Kg (SC) + *MB076* 12.5 mg/Kg (IV)	9	0.862	2.46E+05	100	5.12
MEM 500 mg/Kg + cilastatin 200 mg/Kg (SC) + *MB076* 100 mg/Kg (IV)	10	0.861	1.70E+05	100	5.05
MEM 500 mg/Kg + cilastatin 200 mg/Kg (SC) + *MB076* 50 mg/Kg (IV)	11	0.871	3.28E+05	100	5.34
MEM 500 mg/Kg + cilastatin 200 mg/Kg (SC) + *MB076* 25 mg/Kg (IV)	12	0.893	1.58E+05	100	5.14
MEM 500 mg/Kg + cilastatin 200 mg/Kg (SC) + *MB076* 12.5 mg/Kg (IV)	13	0.897	6.36E+05	99	5.65

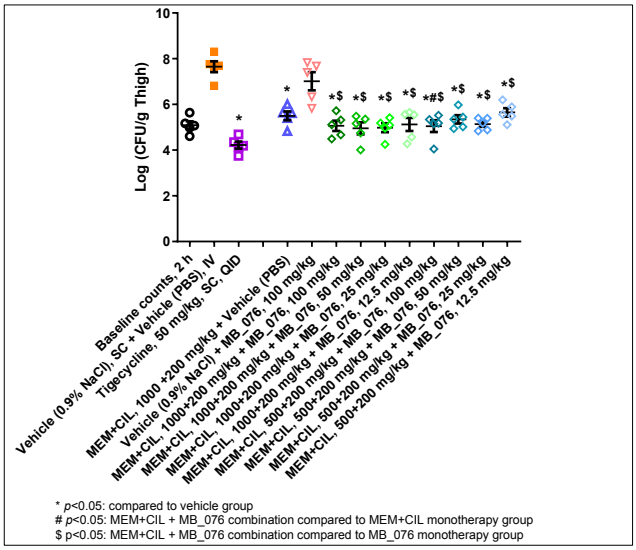

Chart 6. ***MB076*** with meropenem (MEM) plus cilastatin (CIL) in monotherapy and combination therapy in the *K. pneumoniae* AR-BANK#0098 (KPC-2) thigh infection model, scatter plot. (*): Indicates a significant difference ($p < 0.05$) compared to the vehicle control group as determined by one-way ANOVA and Dunnett's test. ($^{\#}$): Indicates a significant difference ($p < 0.05$) compared to MEM + CIL monotherapy as determined by student's t-test. ($^{\$}$): Indicates a significant difference ($p < 0.05$) compared to MB_076 monotherapy as determined by student's t-test

4.3.5 *Pharmacokinetic and Pharmacodynamic profile (PK/PD)*

A single dose PK study with ***MB076*** IV was performed to measure the compound's concentration over time in plasma samples and thigh homogenates LC-MS/MS. The PK study used the same ***MB076*** doses from the efficacy study with eight collection time points after a single IV dose administration.

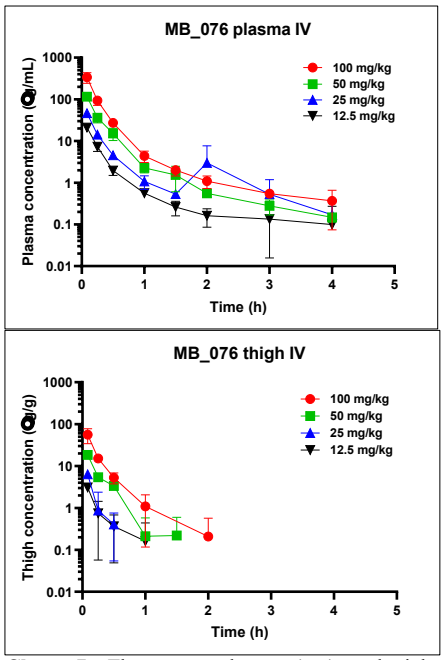

Chart 7. The mean plasma (top) and tight (bottom) concentration-time profiles of ***MB076*** after IV single administration to *K. pneumoniae* AR-BANK#0098 (KPC-2) thigh infected mice.

Among the PK parameters, $t_{1/2}$, C_0, AUC_{last}, AUC_{INF}, Vss and CL were evaluated (Table 12), while for PD parameters, C_0/MIC, AUC_{last}/MIC and T>MIC were calculated (Table 13). In particular, the % time over the minimum inhibitory concentration (T>MIC) was calculated for all dose groups to determine the impact of ***MB076*** efficacy in this animal model. Plots of concentration in plasma and thigh homogenate versus time were created and the linearity of the resulting PK parameters was assessed (Chart 7). Indeed, the concentration time profile of ***MB076*** yielded C_0 and AUC_{last} values that correlated linearly with dose both in plasma and in tight homogenates. In plasma, the C_0 values ranged from 35.6 to 638.1 µg/mL and AUC_{last} values ranged from 7.1 to 103.2 h*µg/mL. In the infected thigh homogenates, C_0 values ranged from 6.3 to 107.6 µg/g and AUC_{last} values ranged from 1.0 to

17.2 h*µg/g. The AUC_{last} thigh / AUC_{last} plasma ranged from 10% to 17% in the dose range of 12.5 to 100 mg/kg.

Table 12. The plasma and thigh PK parameters of ***MB076*** after single IV administration to *K. pneumoniae* AR-BANK#0098 (KPC-2) thigh infected mice (see Appendix 1- Pharmacokinetic and pharmacodynamics parameters, page 120).

MB_076 – Plasma							
Dose, IV (mg/kg)	Time point (h)	$t_{1/2}$ (h)	C_0 (µg/mL)	AUC_{last} (h*µg/mL)	AUC_{Inf} (h*µg/mL)	Vss (L/kg)	CL (mL/min/kg)
12.5	0.083-4.0	0.56	35.6	7.1	7.2	0.65	29.05
25	0.083-4.0	0.61	84.0	17.6	17.8	0.80	23.42
50	0.083-4.0	0.43	206.9	39.0	39.1	0.35	21.31
100	0.083-4.0	0.43	638.1	103.2	103.5	0.21	16.11
MB_076 – Thigh							
Dose, IV (mg/kg)	Time point (h)	$t_{1/2}$ (h)	C_0 (µg/g)	AUC_{last} (h*µg/g)	AUC_{Inf} (h*µg/g)	Vss (kg/kg)	CL (g/min/kg)
12.5	0.083-4.0	0.24	6.3	1.0	1.0	2.96	201.07
25	0.083-4.0	0.11	17.0	1.7	1.8	1.38	231.77
50	0.083-4.0	0.21	34.0	6.3	6.3	1.76	131.74
100	0.083-4.0	0.25	107.6	17.2	17.3	1.07	96.46

Tabella 13. The plasma and thigh PD parameters of ***MB076*** after single IV administration to *K. pneumoniae* AR-BANK#0098 (KPC-2) thigh infected mice (see Appendix 1- Pharmacokinetic and pharmacodynamics parameters, page 120).

MB_076 – Plasma						
Dose, IV (mg/kg)	TimeLow (h)	TimeHigh (h)	Dosage interval (h)	T > MIC (%)	C_0 / MIC	AUC_{last} / MIC (h)
12.5	23.60	0.40	24	1.69	8.91	1.77
25	23.42	0.58	24	2.43	21.01	4.41
50	23.07	0.93	24	3.89	51.73	9.75
100	22.92	1.08	24	4.51	159.52	25.81
MB_076 – Thigh						
12.5	23.94	0.06	24	0.24	1.57	0.25
25	23.88	0.12	24	0.50	4.26	0.43
50	23.58	0.42	24	1.75	8.51	1.56
100	23.35	0.65	24	2.72	26.89	4.30

4.3.6 Mice survival

Five male C57BL/6 mice per treatment group were infected intravenously via the tail-vein by injecting a prepared inoculum of *K. pneumoniae* KP1 (input CFU = 2.1 x 10^8 CFU/mouse) contained in a volume of 0.25 mL per animal. Animals were treated with intraperitoneal 100 mg/kg/dose of cefepime, cefepime + ***MB076*** (1:1, or 1:4 *ratio*) or placebo at the time of infection. Doses were repeated the following morning and afternoon (18h and 24h after infection). Survival was evaluated 24h post-treatment. To evaluate bacterial burden, a similar experiment was performed by infecting eight male C57BL/6 mice and treating with cefepime, cefepime + ***MB076*** (1:4 *ratio*) or placebo at the

time of infection. Blood was drawn from the tail 1 hour post-infection and a cardiac bleed was performed 18h post-infection. Determination of bacterial titers (CFU) was performed in each case. Results showed that mice treated with placebo or cefepime alone died, whereas all mice treated with ***MB076*** plus cefepime 1:4 survived (Figure 56).

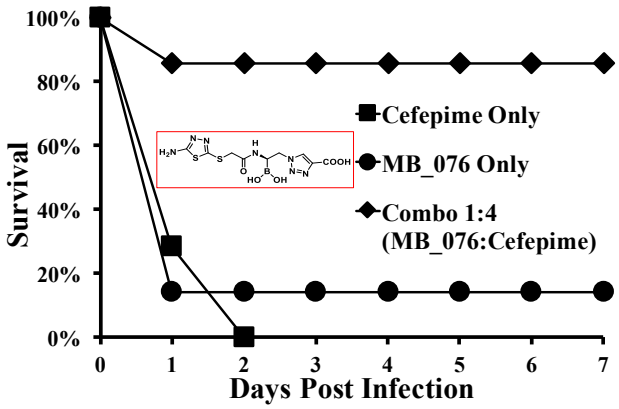

Figure 56. Survival curve of mice infected IV with *K.pneumoniae* Kp1 and treated with cefepime alone or in combination with ***MB076***.

Even if several new antimicrobials are under preclinical and clinical development, the high capabilities of bacteria to develop resistance against new agents encourage the development of new, potent and targeted antimicrobials. ESBL, AmpCs and KPCs producing bacteria are increasingly reported in animals, food, environment and community acquired human infections. Among MDR infections, complicated urinary tract infections (cUTI) and pyelonephritis are of particular concern and could become the target pathologies for ***MB076***. The results obtained for this new BATSI, such as the absence of toxicity demonstrated in MTD assessment, the ability to reduce by 40% the bacterial counts if compared to meropenem/cilastatin monotherapy, the PK/PD profile and the ability to enhance mice survival in combination with cefepime, highlighted the clinical potential of this compound.

4.3.7 Development of an oral agent

The boronic acid inhibitor ***MB076*** in combination with an antibiotic proved to have the potential as a targeted therapy for infections due to extended-spectrum β-lactamases (ESBL)-producing *Enterobacteriaceae* and carbapenem-resistant *Enterobacteriaceae*. To this end, the development of an oral version of the combination β-lactam-β-lactamase inhibitor could reduce hospital length of stay of patients and prevent hospitalization, thus reducing health care costs and enhancing patients' compliance. Therefore, in the last period of my PhD programme I developed a prodrug, oral analogue of ***MB076*** (Figure 57) where the carboxylic acid in position 4 on the triazole ring is bound to a hydrophobic side chain, forming an ester, which can be

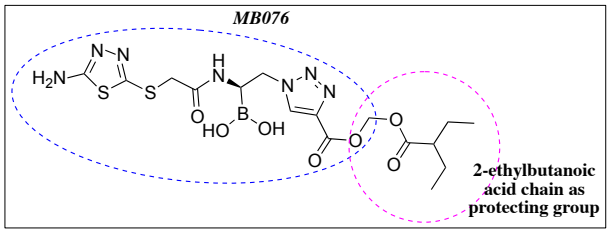

Figure 57. ***MB076*** prodrug as oral agent.

hydrolysed *in vivo* by esterases. The drug should be absorbed in the gastroenteric tract and subsequently hydrolysed to the active form in the blood. The synthesis of the new alkyne to be reacted with the acylated azide ***16*** (see section 4.3.1) was achieved as reported in the experimental section below. The aim of this new oral BATSI is to face the urgent need for an oral treatment for complicated urinary tract infections (cUTI) and pyelonephritis. Moreover, potential application to other highly resistant community-acquired infections, such as Upper Respiratory Tract Infections (URTI) and complicated Intra Abdominal Infections (cIAI) might be explored. Given the evidence that MDR bacterial infections cause an increase in costly emergency department hospitalizations, requiring intravenous (IV) or intramuscular (IM) antibiotic therapies, the identification of a new, oral ESBL, AmpC and KPC inhibitor, able to restore susceptibility to cephalosporins, penicillins and carbapenem is the major request of the antibiotic market and the development of a combination of oral ***MB076***/β-lactam might become an answer to this request.

Appendix 1: Pharmacokinetic and pharmacodynamics parameters

The fundamental principle of ***pharmacokinetic*** is that there is a relationship between the pharmacological effects of a drug and the accessible concentration of that drug (e.g. in the blood). There are four most important parameters that regulate the distribution of a drug in an organism:

- *Bioavailability (F)*: the fraction of the drug absorbed as such into the systemic circulation. For a drug administered intravenously (IV), the bioavailability corresponds to the administered dose, but if the administration route is different, it is necessary to take into account the first pass elimination processes and the bioavailability is given by the equation

  $$F = CL \times C_{ss} / \text{rate of administration}$$

  where *CL* is the clearance and C_{ss} is the concentration at equilibrium (steady state concentration).
- *Volume of distribution (V)*: a measure of the apparent space available to contain the drug in the organism, calculated on the basis of the quantity of drug administered in relation to the concentration found in the systemic circulation (C). This parameter does not necessarily refer to an identifiable physiological volume, but rather to the volume of liquid that would be required to contain all the drug present in the organism at the same concentration measured in the blood. Therefore, it is an imaginary volume that reflects the amount of drug present in extravascular tissues and is calculated by the equation

  $$V = \text{dose administered} / C$$

  The PK parameter V_{ss} reported for ***MB076*** is the volume of distribution at equilibrium. C_0 is the value of the concentration estrapolated at t (time) = 0.
- *Clearance (CL)*: a measure of the efficiency in eliminating the drug from the systemic circulation. In particular, the parameter indicates the volume of blood completely purified from the drug in the unit of time per unit of body weight. It can be determined at equilibrium starting from the rate of administration and the concentration at equilibrium (C_{ss}), but it can also be derived from the equation

  $$CL = \text{dose administered}/AUC_{inf}$$

  where AUC_{inf} (area under the curve) is the total area under the curve describing the drug concentration measured in the systemic circulation as a function of time (from zero to infinity). AUC_{inf} is estrapolated from AUC_{last} that is defined as the AUC from dosing to the time of the last measured concentration.
- *Elimination half-life ($t_{1/2}$)*: a measure of the rate of elimination of the drug from the organism. In particular, it is the time required for the concentration to decrease by 50%. It changes as a function of the clearance and of the volume of distribution

  $$t_{1/2} = 0.693 \times V_{ss}/CL$$

Pharmacodynamics deals with the study of the biochemical and physiological effects of drugs and their mechanisms of action.

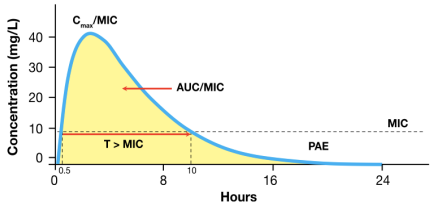

In the figure (adapted from *Journal of Chemotherapy*, **2017**, *29*, 10-18) is reported the concentration/time curve of an antibiotic and the pharmacodynamics parameters are shown. C_{max} is the concentration peak after the administration of the drug, AUC is the area under the curve and T > MIC is the fraction of the dosing range when the drug concentration remains above the MIC value. AUC is a measure of the total concentration of the drug and is calculated based on the integral between two time points (0-24h in the figure). When an antibiotic is administered three times a day instead of one, the total AUC is the same, the ratio C_{max}/MIC decreases by 1/3 and the time when T > MIC increases. For some antimicrobials it is better to have T>MIC for a prolonged time (e.g. penicillins) and this is obtained with a more frequent administration or continued infusion to enhance the $t_{1/2}$. Other antimicrobials, such as aminoglycosides, benefit from a higher concentration peak and they can be administered less frequently thanks to their long post-antibiotic effect (PAE). Indeed, their effect continues also after the decrease of their concentration under the MIC value.

Experimental section

General synthetic information

All reactions were performed under argon using oven-dried glassware and dry solvents. Dry tetrahydrofuran (THF) was obtained by standard methods and freshly distilled under argon from sodium benzophenone ketyl prior to use. Reactions were monitored by using Thin Layer chromatography (TLC) by means of Macherey-Nagel silica gel 0.20 mm (60-F_{254}) under UV light (l = 254 nm) or developed with standard stain solution: $KMnO_4$, ninhydrin, curcumin, Cerium Ammonium Molybdate (Hanessian's Stain) followed by heating. Chromatographic purification and isolation of the compounds was performed on gravimetric silica gel (particle size 0.05-0.20 mm). ^1H and ^{13}C NMR spectra were recorded on a Bruker Avance-400 MHz spectrometer. Chemical shifts (δ) are reported in ppm and were calibrated to the residual signals of the deuterated solvent ($CDCl_3$, CD_3OD). ^{13}C NMR spectra were recorded with ^1H broadband decoupling. Multiplicity is given as s = singlet, d = doublet, t = triplet, q = quartet, m = multiplet, br = broad signal; coupling constants (J) are given in Hz. Two-dimensional NMR techniques (COSY, HMBC, HSQC) were used to aid in the assignment of signals in ^1H and ^{13}C spectra. In particular, the signal of the boron-bearing carbon atom in the ^{13}C spectra tends to be broadened, and the signal is often beyond the detection limit, but its resonance was unambiguously determined by HSQC and HMBC. Mass spectra were determined on an Agilent Technologies LC-MS (n) Ion Trap 6310A (ESI, 70 eV). High-resolution mass spectra were recorded on a LC-MS apparatus: Thermo Scientific UHPLC Ultimate 3000 coupled with Q Exactive™ Hybrid Quadrupole-Orbitrap™ Mass Spectrometer. Melting points were measured in open capillary tubes on a Stuart SMP30 Melting Point apparatus. Optical rotations were determined at +20 °C on a Perkin-Elmer 241 polarimeter and are expressed in 10^{-1} deg cm^2 g^{-1}.

(+)-Pinanediol azido-methylboronate ***2*** and (+)-pinanediol (1*R*)-2-azido-1-*N,N*-bis-(trimethylsilyl)aminoethylboronate ***14*** were obtained as previously described.[6]

Synthesis of (+)-Pinanediol (1R)-2-azido-1-ammonioethylboronate hydrochloride (15)

Compound ***14*** (0.49 mmol, 1 eq.) was solubilized in THF dry (3 mL) under Ar. The temperature was cooled to -10°C and HCl 4M in dioxane was added dropwise. After 5 min at -10°C, the mixture was stirred for 5h at room temperature. The mixture was evaporated under *vacuum* and a white hygroscopic solid was obtained (96%).

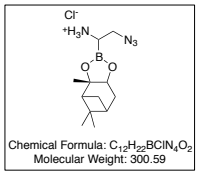

Chemical Formula: $C_{12}H_{22}BClN_4O_2$
Molecular Weight: 300.59

^1H NMR (400 MHz, DMSO-d_6) δ: 4.22 (dd, J = 8.6, 1.9 Hz, 1H, CH_{pin}), *CHB and CH_2 signals are under the H_2O signal at 3.33 ppm*, 2.31-2.24 (m, 1H, $CH_{2\text{-}pin}$), 2.22-2.15 (m, 1H, $CH_{2\text{-}pin}$), 1.92 (t, J = 5.6 Hz, 1H, CH_{pin}), 1.88-1.83 (m, 1H, CH_{pin}), 1.71-1.66 (m, 1H, $CH_{2\text{-}pin}$), 1.29 (s, 3H, $CH_{3\text{-}pin}$), 1.24 (s, 3H, $CH_{3\text{-}pin}$), 1.10 (d, J = 10.6 Hz, 1H, $CH_{2\text{-}pin}$), 0.80 (s, 3H, $CH_{3\text{-}pin}$).

Synthesis of (+)-Pinanediol (1R)-2-azido-1-(2-chloroacetamido)ethylboronate (16)

Compound ***15*** (0.91 mmol, 1 eq.) was solubilized in dry CH_2Cl_2 (10 mL) under Ar and the temperature was cooled to 0°C with an ice bath. Chloroacetylchloride (1.09 mmol, 1.2 eq.) was solubilized in dry CH_2Cl_2 (1 mL) and added dropwise to the mixture. DIPEA (2.00 mmol, 2.2 eq.) was solubilized in dry CH_2Cl_2 (3 mL) and slowly added (15-20 min) to the reaction mixture. After 30 min the light brown mixture obtained was reported to room temperature. The reaction was stirred at room temperature for 4h, then CH_2Cl_2 (10 mL) and H_2O (10 mL) were added, and the mixture was transferred in a separatory funnel where the two phases were separated. The aqueous phase was extracted with CH_2Cl_2 (2x5mL). The organic layers were washed once with H_2O, dried over Na_2SO_4, filtered and evaporated. The crude product was purified by column chromatography (Petroleum ether/ diethyl ether 1:1) and the product was obtained in 31% yield.

One-pot two-step reaction to convert compound 14 into compound 16

Compound ***14*** (4.04 mmol, 1 eq.) was dissolved in dry THF (40 mL) and cooled at 0°C under Ar. Dry MeOH (4.04 mmol, 1 eq.) was added and the reaction mixture was magnetically stirred 15 min at 0 °C, then 1 h at r.t. The mixture was then cooled at -30 °C and chloroacetylchloride (4.44 mmol, 1.1 eq.) dissolved in dry THF (1 mL) was added over 5 min. The solution was stirred for 1h at -30 °C then the mixture was diluted with EtOAc and quenched with saturated $NaHCO_3$ aqueous solution and the phases separated. The aqueous phase was extracted three times with EtOAc and the combined organic phases were washed once with a 1:1 mixture of water and brine and once with brine, dried (Na_2SO_4), filtered, and concentrated *in vacuo* to give a crude residue which was purified by column chromatography purifications on silica gel (DCM/Et_2O 8:2). Compound ***16*** was isolated as a transparent oil (98%).

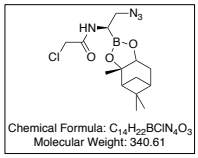

^{1}H NMR (400 MHz, $CDCl_3$) δ: 7.09 (s, 1H, NH), 4.35 (dd, J = 8.8, 2.1 Hz, 1H, CH_{pin}), 4.10 (s, 2H, CH_2Cl), 3.71 (dd, J = 12.6, 3.7 Hz, 1H, CH_2N), 3.54 (dd, J = 12.6, 7.3 Hz, 1H, CH_2N), 3.33 – 3.43 (m, 1H, CHB), 2.18 –2.41 (m, 2H, $CH_{2\text{-pin}}$), 2.06 (t, J = 5.5 Hz, 1H, CH_{pin}), 1.81 – 1.98 (m, 2H, CH_{pin}), 1.42 (s, 3H, $CH_{3\text{-pin}}$), 1.30 (s, 3H, $CH_{3\text{-pin}}$), 1.27 (d, J = 12.4 Hz, 1H, $CH_{2\text{-pin}}$), 0.85 (s, 3H, $CH_{3\text{-pin}}$). ^{13}C NMR (101 MHz, $CDCl_3$) δ: 167.5, 86.9, 78.5, 53.0, 51.5, 42.1, 39.6, 38.4 (CB), 38.3, 35.6, 28.7, 27.2, 26.4, 24.2. ^{11}B NMR (128 MHz, $CDCl_3$) δ: 29.7. LCMSQO: $[M\text{-}H]^-$ theo. 339.1401, found 339.1405. $[\alpha]^{20}_D$ = – 10.6 ($CHCl_3$).

Synthesis of (+)-Pinanediol (R)-(2-(4-(tert-butoxycarbonyl)-1H-1,2,3-triazol-1-yl)-1-(2-chloroacetamido)ethyl)boronate (17)

$CuSO_4$ (0.028 mmol, 0.1 eq.) and sodium ascorbate (0.056 mmol, 0.2 eq.) were subsequently added to degassed water (1 ml) under Ar and the mixture stirred 2 min until a yellow precipitate was formed. Compound ***16*** (0.28 mmol, 1 eq.) was dissolved in 1 ml of degassed *t*-BuOH and added to the mixture. *Tert*-butyl propiolate (0.42 mmol, 1.5 eq) was finally added one portion via syringe and the reaction mixture stirred 3 h at 40 °C. the solution was partitioned between EtOAc (5 mL) and water (3 mL) and the aqueous phase extracted three times with EtOAc. The combined organic phases were washed twice with brine, then dried (Na_2SO_4), filtered, and concentrated *in vacuo* to give the crude which was purified by crystallization from Et_2O/Pentane 1:1 to afford ***17*** as a yellow solid (70 %).

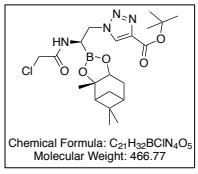

^{1}H NMR (400 MHz, $CDCl_3$) δ: 7.99 (s, 1H, CH_{triaz}), 7.51 (s, 1H, NH), 4.68 (dd, J = 14.2, 4.0 Hz, 1H,CH_2N), 4.57 (dd, J = 14.2, 8.1 Hz, 1H, CH_2N), 4.36 (dd, J = 8.8, 2.2 Hz, 1H, CH_{pin}), 4.09 (s, 2H, CH_2Cl), 3.61 – 3.71 (m, 1H, CHB), 2.15 – 2.40 (m, 2H, $CH_{2\text{-pin}}$), 2.04 (t, J = 5.5 Hz, 1H, CH_{pin}), 1.80 – 1.95 (m, 2H, CH_{pin} + $CH_{2\text{-pin}}$), 1.60 (s, 9H, $(CH_3)_3$), 1.41 (s, 3H, $CH_{3\text{-pin}}$), 1.29 (s, 3H, $CH_{3\text{-pin}}$), 1.26 (d, J = 10.3 Hz, 1H, $CH_{2\text{-pin}}$), 0.85 (s, 3H, $CH_{3\text{-pin}}$). ^{13}C NMR (101 MHz, $CDCl_3$) δ: 168.7, 159.9, 141.42, 128.3, 86.7, 82.6, 78.4, 51.6, 51.5, 41.5, 39.7, 39.3 (CB), 38.4, 35.7, 28.7, 27.2, 26.5, 24.2. ^{11}B NMR (128 MHz, $CDCl_3$) δ: 29.2. LCMSQO: $[M+H]^+$ theo. 467.2227, found 467.2230. $[\alpha]^{20}_D$ = –20.8 ($CHCl_3$).

((2-ethylbutanoyl)oxy)methyl-1-((2R)-2-(2-chloroacetamido)-2-((3aS)-3a,5,5-trimethylhexahydro-4,6-methanobenzo[d][1,3,2]dioxaborol-2-yl)ethyl)-1H-1,2,3-triazole-4-carboxylate

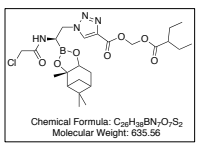

^{1}H NMR (600 MHz, $CDCl_3$): δ 8.11 (s, 1H, CH_{triaz}), 7.29 (s, 1H, NH), 6.01 (s, 2H, OCH_2O), 4.76 – 4.52 (m, 2H, CH_2N_{triaz}), 4.36 (dd, J = 8.8, 2.0 Hz, 1H, CH_{pin}), 4.06 (s, 2H, CH_2Cl), 3.68 (dt, J = 8.8, 4.6 Hz, 1H, CHB), 2.34 (m, 1H, $CH_{2\text{-pin}}$), 2.28 (tt, J = 8.5, 5.6 Hz, 1H, $\underline{CH}(CH_2)_2$), 2.23 – 2.17 (m, 1H, $CH_{2\text{-pin}}$), 2.03 (t, J = 5.5 Hz, 1H, CH_{pin}), 1.91 (m, 1H, CH_{pin}), 1.83 (m, 1H, $CH_{2\text{-pin}}$), 1.68- 1.48 (m, 4H, $(CH_2)_2$), 1.40 (s, 3H, $CH_{3\text{-pin}}$), 1.29 (s, 3H, $CH_{3\text{-pin}}$), 1.25 (d, J = 10.9 Hz, 1H, $CH_{2\text{-pin}}$), 0.88 (t, J = 7.5 Hz, 6H, $(CH_3)_2$), 0.84 (s, 3H, $CH_{3\text{-pin}}$). ^{13}C NMR (151 MHz, $CDCl_3$) δ 174.85, 168.50, 159.14, 138.81, 129.28, 86.98, 79.59, 78.58, 51.60, 51.47, 48.60, 41.60, 39.66, 39.00 (CB), 38.37, 35.60, 28.67, 27.21, 26.46, 24.80, 24.20, 11.78. ^{11}B NMR (600 MHz, $CDCl_3$): δ

22.53. LCMSQO: $[M+H]^+$ theo. 387.12372 found 387.1237 (without pinanediol and without a molecule of H_2O). $[\alpha]^{20}_D$ = - 12.54 (MeOH).

General procedure for the synthesis of compounds 18

The selected heterocycle or potassium thioacetate (1.04 eq.) was suspended in dry CH_3CN (20 ml/mmol)) under Argon and triethylamine (1.05 eq) was added. Compound ***17*** (1 eq) was added as a solid and the reaction mixture was stirred 2 h at r.t. The mixture was concentrated *in vacuo* to reduce the volume. Then it was partitioned between EtOAc and H_2O and the aqueous phase extracted 3 times with EtOAc. The combined organic phases were washed once with H_2O, then dried (Na_2SO_4), filtered, and concentrated *in vacuo* to give the crude product which was triturated with Et_2O and washed with hexane affording the desired product.

Tert-butyl-1-((2R)-2-(2-((5-methyl-4H-1,2,4-triazol-3-yl)thio)acetamido)-2-((3aS)-3a,5,5-trimethylhexahydro-4,6-methanobenzo[d][1,3,2]dioxaborol-2-yl)ethyl)-1H-1,2,3-triazole-4-carboxylate (18a)

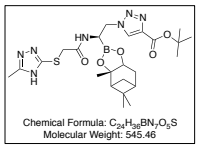

^{1}H NMR (600 MHz, $CDCl_3$): δ 9.06 (s, 1H, NH), 8.08 (s, 1H, CH_{triaz}), 4.63 – 4.47 (m, 2H, CH_2N), 4.29 (dd, *J* = 8.7, 2.1 Hz, 1H, CH_{pin}), 3.78 (s, 2H, CH_2S), 3.38 (dt, *J* = 9.6, 3.5 Hz, 1H, CHB), 2.46 (s, 3H, CH_3), 2.38 – 2.29 (m, 1H, $CH_{2\text{-}pin}$), 2.21 – 2.15 (m, 1H, $CH_{2\text{-}pin}$), 2.02 (t, *J* = 5.6 Hz, 1H, CH_{pin}), 1.90 (m, 1H, CH_{pin}), 1.82 (m, 1H, $CH_{2\text{-}pin}$), 1.58 (s, 9H, $(CH_3)_3$), 1.40 (s, 3H, $CH_{3\text{-}pin}$), 1.35 (d, *J* = 39.9 Hz, 1H, $CH_{2\text{-}pin}$), 1.28 (s, 3H, $CH_{3\text{-}pin}$), 0.86 (s, 3H, $CH_{3\text{-}pin}$). ^{13}C NMR (151 MHz, $CDCl_3$): δ 173.96, 160.56, 157.79, 155.41, 140.84, 128.38, 85.22, 83.02, 77.48, 52.02, 51.68, 42.01 (CB), 39.98, 38.36, 36.35, 32.22, 29.09, 28.36, 27.37, 26.74, 24.30, 12.18. ^{11}B NMR (600 MHz, $CDCl_3$): δ 22.36. LCMSQO: $[M+H]^+$ theo. 546.26644 found 546.2667. $[\alpha]^{20}_D$ = - 23.14 (MeOH).

Tert-butyl-1-((2R)-2-(2-((3-mercapto-4H-1,2,4-triazol-4-yl)amino)acetamido)-2-((3aS)-3a,5,5-trimethylhexahydro-4,6-methanobenzo[d][1,3,2]dioxaborol-2-yl)ethyl)-1H-1,2,3-triazole-4-carboxylate (18b)

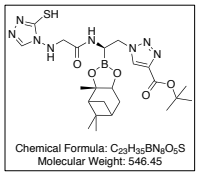

^{1}H NMR (600 MHz, $CDCl_3$): δ 8.61 (d, *J* = 4.2 Hz, 1H, NH), 8.27 (s, 1H, CH_{heter}), 8.09 (s, 1H, CH_{triaz}), 4.64-4.42 (m, *2*H, CH_2N_{triaz}), 4.31 (dd, *J* = 8.8, 2.2 Hz, 1H, CH_{pin}), 3.85 (dd, *J* = 202.7, 14.5 Hz, 2H, CH_2NH), 3.30 (dt, *J* = 8.0, 4.1 Hz, 1H, CHB), 2.34 (m, 1H, $CH_{2\text{-}pin}$), 2.20 – 2.14 (m, 1H, $CH_{2\text{-}pin}$), 2.03 (t, *J* = 5.7, 1H, CH_{pin}), 1.90 (m, 1H, CH_{pin}), 1.82 (m, 1H, $CH_{2\text{-}pin}$), 1.58 (s, 9H, $(CH_3)_3$), 1.39 (s, 3H, $CH_{3\text{-}pin}$), 1.33 (d, *J* = 10.7 Hz, 1H, $CH_{2\text{-}pin}$), 1.28 (s, 3H, $CH_{3\text{-}pin}$), 0.85 (s, 3H, $CH_{3\text{-}pin}$). ^{13}C NMR (101 MHz, $CDCl_3$): δ 172.27, 160.38, 151.79, 146.52, 140.85, 128.34, 85.55, 82.59, 77.74, 51.90, 51.67, 40.97(CB), 39.88, 38.31, 36.18, 32.30, 28.98, 28.38, 27.32, 26.62, 24.25. ^{11}B NMR (600 MHz, $CDCl_3$): δ 22.49. LCMSQO: $[M+H]^+$ theo. 547.26169 found 547.2617. $[\alpha]^{20}_D$ = - 41.77 (MeOH).

Tert-butyl-1-((2R)-2-(2-((4,5-dihydrothiazol-2-yl)thio)acetamido)-2-((3aS)-3a,5,5-trimethylhexahydro-4,6-methanobenzo[d][1,3,2]dioxaborol-2-yl)ethyl)-1H-1,2,3-triazole-4-carboxylate (18c)

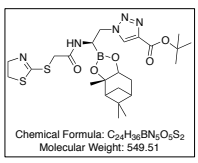

^{1}H NMR (400 MHz, $CDCl_3$): δ 8.62 (d, *J* = 3.6 Hz, 1H, NH), 7.92 (s, 1H, CH_{triaz}), 4.67 – 4.43 (m, 2H, CH_2N), 4.33 (dd, *J* = 8.8, 2.2 Hz, 1H, CH_{pin}), 4.19 – 4.03 (m, 2H, CH_2-S_{heter}), 3.65 (d, *J* = 3.1 Hz, 2H, CH_2S), 3.49 (m, 1H, CHB), 3.47 (t, *J* = 8.2 Hz, 2H, CH_2-N_{heter}), 2.40 – 2.30 (m, 1H, $CH_{2\ pin}$), 2.20 (dtd, *J* = 10.4, 6.0, 2.3 Hz, 1H, $CH_{2\text{-}pin}$), 2.04 (t, *J* = 5.5 Hz, 1H, CH_{pin}), 1.92 (m, 1H, CH_{pin}), 1.84 (dt, *J* = 14.4, 2.7 Hz, 1H, $CH_{2\text{-}pin}$), 1.59 (s, 9H, $(CH_3)_3$), 1.42 (s, 3H, $CH_{3\text{-}pin}$), 1.39 (d, *J* = 11.1 Hz, 1H, $CH_{2\text{-}pin}$), 1.29 (s, 3H, $CH_{3\text{-}pin}$), 0.86 (s, 3H, $CH_{3\text{-}pin}$). ^{13}C NMR (101 MHz, $CDCl_3$): δ 172.43, 166.85, 160.02, 141.21, 128.44, 85.93, 82.27, 78.02, 63.31, 51.88, 51.56, 40.00 (CB), 39.89, 38.38, 36.57, 36.04, 33.35, 28.90, 28.43, 27.34, 26.62, 24.26. ^{11}B NMR (400 MHz, $CDCl_3$): δ 26.10. LCMSQO: $[M+H]^+$ theo. 550.23237 found 550.2324 . $[\alpha]^{20}_D$ = - 24.07 (MeOH).

Tert-butyl-1-((2R)-2-(2-((5-mercapto-1,3,4-thiadiazol-2-yl)amino)acetamido)-2-((3aS)-3a,5,5-trimethylhexahydro-4,6-methanobenzo[d][1,3,2]dioxaborol-2-yl)ethyl)-1H-1,2,3-triazole-4-carboxylate (18d)

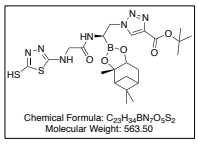

^{1}H NMR (600 MHz, $CDCl_3$): δ 8.69 (s, 1H, NH), 8.32 (s, 1H, CH_{triaz}), 4.87- 4.52 (m, 2H, CH_2N_{triaz}), 4.31 (d, *J* = 8.9, 2.2 Hz, 1H, CH_{pin}), 4.06 (dd, *J* = 162.6, 15.4 Hz, 2H, CH_2NH), 3.52 – 3.42 (m, 1H, CHB), 2.38 (s, 3H, CH_3), 2.33 (m, 1H, $CH_{2\text{-}pin}$), 2.24 – 2.10 (m, 1H, $CH_{2\text{-}pin}$), 2.02 (t, *J* = 5.1 Hz, 1H, CH_{pin}), 1.89 (m, 2H, CH_{pin}), 1.80 (m, 1H, $CH_{2\text{-}pin}$), 1.52 (s, 9H, $(CH_3)_3$), 1.41 (s, 3H, $CH_{3\text{-}pin}$), 1.37 (d, *J* = 10.7 Hz, 1H, $CH_{2\text{-}pin}$), 1.28 (s, 3H, $CH_{3\text{-}pin}$), 0.86 (s, 3H, $CH_{3\text{-}pin}$). ^{13}C NMR (151 MHz, $CDCl_3$): δ 172.54, 168.84, 160.86, 160.14, 158.66, 141.03, 129.21, 85.66, 83.27, 78.02, 52.31, 52.15, 42.03 (CB), 40.10, 38.54, 36.48, 33.61, 29.20, 28.60, 27.54, 27.03, 24.52, 23.29. ^{11}B NMR (600 MHz, $CDCl_3$): δ 22.49. LCMSQO: $[M+H]^+$ theo. 606.23343 found 606.2333. $[\alpha]^{20}_D$ = - 52.38 (MeOH).

Tert-butyl-1-((2R)-2-(2-((5-amino-1,3,4-thiadiazol-2-yl)thio)acetamido)-2-((3aS)-3a,5,5-trimethylhexahydro-4,6-methanobenzo[d][1,3,2]dioxaborol-2-yl)ethyl)-1H-1,2,3-triazole-4-carboxylate (18e)

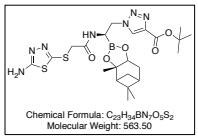

^{1}H NMR (400 MHz, $CDCl_3$) δ: 9.07 (s, 1H, NH), 8.06 (s, 1H, CH_{triaz}), 6.95 (s, 2H, NH_2), 4.54 (d, *J* = 5.7 Hz, 2H, CH_2N), 4.27 (d, *J* = 7.6 Hz, 1H, CH_{pin}), 3.90 (s, 2H, CH_2S), 3.36 – 3.44 (m, 1H, CHB), 2.09 – 2.42 (m, 2H, $CH_{2\text{-}pin}$), 2.01 (t, *J* = 5.5 Hz, 1H, CH_{pin}), 1.75 – 1.94 (m, 2H, CH_{pin} + $CH_{2\text{-}pin}$), 1.57 (s, 9H, $(CH_3)_3$), 1.41 (s, 3H, $CH_{3\text{-}pin}$), 1.35 (d, *J* = 10.4 Hz, 1H, $CH_{2\text{-}pin}$), 1.28 (s, 3H, $CH_{3\text{-}pin}$), 0.86 (s, 3H, $CH_{3\text{-}pin}$). ^{13}C NMR (101 MHz, $CDCl_3$) δ: 173.2, 160.3, 140.9, 128.2, 84.9, 82.6, 77.4, 52.6, 52.1, 42.2 (CB), 40.0, 38.3, 36.4, 33.9, 29.1, 28.4, 27.4, 26.8, 24.3. The two quaternary thiadiazolyl carbons were not detectable. ^{11}B NMR (128 MHz, CH_3OD) δ: 18.6. LCMSQO: $[M+H]^+$ theo. 564.2229, found 564.2240. $[\alpha]^{20}_D$ = - 58.1 ($CHCl_3$).

Tert-butyl-1-((2R)-2-(2-(pyridin-2-ylthio)acetamido)-2-((3aS)-3a,5,5-trimethylhexahydro-4,6-methanobenzo[d][1,3,2]dioxaborol-2-yl)ethyl)-1H-1,2,3-triazole-4-carboxylate (18f)

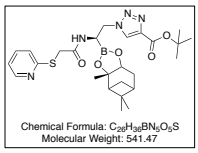

^{1}H NMR (400 MHz, $CDCl_3$) : δ 9.00 (s, 1H, NH), 8.40 – 8.35 (m, 1H, CH_{pyr}), 7.86 (s, 1H, CH_{triaz}), 7.50 (td, *J* = 7.9, 1.8 Hz, 1H, CH_{pyr}), 7.19 (d, *J* = 8.1 Hz, 1H, CH_{pyr}), 7.06 (ddd, *J* = 7.3, 5.0, 0.9 Hz, 1H, CH_{pyr}), 4.59 – 4.39 (m, 2H, CH_2N_{triaz}), 4.29 (dd, *J* = 8.7, 2.1 Hz, 2H, CH_{pin}), 3.83 (d, *J* = 2.6 Hz, 2H, CH_2S), 3.37 (m, 1H, CHB), 2.35 (m, 1H, $CH_{2\text{-}pin}$), 2.22 – 2.13 (m, 1H, $CH_{2\text{-}pin}$), 2.02 (t, *J* = 5.5 Hz, 1H, CH_{pin}), 1.90 (m, 1H, CH_{pin}), 1.82 (m, 1H, $CH_{2\text{-}pin}$), 1.58 (s, 9H, $(CH_3)_3$), 1.41 (s, 3H, $CH_{3\text{-}pin}$), 1.33 (d, *J* = 23.6 Hz, 1H, $CH_{2\text{-}pin}$), 1.28 (s, 3H, $CH_{3\text{-}pin}$), 0.86 (s, 3H, $CH_{3\text{-}pin}$). ^{13}C NMR (101 MHz, $CDCl_3$) δ 174.45, 159.76, 156.30, 149.69, 140.94, 136.73, 127.93, 122.36, 120.66, 84.94, 82.06, 77.21, 52.19, 51.93, 41.33 (CB), 39.86, 38.20, 36.23, 30.72, 28.93, 28.26, 27.25, 26.59, 24.16. ^{11}B NMR (600 MHz, $CDCl_3$): δ 20.70. LCMSQO: $[M+H]^+$ theo. 542.26030 found 542.2608. $[\alpha]^{20}_D$ = - 51.05 (MeOH).

Tert-butyl-1-((2R)-2-(2-mercaptoacetamido)-2-((3aS)-3a,5,5-trimethylhexahydro-4,6-methanobenzo[d][1,3,2]dioxaborol-2-yl)ethyl)-1H-1,2,3-triazole-4-carboxylate (18g)

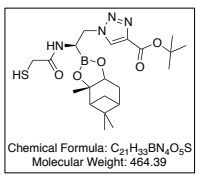

^{1}H NMR (400 MHz, $CDCl_3$) : δ 8.00 (s, 1H, CH_{triaz}), 7.35 (s, 1H, NH), 4.64 – 4.43 (m, 2H, CH_2N_{triaz}), 4.32 (dd, *J* = 8.8, 2.0 Hz, 1H, CH_{pin}), 3.66 – 3.55 (dd, *J* = 15.07, 6.05 Hz, 2H, CH_2S), 3.43 (m, 1H, CHB), 2.37 (s, 3H, CH_3), 2.34 – 2.29 (m, 1H, $CH_{2\text{-}pin}$), 2.23 – 2.11 (m, 1H, $CH_{2\text{-}pin}$), 2.03 (t, *J* = 5.4 Hz, 1H, CH_{pin}), 1.94 – 1.87 (m, 1H, CH_{pin}), 1.82 (m, 1H, $CH_{2\text{-}pin}$), 1.59 (s, 9H, $(CH_3)_3$), 1.40 (s, 3H, $CH_{3\text{-}pin}$), 1.32 (d, *J* = 10.7 Hz, 1H, $CH_{2\text{-}pin}$), 1.28 (s, 3H, $CH_{3\text{-}pin}$), 0.85 (s, 3H, $CH_{3\text{-}pin}$). ^{13}C NMR (101 MHz, $CDCl_3$) δ 195.08, 171.84, 160.37, 141.79, 128.71, 86.19, 82.76, 78.27, 52.16, 52.12, 40.93 (CB), 40.17, 38.66, 36.33, 31.29, 30.65, 29.19, 28.70, 27.64, 26.92, 24.56. ^{11}B NMR (600 MHz, $CDCl_3$): δ 22.47. LCMSQO: $[M+H]^+$ theo. 507.24431 found 507.2443. $[\alpha]^{20}_D$ = - 47.63 (MeOH).

((2-ethylbutanoyl)oxy)methyl-1-((2R)-2-(2-((5-amino-1,3,4-thiadiazol-2-yl)thio)acetamido)-2-((3aS)-3a,5,5-trimethylhexahydro-4,6-methanobenzo[d][1,3,2]dioxaborol-2-yl)ethyl)-1H-1,2,3-triazole-4-carboxylate

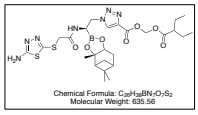

^{1}H NMR (600 MHz, $CDCl_3$): δ 8.47 (s, 1H, NH), 8.18 (s, 1H, CH_{triaz}), 6.09 (s, 2H, NH_2), 6.01 – 5.96 (dd, 2H, *J* = 9.9, 5.5 Hz, OCH_2O), 4.65 – 4.48 (m, 2H, CH_2N_{triaz}), 4.32 – 4.29 (m, 1H, CH_{pin}), 3.91 – 3.79 (dd, 2H, *J* = 28.0, 15.1 Hz,, 2H, CH_2S), 3.48 (dt, *J* = 7.7, 3.6 Hz, 1H, CHB), 2.36 - 2.32 (m, 1H, $CH_{2\text{-}pin}$), 2.31 – 2.27 (m, 1H, $\underline{CH}(CH_2)_2$), 2.19- 2.17 (m, 1H, $CH_{2\text{-}pin}$), 2.02 (t, *J* = 5.4 Hz, 1H, CH_{pin}), 1.92- 1.88 (m, 1H, CH_{pin}), 1.84 – 1.80 (m, 1H, $CH_{2\text{-}pin}$), 1.67- 1.51 (m, 4H, $(CH_2)_2$), 1.40 (s, 3H, $CH_{3\text{-}pin}$), 1.28 (s, 3H, $CH_{3\text{-}pin}$), 0.90 – 0.85 (m, 9H, $CH_{3\text{-}pin}$ + $(CH_3)_2$). ^{13}C NMR (151 MHz, $CDCl_3$) δ 175.34, 172.20, 169.74, 159.38, 152.51, 138.41, 129.41, 85.58, 79.69, 77.74, 52.41, 51.89, 48.59, 40.99 (CB), 39.90, 38.35, 36.19, 34.01, 28.97, 27.34, 26.66, 24.76, 24.28, 11.81. ^{11}B NMR (600 MHz, $CDCl_3$): δ 22.52. LCMSQO: $[M\text{-}H]^-$ theo. 500.11879 found 500.1210 (without pinanediol). $[\alpha]^{20}_D$ = - 21.42 (MeOH).

General procedure for the deprotection of boronic acids and carboxylates

The selected compound ***18*** (1 eq.) was dissolved in dry DCM and TFA (approx. 20 eq.) was added with a syringe at 0°C. The reaction mixture was stirred at r.t. for 12h and then concentrated to dryness. DCM was added and evaporated three times to completely remove TFA, and the oily residue was used as such in the next step without further purification. The crude from above was dissolved in CH_3CN and isobutylboronic acid (1 eq.), HCl 3M (3 eq.) and *n*-hexane were sequentially added, and the resulting biphasic solution was vigorously stirred. After 20 min. the *n*-hexane solution (containing the pinanediol isobutylboronate) was removed and an equal amount of fresh *n*-hexane added. This last procedure was repeated several times until a TLC analysis of the *n*-hexane layer did not revealed isobutylboronate presence. Total reaction time 4-6 hours. Finally, after removal of *n*-hexane phase, the residue was concentrated to dryness. The so-obtained crude product was purified by crystallization or trituration with an appropriate solvent, affording the desired inhibitor.

(R)-1-(2-borono-2-(2-((5-methyl-4H-1,2,4-triazol-3-yl)thio)acetamido)ethyl)-1H-1,2,3-triazole-4-carboxylic acid (19a)

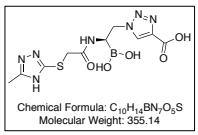

^{1}H NMR (600 MHz,MeOD): δ 8.56 (s, 1H, CH_{triaz}), 4.48 (dd, *J* = 47.1, 11.1 Hz, 2H, CH_2N_{triaz}), 4.16 (s, 2H, CH_2S), 3.27 (d, *J* = 8.8 Hz, 1H, CHB), 2.71 (s, 3H, CH_3). ^{13}C NMR (151 MHz, MeOD): δ 175.40, 162.56, 156.02, 155.01, 140.53, 130.16, 53.51, 45.62 (CB), 34.69, 10.83. ^{11}B NMR (600 MHz, $CDCl_3$): δ 16.84. LCMSQO: $[M\text{-}H]^-$ theo 356.0943 found 356.1239. $[\alpha]^{20}_D$ = - 58.57 (MeOH).

(R)-1-(2-borono-2-(2-((3-mercapto-4H-1,2,4-triazol-4-yl)amino)acetamido)ethyl)-1H-1,2,3-triazole-4-carboxylic acid (19b)

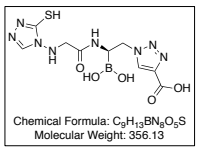

^{1}H NMR (600 MHz,MeOD): δ 9.84 (s, 1H, NCHN), 8.52 (s, 1H, CH_{triaz}), 4.47 (dd, *J* = 46.5, 11.6 Hz, 2H, CH_2N_{triaz}), 4.20 (s, 2H, CH_2S), 3.27 (d, *J* = 9.5 Hz, 1H, CHB). ^{13}C NMR (151 MHz, MeOD): δ 174.50, 168.08, 163.48, 156.25, 141.14, 130.15, 53.46, 45.29 (CB), 34.32. ^{11}B NMR (600 MHz, $CDCl_3$): δ 16.66. LCMSQO: $[M\text{-}H]^-$ theo 355.07839 found 355.0754. $[\alpha]^{20}_D$ = - 55.94 (MeOH).

(R)-1-(2-borono-2-(2-((3-mercapto-4H-1,2,4-triazol-4-yl)amino)acetamido)ethyl)-1H-1,2,3-triazole-4-carboxylic acid (18c)

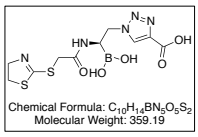

^{1}H NMR (600 MHz,MeOD): δ 8.54 (s, 1H, CH_{triaz}), 4.59-4.45 (m, 2H, CH_2N), 3.62-3.42 (m, 2H, CH_2S), 3.30-3.27 (m, 1H, CHB). ^{13}C NMR (151 MHz, MeOD): δ 174.98, 169.61, 161.68, 129.08, 128.88, 52.42, 45.73 (CB), 39.01, 29.44, 27.99. ^{11}B NMR (600 MHz, $CDCl_3$): δ 18.54. LCMSQO: $[M\text{-}H]^-$ theo 358.04794, found 358.0464. $[\alpha]^{20}_D$ = - 32.18 (MeOH).

(R)-1-(2-borono-2-(2-((5-mercapto-1,3,4-thiadiazol-2-yl)amino)acetamido)ethyl)-1H-1,2,3-triazole-4-carboxylic acid (19d)

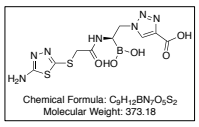

^{1}H NMR (600 MHz,MeOD): δ 8.47 (s, 1H, CH_{triaz}), 4.28 (dd, J = 46.5, 11.6 Hz, 2H, CH_2N_{triaz}), 4.07 (s, 2H, CH_2NH), 3.18 (d, J = 9.5 Hz, 1H, CHB). ^{13}C NMR (151 MHz, MeOD): 169.92, 163.41, 162.52, 155.16, 140.43, 130.13, 53.58, 45.62 (CB), 35.85. ^{11}B NMR (600 MHz, $CDCl_3$): δ 15.94. LCMSQO: $[M-H]^-$ theo 372.03506 found 372.0369. $[\alpha]^{20}_D$ = - 49.53 (MeOH).

(R)-1-(2-(2-((5-amino-1,3,4-thiadiazol-2-yl)thio)acetamido)-2-boronoethyl)-1H-1,2,3-triazole-4-carboxylic acid (19e)

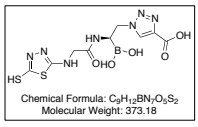

^{1}H NMR (400 MHz, MeOD) δ: 8.50 (s, 1H, CH_{triaz}), 4.47 (dd, J = 14.5, 4.0 Hz, 1H, CH_2N), 4.34 (dd, J = 14.5, 10.2 Hz, 1H, CH_2N), 4.07 (s, 2H, CH_2S), 3.15 – 3.20 (m, 1H, CHB). ^{13}C NMR (151 MHz, MeOD) δ: 175.0, 172.7, 163.4, 155.3, 141.2, 130.3, 53.7, 45.7 (CB), 33.3. ^{11}B NMR (128 MHz, MeOD) δ: 15.51. LCMSQO: $[M-H]^-$ theo. 372.0362, found 372.0364. $[\alpha]^{20}_D$ = - 86.1 (MeOH).

(R)-1-(2-borono-2-(2-(pyridin-2-ylthio)acetamido)ethyl)-1H-1,2,3-triazole-4-carboxylic acid (19f)

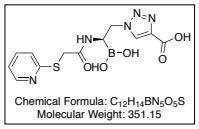

^{1}H NMR (600 MHz,MeOD): δ 8.56 – 8.50 (m, 2H, CH_{triaz}, CH_{pyr}), 8.15 – 8.05 (m, 1H, CH_{pyr}), 7.75 (d, J = 8.3 Hz, 1H, CH_{pyr}), 7.53 – 7.48 (m, 1H, CH_{pyr}), 4.58 – 4.31 (m, 2H, CH_2N_{triaz}), 4.20 (s, 2H, CH_2S), 3.46 (t, J = 5.46 Hz, 1H, CHB). ^{13}C NMR (151 MHz, MeOD): δ 170.63, 163.19, 146.23, 143.21, 141.60, 130.41, 130.07, 125.66, 123.06, 53.56, 41.67 (CB), 33.92. ^{11}B NMR (600 MHz, $CDCl_3$): δ 18.56. LCMSQO: $[M-H]^-$ theo 351.08090 found 351.0802. $[\alpha]^{20}_D$ = - 13.33 (MeOH).

(R)-1-(2-borono-2-(2-mercaptoacetamido)ethyl)-1H-1,2,3-triazole-4-carboxylic acid (19g)

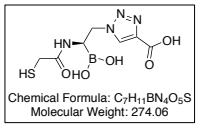

^{1}H NMR (600 MHz, MeOD): δ 8.59 (s, 1H, CH_{triaz}), 4.49-4.41 (m, 2H, CH_2N), 3.71 (s, 2H, CH_2S), 3.28 (t, J = 8.89 Hz, 1H, CHB). ^{13}C NMR (151 MHz, MeOD): δ 177.25, 163.34, 140.41, 130.27, 53.81, 47.16 (CB), 37.74. ^{11}B NMR (600 MHz, $CDCl_3$): δ 12.30. LCMSQO: $[M-H]^-$ theo. 273.04728, found 273.0476. $[\alpha]^{20}_D$ = - 46.49 (MeOH).

(R)-(1-(2-((5-amino-1,3,4-thiadiazol-2-yl)thio)acetamido)-2-(4-((((2-ethylbutanoyl)oxy)methoxy)carbonyl)-1H-1,2,3-triazol-1-yl)ethyl)boronic acid

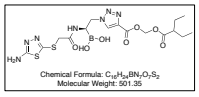

^{1}H NMR (400 MHz,MeOD): δ 8.64 (s, 1H, CH_{triaz}), 6.01 (s, 2H, OCH_2O), 4.73-4.33 (m, 2H, CH_2N_{triaz}), 4.14 (s, 2H, CH_2S), 3.26 (dd, J = 10.01, 3.6 Hz, 1H, CHB), 2.32-2.25 (m, 1H, CH), 1.67-1.50 (m, 4H, $(CH_2)_2$), 0.89 (t, J = 7.4 Hz, 6H, $(CH_3)_2$). ^{13}C NMR (101 MHz, MeOD): δ 176.01, 168.79, 160.52, 155.01, 139.60, 130.88, 80.64, 53.57, 49.90, 45.51 (CB), 33.37, 25.88, 11.97. ^{11}B NMR (400 MHz, $CDCl_3$): δ 17.05. $[\alpha]^{20}_D$ = - 39.85 (MeOH).

Synthesis of (propiolyloxy)methyl-2-ethylbutanoate

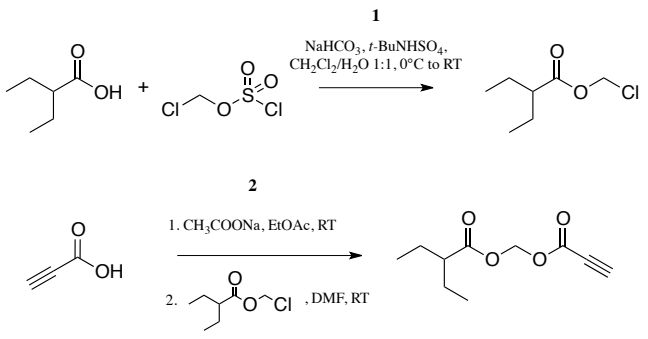

1. 2-Ethylbutirric acid (4.3 mmol, 1 eq.) was dissolved in CH_2Cl_2 (10 mL). Distilled H_2O (17 mL), $NaHCO_3$ (16.7 mmol, 3.9 eq.) and *t*-$BuNHSO_4$ (0.43 mmol, 0.1 eq.) were added. The mixture was cooled to 0°C and stirred for 10 min.

Chloromethyl-chlorosulfate (7.5 mmol, 1.5 eq.) was dissolved in 7 mL of CH_2Cl_2 and added to the mixture. The mixture was allowed to reach room temperature and stirred vigorously for 24h. The two phases were separated and the aqueous phase was extracted with CH_2Cl_2 (2 x 10 mL). The organic phases were dried over Na_2SO_4, filtered and evaporated *in vacuo*. The crude was purified by column chromatography (Petroleum ether / CH_2Cl_2 1:1) and the product was obtained in 80% yield.

2. Propriolic acid (1.4 mmol, 1 eq.) was dissolved in ethyl acetate (15 mL) and CH_3COONa (1.4 mmol, 1 eq.) was added. The mixture was stirred vigorously for 1h. The solvent was evaporated and the solid was suspended in hexane, which was then evaporated to eliminate the acetic acid. The solid was dissolved in DMF (1 mL) and chloromethyl-2-ethylbutanoate (1.27 mmol, 1.1 eq.) in DMF (2.5 mL) was added. The mixture was stirred at room temperature for 18h. A mixture of H_2O/NH_4Cl 1:1 (10 mL) was added. The acqueous phase was extracted with diethyl ether (6 x 10 mL). The organic phases were dried over Na_2SO_4, filtered and evaporated *in vacuo*. The crude was purified by column chromatography (Petroleum ether/ diethyl ether 9:1) and the product was obtained in 30% yield.

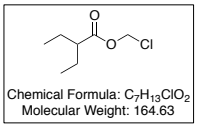

Chemical Formula: $C_7H_{13}ClO_2$
Molecular Weight: 164.63

^{1}H NMR (400 MHz, $CDCl_3$): δ 5.73 (s, 2H, CH_2Cl), 2.32-2.25 (m, 1H, CH), 1.72-1.53 (m, 4H, CH_2), 0.91 (t, J = 7.5 Hz, 6H, CH_3). ^{13}C NMR (101 MHz, $CDCl_3$): δ 174.29, 68.64, 48.71, 24.87 (2C), 11.75 (2C).

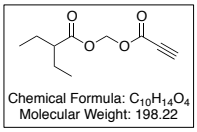

Chemical Formula: $C_{10}H_{14}O_4$
Molecular Weight: 198.22

^{1}H NMR (400 MHz, $CDCl_3$): δ 5.84 (s, 2H, OCH_2O), 2.97 (s, 1H, CCH), 2.32-2.25 (m, 1H, CH), 1.69-1.50 (m, 4H, CH_2), 0.91 (t, J = 7.4 Hz, 6H, CH_3).

Purification and Kinetics

β-Lactamases were expressed as described in precedent works[1,2] and purified using cation exchange chromatography. The inhibition constants (K_i) for each of the BATSIs with KPC-2 and PDC-3/ADC-7 were determined using competition kinetics using nitrocefin (NCF) as colorimetric substrate. The measurements of the initial velocities were performed with the addition of 100 μM NCF after a 5 min preincubation of the enzyme (2 nM) with increasing concentration of the inhibitor. To determine the average velocities (v_0), data from three experiments were fit to the equation:

$$v_0 = v_u - (v_u [I] / IC_{50} + [I])$$

where v_u represents the NCF uninhibited velocity and IC_{50} represents the inhibitor concentration that results in a 50% reduction of v_u. The K_i values for all BATSIs were corrected for the NCF affinity (Km = 20 μM) with the Cheng-Prusoff equation:

$$K_i = IC_{50} / (1 + [NCF] / K_{mNCF}).$$

The data analysis was performed using EnzFitter and Origin 2019b.

Crystallization and Structure Determination for MB076 in complex with KPC-2

The structure of KPC-2 in complex with the inhibitor was obtained via co-crystallization. The KPC-2 β-lactamase and ***MB076*** were incubated overnight, with a molar ratio of protein:inhibitor of 1:10. The co-crystallization condition was 30% PEG 8000, 0.2 M lithium sulphate and 0.1 M sodium acetate (pH 4.5). Once KPC-2:***MB076*** co-crystals grew to their final size, they were mounted and cryoprotected with perfluoropolyether oil prior to flash freezing in liquid nitrogen.

Microbiology

MICs were performed as described in published articles[1,2] and according to Clinical and Laboratory Standards Institute (CLSI) guidelines. Bacterial cultures were grown overnight in Mueller-Hinton (MH) broth supplemented with 20 μg/mL chloramphenicol. The *E. Coli* DH10B cells carrying pBC-SK bla_{KPC-2} were employed. Bacterial liquid culture was diluted using MH broth to a 6 × 104 cfu/mL final concentration, and the antibiotic partner, FEP, was added at concentrations from 256 to 0.25 μg/ mL. BATSIs were constant at 4 μg/mL. The plates were incubated at 37 °C overnight, and the results were recorded the next day.

Materials and Methods for the preclinical development of MB076 for ESBL and carbapenemase expressing pathogens

This study was sponsored by the Division of Microbiology and Infectious Diseases of the National Institute of Allergy and Infectious Diseases (NIH), requested by Prof. Robert Bonomo of the Case Western Reserve University (Cleveland, Ohio) and performed by the Pharmacology Discovery Services of Taiwan, which is a Partner Lab of Eurofins Pharma Discovery services.

The *K. pneumoniae* strains for MIC testing were obtained from the American Type Culture Collection (ATCC) and the CDC & FDA AR Isolate Bank. The thigh infection model for these *K. pneumoniae* strains were developed and validated by Pharmacology Discovery Services (PDS). Susceptibility was determined following the Clinical Laboratory Standards Institute (CLSI) M07-A10 microdilution procedure and the CLSI M100 interpretive criteria. The susceptibility is similar to that reported by the AR Bank. The species identity is confirmed with 16S analysis.

Case Western Reserve University supplied the test articles, ***MB076*** and cilastatin ammonium salt, both in powder form. The test articles were stored at -20˚C upon arrival at PDS. PDS supplied meropenem (both Cat#1392454, USP grade for MIC, and meropenem powder for Intravenous Injection, Savior Lifetec Corporation for animal studies) and tigecycline (TYGACIL®(Tigecycline) 50 mg Lyophilized Powder, Wyeth Lederle S.R.L., Italy).

Minimum Inhibitory Concentration (MIC) Study

MB076 in combination with cefepime was tested in an 11-point titration with ***MB076*** fixed at 4 μg/mL and cefepime ranging from 32 to 0.0313 μg/mL. The MIC of ***MB076***, meropenem and cefepime were tested alone. The direct colony suspension method was used to prepare inoculated broth. Isolated colonies were taken from an 18–24 h culture plate. Optical density measurements (OD_{620nm}) were used to estimate the bacterial density.

MB076 was dissolved in 100% DMSO to generate a 50-fold stock solution, and diluted by 2-fold serial titrations for a total of 11 concentrations (16 to 0.016 mg/mL) for testing of ***MB076*** alone at a final concentration of 32 to 0.0313 μg/mL. Meropenem was dissolved in Water for Injection (WFI, sterilized water) to generate a 50-fold stock, and diluted by 2-fold serial titrations for a total of 11 concentrations (16 to 0.016 mg/mL) for testing of meropenem alone at a final concentration of 32 to 0.0313 μg/mL. Cefepime was dissolved in 0.1 M of PBS at pH 6.0 to generate a 50-fold stock solution, and diluted by 2-fold serial titrations for a total of 11 concentrations (16 to 0.016 mg/mL) for testing of cefepime alone at a final concentration of 32 to 0.0313 μg/mL. For combination testing, ***MB076*** was dissolved in 100% DMSO at 0.4 mg/mL (100x stock). Meropenem and cefepime were dissolved in their respective vehicles at 100x stock for a total of 11 concentrations. The 100x stock of ***MB076*** was mixed at 1:1 ratio with 100x dilutions of meropenem or cefepime to generate 50x solutions for testing of ***MB076*** at 4 μg/mL with meropenem combination at 4 to 0.004μg/mL, and ***MB076*** at 4 μg/mL with cefepime combination at 32 to 0.0313 μg/mL. A 4 μL aliquot of each test article dilution was added to 196 μL of broth medium seeded with the organism in wells of a sterilized 96 well plate. The final bacterial count will be approximately 5 x 10^5 CFU/mL with a range of 2–8 x 10^5 CFU/mL. Medium was cation adjusted Mueller Hinton Broth. The final test article concentration range was as follows: (i) ***MB076***, meropenem and cefepime alone at 32 to 0.0313 μg/mL, (ii) ***MB076*** at 4 μg/mL with meropenem combination at 4 to 0.004 μg/mL, and (iii) ***MB076*** at 4 μg/mL with cefepime combination at 32 to 0.0313 μg/mL. The final vehicle concentration was 2 percent (2%) in all assay wells.

Each test substance dilution was evaluated in duplicate on one test occasion. Vehicle-control and reference controls were used as blank and positive controls, respectively. Plates were incubated at 35-37°C for 18 h. The test plates were visually examined and each well was visually scored for growth or complete inhibition of growth. The MIC value was recorded. The CLSI guidelines of 100% visual growth inhibition were used to call an MIC endpoint.

MTD assessment of meropenem and cilastatin with *MB076* in neutropenic mouse

i. Animal Preparation

For the MTD assessment, cyclophosphamide (CP) was administered by two intraperitoneal (IP) injections to induce neutropenia following the industry standard method used for the mouse thigh infection[3]. The first CP dose, 150 mg/kg, was administered at four days before test article treatment (Day –4); and the second, 100 mg/kg, at 24 h before test article treatment (Day –1), prior to treatment on Day 0. PDS determined in prior complete blood count studies that this cyclophosphamide treatment schedule resulted in neutropenia (< 100 neutrophils per µL) until Day 2 (data not shown).

ii. Treatment and evaluation

Meropenem combined with cilastatin in 0.9% NaCl was subcutaneously (SC) administered followed by intravenous (IV) administration of ***MB076*** within 10 minutes. ***MB076*** dosing solutions was prepared in PBS and pH adjusted to pH 5 to 7 for IV injection. Animals were observed for the presence of acute toxic symptoms (mortality, convulsions, tremors, muscle relaxation, sedation…) and autonomic effects (diarrhea, salivation, lacrimation, vasodilation, piloerection…) after 5 minutes of the first SC+IV administration. Cage side observations, including gait, posture, ruffled fur, immobility, mucous membrane, salivation, tremors, convulsions, reactivity to handling, respiratory, stool, mortality and body weight were observed after each subsequent QID doses and recorded. Mortality and body weight was observed and recorded daily for 3 days after treatment. Animals were humanely euthanized at earlier time points if they are found to be in distress or a moribund state.

Efficacy analysis of meropenem and cilastatin with *MB076* in the thigh infection model

i. Animal Preparation

The *K. pneumoniae* strain AR-BANK#0098 (KPC-2) thigh infection model was performed with neutropenic female ICR mice, weighing 22 ± 2 g following the general guidelines of Andes DR and Lepak AJ (2017). All animals were specific pathogen free. Cyclophosphamide (CP) was administered by two intraperitoneal (IP) injections to induce neutropenia following a standard method for mouse thigh infection models[3]. The first CP dose, 150 mg/kg, was administered at four days before infection (Day –4); and the second, 100 mg/kg, at 24 h before infection (Day –1), prior to infection on Day 0. PDS determined in prior complete blood count studies that this cyclophosphamide treatment schedule resulted in neutropenia (< 100 neutrophils per µL) until Day 2 after infection (data not shown).

ii. Inoculum Preparation

The PDS standard protocol for preparing *K. pneumoniae* cultures for mouse infection studies was followed. A 0.2 mL aliquot of a single-use glycerol stock (at -80 °C) was used to seed 20 mL Brain Heart Infusion (BHI) and then incubated at 35-37 °C with shaking (120 rpm) for 8 h. Cells in the 20 mL culture were pelleted by centrifugation (3,500 × g) for 15 minutes, and then re-suspended in 10 mL cold phosphate buffer saline (PBS). The optical density, OD_{620nm}, was measured and used to guide dilution. The PBS suspensions were stored on ice for no more than 1 h prior to animal inoculation. The bacterial count in the challenge organism suspension was enumerated by dilution plating to Nutrient agar (NA) plates followed by 20-24 h incubation. The target inoculum of the thigh infection model is 1×10^5 CFU/mouse and the actual CFU count was 1.47×10^5 CFU/mouse for *K. pneumoniae* strain AR-BANK#0098 (KPC-2).

iii. Treatment

Meropenem combined with cilastatin in 0.9% NaCl was subcutaneously (SC) administered followed by intravenous (IV) administration of ***MB076*** within 10 minutes. ***MB076*** dosing solutions was prepared in PBS and pH adjusted to pH 5 to 7 for IV injection. Animals were observed at 5 minutes after dosing to detect acute toxicity, which was recorded and reported, if observed. Animals were humanely euthanized if severe acute toxicity is observed.

Animals were checked at 12 h after infection for humane endpoints. Animals were humanely sacrificed if animals were found in a moribund state. Animals were sacrificed with CO_2 asphyxiation at the scheduled time points for tissue harvest, at 2 or 26 h after infection. The thigh tissue was aseptically harvested from each of the sacrificed animals, weighed, and homogenized in 3 mL sterile PBS (pH 7.4) with a Polytron homogenizer. Bacterial burden in the tissue homogenates was determined by performing 10-fold serial dilutions and plating 0.1 mL of each to nutrient agar plates. Colonies were counted after 18 - 24 h incubation. The colony-forming unit value per g tissue (CFU/g) was calculated.

PK assessment in the thigh infection model with neutropenic animals

i. Animal Preparation

The *K. pneumoniae* strain AR-BANK#0098 (KPC-2) thigh infection model was performed with neutropenic female ICR mice, weighing 22 ± 2 g. All animals were specific pathogen free. Cyclophosphamide (CP) was administered by two intraperitoneal (IP) injections to induce neutropenia following a standard method for mouse thigh infection models.[4] The first CP dose, 150 mg/kg, was administered at four days before infection (Day –4); and the second, 100 mg/kg, at 24 h before infection (Day –1), prior to infection on Day 0. PDS determined in prior complete blood count studies that this cyclophosphamide treatment schedule resulted in neutropenia (< 100 neutrophils per µL) until Day 2 after infection (data not shown).

ii. Inoculum Preparation

The PDS standard protocol for preparing *K. pneumoniae* cultures for mouse infection studies was followed. A 0.2 mL aliquot of a single-use glycerol stock (at -80°C) was used to seed 20 mL brain heart infusion (BHI) and then incubated at 35-37°C with shaking (120 rpm) for 8 h. Bacterial cells in the 20 mL was pelleted by centrifugation (3,500 × g) for 15 minutes, and then re-suspended in 10 mL cold phosphate buffer saline (PBS). The optical density, OD_{620nm}, was measured and used to guide dilution. The PBS suspensions were stored on ice for no more than 2 h prior to animal inoculation. The bacterial count in the challenge organism suspension was enumerated by dilution plating to nutrient agar (NA) plates followed by 20-24 h incubation. The target inoculum of the thigh infection model is 1×10^5 CFU/mouse and the actual CFU count was 1.38×10^5 CFU/mouse for *K. pneumoniae* strain AR-BANK#0098 (KPC-2).

iii. Treatment

Test article, ***MB076***, was IV administered once at 2 h post-infection followed by terminal blood sampling at 8 time points with cardiac puncture: 5, 15, 30, 60, 90, 120, 180, and 240 minutes. Terminal blood collection from cardiac puncture was conducted under CO_2 euthanasia. Blood, 0.3-0.4 mL, was drawn into tubes coated with K_2EDTA, mixed gently and kept on ice and centrifuged at 12,000 × g for 5 minutes at 4°C within 1 hour of collection. The plasma was harvested and stored at -80°C until further processing. The thigh tissue was aseptically harvested from each of the sacrificed animals, weighed, and homogenized in 3 mL sterile PBS (pH 7.4) with a Polytron homogenizer. The thigh homogenate was collected and stored at -80°C until further processing.

iv. Processing of plasma and thigh homogenates for bioanalysis

Sample processing for LC-MS/MS was conducted using the procedures as developed by the PDS PK team. A 20 µL aliquot of each plasma and thigh sample was transferred to 96 well plate. A 500 µL aliquot of 0.01 ng/µL internal standard (IS), Oxybutynin, in ACN/FA=95/5 was added to each tube except for the double blank and carryover controls. A 500 µL aliquot of ACN/FA=95/5, without oxybutynin, was added to the double blank and carryover assay wells. The equilibrated mixture was vortexed for 1 min and then centrifuged at 4,000 rpm for 10 min at 20˚C to precipitate protein. After centrifugation, 500 µL of the supernatant was transferred to a new well of the 96 well plate for LC-MS/MS analysis.

Plasma and thigh samples from treatment groups and the calibration curve samples were processed on the same test occasion using the same procedure. The calibration curve samples were generated by spiking aliquots of drug-free plasma or thigh homogenates with the test article dilution. The quality control (QC) samples, QH (high), QM (medium) and QL (low) were each assayed in duplicate.

v. LC-MS/MS analysis

LC-MS/MS was conducted with a SCIEX Triple Quad™ 5500+ mass spectrometer. Method development was conducted to determine appropriate conditions for LC-MS/MS analysis of ***MB076***. A titration of a stock solution was performed to correlate peak areas and the corresponding concentration. The reportable linear range of the assay was determined along with the lower and upper limit of quantitation (LLOQ and ULOQ).

To develop the bioanalytical method, the ***MB076*** was prepared in ACN/H_2O=50/50 at 1 ng/µL and this test compound solution was infused into the MS source via syringe pump at a constant rate. Full scan MS analyses were conducted and total ion current chromatograms and corresponding mass spectra were reviewed for ***MB076*** in both positive and negative ionization modes. The precursor ions for MS/MS were selected from either the positive or the negative mass spectrum, as a function of the respective ion abundance. In addition, product ion MS/MS analysis was performed in order to determine the appropriate selected fragmentation reaction for use in quantitative analysis. The final reaction monitoring parameters were chosen to maximize the ability to quantify the test compound when present within a complex mixture of components. Following identification of the specific multiple reaction monitoring (MRM) transition to be used for each test compound, the detection parameters were optimized. ***MB076*** was observed as one charged ion $[M+H]^+$ and the MRM chosen was m/z = 374.0 to m/z = 243.2 for ***MB076*** in electrospray positive ion mode.

The chromatographic conditions used for LC-MS analysis were identified by injection and separation of the analyte on a suitable LC column followed by adjustment of the gradient conditions as necessary. A suitable internal standard (IS), oxybutynin, was selected from a collection of commonly used compounds whose LC-MS/MS properties had already been characterized, m/z = 358.3 → 142.3. In brief, the chromatography was done with the XSelect Peptide HSS T3 XP column 2.5 µm (2.1 x 150 mm) column for both plasma and thigh samples. LC was conducted with an isocratic elution of H_2O/FA= 99/1 (v/v) (mobile Phase A) and ACN/MeOH/FA= 80/20/1(v/v) (mobile Phase B). The total run time was 4 min and the injection volume was 2 µL. A titration of a stock solution was performed to correlate peak areas and the corresponding nominal concentration. The reportable linear range of the assay was determined along with the lower and upper limit of quantitation (LLOQ and ULOQ). For each sample run, a titration of ***MB076*** was performed and combined with plasma or thigh homogenates, to generate a calibration standard curve with the same biological material under evaluation. Calibration standard of ***MB076*** was included in each test occasion at eight concentrations, 100, 200, 1000, 3000, 10000, 30000, 60000, and 100000 ng/mL, for each run. The ranges include the lower limit and upper limit of quantification (LLOQ and ULOQ). Each run also included six QC standards of ***MB076*** at high (QH), mid (QM) and low (QL) concentrations of 80000, 50000, and 300 ng/mL, respectively. All three QC concentrations were tested twice per run resulting in six QC standards. ACN extracts of the calibration and QC standards were prepared in wells of a 96-well plate following the same method and at the same time as the plasma or thigh samples from treated animals. Peak areas of test plasma and thigh samples were recorded

and ***MB076*** concentrations were determined using the respective calibration standard. Oxybutynin was analyzed concurrently with the test samples to identify variation in sample processing.

vi. Analysis of bioanalytical data and acceptance criteria

Samples from in-life treatment groups, STDs and QCs were processed on the same test run using the same procedure. LC-MS/MS data were processed using Analyst 1.7 software. Peak area ratios of ***MB076*** to IS (oxybutynin) were determined from the STD samples and used to generate a calibration curve. The simplest regression analysis resulting in the best r correlation coefficient was used. In this case the $1/x^2$ weighting was used. In-life treatment samples and the QCs were analysed by the same method in the same run and the concentrations determined by back-calculation from the calibration curves. Calibration standards must be within ± 25% of their nominal value, otherwise they were removed from the analysis. At least 67% (2/3) of the eight STDs in the calibration curve must meet the acceptance criteria. If an LLOQ or ULOQ failed this test, the linear range of the calibration curve was reduced accordingly and in-life treatment samples outside the range were rejected. QC samples also must be ± 25% of their nominal value and at least 67% (2/3) of the QCs must pass to meet the acceptance criteria. If two QCs of the low or high concentration failed, the linear range of the calibration curve was reduced and in-life treatment samples outside of this range were rejected.

The analytical concentrations of ***MB076*** in-life treatment samples were recorded as 0 if no peak was observed or if the concentrations were <LLOQ. If the analytical concentrations in the in-life treatment samples were above the 150% ULOQ, they were coded "AU" (above the curve limit). The original samples were then diluted with the appropriate matrix and analyzed again in a separate run.

vii. Calculation of PK and PD parameters

Data tabulation of analyte concentration in plasma and thigh homogenates over time were supplied with plots generated for plasma and thigh. The PK parameters with settings for Phoenix® Build 8.3.1.5014 was used for each IV dose level of ***MB076*** from the non-compartmental analysis (NCA) of the plasma and thigh data: $t_{1/2}$, C_0, AUC_{last}, AUC_{inf}, Vss and CL (see Appendix 1 for definitions).

Mice survival

Five male C57BL/6 mice per treatment group were infected intravenously via the tail-vein by injecting a prepared inoculum of *K. pneumoniae* KP1, input CFU = 2.1×10^8 CFU/mouse, contained in a volume of 0.25 mL per animal. Animals were treated with intraperitoneal 100mg/kg/dose of cefepime, cefepime + ***MB076*** (1:1, or 1:4 ratio) or placebo at the time of infection. Doses were repeated the following morning and afternoon (18h and 24h after infection). Survival was evaluated 24h post-treatment.

References

(1) Morandi, S.; Morandi, F.; Caselli, E.; Shoichet, B. K.; Prati, F. Structure-Based Optimization of Cephalothin-Analogue Boronic Acids as β-Lactamase Inhibitors. *Bioorganic Med. Chem.* **2008**, *16* (3), 1195–1205. https://doi.org/10.1016/j.bmc.2007.10.075.

(2) Drawz, S. M.; Taracila, M.; Caselli, E.; Prati, F.; Bonomo, R. A. Exploring Sequence Requirements for C3/C4 Carboxylate Recognition in the Pseudomonas Aeruginosa Cephalosporinase: Insights into Plasticity of the AmpC β-Lactamase. *Protein Sci.* **2011**, *20* (6), 941–958. https://doi.org/10.1002/pro.612.

(3) Caselli, E.; Romagnoli, C.; Powers, R. A.; Taracila, M. A.; Bouza, A. A.; Swanson, H. C.; Smolen, K. A.; Fini, F.; Wallar, B. J.; Bonomo, R. A.; et al. Inhibition of Acinetobacter -Derived Cephalosporinase: Exploring the Carboxylate Recognition Site Using Novel β-Lactamase Inhibitors. *ACS Infect. Dis.* **2018**, *4* (3), 337–348. https://doi.org/10.1021/acsinfecdis.7b00153.

(4) Treiber, A.; Dansette, P. M.; El Amri, H.; Girault, J.-P.; Ginderow, D.; Mornon, J.-P.; Mansuy, D. Chemical and Biological Oxidation of Thiophene: Preparation and Complete Characterization of Thiophene S-Oxide Dimers and Evidence for Thiophene S-Oxide as an Intermediate in Thiophene Metabolism in Vivo and in Vitro. *J. Am. Chem. Soc.* **1997**, *119* (7), 1565–1571. https://doi.org/10.1021/ja962466g.

(5) Jernigan, J. A.; Hatfield, K. M.; Wolford, H.; Nelson, R. E.; Olubajo, B.; Reddy, S. C.; McCarthy, N.; Paul, P.; McDonald, L. C.; Kallen, A.; et al. Multidrug-Resistant Bacterial Infections in U.S. Hospitalized Patients, 2012–2017. *N. Engl. J. Med.* **2020**, *382* (14), 1309–1319. https://doi.org/10.1056/nejmoa1914433.

(6) Caselli, E.; Romagnoli, C.; Vahabi, R.; Taracila, M. A.; Bonomo, R. A.; Prati, F. Click Chemistry in Lead Optimization of Boronic Acids as β-Lactamase Inhibitors. *J. Med. Chem.* **2015**, *58* (14), 5445–5458. https://doi.org/10.1021/acs.jmedchem.5b00341.

5 Strategies for new inhibitors

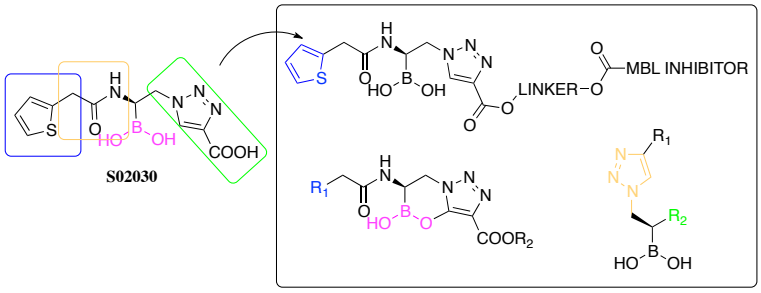

The aim of this chapter is to describe some other projects I worked on, which provided useful synthetic strategies to obtain new boronic acids with interesting structural change. *In vitro* analyses of such compounds were not yet performed at the time of writing this thesis and some of these projects are currently on going. The starting point was always **S02030** as lead compound for further modifications and the major objective is to succeed in the inhibition of class B and class D β-lactamases. Indeed, we developed some molecules with a certain activity against these enzymes, but always in the micromolar range: compound ***6h*** demonstrated to inhibit class B, VIM-2 with K_i = 7.7 μM (see section 3.1.4) and compound ***12f*** was able to inhibit class D, OXA-24/40 with K_i = 4.4 μM (see section 3.2.2). Therefore, different strategies were developed to improve potency against these classes of β-lactamases, but also to obtain inhibitors with multiple activity against different and hopefully all classes of enzymes.

5.1 β-Triazolylboronic acid as new scaffold for the inhibition of class D β-lactamases

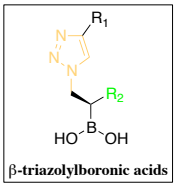

As described previously (see section 3.2.2), the most important feature, which differentiates class D β-lactamases from other SBLs, is the presence of a tunnel-like entrance to the active site, first identified in OXA-24/40 enzymes, where it is formed through the specific arrangement of Tyr112 and Met223 side chains. These residues create a barrier, which avoids the entrance of antibiotics with bulky substituents, while little substituents, such as the hydroxyethyl side chains of carbapenems, are easily accommodated under the barrier.

All the α-triazolylboronic acids library described in 3.1.2 showed poor affinity against class D β-lactamases with K_i values > 100 mM. Therefore, based on crystallographic structures of OXA enzymes, the insertion of one more carbon atom between the boron atom and the triazole was designed to overcome the hydrophobic bridge and to extend the activity of α-triazolylboronic acids towards

class D β-lactamases. I developed the synthesis of achiral and chiral β-triazolylboronic acids and a series of ten molecules (***24a-k***, Figure 58) was obtained.

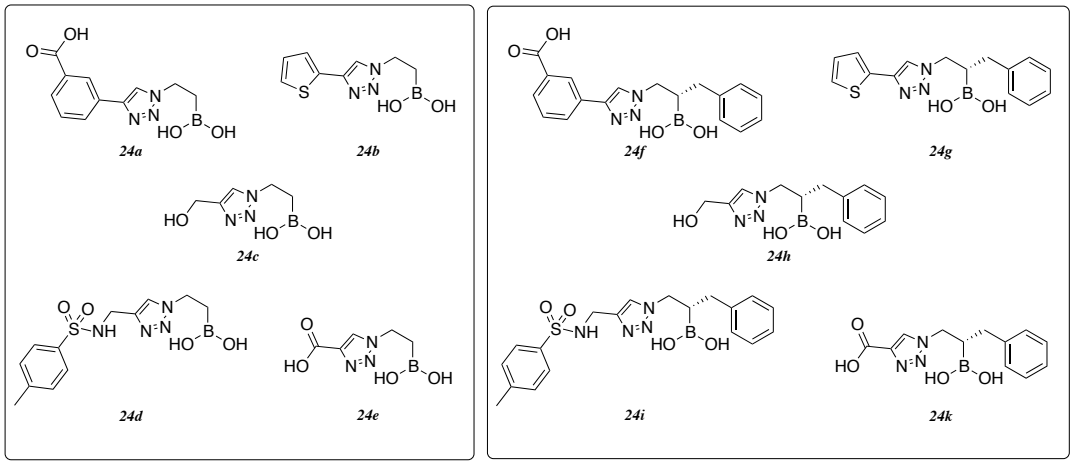

Figure 58. Achiral (left) and chiral (right) β-triazolylboronic acids (***24a-k***).

5.1.1 Synthesis of achiral β-triazolylboronic acids

Both synthesis started from the (+)-pinanediol α-azidomethaneboronate ***2***. For the achiral compounds (Scheme 12), ***2*** was converted into the corresponding β-azidoethaneboronate ***20*** through homologation with chloromethyl-lithium, generated *in situ* by reaction of bromochloromethane (1.5 eq.) with *n*-BuLi (1.2 eq.) at -78 °C. Compound ***20*** was then reacted with desired alkynes in CuAAC reaction: the azide was reacted with an excess of alkyne (1.5 eq.) in a 1:1 mixture of *tert*-butanol and water, together with copper sulphate (0.05 eq.), which was reduced *in situ* by sodium ascorbate (0.2 eq.). The expected 1,4-disubstituted triazoles (***21***), differently substituted at the R_1 group, were easily isolated by extraction (85-99% yield) and used as such for the next step. Final deprotection of (+)-pinanediol esters was accomplished either by transesterification with isobutylboronic acid (0.95 eq.) and HCl (3 eq.) or by transesterification with methylboronic acid (10 eq.) and HCl 0.2 M in a mixture of H_2O and acetone, allowing to obtain final boronic acids ***24a-e***.

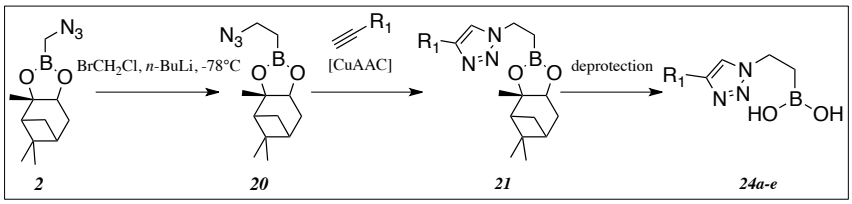

Scheme 12. Synthesis of achiral β-triazolylboronic acids ***24a-e***.

5.1.2 Synthesis of chiral β-triazolylboronic acids

For the synthesis of chiral compounds (Scheme 13), the chiral (+)-pinanediol α-chloro-β-azidoethaneboronate ***13*** was obtained from the α-azidomethaneboronate ***2*** through a stereoselective Matteson homologation, as already described in section 4.1. Compound ***13*** was obtained in 90% yield

and then reacted with a Grignard reagent to generate the α-benzyl-β-azidoethaneboronate ***22***. Compound ***22*** was then reacted with desired alkynes in CuAAC reaction in the same way described before for achiral compounds. Final deprotection of (+)-pinanediol esters was accomplished and allowed to obtain the desired products ***24f-k***. In this case, the stereochemistry of the compound is inverted in respect to that commonly observed in other compounds, such as α-amido-β-triazolylboronic acids. The triazole ring, which should behave as bioisoster of the amide side chain of β-lactams is on the other side of the molecule, while the benzyl chain occupies the α-position where we usually positioned the amide. These changes are based on the analysis of the structure of OXA-24/40 in complex with doripenem (section 3.2.2). The site where the R_1 hydroxyethyl chain of doripenem binds does not offer much space to expand. However, it is important to notice the different conformation of the R_1 side chain between carbapenems and other β-lactam antibiotics. In fact, the stereochemistry at C(7) in cephalosporins is *opposite* with respect to C(6) in carbapenems (Figure 59).Therefore, even if the hydroxyethyl chain occupies a little binding site, trajectory can be changed > 90 degrees to occupy the commonly called R_1 binding site, where there is more space and lots of hydrophobic side chains (Val130, Trp167, Leu168, Val169). The benzyl group of compounds ***24f-k*** is in the same position of the amide chain of cephalosporins. Therefore, it could occupy the R_1 hydrophobic pocket of OXA enzymes.

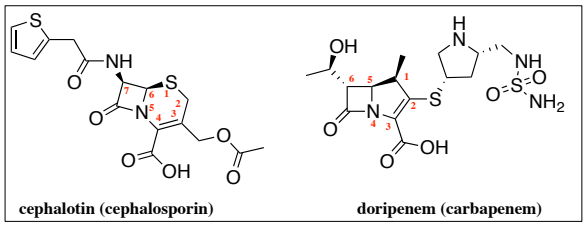

Figure 59. Comparison between cephalosporins and carbapenems.

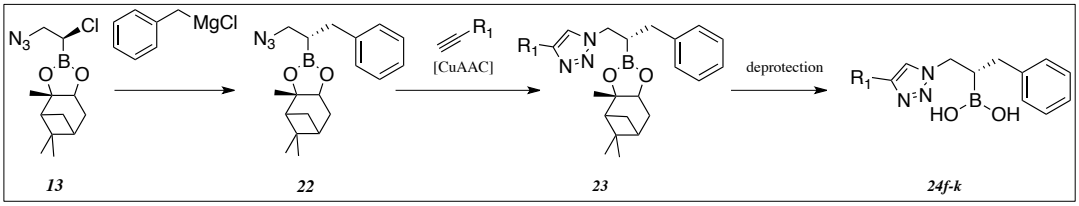

Scheme 13. Synthesis of chiral β-triazolylboronic acids ***24f-k***.

In conclusion, the synthesis of ten β-triazolylboronic acids was accomplished with good yields and purification of final compounds. The next step will be the development of kinetic analysis and microbiological assays to assess the inhibitory activity of such compounds. β-Amidoboronic acids and their triazole bioisosters are poorly explored. A recent study reported the activity of β-amidoboronates against *M. tuberculosis*,[1] but there are not many other studies concerning this class of compounds. This lack of data opens the door to a mostly unexplored field of great interest and the success obtained in the synthesis of this class of compounds makes possible the synthesis of a larger library where also β-amido and β-sulphonamidoboronic acids could be inserted.

5.2 Design and synthesis of co-drugs with dual activity against SBLs and MBLs

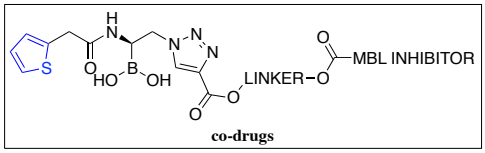

The idea and use of the "co-drug" dates to the 1960s and still continues to allow the development of new drugs. “Co-drug” or “mutual prodrug” is an approach where two different pharmacophores with similar or different pharmacological activities are attached directly or via a linkage. In this way, by attaching them with other drugs of same or different categories, effective drugs, maybe associated with some drawbacks, can develop synergistic action or reach more effectively specific site/organ/cells. This approach is commonly used to improve physicochemical, biopharmaceutical and drug delivery properties of therapeutic agents. Indeed, the union of two molecules with different pharmacokinetic profile in a single structure allows obtaining an entity with a single pharmacokinetic profile, which can guarantee absorption of the two compounds at the same time and with a constant 1: 1 *ratio*. Furthermore, each molecule of the co-drug can improve the pharmaceutical properties of the other, thus acting as a "mutual pro-drug".[2]

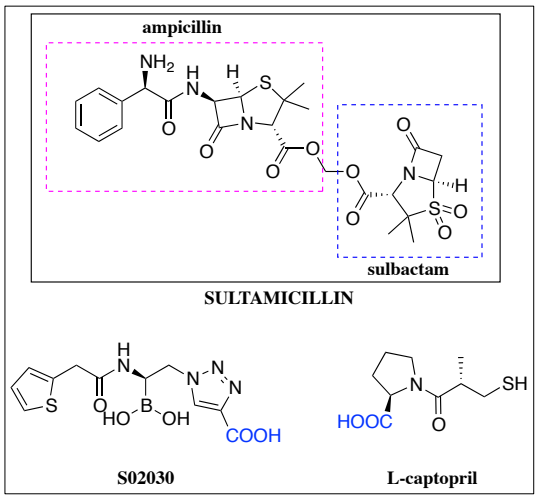

Figure 60. The commercially – available sultamicillin and the two compounds selected for the synthesis of co-drugs.

While reading about a commercially - available co-drug, namely sultamicillin (Figure 60), I was inspired to try to couple an inhibitor of MBLs with a SBLs inhibitor. Two co-drugs were designed containing **S02030** (Figure 60), which proved to be an excellent inhibitor against SBLs and an inhibitor of MBLs. As described before, **S02030** is active towards class A β-lactamases such as KPC-2 (IC_{50} = 80 nM), SHV-1 (IC_{50} = 130 nM) and CTXM-96 (IC_{50} = 2 nM) and towards those of class C, such as ADC-7 (K_i = 44 nM), P-99 (IC_{50} = 23 nM) and PDC-3 (IC_{50} = 4 nM). The choice of the MBLs inhibitor to combine with **S02030**, was made between the molecules identified in the literature, which however did not undergo pre-clinical development. Among the many possible examples, **L-captopril** (Figure 60), used as an Angiotensin- Converting- Enzyme (ACE) inhibitor and active on some of the most relevant MBLs, such as NDM-1 (IC_{50} = 202 μM), IMP-1 (K_i = 12.5 μM) and BcII (K_i = 65.5 μM), was selected.[3]

The two molecules were linked through their carboxyl groups and esterified with a diol linker. Diols can easily form ester bonds and these bonds are easily hydrolysed *in vivo* by cell esterases. In particular, among the possible diols 1,3-propanediol, which separates ester groups with three carbon atoms and methylene glycol, a geminal diol (hydrated formaldehyde), which has only one carbon atom between the hydroxyl groups, have been chosen (Figure 61).

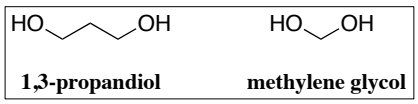

Figure 61. Linkers.

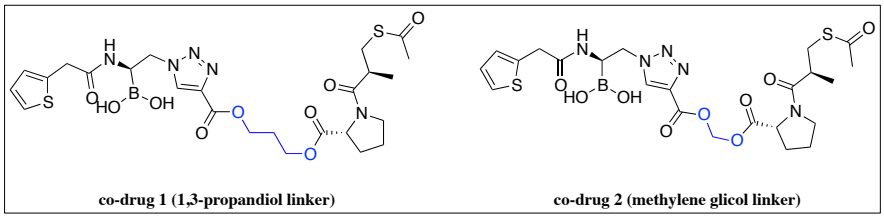

Figure 62. The two co-drugs synthesised.

Key intermediates for the synthesis of both co-drugs were the azide ***25*** (Figure 63), intermediate in the synthesis of **S02030**, propiolic acid and captopril protected with an acetyl group on the thiol. For the introduction of 1,3-propandiol linker, the diol was used directly in the synthesis, while, for the introduction of methylene glycol, chloromethane chlorosulfate was used to introduce the linker in the co-drug structure.

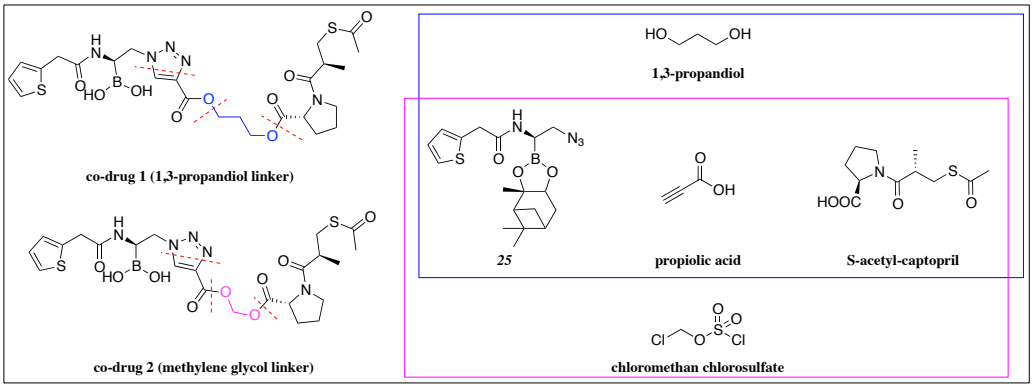

Figure 63. Key compounds for the synthesis of co-drugs.

5.2.1 Synthesis of co-drug 1

For the synthesis of **co-drug 1** propiolic acid (Scheme 14) was esterified first with propandiol protected with a *tert*-butyl-dimethylsilyl (TBDMS) group in dry CH_2Cl_2, in the presence of DCC and DMAP. The expected propiolic ester ***26*** was obtained in 75% yield subjected to the click reaction with azide ***25*** as described before, using $CuSO_4$/ascorbate as catalyst, affording in nearly quantitative yield the triazole ***27***. Subsequently, deprotection of the alcohol was performed with tetrabutylammonium fluoride (TBAF, 3 eq.) and allowed to obtain compound ***28*** in 80% yield. The coupling between the two inhibitors occurs with an esterification similar to that used for the synthesis of alkyne ***26***, with the only difference being the use of EDC •HCl (hydrochloride of 1-ethyl-3- (3-dimethylaminopropyl)

carbodiimide) instead of DCC. Finally, deprotection of the (+)-pinanediol was accomplished using methylboronic acid and HCl 0.2 M and allowed to obtain **co-drug 1** in 70% yield.

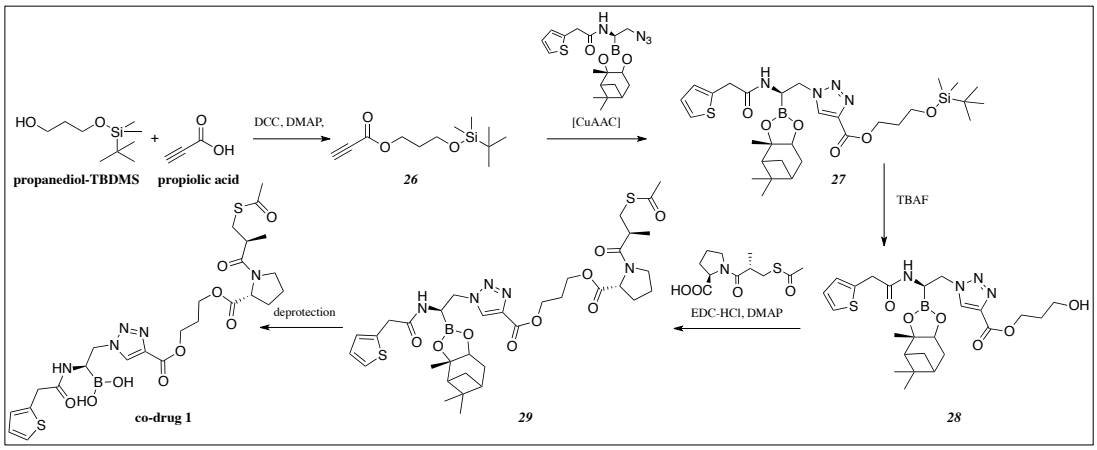

Scheme 14. Synthesis of **co-drug 1**.

5.2.2 Synthesis of co-drug 2

The synthetic pathway for **co-drug 2** is resumed in Scheme 15 and started with the esterification of the acidic group of *S*-acetyl-captopril with a chloromethyl group, affording compound ***30*** in 58% yield. The substitution of the chlorine of ***30*** with iodine, which is a better leaving group, had the purpose of facilitating the subsequent nucleophilic substitution with the carboxylate anion of propiolic acid, which is not a very good nucleophile. The iodo-derivative ***31*** was, thus, obtained by substitution SN_2 with sodium iodide in acetone. The product was not further purified and was used for next reaction where it was reacted with propiolic acid in basic conditions to obtain alkyne ***32*** (74% yield). This latter and azide ***25*** were subjected to CuAAC, which allowed obtaining ***33***, the pinandiol ester of **co-drug 2**. Unfortunately, this reaction displayed an unusual low yield (6%), due to difficulties in purification steps and the amount of ***33*** was not enough to perform deprotection of pinanendiol, affording **co-drug 2**.

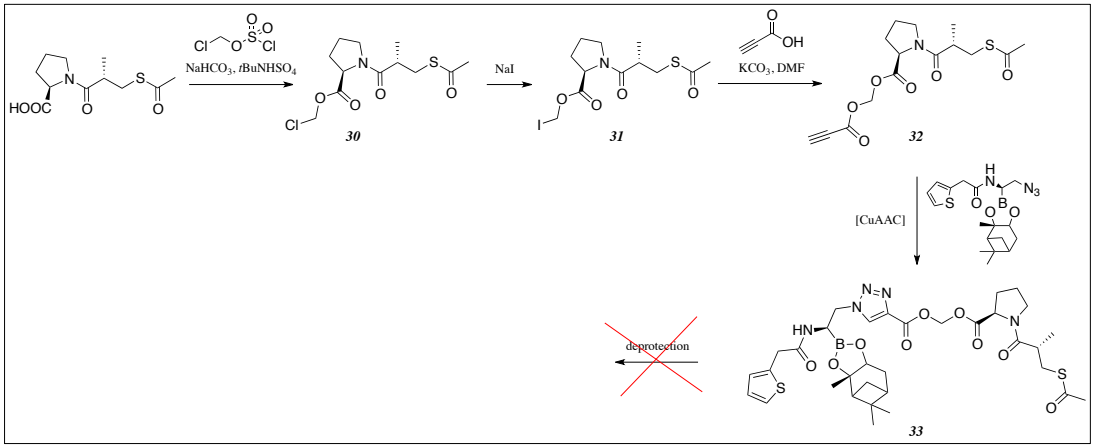

Scheme 15. Synthesis of **co-drug 2**.

In conclusion, two co-drugs were designed and synthesised with the aim of inhibiting both SBLs and MBLs. **S02030** for the inhibition of class A and class C β-lactamases and **L-captopril** for the inhibition of class B β-lactamases were bound together through a linker. In one case the linker was 1,3-propandiol and in the other case, methylene glycol, both able to form ester bonds, which can be hydrolysed *in vivo*. The synthesis of both co-drugs was successfully accomplished and this is the starting point for a new kind of BATSI: not just one molecule with multiple inhibitory activity, but two molecules with different target bound together in a single co-drug.

5.3 *Cyclic boronic acids as broad spectrum β-lactamases inhibitors*

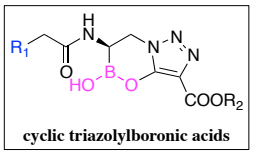

cyclic triazolylboronic acids

In 2015 Hecker et al. performed a docking study to find cyclic boronic acid as potential inhibitors of class A, C and D β-lactamases: the aim was to constrain the structure into a single conformation able to better interact with the active site of the enzymes and to improve selectivity. Several molecules were synthesised and evaluated, resulting in the discovery of vaborbactam, the first cyclic boronate compound on the market.[4]

The evidence that all the boronic inhibitors of β-lactamases that reached the clinic were cyclic boronates, forced my research in the direction of cyclic triazolylboronic compounds. If **S02030**, ***MB076*** (see section 4.2) and also α-tryazolylboronic acids are so good inhibitors of class A and class C β-lactamases, their cyclic analogues could be broad spectrum inhibitors of all classes, like **QPX7728** (Figure 64).[5]

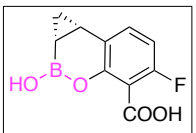

QPX7728

Figure 64. Broad spectrum inhibitor of β-lactamases in phase I clinical trial.

5.3.1 *Attempts to obtain cyclic analogues of S02030*

Initially, the objective was to obtain the cyclic analogue of **S02030**. To this end, the easy and mild synthesis of the triazole ring by CuAAC, leading exclusively to 1,4-disubstituted rings, was no more exploitable and two alternative synthetic strategies were therefore designed. In one case the cyclization should be obtained installing a hydroxyl in position 5 on the triazole, thus favouring, during deprotection of the pinacol ester, the attack to the boron atom. The second strategy, instead, install a halogen atom on position 5 of the triazole ring which will be substituted with – OH group of the boronic acid after deprotection of the pinanendiol ester (Figure 65).

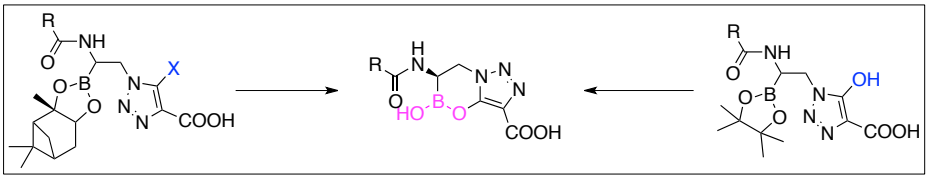

Figure 65. Strategies to obtain cyclic **S02030** and analogues.

In both cases the final product was not obtained. In the first case, the synthetic procedure involved ten synthetic steps and the low amount of compound obtained after six or seven steps avoided the development of next reactions. The procedure was repeated three times, but the same problem was found every time. Therefore, we decided not to definitively withdrawing this procedure, but to set it aside and try other strategies.

In the second case, we found a way to insert an iodide atom in position 5 on the triazole through a modification of the click reaction (Scheme 16).[6] However, not only the synthesis was not selective and also the triazole without the iodide was obtained in a 1:1 *ratio*, but we didn't succeeded also in its intramolecular substitution. The synthesis of the cyclic version of **S02030** was therefore abandoned.

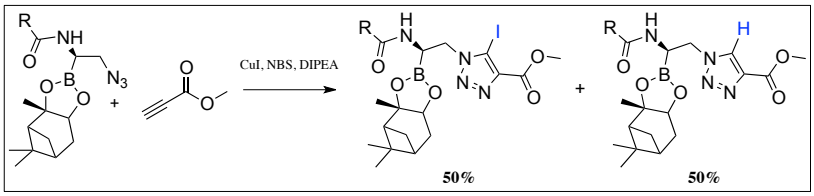

Scheme 16. Reaction to introduce an iodide atom in position 5 on the triazole ring.

5.3.2 Cyclic boronic acids starting from (+)-pinanediol α-azidomethaneboronate

The starting azide was changed and the less hindered (+)-pinanediol α-azidomethaneboronate was used to facilitate the introduction of a halogen atom, of another nucleophile and/or the cyclization, obtaining this time a five-member ring (Figure 66).

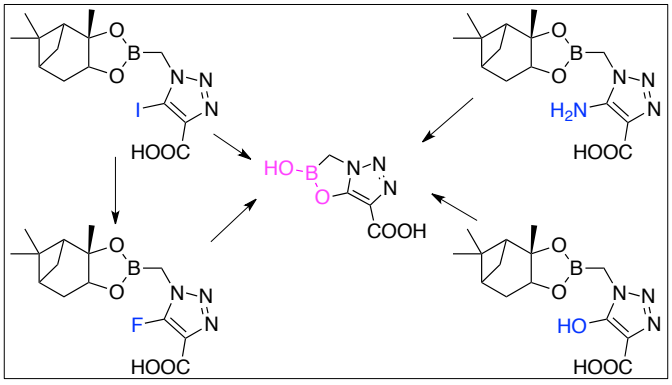

Figure 66. Strategies starting from the α-azidomethaneboronate.

Initially, the introduction of an iodide was developed (Scheme 17). In this case, the click reaction performed better and we obtain only the product with the iodide atom in position 5, confirming that the presence of the α-amido chain reduced the attack of the halogen atom. Therefore, the deprotection of the (+)-pinanediol ester was achieved, hoping to obtain also the cyclization of the boronic acid. Unfortunately, the cyclization didn't occur, but the reaction gave the boronic acid with high yield (85%). Different reactions (H_2O, refluxing for 1-4h; basic media etc.) were developed to force the cyclization through the substitution of the iodide atom by the –OH group of the boronic acid, but only the elimination of the boronic acid was observed.

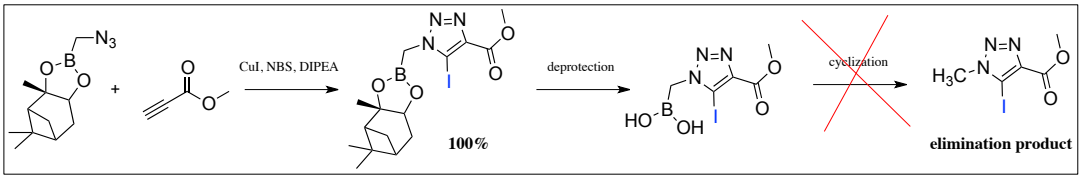

Scheme 17.Introduction of an iodide atom in position 5 of the triazole in a α-triazolylboronate.

The attempts to change the nucleophile in position 5 on the triazole ring, by substitution of the iodide with a fluoride or by direct introduction of a fluoride, of an amino-group or of a hydroxyl group were disappointing and this time we decided to abandon this synthetic strategy.

5.3.3 Attempts to obtain cyclic boronic acids currently on going

Exploiting decarboxylative borilation

In 2017, Baran et al. demonstrated that through simple redox-active esters (RAEs, e.g., N-hydroxyphthalimide esters), alkyl carboxylic acids could be convert into boronate esters, using an inexpensive nickel catalyst.[7] This reaction possesses a high potential for the synthesis of cyclic β-triazolylboronic acids. Therefore, a synthetic pathway to obtain cyclic boronates starting from the amino acid serine or from its precursor 3-aminooxetan-2-one was designed (Scheme 18).

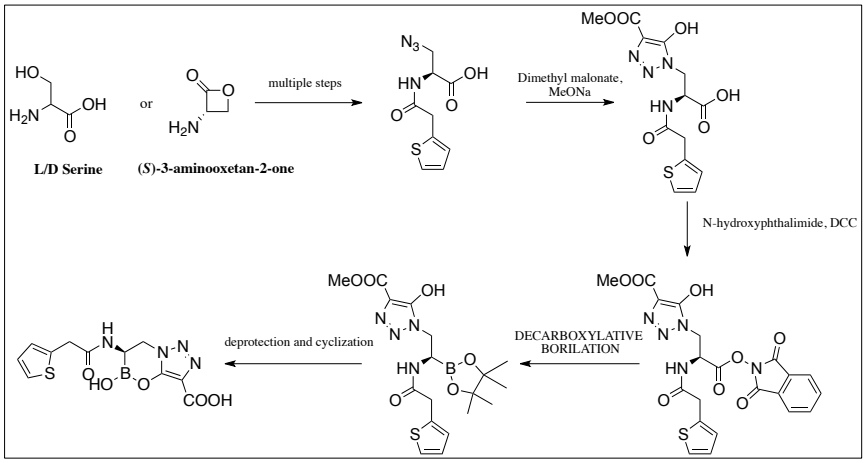

Scheme 18. Synthetic pathway for the synthesis of cyclic β-triazolylboronic acids, exploiting decarboxylative borilation.

This synthetic project is currently on going. At present the boron as pinacolate has been successfully inserted through decarboxylative borilation on other substrates in order to verify the feasibility of this experimental procedure.

Experimental section

General synthetic information

Unless otherwise stated, all reagents were purchased and used without further purification. Deoxygenated water was obtained through sonication Anhydrous tetrahydrofuran (THF dry) was freshly distilled from Na (s), under an argon flow, using benzophenone as an indicator. The reactions that require a particularly anhydrous environment were carried out in a glassware previously heated in an oven at 130 ° C for at least 2h, hot assembled, greasing the emery and cooled under an argon flow. All transfers of anhydrous solvents or mixtures were carried out through porous septa, using glass syringes previously dried in an oven, under the same conditions. The temperature of – 80 °C was reached and maintained by adding CO_2 to a 1: 1 ethanol / methanol mixture previously cooled with a cryostat; the heating of the reaction mixture was carried out by means of a silicone bath and controlled through a probe. All reactions were monitored through Thin Layer Chromatografy (TLC) with 0.20 mm Machery-Nagel silica plates (60-F254), using as developing agents: UV light (λ = 254 nm), potassium permanganate ($KMnO_4$), Pancaldi's reagent (phosphomolybdic reactive), sulfuric acid (H_2SO_4), ninhydrin or curcumin solutions. All optical activity measurements were performed at a temperature of 20 ° C, using the Perkin-Elmer mod. 241 polarimeter with a 10 cm long and 0.5 cm diameter cell. Unless otherwise indicated, the ^{1}H-NMR, ^{13}C-NMR and ^{11}B-NMR spectra were recorded with a Brucker DPX-400 spectrometer or with a Brucker FT-NMR Avance III HD 600 MHz spectrometer. Deuterated solvents (DMSO-d_6, $CDCl_3$, MeOD etc.) were used. Chemical shifts (δ) are reported in ppm and were calibrated to the residual signals of the deuterated solvent. Multiplicity is given as s = singlet, d = doublet, t = triplet, q = quartet, m = multiplet; coupling constants (J) are given in Hz. Two-dimensional NMR techniques (COSY, HMBC, HSQC) were used to aid in the assignment of signals in ^{1}H and ^{13}C spectra. Particularly, in the ^{13}C spectra, the signal of the boron-bearing carbon atom, which tend to be broadened, and the signal of the quaternary triazole carbon (when present) are often beyond the detection limit, but their resonances were unambiguously determined by HSQC and HMBC. Mass spectra were determined on an Agilent Technologies LC-MS (n) Ion Trap 6310A (ESI, 70 eV). High-resolution mass spectra were recorded on an Agilent Technologies 6520 Accurate-Mass Q-TOF LC/MS.

β-Triazolylboronic acids

Synthesis of (+)-pinanediol-azidoethaneboronate (20)

(+)-Pinenediol-azidomethaneboronate ***2*** and chlorobromomethane are dissolved in dry THF. The mixture is brought to - 80 °C and *n*-BuLi is added dropwise over 15 minutes, under mechanical stirring. The reaction mixture stirred all night, allowing the temperature to rise slowly. The volume of solvent was reduced under vacuum and the resulting mixture was diluted with petroleum ether and washed with a saline solution obtained by mixing equal volumes of H_2O and saturated NaCl solution. The aqueous phase was extracted three times with petroleum ether and the combined organic phases were washed with saturated NaCl solution and subsequently dried with anhydrous Na_2SO_4. The mixture is filtered and the solvent removed *in vacuo*. The residue was purified by chromatographic column (petroleum ether / ethyl ether 9: 1) giving the expected product (30%).

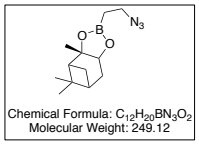

Chemical Formula: $C_{12}H_{20}BN_3O_2$
Molecular Weight: 249.12

^{1}H NMR (400 MHz, $CDCl_3$) *δ:* 4.28 (dd, *J* = 2.0, 8.6 Hz, 1H, CH_{pin}), 3.41 (t, *J* = 8.0 Hz, 2H, CH_2N_3), 2.37-1.83 (m, 5H, pinanediol), 1.39 (s, 3H, $CH_{3\text{-}pin}$), 1.29 (s, 3H, $CH_{3\text{-}pin}$), 1.21 (t, *J* = 8 Hz, 2H CH_2B)), 1.11 (d, *J* = 10 Hz, 1H, $CH_{2\text{-}pin}$), 0.84 (s, 3H, $CH_{3\text{-}pin}$). ^{13}C NMR (101 MHz, $CDCl_3$) δ: 77.99, 77.22, 44.77, 51.25, 39.52, 38.16, 35.39, 28.62, 27.09, 26.47, 24.01, 12.95 (CB). ^{11}B NMR: (128 MHz, $CDCl_3$) *δ*: 32.63. $[\alpha]^{20}_{D}$ = + 25.74 ($CHCl_3$).

General procedure for the synthesis of (+)-pinanediol-β-triazolylethaneboronates (21a-e)

Compound ***20*** (0.40 mmol, 1 eq.) and $CuSO_4$ 0.03 M (0.8 mL, 0.1 eq.) were added to a solution containing sodium ascorbate (0.08 mmol, 0.2 eq.) and the selected alkyne (0.42 mmol, 1.05 eq.) solubilized in *tert*-butanol (0.8 mL). The reaction mixture was heated at 65 °C for 2-3 hours. The reaction mixture was allowed to cool down to room temperature and ethyl acetate (15 mL) was added. The organic layer was washed with 6 ml of saline solution obtained by mixing equal volumes of H_2O and saturated NaCl solution. The aqueous phase was extracted with ethyl acetate (2 x 10 mL) and the combined organic phases were washed with saturated NaCl, dried over Na_2SO_4, filtered and concentrated affording the desired product.

3-(1-(2-((3aS)-3a,5,5-trimethylhexahydro-4,6-methanobenzo[d][1,3,2]dioxaborol-2-yl)ethyl)-1H-1,2,3-triazol-4-yl)benzoic acid (21a)

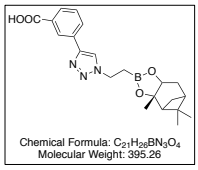

White solid (54%). ^{1}H NMR (400 MHz, $CDCl_3$) δ: 8.49 (s, 1H, CH_{triaz}), 8.19 (d, J = 7.4 Hz, 1H, CH_{phen}), 8.08 (d, J = 7.7 Hz, 1H, CH_{phen}), 7.96 (s, 1H, CH_{phen}), 7.55 (t, J = 7.7 Hz, 1H, CH_{phen}), 4.58 (t, J = 7.6 Hz, 2H, CH_2N_3), 4.30 (d, J = 7.4 Hz, 1H, CH_{pin}), 2.40-1.75 (m, 5H, pinanediol), 1.60 (t, J = 7.7 Hz, 2H, CH_2B), 1.40 (s, 3H, $CH_{3\text{-}pin}$), 1.28 (s, 3H, $CH_{3\text{-}pin}$), 1.00 (d, J = 10.9 Hz, 1H, $CH_{2\text{-}pin}$), 0.84 (s, 3H, $CH_{3\text{-}pin}$). ^{13}C NMR (101 MHz, $CDCl_3$) δ: 131.38, 130.77, 130.03, 129.66, 129.17, 127.34, 120,12, 86.40, 78.16, 65.86, 51.20, 46.82, 39.49, 38.17, 35.30, 29.70, 28.61, 27.04, 26.41, 24.00, 12.95 (CB). ^{11}B NMR (128 MHz, $CDCl_3$) δ: 34.56. HRMS (ESI-QTOF) m/z: $[M\text{-}H]^-$ 394.1948. $[\alpha]^{20}_D$ = + 10.8 (MeOH).

4-(thiophen-2-yl)-1-(2-((3aS)-3a,5,5-trimethylhexahydro-4,6-methanobenzo[d][1,3,2]dioxaborol-2-yl)ethyl)-1H-1,2,3-triazole (21b)

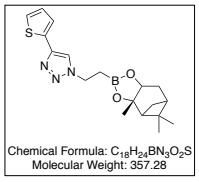

Brown solid (89%). ^{1}H NMR (400 MHz, $CDCl_3$) δ: 7.72 (s, 1H, CH_{triaz}), 7.66 (s, 1H, CH_{tioph}), 7.44 (d, J = 4.9 Hz, 1H, CH_{tioph}), 7.39 – 7.35 (m, 1H, CH_{tioph}), 4.53 (t, J = 7.8 Hz, 2H, CH_2N), 4.31 (d, J = 14.4 Hz, 1H, CH_{pin}), 2.42-1.71 (m, 5H, pinanediol), 1.56 (t, J = 7.8 Hz, 2H, CH_2B), 1.39 (s, 3H, $CH_{3\text{-}pin}$), 1.27 (s, 3H, $CH_{3\text{-}pin}$), 1.03 (d, J = 10.9 Hz, 1H, $CH_{2\text{-}pin}$), 0.84 (s, 3H, $CH_{3\text{-}pin}$). ^{13}C NMR (101 MHz, $CDCl_3$) δ: 126.23, 125.85, 120.84, 119.18, 86.32, 84.87, 78.12, 77.21, 51.22, 46.64, 39.49, 38.16, 35.31, 28.61, 27.04, 26.43, 24.00, 13.49 (CB). ^{11}B NMR (128 MHz, $CDCl_3$) δ: 32.95. HRMS (ESI-QTOF) m/z: $[M+H]^+$ 358.1753. $[\alpha]^{20}_D$ = + 10.58 (MeOH).

(1-(2-((3aS)-3a,5,5-trimethylhexahydro-4,6-methanobenzo[d][1,3,2]dioxaborol-2-yl)ethyl)-1H-1,2,3-triazol-4-yl)methanol (21c)

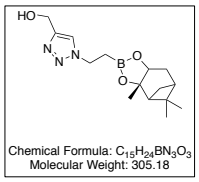

Colourless solid (88%). ^{1}H NMR (400 MHz, $CDCl_3$) δ: 7.74 (s, 1H, CH_{triaz}), 4.84 (s, 2H, CH_2OH), 4.51 (t, J = 7.6 Hz, 2H, CH_2N), 4.28 (d, J = 8.4 Hz, 1H, CH_{pin}), 2.43-1.68 (m, 5H, pinanediol), 1.53 (t, J = 7.7 Hz, 2H, CH_2B), 1.38 (s, 3H, $CH_{3\text{-}pin}$), 1.29 (s, 3H, $CH_{3\text{-}pin}$), 0.99 (d, J = 10.9 Hz, 1H, $CH_{2\text{-}pin}$), 0.84 (s, 3H, $CH_{3\text{-}pin}$). ^{13}C NMR (101 MHz, $CDCl_3$) δ: 86.27, 78.07, 77.22, 56.75, 51.16, 46.89, 39.44, 38.12, 35.26, 28.54, 27.01, 26.39, 23.95, 12.88 (CB). ^{11}B NMR (128 MHz, $CDCl_3$) δ: 33.33. HRMS (ESI-QTOF) m/z: $[M+H]^+$ 306.1984. $[\alpha]^{20}_D$ = + 15.0 (MeOH).

4-methyl-N-(2-(1-(2-((3aS,4S,6S)-3a,5,5-trimethylhexahydro-4,6-methanobenzo[d][1,3,2]dioxaborol-2-yl)ethyl)-1H-1,2,3-triazol-4-yl)ethyl)benzenesulfonamide (21d)

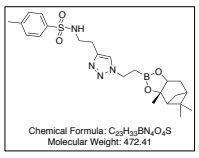

Brown solid (88%). ^{1}H NMR (400 MHz, $CDCl_3$): δ 7.73 (d, J = 8.1 Hz, 2H, CH_{phen}), 7.58 (s, 1H, CH_{triaz}), 7.29 (d, J = 8.1 Hz, 2H, CH_{phen}), 5.15 (s, 1H, NH), 4.53 (t, J = 7.8 Hz, 2H, CH_2N), 4.38 (dd, J = 8.8, 1.7 Hz, 1H, CH_{pin}), 4.23 (d, J = 6.1 Hz, 2H, CH_2NH), 4.14 (s, 2H, CH_2), 2.42 (s, 3H, CH_3), 2.38-2.32 (m, 1H, $CH_{2\text{-}pin}$), 2.30- 2.24 (m, 1H, $CH_{2\text{-}pin}$), 2.08 (t, J = 5.5 Hz, 1H, CH_{pin}), 1.97-1.92 (m, 1H, CH_{pin}), 1.89-1.84 (m, 1H, $CH_{2\text{-}pin}$), 1.53 (t, J = 7.7 Hz, 2H, CH_2B), 1.43 (s, 3H, $CH_{3\text{-}pin}$), 1.0 (d, J = 11.1 Hz, 1H, $CH_{2\text{-}pin}$), 0.85 (s, 3H, $CH_{3\text{-}pin}$), 0.79 (s, 3H, $CH_{3\text{-}pin}$). ^{13}C NMR (100 MHz, $CDCl_3$) δ 143.7, 143.2, 136.7, 129.9 (2C), 127.3 (2C), 123.6,

87.7, 79.0, 51.2, 46.84, 39.5, 39.0, 38.3, 35.8 (CB), 35.2, 28.6, 27.1, 26.6, 24.1, 21.7. ^{11}B NMR (128 MHz, DMSO-*d*6): *δ* 31.60.

tert-butyl-1-(2-((3aS)-3a,5,5-trimethylhexahydro-4,6-methanobenzo[d][1,3,2]dioxaborol-2-yl)ethyl)-1H-1,2,3-triazole-4-carboxylate (21e)

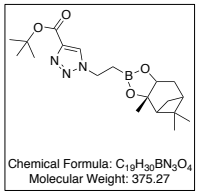

Colourless liquid (52%). ^{1}H NMR (400 MHz, $CDCl_3$) δ 8.05 (s, 1H, CH_{triaz}), 4.51 (t, *J* = 7.7 Hz, 2H, CH_2N_3), 4.27 (dd, *J* = 8.7, 1.8 Hz, CH_{pin}), 2.39-1.75 (m, 5H, pinanediol), 1.59 (s, 9H, $(CH_3)_3$), 1.52 (t, *J* = 7.7, 2H, CH_2B) 1.37 (s, 3H, $CH_{3\text{-}pin}$), 1.27 (s, 3H, $CH_{3\text{-}pin}$), δ 0.94 (d, J = 11 Hz, 1H, $CH_{2\text{-}pin}$), δ 0.84 (s, 3H, $CH_{3\text{-}pin}$). ^{13}C NMR (100 MHz, $CDCl_3$) δ 160.14, 140. 31, 127.04, 86.37, 82.07, 78.11, 77.95, 51.12, 50.80, 46.84, 39.43, 38.11, 35.20, 28.51, 28.24, 27.00, 26.39, 23.94, 12.80 (CB). ^{11}B NMR (128 MHz, $CDCl_3$) δ 31.98. HRMS (ESI-QTOF) *m*/*z*: $[M+H]^+$ 376.2396.

Deprotection of compound 21e

A solution of trifluoroacetic acid in CH_2Cl_2 (1:1) was added to ***21e*** solid at 0 °C. The reaction mixture was left at 0 °C for 30 min, then at room temperature for 4h. The solvent and the trifluoroacetic acid were removed *in vacuo*. A sticky yellow solid was obtained which was washed with a mixture of CH_2Cl_2 and *n*-hexane (1:1). The expected product was isolated as a white powdery solid (99%).

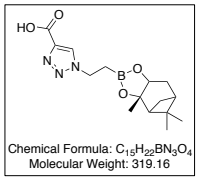

^{1}H NMR (400 MHz, $CDCl_3$) *δ:* 4.28 (dd, *J* = 2.0, 8.6 Hz, 1H, CH_{pin}), 3.41 (t, *J* = 8.0 Hz, 2H, CH_2N), 2.37-1.83 (m, 5H, pinanediol), 1.39 (s, 3H, $CH_{3\text{-}pin}$), 1.29 (s, 3H, $CH_{3\text{-}pin}$), 1.21 (t, *J* = 8 Hz, 2H CH_2B)), 1.11 (d, *J* = 10 Hz, 1H, $CH_{2\text{-}pin}$), 0.84 (s, 3H, $CH_{3\text{-}pin}$). ^{13}C NMR (101 MHz, MeOD) *δ*:129.68, 87.72, 77.99, 44.77, 51.25, 50.15, 41.11, 39.52, 38.16, 35.39, 28.62, 27.09, 26.47, 24.01, 12.95 (CB). ^{11}B NMR (128 MHz, $CDCl_3$) *δ:* 32.63.

General procedure for the deprotection of boronic acid by transesterification with isobutylboronic acid

β-Triazolylboronate ***21*** (0.36 mmol, 1 eq.) was dissolved in dry CH_3CN (2 mL). HCl 3M (1.08 mmol, 3 eq.) and isobutylboronic acid (0.34 mmol, 0.95 eq.) were added. The mixture was stirred for 5 min, then *n*-hexane (2 mL) was added. The biphasic mixture was vigorously stirred and after 30 min the *n*-hexane layer, containing the pinanediol isobutylboronate, was removed and fresh *n*-hexane (2 mL) was added. The last procedure was repeated several times until the disappearance of isobutylboronate from the *n*-hexane layer, monitored by TLC analysis (total reaction time 3-6 hours). The acetonitrile phase was then concentrated and the crude recrystallized to afford the desired β–triazolylboronic acid.

3-(1-(2-boronoethyl)-1H-1,2,3-triazol-4-yl)benzoic acid (24a)

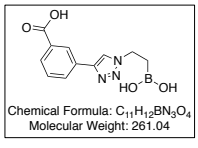

White solid (99%). HRMS (ESI-QTOF) *m*/*z*: $[M-H]^-$ 260.0848.

Characterization not completed.

1-(2-boronoethyl)-1H-1,2,3-triazole-4-carboxylic acid (24e)

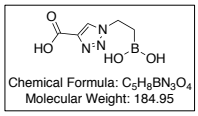

^{1}H NMR (600 MHz, MeOD) *δ:* 8.42 (s, 1H, CH_{triaz}), 4.41 (t, *J* = 7.64 Hz, 2H, CH_2N), δ 1.44 (t, *J* = 7.8 Hz, 2H, CH_2B). *Characterization not completed.*

General procedure for the deprotection of boronic acid by transesterification with methylboronic acid

Methyl boronic acid (3.6 mmol, 10 eq.) and HCl 0.2 M (1 mL) were added to a solution of β-triazolylboronate ***21*** (0.36 mmol, 1 eq.) in acetone (1 mL). The mixture was stirred at room temperature for 36h. The solvent was removed *in vacuo*. CH_2Cl_2 was added and evaporated several times to eliminate all the residual solvents from the solid.

(2-(4-(thiophen-2-yl)-1H-1,2,3-triazol-1-yl)ethyl)boronic acid (24b)

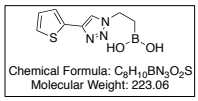

Brown powdery solid (99%). ^{1}H NMR (600 MHz, MeOD) δ: 8.52 (s, 1H, CH_{triaz}), 7.87 – 7.83 (m, 1H, CH_{tioph}), 7.53 (dt, J = 15.2, 7.6 Hz, 1H, CH_{tioph}), 7.43 (d, J = 5.0 Hz, 1H; CH_{tioph}), 4.51 (t, J = 8.2 Hz, 2H, CH_2N), 1.52 (t, J = 7.8, 2H, CH_2B). ^{13}C NMR (151 MHz, MeOD) δ: 128.49, 128.34, 127.36, 126.17, 124.78, 123.78, 49.91, 15.23 (CB). HRMS (ESI-QTOF) m/z: $[M-H]^-$ 222.0510.

(2-(4-(hydroxymethyl)-1H-1,2,3-triazol-1-yl)ethyl)boronic acid (21c)

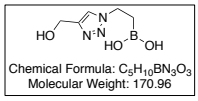

White powdery solid (99%). ^{1}H NMR (600 MHz, MeOD) δ: 8.36 (s, 1H, CH_{triaz}), 4.73 (s, 2H, CH_2OH), 4.49 (t, J = 7.98, 2H, CH_2N), 1.46 (t, J = 7.9 Hz, 2H, CH_2B). ^{13}C NMR (151 MHz, MeOD) δ: 54.64, 51.42, 50.00, 48.46, 15.39 (CB).

(2-(4-(((4-methylphenyl)sulfonamido)methyl)-1H-1,2,3-triazol-1-yl)ethyl)boronic acid (24d)

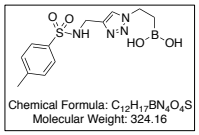

White solid (99%). ^{1}H NMR (400 MHz, MeOD): δ 8.23 (s, 1H, CH_{triaz}), 7.72 (t, J = 7.6 Hz, 2H, CH_{phen}), 7.36 (dd, J = 15.4, 8.0 Hz, 2H, CH_{phen}), 4.35 (s, 2H, CH_2NH), 4.50 (t, J = 8.2 Hz, 2H, CH_2N), 2.40 (s, 3H, CH_3), 1.50 (t, J = 7.8, 2H, CH_2B). ^{13}C NMR (100 MHz, MeOD): δ 143.9, 141.2, 136.5, 129.6 (2C), 127.5, 126.8 (2C), 40.1, 20.1, 15.39 (CB). ^{11}B NMR (128 MHz, MeOD): δ 27.21.

Synthesis of (3aS,4S,6S)-2-((R)-2-azido-1-chloroethyl)-3a,5,5-trimethylhexahydro-4,6-methanobenzo[d][1,3,2]dioxaborole (13)

CH_2Cl_2 (17 mmol, 2 eq.) was solubilized in dry THF (25 mL). The solution was cooled to -100 °C and *n*-BuLi (10.2 mmol, 1.2 eq.) was added dropwise over 30 min, under mechanical stirring. Compound ***2*** (8.5 mmol, 1 eq.) was solubilized in THF (10 mL) and dropped into the mixture. The temperature was leaved to reach -80 °C, then $ZnCl_2$ (17 mmol, 2 eq.) was added. The reaction mixture was left under stirring overnight, allowing the temperature to rise slowly. The volume of solvent was reduced *in vacuo* and the resulting mixture is diluted with petroleum ether (100 mL) and washed with 40 ml of saline solution obtained by mixing equal volumes of H_2O and saturated NH_4Cl solution. The aqueous phase was extracted three times with petroleum ether (30 mL) and the combined organic phases were washed with saturated NaCl, dried over Na_2SO_4, filtered and the solvent removed *in vacuo*. The residue was an slightly yellow oil (75%), which was not further purified.

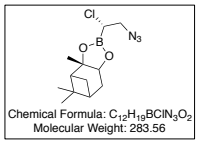

^{1}H NMR (400 MHz, $CDCl_3$) δ: 4.40 (dd, J = 2.0, 9.0 Hz, 1H CH_{pin}), 3.65 (m, 3H, CHB + CH_2), 2.32 (m, 2H, $CH_{2\text{-pin}}$), 2.10 (m, 1H, $CH_{2\text{-pin}}$), 1.92 (m, 2H, CH_{pin}), 1.44 (s, 3H, $CH_{3\text{-pin}}$), 1.30 (s, 3H, $CH_{3\text{-pin}}$), 1.17 (d, J = 11.4 Hz, 1H, $CH_{2\text{-pin}}$), 0.85 (s, 3H, $CH_{3\text{-pin}}$). ^{13}C NMR 87.1, 78.7, 54.4, 50.9,39.1, 38.0, 34.9, 28.2, 26.8, 26.1, 23.8.

Synthesis of benzylmagnesium chloride

Magnesium (9.7 mmol, 1.08 eq.) and Iodine (0.45 mmol, 0.95 eq.) solids were heated to 40 ° C for 5 min in order to sublimate the iodine. The mixture was cooled to 0 °C and dry diethyl ether (1 mL) was added. Benzyl chloride (9 mmol, 1 eq.) was solubilized in dry diethyl ether (10 mL). By keeping the mixture at 0 °C about 10% of the benzyl chloride solution was added; after a few minutes the discoloration of the reaction mixture and the development of heat were observed. The

remaining benzyl chloride solution was slowly added over 40 min. At the end of the addition, a solution of benzyl magnesium chloride was obtained which could be used directly in the next step.

Synthesis of (3aS,4S,6S)-2-((S)-1-azido-3-phenylpropan-2-yl)-3a,5,5-trimethylhexahydro-4,6-methanobenzo[d][1,3,2]dioxaborole (22)

Compound ***13*** (1.76 mmol, 1 eq.) was solubilized in anhydrous diethyl ether (7 mL). The mixture was cooled to - 80 °C and benzyl magnesium chloride solution was dropped over 10 minutes, under magnetic stirring. The reaction mixture was left under stirring overnight, allowing the temperature to rise slowly. The volume of solvent was reduced *in vacuo* and the resulting mixture diluted with petroleum ether (40 mL) and washed with 10 ml of saturated NH_4Cl solution. The aqueous phase was extracted petroleum ether (3 x 15 mL). The combined organic phases were washed with saturated NaCl, dried over anhydrous Na_2SO_4, filtered and the solvent was removed *in vacuo*. The residue was purified by column chromatography (petroleum ether / diethyl ether 95: 5) giving the expected product as a colourless liquid (50%).

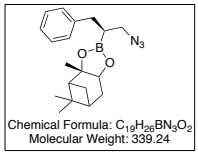

Chemical Formula: $C_{19}H_{26}BN_3O_2$
Molecular Weight: 339.24

^{1}H NMR (600 MHz, $CDCl_3$) δ: 7.30 – 7.16 (m, 5H, CH_{phen}), 4.27 (dd, J = 8.8, 2.0 Hz, 1H, CH_{pin}), 3.43 – 3.32 (m, 2H, CH_2N_3), 2.81 (ddd, J = 21.9, 13.8, 7.7 Hz, 2H, CH_2), 2.37 – 1.77 (m, 5H, pinanediol), 1.75 – 1.63 (m, 1H, CHB), 1.32 (s, 3H, $CH_{3\text{-pin}}$), 1.28 (s, 3H, $CH_{3\text{-pin}}$), 1.06 (dd, J = 10.9, 4.4 Hz, 1H, $CH_{2\text{-pin}}$), 0.83 (s, 3H, $CH_{3\text{-pin}}$). ^{13}C NMR (151 MHz, $CDCl_3$) δ 140.65, 128.92 (2C), 128.31 (2C), 126.04, 86.07, 78.51, 78.00, 52.41, 51.13 (CB), 39.44, 38.12, 35.33, 34.10, 28.53, 27.04, 26.27, 23.98. ^{11}B NMR: (128 MHz, $CDCl_3$) δ: 32.77.

General procedure for the synthesis of α-benzyl-β-triazolylboronates (23f-k)

Compound ***22*** (0.30 mmol, 1 eq.) and $CuSO_4$ 0.03 M (0.53 mL, 0.1 eq.) were added to a solution containing sodium ascorbate (0.06 mmol, 0.2 eq.) and the selected alkyne (0.31 mmol, 1.05 eq.) solubilized in *tert*-butanol (0.53 mL). The reaction mixture was heated at 65 °C for 2-3 hours. The reaction mixture was allowed to cool down to room temperature and ethyl acetate (15 mL) was added. The organic layer was washed with 6 ml of saline solution obtained by mixing equal volumes of H_2O and saturated NaCl solution. The aqueous phase was extracted with ethyl acetate (2 x 10 mL) and the combined organic phases were washed with saturated NaCl, dried over Na_2SO_4, filtered and concentrated affording the desired product.

3-(1-((2S)-3-phenyl-2-((3aS)-3a,5,5-trimethylhexahydro-4,6-methanobenzo[d][1,3,2]dioxaborol-2-yl)propyl)-1H-1,2,3-triazol-4-yl)benzoic acid (23f)

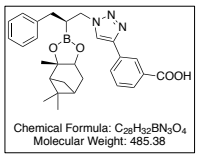

Chemical Formula: $C_{28}H_{32}BN_3O_4$
Molecular Weight: 485.38

^{1}H NMR (400 MHz, $CDCl_3$) δ 8.46 (s, 1H, CH_{triaz}), 8.17 (d, J = 1.4 Hz, 1H, CH_{phen}), 8.07 (d, J = 1.4 Hz, 1H, CH_{phen}), 7.86 (s, 1H, CH_{phen}), 7.55 (t, J = 7.8 Hz, 1H, CH_{phen}), 7.36 – 7.11 (m, 5H, CH_{benz}), 4.48 (qd, J = 13.6, 7.1 Hz, 2H, CH_2N), 4.27 (dd, J = 8.8, 2.0 Hz, 1H, CH_{pin}), 2.84 (ddd, J = 62.0, 14.0, 7.6 Hz, 2H, CH_2), 2.32 - 2.26 (m, 1H, $CH_{2\text{-pin}}$), 2.20 – 2.15 (m, 1H, $CH_{2\text{-pin}}$), 2.14 – 2.07 (m, 1H, CH_{pin}), 2.02 (t, J = 5.5 Hz, 1H, CHB), 1.88 – 1.84 (m, 1H, CH_{pin}), 1.77 (dt, J = 14.8, 2.6 Hz, 1H, $CH_{2\text{-pin}}$), 1.32 (s, 3H, $CH_{3\text{-pin}}$), 1.26 (s, 3H, $CH_{3\text{-pin}}$), 0.86 (m, 1H, $CH_{2\text{-pin}}$), 0.81 (s, 3H, $CH_{3\text{-pin}}$). ^{13}C NMR (101 MHz, $CDCl_3$) δ 170.85, 146.45, 140.16, 131.49, 130.90, 130.05, 129.73, 129.27, 129.13, 128.62 (2C), 127.44, 126.50, 120.93, 86.59, 78.30, 51.26 (CB), 51.14, 39.54, 38.29, 35.36, 34.41, 28.61, 27.82, 27.15, 26.37, 24.11. ^{11}B NMR (128 MHz, $CDCl_3$) δ 34.92. $[\alpha]^{20}_D$ = + 18.37 (MeOH).

1-((2S)-3-phenyl-2-((3aS)-3a,5,5-trimethylhexahydro-4,6-methanobenzo[d][1,3,2]dioxaborol-2-yl)propyl)-4-(thiophen-3-yl)-1H-1,2,3-triazole (23g)

^{1}H NMR (400 MHz, $CDCl_3$) δ 7.65 (dd, J = 3.2, 1.2 Hz, 1H, CH_{tioph}), 7.64 (s, 1H, CH_{triaz}), 7.42– 7.35 (m, 3H, CH_{tioph}), 7.30 - 7.17 (m, 4H, CH_{benz}), 4.43 (qd, J = 13.6, 7.2 Hz, 2H, CH_2N), 4.25 (dd, J = 8.8, 2.0 Hz, 1H, CH_{pin}), 2.81 (ddd, J = 22.1, 14.0,

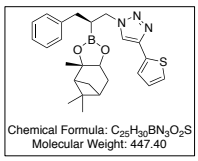

7.6 Hz, 2H, CH_2), 2.32 – 2.26 (m, 1H, $CH_{2\text{-pin}}$), 2.17 – 2.12 (m, 1H, $CH_{2\text{-pin}}$), 2.10 – 2.08 (m, 1H, CH_{pin}), 1.99 (t, *J* = 5.6 Hz, 1H, CHB), 1.86 - 1.83 (m, 1H, CH_{pin}), 1.78 – 1.71 (m, 1H, $CH_{2\text{-pin}}$), 1.31 (s, 3H, $CH_{3\text{-pin}}$), 1.25 (s, 3H, $CH_{3\text{-pin}}$), 0.88 (m, 1H, $CH_{2\text{-pin}}$), 0.81 (s, 3H, $CH_{3\text{-pin}}$). ^{13}C NMR (101 MHz, $CDCl_3$) δ 144.04, 140.54, 132.57, 129.46 (2C), 129.05, 128.91 (2C), 126.78, 126.65, 126.29, 121.26, 120.48, 86.81, 78.58, 51.58 (CB), 51.29, 39.86, 38.60, 35.67, 34.68, 28.92, 27.48, 26.68, 24.42. ^{11}B NMR (128 MHz, $CDCl_3$) δ 33.98. $[\alpha]^{20}_D$ = + 17.18 (MeOH).

(1-((2S)-3-phenyl-2-((3aS)-3a,5,5-trimethylhexahydro-4,6-methanobenzo[d][1,3,2]dioxaborol-2-yl)propyl)-1H-1,2,3-triazol-4-yl)methanol (23h)

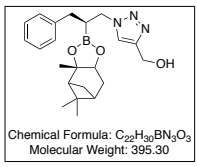

^{1}H NMR (400 MHz, $CDCl_3$) δ 7.53 (s, 1H, CH_{triaz}), 7.29- 7.15 (m, 5H, CH_{benz}), 4.77 (s, 1H, CH_2OH), 4.46 – 4.32 (m, 2H, CH_2N), 4.23 (d, *J* = 1.9 Hz, 1H, CH_{pin}), 2.71 (ddd, J = 22.1, 14.0, 7.5 Hz, 2H, CH_2), 2.28 – 2.16 (m, 1H, $CH_{2\text{-pin}}$), 2.04 (m, 2H, $CH_{2\text{-pin}}$ + CH_{pin}), 1.92 (t, *J* = 5.6 Hz, 1H, CHB), 1.81 – 1.74 (m, 1H, CH_{pin}), 1.72 – 1.64 (m, 1H, $CH_{2\text{-pin}}$), 1.55 (s, 1H, OH), 1.29 (s, 3H, $CH_{3\text{-pin}}$), 1.26 (s, 3H, $CH_{3\text{-pin}}$), 0.87 (d, J = 11.0 Hz, 1H, $CH_{2\text{-pin}}$), 0.81 (s, 3H, $CH_{3\text{-pin}}$). ^{13}C NMR (101 MHz, CDCl3) δ 140.18, 129.06 (3C), 128.58 (2C), 126.42, 86.47, 78.24, 56.71, 51.26 (CB), 51.11, 39.54, 38.29, 35.34, 34.36, 29.58, 28.56, 27.16, 26.38, 24.11. ^{11}B NMR (128 MHz, $CDCl_3$) δ 33.80. $[\alpha]^{20}_D$ = + 12.60 (MeOH).

4-methyl-N-((1-((2S)-3-phenyl-2-((3aS)-3a,5,5-trimethylhexahydro-4,6-methanobenzo[d][1,3,2]dioxaborol-2-yl)propyl)-1H-1,2,3-triazol-4-yl)methyl)benzenesulfonamide (23i)

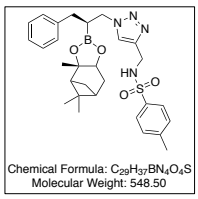

^{1}H NMR (400 MHz, $CDCl_3$) δ 7.74 (d, *J* = 8.3 Hz, 2H, CH_{phen}), 7.38 (s, 1H, CH_{triaz}), 7.32 – 7.22 (m, 4H, CH_{phen} + CH_{benz}), 7.23 – 7.13 (m, 3H, CH_{benz}), 4.32 – 4.28 (m, 2H, CH_2N), 4.25 – 4.20 (m, 1H, CH_{pin}), 4.22 - 4.20 (m, 2H, CH_2NH), 2.84 - 2.61 (m, 2H, CH_2), 2.40 (s, 3H, CH_3), 2.43 – 2.28 (m, 1H, $CH_{2\text{-pin}}$), 2.25 - 2.10 (m, 2H, $CH_{2\text{-pin}}$), 2.08 – 2.03 (m, 1H, CH_{pin}), 2.00 – 1.97 (m, 1H, CHB) 1.90 – 1.86 (m, 1H, CH_{pin}), 1.79 – 1.68 (m, 1H, CH_{pin}), 1.28 (s, 3H, $CH_{3\text{-pin}}$), 1.26 (s, 3H, $CH_{3\text{-pin}}$), 0.85 (d, *J* = 10.9 Hz, 1H, $CH_{2\text{-pin}}$), 0.81 (s, 3H, $CH_{3\text{-pin}}$). ^{13}C NMR (101 MHz, $CDCl_3$) δ 143.76, 143.19, 140.08, 136.77, 129.88 (2C), 129.04 (2C), 128.58 (2C), 127.33 (2C), 126.44, 122.83, 86.49, 78.25, 51.24 (CB), 51.04, 39.52, 38.93, 38.28, 35.33, 34.29, 29.84, 28.57, 27.15, 26.38, 24.10, 21.65. ^{11}B NMR (128 MHz, $CDCl_3$) δ 34.08. $[\alpha]^{20}_D$ = + 12.20 (MeOH).

tert-butyl-1-((2S)-3-phenyl-2-((3aS)-3a,5,5-trimethylhexahydro-4,6-methanobenzo[d][1,3,2]dioxaborol-2-yl)propyl)-1H-1,2,3-triazole-4-carboxylate (23k)

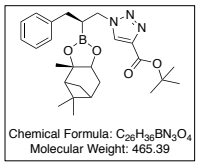

^{1}H NMR (400 MHz, $CDCl_3$) δ 8.02 (s, 1H, CH_{triaz}), 7.37 – 7.29 (m, 3H, CH_{benz}), 7.24 (m, 2H, CH_{benz}), 4.47 (dd, *J* = 7.2, 4.4 Hz, 2H, CH_2N), 4.29 (dd, J = 8.8, 2.0 Hz, 1H, CH_{pin}), 2.99 – 2.66 (m, 2H, CH_2), 2.43 – 2.28 (m, 1H, $CH_{2\text{-pin}}$), 2.25 – 2.10 (m, 2H, $CH_{2\text{-pin}}$), 2.05 (t, *J* = 5.6 Hz, 1H, CHB), 1.91 (dt, J = 5.7, 2.8 Hz, 1H, CH_{pin}), 1.79 (ddd, J = 14.8, 3.5, 2.1 Hz, 1H, $CH_{2\text{-pin}}$), 1.65 (s, 9H, $(CH_3)_3$) 1.36 (s, 3H, $CH_{3\text{-pin}}$), 1.31 (s, 3H, $CH_{3\text{-pin}}$), 0.88 (d, J = 10.9 Hz, 1H, $CH_{2\text{-pin}}$), 0.86 (s, 3H, $CH_{3\text{-pin}}$). ^{13}C NMR (101 MHz, $CDCl_3$) δ 160.20, 141.20, 139.91, 129.06 (2C), 128.61 (2C), 127.92, 126.51, 86.59, 82.13, 78.29, 51.22 (CB), 51.13, 39.53, 38.26 (2C), 35.26, 34.25, 28.54, 28.39 (3C), 27.14, 26.40, 24.08. ^{11}B NMR (128 MHz, $CDCl_3$) δ 33.51. $[\alpha]^{20}_D$ = +17.82 (MeOH).

The chiral β-triazolylboronic acids had not yet been deprotected at the time of writing this doctoral thesis.

Synthesis of co-drug 1

Compound ***25*** was synthesised as previously described.[8]

Synthesis of 3-((tert-butyldimethylsilyl)oxy)propyl propiolate (26)

In anhydrous conditions at 0 °C, dimethyl-aminopyridine (DMAP, 0.195 mmol, 0.1 eq.), propiolic acid (2.14 mmol, 1.1 eq.) and dicyclohexylcarbodiimide (DCC, 2.33 mmol, 1.2 eq.) were added to a solution of propanediol-TBDMS (1.95 mmol, 1 eq.) in dry CH_2Cl_2 (11 mL). The formation of a brown suspension was observed. The reaction was left under vigorous stirring overnight at room temperature. Diethyl ether (20ml) was added to favour the precipitation of dicyclohexylurea (DCU) and its removal by filtration on celite. The filtrate was evaporated. The crude was purified by column chromatography (petroleum ether / diethyl ether 9: 1) to obtain the desired product as a colourless liquid (74.5%).

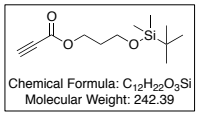

^{1}H NMR (400 MHz, $CDCl_3$) δ 4.30 (t, *J* = 6.4 Hz, 2H, OCH_2), 3.71 (t, *J* = 5.9 Hz, 2H, CH_2O), 2.86 (s, 1H, CH), 1.88 (d, *J* = 6.2 Hz, 2H, CH_2), 0.89 (s, 9H, $(CH_3)_3$), 0.05 (s, 6H, $(CH_3)_2Si$). ^{13}C NMR (101 MHz, $CDCl_3$) δ 152.59, 74.61, 74.23, 63.22, 58.89, 31.22, 25.71, 18.11, -5.62. MS: LC-MSQO m/z $[M+H]^+$ theo. 243.39, found 191.1462 (without the alkyne).

Synthesis of 3-((tert-butyldimethylsilyl)oxy)propyl1-(2-(2-(thiophen-2-yl)acetamido)-2-((3aS)-3a,5,5-trimethylhexahydro-4,6-methanobenzo[d][1,2,3]dioxaborol-2-yl)ethyl)-1H-1,2,3-triazole-4-carboxylate (27)

In anhydrous conditions, sodium ascorbate (0.28 mmol, 0.2 eq.) and 0.03 M $CuSO_4$ solution (4.6 mL, 0.1 eq.) were added to a suspension of alkyne ***26*** (1.40 mmol, 1 eq.) and azide ***25*** (1.40 mmol, 1 eq.) in *tert*-butanol (4.6 mL). The reaction was heated to 60 °C and stirred for 4h. The suspension obtained was extracted with ethyl acetate (10 ml) and water (10 ml). The aqueous phase was re-extracted with EtOAC (3 x 10 ml). Finally the organic phases were washed with saturated NaCl solution, dried over Na_2SO_4, filtered and evaporated *in vacuo*, giving the final compound as a white solid (92%).

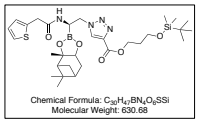

^{1}H NMR (400 MHz, $CDCl_3$) δ 8.00 (s, 1H, CH_{triaz}), 7.44 (s, 1H, NH), 7.24 (dd, *J* = 5.2, 1.3 Hz, 1H, CH_{tioph}), 7.00 – 6.91 (m, 2H, CH_{tioph}), 4.58 – 4.46 (m, 2H, CH_2N), 4.43 (t, *J* = 6.5 Hz, 2H, OCH_2), 4.27 (dd, *J* = 8.7, 2.3 Hz, 1H, CH_{pin}), 3.91 (s, 2H, CH_2CO), 3.74 (t, *J* = 6.0 Hz, 2H, CH_2O), 3.27 (d, *J* = 9.5 Hz, 1H, CHB), 2.40 – 2.32 (m, 1H, $CH_{2\text{-}pin}$), 2.18 (dtd, *J* = 10.4, 6.0, 2.0 Hz, 1H, $CH_{2\text{-}pin}$), 2.02 (t, *J* = 5.5 Hz, 1H, CH_{pin}), 1.99 – 1.92 (m, 2H, CH_2), 1.91 (dt, *J* = 5.4, 2.7 Hz, 1H, CH_{pin}), 1.82 (dt, *J* = 14.1, 2.8 Hz, 1H, $CH_{2\text{-}pin}$), 1.41 (s, 3H, $CH_{3\text{-}pin}$), 1.29 (s, 3H, $CH_{3\text{-}pin}$), 0.88 (s, 12H, $CH_{3\text{-}pin}$ + $(CH_3)_3$), 0.04 (s, 6H, $(CH_3)_2Si$). ^{13}C NMR (101 MHz, $CDCl_3$) δ 174.95, 160.37, 139.54, 132.68, 127.95, 127.43, 126.09, 84.39, 62.29, 59.18, 52.37, 51.91, 39.79, 38.04, 36.28, 33.51, 31.67, 28.85, 27.12, 26.51, 25.72, 24.01, 18.10, -5.55.

Deprotection of the hydroxyl group

In anhydrous conditions, a solution of tetrabutylammoniofloride (TBAF, 2.88 mmol, 3 eq.) 1M in THF (2.88 mL) was added to the orange-brown solution of compound ***27*** (0.96 mmol, 1 eq.) in dry THF (27 mL). After 2.5h, ethyl acetate (20ml) was added. The organic phase was washed with a mixture of NH_4Cl / H2O 1: 1 (4 x 20 ml) and dried over Na_2SO_4, filtered and evaporated. The crude was purified by fragmentation with ethyl ether (1ml x 5) affording the desired product ***28*** as a beige solid (88%).

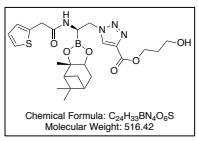

^{1}H NMR (400 MHz, MeOD) δ 8.60 (s, 1H, CH_{triaz}), 7.32 (dd, *J* = 5.0, 1.4 Hz, 1H, CH_{tioph}), 6.97 (tt, *J* = 5.1, 2.4 Hz, 2H, CH_{tioph}), 4.59 (dd, *J* = 14.5, 4.2 Hz, 1H, CH_2N), 4.48 – 4.40 (m, 3H, CH_2N + CH_2OH), 4.20 (dd, *J* = 8.7, 2.3 Hz, 1H, CH_{pin}), 3.95 (s, 1H, CH_2CO), 3.71 (t, *J* = 6.2 Hz, 2H, OCH_2), 3.19 (dd, *J* = 10.2, 4.2 Hz, 1H, CHB), 2.37 – 2.33 (m, 1H, $CH_{2\text{-}pin}$), 2.15 – 2.11 (m, 1H, $CH_{2\text{-}pin}$), 2.02 – 1.91 (m, 2H, CH_2), 1.86 (dt, *J* = 5.6, 2.7 Hz, 1H, CH_{pin}), 1.79 (dt, *J* = 14.0, 2.8 Hz, 1H, $CH_{2\text{-}pin}$), 1.36 (s, 3H, $CH_{3\text{-}pin}$), 1.29 (s, 3H, $CH_{3\text{-}pin}$), 0.88 (s, 3H, $CH_{3\text{-}pin}$). ^{13}C NMR (101 MHz, MeOD) δ 178.66, 162.07, 140.61, 134.53, 130.22, 128.64, 128.06, 126.75, 84.57, 77.53, 63.25, 59.34, 53.80, 53.65, 45.49(CB), 41.42, 39.18, 37.72, 32.71, 32.19, 29.71, 27.79, 27.60, 24.57.

^{11}B NMR (128 MHz, MeOD) δ 15.65. MS: LC-MSQO m/z [M-H]$^-$ theo. 515.2130, found 515.2149. $[\alpha]_D^{20}$ = - 70.7 (MeOH).

Synthesis of ((S)-3-(acetylthio)-2-methylpropanoyl)-L-proline

In anhydrous conditions at -5 ° to 0 °C, acetyl chloride (5.52 mmol, 1.2 eq.) was added dropwise (30 min) to the solution of L-captopril (4.6 mmol, 1 eq.) in DCM dry (8.6 mL). The pH was adjusted to 8-9 with triethylamine (TEA, 0.6 mL). After 4h there was a suspension that was filtered on celite and the filtrate was washed with 0.1M HCl, dried over Na_2SO_4, filtered and evaporated, obtaining a white solid. The crude was initially purified by fragmentation with tert-butyl-methyl ether (MTBE) and then by column chromatography (DCM / MeOH 95: 5) obtaining a white solid (58%).

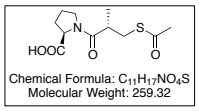

^{1}H NMR (400 MHz, $CDCl_3$) δ 4.56 (dd, *J* = 8.8, 3.9 Hz, 1H, $CH_{proline}$), 3.65 - 3.59 (m, 2H, CH_2N), 3.10 – 2.99 (m, 2H, CH_2S), 2.80 (q, *J* = 7.0 Hz, 1H, CH), 2.32 (s, 3H, CH_3CO), 2.28 – 2.14 (m, 2H, $CH_{2\text{-proline}}$), 2.13 – 2.01 (m, 2H, $CH_{2\text{-proline}}$), 1.23 (d, *J* = 6.9 Hz, 3H, CH_3). ^{13}C NMR (101 MHz, $CDCl_3$) δ 195.94, 173.45, 166.97, 58.88, 46.74, 38.26, 32.01, 30.46, 28.04, 24.57, 16.63. MS: LC-MSQO m/z [M-H]$^-$ theo. 258.0794, found 258.0807. $[\alpha]_D^{20}$ = - 200 (MeOH).

3-((((S)-3-(acetylthio)-2-methylpropanoyl)-L-prolyl)oxy)propyl-1-((2R)-2-(2-(thiophen-2-yl)acetamido)-2-((3aS)-3a,5,5-trimethylhexahydro-4,6-methanobenzo[d][1,2,3]dioxaborol-2-yl)ethyl)-1H-1,2,3-triazole-4-carboxylate (29)

In anhydrous conditions, L-captopril acetylated (0.31 mmol, 1 eq.), ***27*** (0.37 mmol, 1.2 eq.), 1-ethyl-3-(3-dimethyl-aminopropyl)-carbodiimide (EDC, 0.46 mmol, 1.3 eq.) and DMAP (0.42 mmol, 1.3 eq.) were dissolved in dry DCM (3 mL). The reaction was stirred at room temperature for 1.5h. DCM (5 ml) and 1% HCl (5 ml) were added. The two phases were separated and the organic phase was washed with saturated NaCl solution, dried over Na_2SO_4, filtered and evaporated. Compound ***29*** was purified by fragmentation with MTBE obtaining a beige solid (70%).

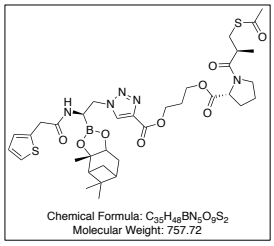

^{1}H NMR (400 MHz, $CDCl_3$) δ 8.05 (s, 1H, CH_{triaz}), 7.46 (s, 1H, NH), 7.25 – 6.93 (m, 3H, tiophene), 4.57 – 4.40 (m, 5H, CH_2N, OCH_2, $CH_{proline}$), 4.30 – 4.24 (m, 3H, CH_{pin} + CH_2O), 3.92 (s, 2H, CH_2CO), 3.61 (t, *J* = 6.6 Hz, 2H, $CH_2N_{proline}$), 3.25 (d, *J* = 4.6 Hz, 1H, CHB), 3.12 – 2.91 (m, 2H, CH_2S), 2.84 – 2.75 (m, 1H, CH), 2.32 (s, 3H, CH_3CO), 2.22 – 1.79 (m, 12H, pinanediol + CH_2 + $CH_{2\text{-proline}}$), 1.41 (d, *J* = 1.3 Hz, 3H, $CH_{3\text{-pin}}$), 1.29 (s, 3H, $CH_{3\text{-pin}}$), 1.22 (d, *J* = 6.9 Hz, 3H, CH_3), 0.87 (s, 3H, $CH_{3\text{-pin}}$). ^{13}C NMR (151 MHz, $CDCl_3$) δ 196.20, 175.35, 173.48, 172.10, 160.36, 139.47, 132.80, 128.12, 127.56-126.25 (tiophene), 84.44, 61.70, 61.52, 58.75, 52.66, 52.08, 46.97, 42.54 (CB), 39.96, 38.43, 36.50, 33.49, 32.24, 30.64, 29.14, 29.05, 28.01, 27.30, 26.71, 24.88, 24.19, 16.79. ^{11}B NMR (128 MHz, $CDCl_3$) δ 22.23. MS: LC-MSQO m/z [M-H]$^-$ theo. 756.2902, found 756.2932. $[\alpha]_D^{20}$ = - 80 (MeOH).

Deprotection of boronic acid to obtain co-drug 1

In anhydrous conditions, at room temperature, methyl-boronic acid (0.96 mmol, 10 eq.) and 0.2 M HCl (0.48 mL, 1 eq.) were added to a solution of ***29*** (0.096 mmol, 1 eq.) in acetone (1 mL). After 53h the solution was evaporated *in vacuo*. The compound obtained was subjected to lyophilisation, cooling the flask in liquid nitrogen and subjecting it to high vacuum. The crude obtained was purified by crystallization with DCM / *n*-hexane giving **co-drug 1**, as a beige solid (70%).

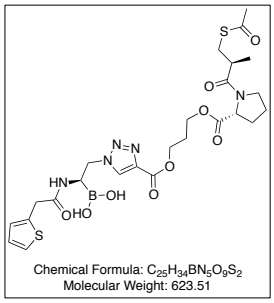

^{1}H NMR (400 MHz, MeOD) δ 8.59 (d, *J* = 1.9 Hz, 1H, CH_{triaz}), 7.34 (dd, *J* = 5.1, 1.3 Hz, 1H, CH_{tioph}), 7.04 – 6.89 (m, 2H, CH_{tioph}), 4.61 – 4.36 (m, 5H, CH_2N, OCH_2, $CH_{proline}$), 4.27 (td, *J* = 6.2, 3.0 Hz, 2H, CH_2O), 3.99 (s, 2H, CH_2CO), 3.69 – 3.59 (m, 2H, $CH_2N_{proline}$), 3.22 – 3.16 (m, 1H, CHB), 3.07 – 2.81 (m, 3H, CH + CH_2S), 2.30 (s, 3H, CH_3CO), 2.25 – 1.92 (m, 6H,

CH_2 + $CH_{2\text{-proline}}$), 1.18 (d, *J* = 6.7 Hz, 3H, CH_3). ^{13}C NMR (151 MHz, MeOD) δ 195.81, 177.73, 174.28, 172.22, 160.56, 139.27, 128.99, 127.47, 126.79, 125.51, 107.68, 61.44, 61.34, 59.05, 52.48, 46.28, 45.59 (CB), 38.12, 31.58, 30.74, 29.13, 28.81, 27.73, 24.43, 15.60. ^{11}B NMR (193 MHz, MeOD) δ 11.70. MS: LC-MSQO m/z $[M-H]^-$ theo. 624.1963, found 624.1970. $[\alpha]_D^{20}$ = - 99 (MeOH).

Synthesis of chloromethyl ((R)-3-(acetylthio)-2-methylpropanoyl)-D-prolinate (30)

L-Captropril acetylate (0.38 mmol, 1 eq.), sodium bicarbonate (1.46 mmol, 3.8 eq.), *tetra*-butyl-ammonium bisulphate (0.038 mmol, 0.1 eq.) were solubilized at 0 °C in a 1:1 DCM /H_2O biphasic solvent (0.8 mL). After 10 min at 0 °C, chloro-methyl-chlorosulfate (0.58 mmol, 1.5 eq.), solubilized in DCM, was added dropwise. The reaction was stirred overnight. The two phases were separated: the aqueous phase was re-extracted with DCM (3 x 1 mL). The organic phase was dried over Na_2SO_4, filtered and evaporated. The crude was purified by column chromatography (DCM / MeOH 95: 5) affording compound ***30*** as an colourless oil (58%).

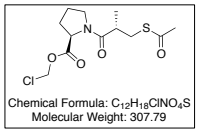
Chemical Formula: $C_{12}H_{18}ClNO_4S$
Molecular Weight: 307.79

^{1}H NMR (400 MHz, $CDCl_3$) δ 5.86 (d, *J* = 6.0 Hz, 1H, CH_2Cl), 5.58 (d, *J* = 6.0 Hz, 1H, CH_2Cl), 4.54 (dd, *J* = 8.9, 4.1 Hz, 1H, $CH_{proline}$), 3.64 (dd, *J* = 7.1, 6.1 Hz, 2H, CH_2N), 3.14 – 2.92 (m, 2H, CH_2S), 2.81 (dt, *J* = 7.9, 6.6 Hz, 1H, CH), 2.32 (s, 3H, CH_3CO), 2.28 – 1.99 (m, 4H, $CH_{2\text{-proline}}$), 1.24 (d, *J* = 6.9 Hz, 3H, CH_3). ^{13}C NMR (101 MHz, $CDCl_3$) δ 196.30, 173.75, 170.36, 69.26, 58.63, 47.08, 38.59, 32.36, 30.77, 28.76, 25.03, 16.90. MS: LC-MSQO m/z $[M-H]^-$ theo. 308.0717, found 308.0716. $[\alpha]_D^{20}$ = - 179.4 (MeOH).

Synthesis of iodomethyl ((R)-3-(acetylthio)-2-methylpropanoyl)-D-prolinate (31)

In anhydrous conditions, NaI (0.81 mmol, 1.5 eq.) was added to the solution of the chlorine derivative ***30*** (0.54 mmol, 1 eq.) in acetone (0.8 mL), obtaining a yellow solution, which after 1 hour became a yellow suspension due to the formation of NaCl. The reaction was left under vigorous stirring for 24h and then the solvent was evaporated. DCM (1ml) was added to favour the precipitation of NaCl, which was removed by filtration on celite. The filtrate was then washed with 10% sodium-thio-sulphate solution (2 x 1 ml), water (2 x 1 ml) and saturated NaCl solution (2 x 1 ml). The organic phase was dried over Na_2SO_4, filtered and evaporated *in vacuo*, giving the final compound ***31***, as a yellowish oil (59%). The product obtained was used directly for the subsequent reaction.

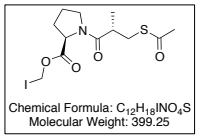
Chemical Formula: $C_{12}H_{18}INO_4S$
Molecular Weight: 399.25

^{1}H NMR (400 MHz, $CDCl_3$) δ 6.03 (d, *J* = 4.8 Hz, 1H, CH_2I), 5.82 (d, *J* = 4.8 Hz, 1H, CH_2I), 4.50 (dd, *J* = 8.6, 4.2 Hz, 1H, $CH_{proline}$), 3.63 (dd, *J* = 7.4, 6.1 Hz, 2H, $CH_2N_{proline}$), 3.14 – 2.92 (m, 2H, CH_2S), 2.84 – 2.76 (m, 1H, CH), 2.32 (s, 3H, CH_3CO), 2.25 – 1.95 (m, 4H, $CH_{2\text{-proline}}$), 1.24 (d, *J* = 6.9 Hz, 3H, CH_3).

Synthesis of (propioloyloxy)methyl ((R)-3-(acethylthio)-2-methylpropanoyl)-D-prolinate (32)

Propiolic acid (0.40 mmol, 1 eq.) was added to a suspension of K_2CO_3 (0.44 mmol, 1.1 eq.) in DMF (0.85 mL). The reaction was left under vigorous stirring for 2h. The iodine derivative ***31*** (0.40 mmol, 1 eq.) was solubilized in DMF and added to the mixture. The reaction was left under vigorous stirring at room temperature for 24h. Diethyl ether (20 mL) and H_2O (5 mL) were added. The two phases were separated and the aqueous phase was re-extracted with diethyl ether (2 x 10 mL). The combined organic phases were washed with saturated NaCl, dried over Na_2SO_4, filtered and evaporated. Alkyne ***32*** was purified by column chromatography (DCM / MeOH 95: 5) and obtained as yellow oil (73.5%).

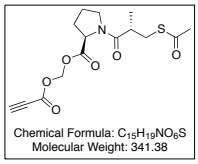
Chemical Formula: $C_{15}H_{19}NO_6S$
Molecular Weight: 341.38

^{1}H NMR (400 MHz, $CDCl_3$) δ 5.92 (d, *J* = 5.8 Hz, 1H, OCH_2O), 5.73 (d, *J* = 5.7 Hz, 1H, OCH_2O), 4.53 (dd, *J* = 8.7, 4.2 Hz, 1H, $CH_{proline}$), 3.66 – 3.58 (m, 2H, $CH_2N_{proline}$), 3.09 (dd, *J* = 13.5, 7.9 Hz, 1H, CH_2S), 2.99 (d, *J* = 1.3 Hz, 1H, CCH), 2.95 (dd, *J* = 13.6, 6.8, 1H, CH_2S), 2.83 – 2.76 (m, 1H, CH), 2.31 (s, 3H, CH_3CO), 2.29– 1.96 (m, 4H, $CH_{2\text{-proline}}$), 1.22 (d, *J* = 6.9 Hz, 3H, CH_3). ^{13}C NMR

(101 MHz, $CDCl_3$) δ 196.17, 173.53, 170.33, 151.10, 80.09, 73.69, 58.49, 46.88, 38.42, 32.20, 30.61, 28.86, 24.89, 16.70. MS: LC-MSQO m/z $[M-H]^-$ theo. 342.1005, found 342.1003. $[\alpha]_D^{20}$ = - 99 (MeOH).

Synthesis of ((((S)-3-(acetylthio)-2-methylpropanoyl)-L-prolyl)oxy)methyl 1-((2R)-2-(2-(thiophen-2-yl)acetamido)-2-((3aS)-3a,5,5-trimethylhexahydro-4,6-methanobenzo[d][1,2,3]dioxaborol-2-yl)ethyl)-1H-1,2,3-triazole-4-carboxylate (33)

In anhydrous conditions, alkyne ***32*** (0.25 mmol, 1 eq.), Na ascorbate (0.050 mmol, 0.2 eq.) and 0.03 M $CuSO_4$ solution (0.84 mL, 0.1 eq.) were added to the suspension of azide ***25*** (0.25 mmol, 1 eq.) in *tert*-butanol (0.84 mL). The reaction was heated to 60 °C for 7h. The suspension obtained was extracted with ethyl acetate (10 ml) and water (10 ml). The aqueous phase was re-extracted with EtOAC (3 x 10 ml). Finally, the organic phase was washed with saturated NaCl, dried over Na_2SO_4, filtered and evaporated. A purification test was carried out on a preparative 20 mm TLC (DCM / Et_2O / MeOH 1: 1: 0.1): 10 mg of crude were used, from which 8 mg of product was purified and 2 mg of azide ***25***. Since it was not possible to use the same method to purify all the crude, the remainder was subjected to column chromatography purification (DCM / Et2O / MeOH 1: 1: 0.1): the analysis of the product obtained showed the presence of free azide ***25*** and a smaller amount of the desired product ***33***, a beige solid which was isolated with a yield of 6%. Column chromatography may have damaged the product due to the instability of the boronic group and the linker exposed to acid silica.

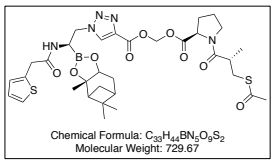

^{1}H NMR (400 MHz, $CDCl_3$) δ 8.10 (d, *J* = 5.9 Hz, 1H, CH_{triaz}), 7.28 (d, *J* = 1.2 Hz, 1H, CH_{tioph}), 7.17 (s, 1H, NH), 7.04 – 6.90 (m, 2H, CH_{tioph}), 6.07 -5.93 (dd, *J* = 5.6 Hz, 2H, OCH_2O), 4.67 – 4.40 (m, 3H, CH_2N + $CH_{proline}$), 4.28 (dd, *J* = 8.7, 2.3 Hz, 1H, CH_{pin}), 3.91 (s, 2H, CH_2CO), 3.62 (t, *J* = 6.7 Hz, 2H, $CH_2N_{proline}$), 3.27 (d, *J* = 9.2 Hz, 1H, CHB), 3.12 – 2.87 (m, 2H, CH_2S), 2.77 (dt, *J* = 14.5, 7.8 Hz, 1H, CH), 2.31 (s, 3H, CH_3CO), 2.29 – 1.74 (m, 10H, pinanediol + $CH_{2\text{-proline}}$), 1.41 (s, 3H, $CH_{3\text{-pin}}$), 1.29 (s, 3H, $CH_{3\text{-pin}}$), 1.19 (d, *J* = 6.9 Hz, 3H, CH_3), 0.85 (s, 3H, $CH_{3\text{-pin}}$). ^{13}C NMR (151 MHz, $CDCl_3$) δ 196.14, 175.17, 173.54, 170.70, 158.88, 138.45, 132.73, 129.19, 128.25-127.70-126.43(thiophene), 84.65, 79.74, 58.66, 52.60, 52.04, 46.94, 42.10(CB), 39.93, 38.21, 36.44, 33.75, 32.20, 30.64, 29.37, 29.01, 27.29, 26.70, 24.93, 24.20, 16.68. ^{11}B NMR (193 MHz, $CDCl_3$) δ 22.79. MS: LC-MSQO m/z $[M-H]^-$ theo. 728.2589, found 728.2617.

A new target: α-triazolylboronic acids as protein kinase (PK) inhibitors in Acute Myeloid Leukaemia (AML)

Recently, I worked in collaboration with the research group of prof. Zambon at the Department of Chemical and Geological Sciences, to find a new target for our boronic acids. Prof. Zambon works in the field of medicinal chemistry and on the synthesis of kinase inhibitors against acute myeloid leukaemia (AML).

Brief introduction about protein kinases (PKs) and AML

The family of protein kinases, which in humans have more than 500 types of different proteins, plays a crucial role in the regulation of multiple signal pathways involved in cell proliferation, differentiation and apoptosis. The role of kinases is to phosphorylate serine, threonine or tyrosine residues of specific protein substrates by transferring a terminal γ-phosphate group of the adenosine triphosphate (ATP) molecule. Kinases can be divided into different subgroups based on the residue they are capable of phosphorylating; the main ones are serine / threonine kinases and tyrosine kinases.[9,10]

The receptor protein kinases (RTKs) are tyrosine kinases incorporated into the cell membrane: they have an extracellular receptor part that is able to bind specific signal molecules and activates the intracellular catalytic site of the kinase, promoting substrate phosphorylation. Whereas deregulation of the signal cascade is closely linked to tumour genesis, RTK aberrations are associated with the onset of various types of cancer.[10]

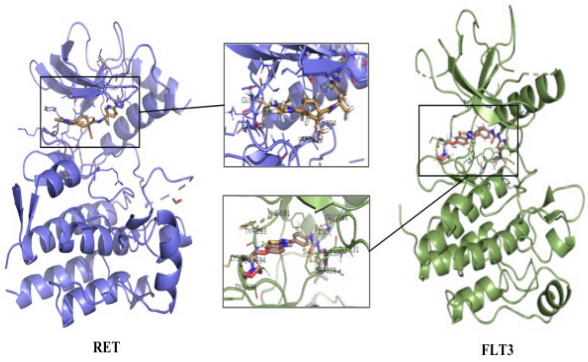

Figure 67. RET and FLT3 in complex with a dual inhibitor.

RET (REarranged during Transfection; Figure 67, left) is an RTK, involved in multiple signal pathways, which promote cell growth, proliferation, survival and / or differentiation. An overexpression of RET was observed in about 70% of patients with AML, ensuring high proliferation of leukemic cells.

FLT3 (Figure 67, right) is an RTK involved in the proliferation, differentiation and survival of dendritic cells and hematopoietic stem cells. Mutations of this kinase, resulting in enhanced cell proliferation, were found in 20-40% of cases of AML with negative prognosis.[11,12] FLT3 is therefore a therapeutic target for the development of anticancer drugs for various forms of cancer, including AML. However, it has been observed that the inhibition of FLT3 alone has a rather low clinical efficacy.[13]

RET and FLT3 are simultaneously activated in cases of AML presenting mutated FLT3.[14,15] There is, thus, a strong clinical rationale for the simultaneous inhibition of RET and FLT3 in the treatment of AML.

Recently, RET has been validated as a therapeutic target and various inhibitors of RET are in clinical evaluation or approved for the treatment of specific cancers. Nonetheless, the currently available RET inhibitors show low selectivity (i.e. they inhibit numerous kinases) and therefore a limited therapeutic window.[16] Similarly, the FLT3 inhibitors now used (e.g. midostaurin), exhibited a low selectivity profile.[17] Moreover, both FLT3 and RET can develop drug resistance following mutations that prevent binding to the inhibitor. The development of inhibitors with high selectivity and capable of simultaneously inhibiting RET and FLT3 is of considerable interest in the treatment of AML. This kind of "dual" inhibitor would avoid the simultaneous administration of several

drugs, and by acting on several parallel signal pathways at the same time, it should be able to avoid the signal bypass mechanisms that contribute to the drug resistance of cancer cells.

Boronic acids as inhibitors of FLT3 and RET PKs

As described previously, boronic compounds are attractive scaffolds for the development of new agents due to their favourable physic-chemical properties such as low lipophilicity, water solubility and stability. As kinase-targeting agents, boronic compounds are only scantly reported, thus presenting a relatively unhindered IP landscape. A library comprising several classes of in house boronic compounds (Figure 68) was docked on the available co-crystal structures of FLT3 and RET; a selection of the best-ranking compounds was made on the ground of structural diversity, high polarity and number of H-bond donor and acceptor groups, and assessed initially against FLT3.

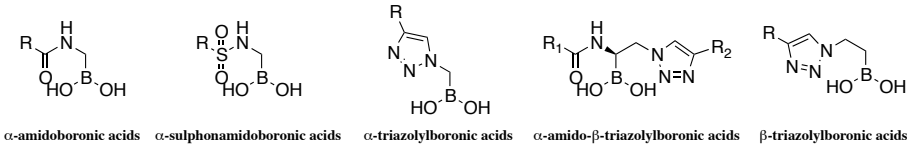

Figure 68. Classes of boronic acids docked on FLT3 and RET.

Recurrent binding interactions were observed in FLT3 and RET with important residues, such as the salt bridge (Glu661-Lys644), the DFG motif (Asp829-Phe830-Gly831) and the hinge region (Cys694-Cys695) of the ATP binding site.[6] The binding mode of α-triazolylboronic acids in particular is characterized by the formation of strong hydrogen bonds between the boronic acid and the salt bridge, the π-stacking of the triazole with two Phe and the interaction of the R group with the hinge region.

Thirty compounds among the boronic acids with the highest docking scores were assessed in enzymatic and cellular assays, leading to the identification of five triazolyl-boronic acids as micromolar hits (Chart 8).

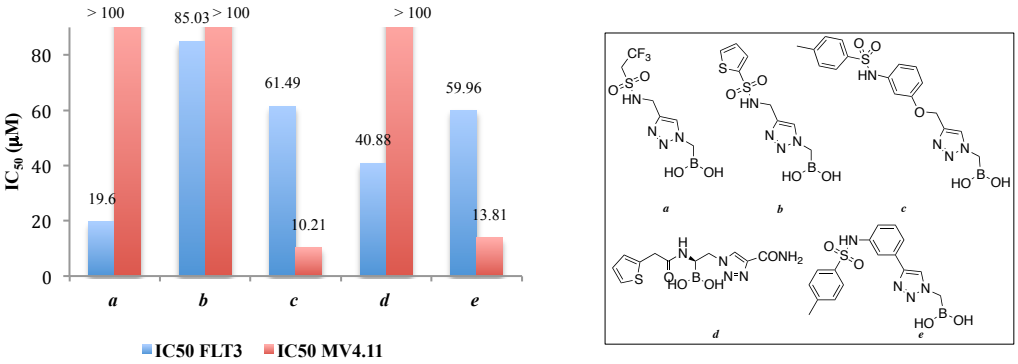

Chart 8. Enzymatic and cellular results on FLT3. MV4.11 is a cell line expressing FLT3 protein kinase.

Based on the results obtained from the first enzymatic and cellular assays, we ran a second *in silico* study focusing on α-triazolyl-boronic acids, the scaffold that showed the greatest activity. Twenty other compounds were, thus, identified and further profiled for activity against FLT3 in cellular assays on MV4.11 and MOLM.14 cell lines. Results for the most active compounds of the second selection are reported in Chart 9.

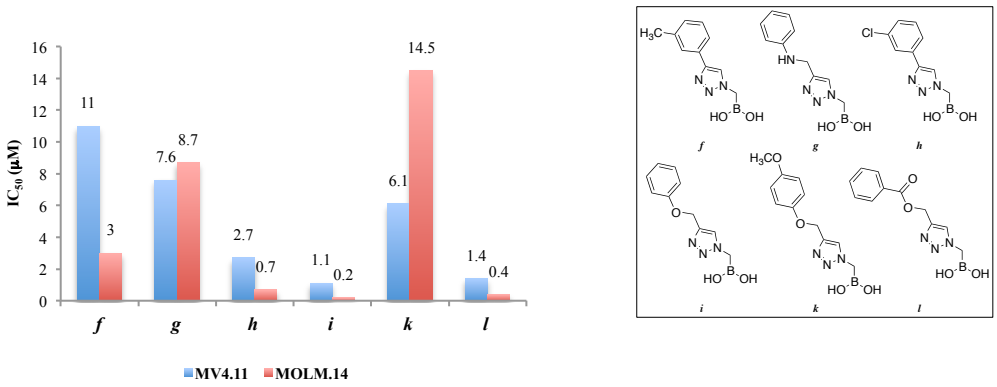

Chart 9. Cellular assays for the second series of α-triazolylboronic acids on FLT3 expressing cells.

Starting from the evidence that there is an active interest in the field of protein kinase (PK) inhibitors to develop dual-targeting agents to improve treatment outcomes, it is possible to say that boronic acids are interesting and promising compounds never tested in the field of AML. The presence of the boronic acid moiety improves the bioavailability and the pharmacokinetic profile of common anticancer chemotypes.[18,19] Moreover, the enzymatic and cellular activities together with the docking results highlighted a promising new kinase inhibitor scaffold, which is an interesting starting point for the design of α-triazolylboronic acids for a possible application as PK inhibitors. We are now waiting for more results about the activity of α-triazolylboronic acids in enzymatic assays on both kinasis and in cellular assays on RET. Then, the next step will be the development of new boronic compounds specifically designed to target PKs in order to improve the activity found in this preliminary screening.

It is really important to notice that this project highlights once more the potential of our compounds: they could be employed in more therapeutic fields than the antimicrobial one, in which we tested them until now. The possibility to target more diseases and to exploit the abilities of boron in different ways expands the frontiers of our research, making it the more and more exciting and promising.

References

(1) Gorovoy, A. S.; Gozhina, O. V; Svendsen, J. S.; Domorad, A. A.; Tetz, G. V; Tetz, V. V; Lejon, T. Boron-Containing Peptidomimetics – A Novel Class of Selective Anti-Tubercular Drugs. *Chem. Biol. Drug Des.* **2013**, *81* (3), 408–413. https://doi.org/https://doi.org/10.1111/cbdd.12091.

(2) Das, N.; Dhanawat, M.; Dash, B.; Nagarwal, R. C.; Shrivastava, S. K. Codrug: An Efficient Approach for Drug Optimization. *Eur. J. Pharm. Sci.* **2010**, *41* (5), 571–588. https://doi.org/10.1016/j.ejps.2010.09.014.

(3) Berkel, S. S. Van; Zollman, D.; Lee, S. Y.; Gileadi, O.; Mchugh, P. J.; Walsh, T. R.; Mcdonough, M. A.; Schofield, C. J. Structural Basis of Metallo-β-Lactamase Inhibition by Captopril Stereoisomers. *Antimicrob. Agents Chemother.* **2016**, *60* (1), 142–150. https://doi.org/10.1128/AAC.01335-15.Address.

(4) Tarazi, Z.; Lomovskaya, O.; Loutit, J. S.; Atkins, K.; Boyer, S. H.; Morgan, E. E.; Hirst, G. C.; Dudley, M. N.; Totrov, M.; Durso, S.; et al. Discovery of a Cyclic Boronic Acid β-Lactamase Inhibitor (RPX7009) with Utility vs Class A Serine Carbapenemases. *J. Med. Chem.* **2015**, *58* (9), 3682–3692. https://doi.org/10.1021/acs.jmedchem.5b00127.

(5) Hecker, S. J.; Reddy, K. R.; Lomovskaya, O.; Griffith, D. C.; Rubio-Aparicio, D.; Nelson, K.; Tsivkovski, R.; Sun, D.; Sabet, M.; Tarazi, Z.; et al. Discovery of Cyclic Boronic Acid QPX7728, an Ultrabroad-Spectrum Inhibitor of Serine and Metallo-β-Lactamases. *J. Med. Chem.* **2020**, *63* (14), 7491–7507. https://doi.org/10.1021/acs.jmedchem.9b01976.

(6) Li, N.; Zhang, G.; Zhu, A.; Zhang, L. A Convenient Preparation of 5-Iodo-1,4-Disubstituted-1,2,3-Triazole: Multicomponent One-Pot Reaction of Azide and Alkyne Mediated by CuI-NBS. *J. Org. Chem.* **2008**, *73* (9), 3630–3633. https://doi.org/10.1021/jo800035v.

(7) Chao, L.; Jie, W.; M., B. L.; Shan, Y.; Maoqun, T.; S., P. D.; Manoj, K.; W., Y. A.; A., J. K.; K., C. A.; et al. Decarboxylative Borylation. *Science (80-.).* **2017**, *356* (6342), eaam7355. https://doi.org/10.1126/science.aam7355.

(8) Powers, R. A.; Prati, F.; Bonomo, R. A.; Romagnoli, C.; Taracila, M. A.; Swanson, H. C.; Wallar, B. J.; Florek, N. W.; Caselli, E. Biochemical and Structural Analysis of Inhibitors Targeting the ADC-7 Cephalosporinase of Acinetobacter Baumannii . *Biochemistry* **2014**, *53* (48), 7670–7679. https://doi.org/10.1021/bi500887n.

(9) Huse, M.; Kuriyan, J. The Conformational Plasticity of Protein Kinases. *Cell* **2002**, *109* (3), 275–282. https://doi.org/10.1016/S0092-8674(02)00741-9.

(10) Hanahan, D.; Weinberg, R. A. Hallmarks of Cancer: The next Generation. *Cell* **2011**, *144* (5), 646–674. https://doi.org/10.1016/j.cell.2011.02.013.

(11) Glenjen, N.; Hovland, R.; Wergeland, L.; Wendelbo, Ø.; Ernst, P.; Bruserud, Ø. The Angioregulatory Phenotype of Native Human Acute Myelogenous Leukemia Cells: Influence of Karyotype, Flt3 Abnormalities and Differentiation Status. *Eur. J. Haematol.* **2003**, *71* (3), 163–173. https://doi.org/https://doi.org/10.1034/j.1600-0609.2003.00130.x.

(12) Daver, N.; Schlenk, R. F.; Russell, N. H.; Levis, M. J. Targeting FLT3 Mutations in AML: Review of Current Knowledge and Evidence. *Leukemia* **2019**, *33* (2), 299–312. https://doi.org/10.1038/s41375-018-0357-9.

(13) Mologni, L.; Marzaro, G.; Redaelli, S.; Zambon, A. Dual Kinase Targeting in Leukemia. *Cancers (Basel).* **2021**, *13* (1), 1–26. https://doi.org/10.3390/CANCERS13010119.

(14) Barabé, F.; Gil, L.; Celton, M.; Bergeron, A.; Lamontagne, V.; Roques, É.; Lagacé, K.; Forest, A.; Johnson, R.; Pécheux, L.; et al. Modeling Human MLL-AF9 Translocated Acute Myeloid Leukemia from Single Donors Reveals RET as a Potential

Therapeutic Target. *Leukemia* **2017**, *31* (5), 1166–1176. https://doi.org/10.1038/leu.2016.302.

(15) Rudat, S.; Pfaus, A.; Cheng, Y. Y.; Holtmann, J.; Ellegast, J. M.; Bühler, C.; Marcantonio, D. Di; Martinez, E.; Göllner, S.; Wickenhauser, C.; et al. RET-Mediated Autophagy Suppression as Targetable Co-Dependence in Acute Myeloid Leukemia. *Leukemia* **2018**, *32* (10), 2189–2202. https://doi.org/10.1038/s41375-018-0102-4.

(16) Choudhury, N. J.; Drilon, A. Decade in Review: A New Era for RET-Rearranged Lung Cancers. *Transl. Lung Cancer Res.* **2020**, *9* (6), 2571–2580. https://doi.org/10.21037/tlcr-20-346.

(17) Kadia, T. M. FLT3 Inhibitors in Acute Myeloid Leukemia: Increasing Options. *Clin. Adv. Hematol. Oncol.* **2021**, *19* (6), 352–355.

(18) Silva, M. P.; Saraiva, L.; Pinto, M.; Sousa, M. E. Boronic Acids and Their Derivatives in Medicinal Chemistry: Synthesis and Biological Applications. *Molecules* **2020**, *25* (18). https://doi.org/10.3390/molecules25184323.

(19) Maslah, H.; Pethe, S.; Labruère, R. Boronic Acid/boronate Prodrugs for Cancer Treatment: Current Status and Perspectives. *Future Med. Chem.* **2021**, *13* (10), 859–861. https://doi.org/10.4155/fmc-2021-0037.

Concluding Remarks

The aim of my doctoral research was to contribute to the identification of boronic acids as effective tools to contrast the worldwide alarming problem of antibiotic resistance. This research encompassed design, stereoselective synthesis, X-ray diffraction analysis, kinetic and microbiological studies and *in vivo* tests and gave me the possibility to exploit all the aspects of my pharmaceutical chemistry preparation. This multidisciplinary approach afforded the identification of several potent inhibitors of β-lactamases capable of restoring *in vitro* and *in vivo* the activity of β-lactams.

I started from the structure of the lead compound **S02030**, the most promising compound already synthesised by the research group. My project involved changes in the three different determinants of **S02030** structure: the amide group, the R_1 side chain attached to it and the R_2 side chain. Different approaches allowed obtaining important results:

- The bioisosteric substitution of the amide with its non-classical bioisostere triazole lead to the identification of α-triazolylboronic acids as potent inhibitors of class A and class C β-lactamases and good preliminary results were obtained against class B MBLs too. All the twenty-four compounds tested against ADC-7 displayed K_i values spanning from low micromolar to nanomolar values, with compound ***5o*** being among the best achiral inhibitors of class C β-lactamases (K_i = 0.09 μM; MIC lowered from 16 to 2 μg/ mL). Fourteen compounds were tested on KPC-2 and emerged as a new promising scaffold for *K. pneumoniae* carbapenemases inhibition. In particular, compound ***5q*** bearing a sulphonamide substituted by a tiophene ring proved to be an excellent inhibitor (K_i = 30 nM, MIC lowered from 32 to 0.5 μg/mL). Eight α-triazolylboronic acids decorated with zinc binding groups were also obtained; among these, compound ***6h*** demonstrated to inhibit VIM-2, with a K_i value of 7.7 μM.
- The bioisosteric substitution of the amide with a sulphonamide, the introduction of a little R_1 substituent and the different stereochemical arrangement of the substituents at the stereogenic center were explored to gain activity against class D β-lactamases. The results obtained suggested the best structural determinants for the inhibitions of this difficult to inhibit class of β-lactamases. In particular, i) the preferred configuration is *opposite* with respect to the inhibition of class C enzymes, ii) the smaller alkyl group (methyl/ethyl) attached to the stereocenter, the better the binding, iii) the presence of a carboxylate group on the sulphonamide chain strongly contributes to affinity. All the results obtained encourage the development of new compounds to improve inhibitory activity, starting from compound ***12f***, which is the best boronic inhibitor of class D β-lactamases identified so far (K_i = 4.4 μM).
- The modification of the R_1 group attached to the amide was made with the synthesis of a series of **S02030** derivatives, bearing an extra heteroatom directly bound to different heterocycles. Among

the seven compounds synthesised, ***19e*** (***MB076***) proved the best inhibitor of class A and class C β-lactamases in all assays performed (kinetic and microbiological analysis). ***MB076*** entered a program for preclinical development supported by the NIAID and it demonstrated to be not toxic in MTD assessment and to reduce by 40% the bacterial counts if compared to meropenem/cilastatin monotherapy. Moreover, it possesses a good PK/PD profile and it is able to enhance mice survival in combination with cefepime: mice treated with placebo or cefepime alone died, whereas all mice treated with a combination of ***MB076*** and cefepime survived.

Even if several new antimicrobials are under preclinical and clinical development, the high capabilities of bacteria to develop resistance against new agents encourage the development of new, potent and targeted antimicrobials. ESBL, AmpCs and KPCs producing bacteria are increasingly reported in animals, food, environment and community acquired human infections. Among MDR infections, complicated urinary tract infections (cUTI) and pyelonephritis are of particular concern and could become the target pathologies for our compounds and, in particular, for ***MB076***, which is the most promising compound synthesised.

The unique chemistry of boron compared to its adjacent neighbour carbon offers great promise in the search for new drug leads, with pharmaceutical companies now beginning to take notice of its great potential. Therefore, this is just the beginning and the best is all to discover!

Pubblications and Communications

Full Papers:

1. **α-Triazolylboronic Acids: A Promising Scaffold for Effective Inhibitors of KPCs.** Maria Luisa Introvigne, Magdalena A. Taracila, Fabio Prati, Emilia Caselli and Robert A. Bonomo. *ChemMedChem* **2020**, *15*, 1283-1288. https://doi.org/10.1002/cmdc.202000126.

2. **1,2,3-Triazolylmethaneboronate: A Structure Activity Relationship Study of a Class of β-Lactamase Inhibitors against *Acinetobacter baumannii* Cephalosporinase.** Emilia Caselli, Francesco Fini, Maria Luisa Introvigne, Mattia Stucchi, Magdalena A. Taracila, Erin R. Fish, Kali A. Smolen, Philip N. Rather, Rachel A. Powers, Bradley J. Wallar, Robert A. Bonomo, and Fabio Prati. *ACS Infect. Dis.* **2020**, *6* (7), 1965-1975. https://dx.doi.org/10.1021/10.1021/acsinfecdis.0c00254.

3. **Straightforward synthesis of chiral non-racemic α-boryl isocyanides.** Francesco Fini, Alessandro Zanni, Maria Luisa Introvigne, Mattia Stucchi, Emilia Caselli and Fabio Prati. *Org. Biomol. Chem.*, **2021**, *19*, 6687-6691. https://doi.org/10.1039/D1OB00616A.

Posters:

1. **XVIII Giornata della Chimica dell'Emilia Romagna**, December 17th, 2018 – Poster presentation: ***FACE TO FACE WITH ANTIBIOTIC RESISTANCE: NEW BORONIC ACID TRANSITION STATE INHIBITORS (BATSIs)*** *Maria Luisa Introvigne, Michele Menconi, Mattia Stucchi, Francesco Fini, Fabio Prati and Emilia Caselli.*

2. **National Meeting of Medicinal Chemistry 2019**, Milano, July 16th- 19th, 2019 – Poster Presentation: **OVERCOMING EXTENDED SPECTRUM BETA-LACTAMASE RESISTANCE IN *ACINETOBACTER BAUMANII* WITH BORONIC ACID TRANSISTION STATE INHIBITORS (BATSIs)** *Introvigne, M.L.; Fini, F; Powers, R ; Wallar, B; Taracila, M; Bonomo, R. A.; Caselli, E; Prati, F.*

3. **XIX Giornata della Chimica dell'Emilia Romagna**, December 6th, 2019 – Poster presentation*:* ***α−TRIAZOLYL-BORONIC ACIDS: A NEW CLASS OF β−LACTAMASE INHIBITORS ACTIVE AGAINST KLEBSIELLA PNEUMONIAE CARBAPENEMASE (KPC-2).*** *Maria Luisa Introvigne, Francesco Fini, Magdalena Taracila, Robert Bonomo, Fabio Prati and Emilia Caselli.*

4. **13th Young Medicinal Chemist Symposium: Nuove prospettive in Chimica Farmaceutica (NPCF2021)**, online event, April 26th, 27th, 28th, 29th, 2021 – Poster

presentation: ***CHIRAL SULFONAMMIDO-BORONIC ACIDS AS INHIBITORS OF CLASS C AND CLASS D - β−LACTAMASES: DESIGN, SYNTHESIS AND PRELIMINARY DATA.*** Introvigne, M.L.; Zhou, R; Powers, R; Wallar, B; Taracila, M; Bonomo, R. A.; Caselli, E; Prati, F.

5. **XXVI EFMC International Symposium on Medicinal Chemistry**, virtual event, August, 29th- September, 2nd, 2021 – Poster presentation: ***α*−TRIAZOLYL-BORONIC ACIDS: A PROMISING SCAFFOLD AS PROTEIN KINASE (PK) INHIBITORS IN ACUTE MYELOID LEUKAEMIA (AML).** Introvigne, M.L., Destro, L.; Mologni, L., Prati, F.; Caselli, E.; Zambon, A.

6. **European School of Medicinal Chemistry**, virtual event from Urbino, June, 28th- July, 1st 2021 – Poster presentation: **BORONIC ACIDS IN THE FIGHT AGAINST ANTIMICROBIAL RESISTANCE. A BIG ENEMY, A LOT OF WEAPONS: OUR SOLUTIONS.** Introvigne, M.L.; Zhou, R; Powers, R; Wallar, B; Taracila, M; Bonomo, R. A.; Caselli, E; Prati, F.

Oral presentations:

1. **European School of Medicinal Chemistry**, virtual event from Urbino, June, 28th- July, 1st 2021 – Oral communication: **BORONIC ACIDS IN THE FIGHT AGAINST ANTIMICROBIAL RESISTANCE. A BIG ENEMY, A LOT OF WEAPONS: OUR SOLUTIONS.**